GA–A24285

HIGH EFFICIENCY GENERATION OF HYDROGEN FUELS USING NUCLEAR POWER

FINAL TECHNICAL REPORT FOR THE PERIOD AUGUST 1, 1999 THROUGH SEPTEMBER 30, 2002

by
L.C. BROWN, G.E. BESENBRUCH, R.D. LENTSCH,
K.R. SCHULTZ, J.F FUNK, P.S. PICKARD,
A.C. MARSHALL, S.K. SHOWALTER

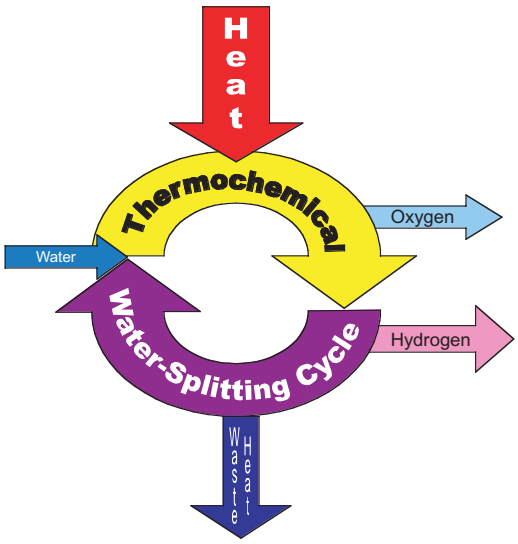

Prepared under the
Nuclear Energy Research Initiative (NERI) Program
Grant No. DE-FG03-99SF21888
for the U.S. Department of Energy

DATE PUBLISHED: JUNE 2003

GENERAL ATOMICS

DISCLAIMER

This report was prepared as an account of work sponsored by an agency of the United States Government. Neither the United States Government nor any agency thereof, nor any of their employees, makes any warranty, express or implied, or assumes any legal liability or responsibility for the accuracy, completeness, or usefulness of any information, apparatus, product, or process disclosed, or represents that its use would not infringe privately owned rights. Reference herein to any specific commercial product, process, or service by trade name, trademark, manufacturer, or otherwise, does not necessarily constitute or imply its endorsement, recommendation, or favoring by the United States Government or any agency thereof. The views and opinions of authors expressed herein do not necessarily state or reflect those of the United States Government or any agency thereof.

GA–A24285

HIGH EFFICIENCY GENERATION OF HYDROGEN FUELS USING NUCLEAR POWER

FINAL TECHNICAL REPORT FOR THE PERIOD AUGUST 1, 1999 THROUGH SEPTEMBER 30, 2002

by
L.C. BROWN, G.E. BESENBRUCH, R.D. LENTSCH,
K.R. SCHULTZ, J.F FUNK,* P.S. PICKARD,†
A.C. MARSHALL,† S.K. SHOWALTER†

*University of Kentucky, Lexington, Kentucky
†Sandia National Laboratory, Albuquerque, New Mexico

Prepared under the
Nuclear Energy Research Initiative (NERI) Program
Grant No. DE-FG03-99SF21888
for the U.S. Department of Energy

GENERAL ATOMICS PROJECT 30047
DATE PUBLISHED: JUNE 2003

EXECUTIVE SUMMARY

Hydrogen is a promising energy carrier, which potentially could replace the fossil fuels used in the transportation sector of our economy. Fossil fuels are polluting and carbon dioxide emissions from their combustion are thought to be responsible for global warming. However, no large scale, cost-effective, environmentally attractive hydrogen production process is currently available for commercialization.

This report describes work accomplished by the team of General Atomics (GA), Sandia National Laboratories (SNL) and the University of Kentucky (UK) during a three-year project whose objective was to "define an economically feasible concept for production of hydrogen, by nuclear means, using an advanced high temperature nuclear reactor as the energy source." The purpose of this work was to determine the potential for efficient, cost-effective, large-scale production of hydrogen utilizing high temperature heat from an advanced nuclear power station. The benefits of this technology include generation of a low-polluting transportable energy feedstock in a highly efficient method that has no greenhouse gas emissions, from an energy source whose availability and sources are domestically controlled. The work was divided into three phases. The work of Phases 1 [E–1] and 2 [E–2] have been reported earlier but are also summarized here for completeness.

The purpose of the first phase was to evaluate thermochemical processes which offer the potential for efficient, cost-effective, large-scale production of hydrogen from water, in which the primary energy input is high temperature heat from an advanced nuclear reactor and to select one for further detailed consideration. This was done in several steps: (1) a detailed literature search was performed to develop a database of all published thermochemical cycles, (2) a set of objective screening criteria was developed to rate each cycle and was used to reduce the initial list to 25 cycles [E–3], and (3) a detailed analysis was used to reduce the number of cycles under consideration to two and finally to one. The Phase 1 report is included as the Attachment. Appendix A presents an introduction to thermochemical water splitting.

Ten databases were searched (e.g., Chemical Abstracts, NTIS, etc.), and over 800 literature references, pertaining to thermochemical production of hydrogen from water, were organized in a computerized database. In the process, over 100 thermochemical water-splitting cycles were identified and organized into a separate, computer searchable database.

The first round of screening, using defined screening criteria and quantifiable metrics, yielded 25 cycles for more detailed study. The second round of screening, using refined criteria, reduced the 25 candidate cycles to 2 final options.

The two cycles selected for final consideration are the UT-3 cycle and the Sulfur-Iodine (S-I) cycle. The UT-3 cycle was invented at the University of Tokyo and much of the early development was done there. This cycle has been studied extensively by the Japan Atomic Energy Research Institute (JAERI). After considering several different flowsheets making use of the UT-3 cycle, JAERI selected the so-called Adiabatic UT-3 process for further development. The predicted efficiency of the Adiabatic UT-3 process varies between 35% and 40% depending upon the efficiency of membrane separators which are under development. A 10% overall efficiency increase is projected if electricity is co-generated along with the hydrogen.

The S-I cycle is the cycle with the highest reported efficiency based on an integrated flowsheet. The last full flowsheet of the process, developed in 1981–1984, had a predicted efficiency of 38% when coupled to a fusion reactor. Since that time, various researchers have pointed out improvements that should increase the already high efficiency of this cycle and, in addition, lower the capital cost. As the S-I cycle had both the highest predicted efficiency and the most potential for further improvement, it was selected as the basis for the ongoing effort. A schematic for the nuclear-matched S-I cycle is shown in Fig. Ex–1.

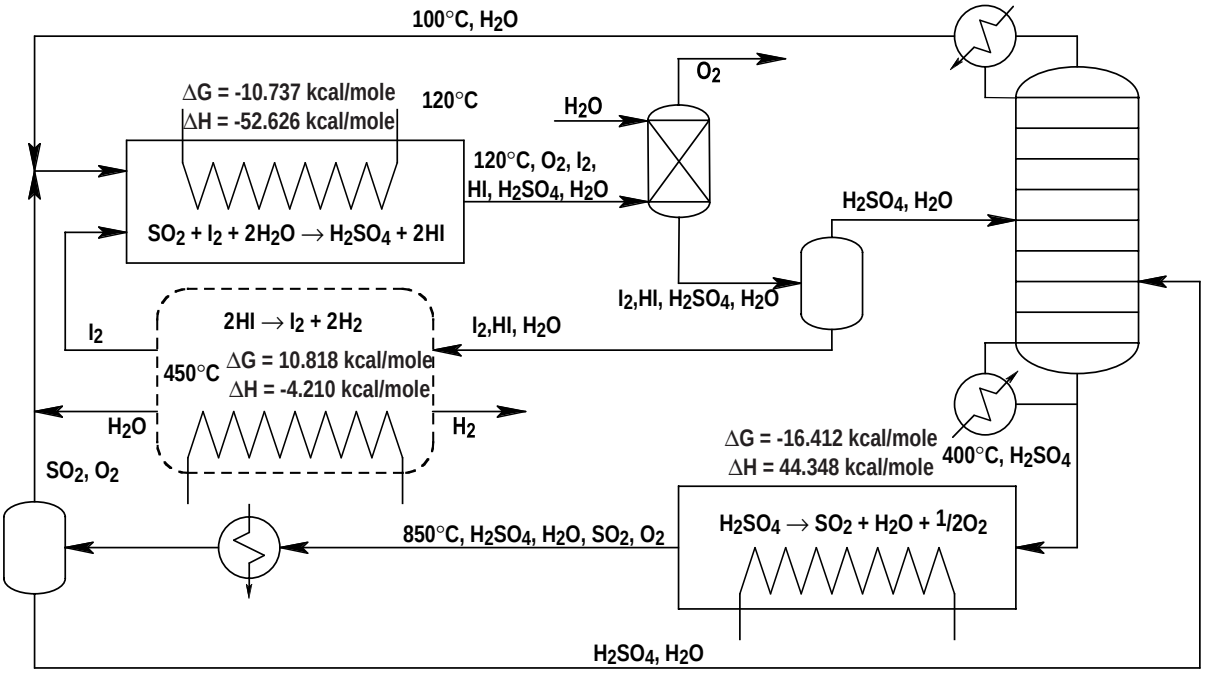

Fig. Ex–1. S-I cycle process flow diagram.

The goal of Phase 2 and 3 efforts was to determine the optimal configuration of a high temperature nuclear reactor coupled to a thermochemical hydrogen plant so as to deliver hydrogen at the minimum total cost. The reactor selection and integration task was headed by

SNL while the hydrogen production flowsheet and costing effort was split between GA and UK.

The main elements comprising Phases 2 and 3 are:

- Evaluate and select the nuclear reactor best suited for production of hydrogen by the S-I thermochemical cycle process.
  - — Develop the concept for the interface which matches the reactor to the process.
  - — Develop the flowsheets for the chemical process.
  - — Conceptually design each major piece of process equipment to the degree necessary for estimating the capital equipment cost and then determine that cost.
  - — Using standard chemical engineering cost estimating techniques, estimate the total chemical plant capital cost based on the equipment costs.
  - — Combine the chemical plant capital costs with estimates of the reactor capital cost and operating costs to predict the cost of hydrogen from the project.

During Phase 2, a detailed evaluation of alternative nuclear reactor concepts was performed to select the reactor best suited to thermochemical hydrogen production using the selected S-I process. SNL evaluated nine categories of nuclear reactor, identified by their coolants. These ranged from reactors that have been successfully commercialized [the Light Water Reactors (LWRs)], to those that have been demonstrated but not successfully commercialized (helium and liquid metal-cooled reactors), to reactors that have been conceptualized but never built. SNL evaluated these reactors against a set of five design requirements and five performance criteria. Today's LWRs simply cannot achieve adequate temperature to be used for thermochemical water-splitting. Several nonwater-cooled reactors do appear to have high enough temperature potential to drive the S-I cycle. Of these, the helium-cooled reactor, the heavy metal (Pb-Bi) cooled reactor and the molten salt-cooled reactor rated best. The SNL study, Appendix B, indicated that although heavy metal and molten salt-cooled reactor concepts could potentially be developed to the point that they could support hydrogen production, helium gas-cooled reactors had reached the point in development where nuclear hydrogen production would be possible with essentially no further development. We selected the helium gas-cooled reactor for our study.

The starting point for process development and improvement is the S-I cycle flowsheet developed in 1979–1984 [E–4]. This flowsheet was produced at the time when computer simulation of chemical processes was coming into vogue using general-purpose chemical flowsheet simulators. Several attempts were made at that time to use various simulation programs then extant but the thermodynamic models available at that time could not deal with the nonidealities of even the simplest part of the process and hand calculations were used for the entire flowsheet.

When beginning this effort, we assumed that current computer simulation programs could adequately represent the complex behaviors characteristic of the S-I cycle. This is, to a large extent, true but transforming the available data into computer usable form proved to be a considerable undertaking. Aspen Plus, the process simulation program selected for this effort, has, perhaps, the best implementation of electrolytic solution thermodynamics available. But, even for the simple system H_2SO_4/H_2O, there was no valid model covering the range of temperature, pressure and composition needed to describe the thermochemistry of the S-I cycle. The services of Aspen Technology, licenser of Aspen Plus, were utilized to regress sulfuric acid thermodynamics data to generate the model used for our analysis. The resulting electrolytic nonrandom two-liquid sulfuric acid model is a good representation of the H_2SO_4/H_2O system and was used to model Section 2 of the flowsheet.

We were unable to develop Aspen Plus models for $HI/I_2/H_20$ system (Section 3) or the $H_2SO_4/HI/I_2/H_2O$ system (Section 1). The current state of the equilibrium data for the $HI/I_2/H_20$ system appears to be inadequate to be able to regress a model that will successfully converge. The flowsheets for Sections 1 and 3 were based on earlier analyses, calculated by hand without a chemical simulation computer program. For Section 3, HI decomposition, we use the reactive distillation process calculated by Roth and Knocke [E–5] at the University of Aachen. For Section 1, we started with the 1982 flow sheet and calculated the compositions after accounting for the large recycle flows from Section 3. While these analyses are adequate to calculate self-consistent flowsheets, they did not allow us to optimize the overall S-I system to the extent desired. We believe that recuperation of heat from Section 2 into Section 3 would allow still further increases in the efficiencies we calculated for the current flowsheet. This can be done when the $HI/I_2/H_20$ system equilibrium data are measured, a full chemical system model is regressed from these data, and a complete Aspen Plus model for the entire S-I flowsheet is developed. Measurement of the equilibrium data is a high priority R&D need identified by this study.

In Phase 2, we investigated several alternatives to the 1982 flowsheet, which was based on the use of phosphoric acid, H_3PO_4, to pull the water out of the $HI/I_2/H_2O$ mixture in Section 3 prior to HI decomposition. While this process is effective, the energy needed and capital cost of the equipment used to then extract the water to regenerate the H_3PO_4 are high and they reduce the efficiency and increase the cost of the 1982 S-I system. At that time, GA suggested reactive distillation as an alternative but did not pursue it. Roth and Knocke at the University of Aachen analyzed this option and predicted that a higher efficiency and up to 40% lower capital cost might be obtained. We chose the reactive distillation option for Section 3 of our flowsheet design. This process only decomposes one-sixth of the HI and recycles the remaining five-sixths to Section 1. This results in increased costs and we had hoped to further optimize the process to increase the fractional decomposition. The computational difficulties described above prevented us from completing this step and we adopted the original Roth and Knocke reactive distillation process for our design.

In Phase 3 of the study, we completed a flowsheet for each Section of the S-I process. These are presented in detail in this report. These flowsheets were developed with an assumed peak process temperature of 827°C. This matched the peak temperature of the 1978 flowsheet and we expect that this temperature could be attained using the current 850°C Modular Helium Reactor outlet temperature and a high effectiveness compact heat exchanger. The complete design at this temperature only achieved 42% thermal efficiency. We estimated the increase in efficiency that could be achieved at higher peak process temperature and believe that at 900°C peak process temperature, we will be able to achieve 52% efficiency. This would require about 950°C reactor outlet temperature. We have used this system for our economics estimates.

We performed preliminary equipment sizing calculations to determine the capital cost of the equipment and then estimated the total capital and operating costs of the integrated hydrogen plant. Finally, we incorporated the reactor capital cost and operating costs for an estimated 950°C Modular Helium Reactor to estimate the cost of the hydrogen produced by a high temperature nuclear reactor coupled to the S-I process. Selected results of this economics analysis are shown below. The capital costs are for an "nth of a kind" plant and include all direct and indirect costs, plus interest during construction. The Reactor operating costs include all fuel cycle costs (fuel, conversion, enrichment, fabrication, and waste disposal) plus normal operation and maintenance costs. The Hydrogen Plant operating costs include normal operation and maintenance costs plus the cost of high purity water. All costs are in 2002 funding. Since both the reactor and the hydrogen plant are capital intensive, the hydrogen cost using several different capital recovery factors (CRF) are shown in Table Ex–1.

Table Ex–1
Cost of 2400 MWt 4-module Modular Helium Reactor Hydrogen Production Plant

	850°C, 42% Efficiency	950°C, 52% Efficiency
Reactor Capital Cost, M$	968.2	1,098.0
Hydrogen Plant Capital Cost, M$	643.2	796.3
Reactor Fuel + Operating Cost, M$/yr	93.9	97.1
Hydrogen Plant Operating Cost, M$/yr	50.7	62.7
Hydrogen Production Rate, kg/yr	213×10^6	264×10^6
Cost of Hydrogen, $/kg		
— Public utility – 10.5% CRF	1.53	1.42
— Regulated utility – 12.5% CRF	1.69	1.57
— Unregulated utility – 16.5% CRF	2.01	1.87

On the basis of these results, we recommend that work be carried out to demonstrate and develop the S-I cycle for production of hydrogen from nuclear energy.

TABLE OF CONTENTS

LIST OF FIGURES

LIST OF TABLES

1. INTRODUCTION

Combustion of fossil fuels, used to power transportation, generate electricity, heat homes and fuel industry provides 86% of the world's energy [1–1,1–2]. Drawbacks to fossil fuel utilization include limited supply, pollution, and carbon dioxide emissions. Carbon dioxide emissions, thought to be responsible for global warming, are now the subject of international treaties [1–3,1–4]. Together, these drawbacks argue for the replacement of fossil fuels with a less-polluting potentially renewable primary energy such as nuclear energy. Conventional nuclear plants readily generate electric power but fossil fuels are firmly entrenched in the transportation sector. Hydrogen is an environmentally attractive transportation fuel that has the potential to displace fossil fuels. Hydrogen will be particularly advantageous when coupled with fuel cells. Fuel cells have higher efficiency than conventional battery/internal combustion engine combinations and do not produce nitrogen oxides during low-temperature operation. Contemporary hydrogen production is primarily based on fossil fuels and most specifically on natural gas. When hydrogen is produced using energy derived from fossil fuels, there is little or no environmental advantage.

There is currently no large scale, cost-effective, environmentally attractive hydrogen production process available for commercialization, nor has such a process been identified. The objective of this work is to find an economically feasible process for the production of hydrogen, by nuclear means, using an advanced high-temperature nuclear reactor as the primary energy source. Hydrogen production by thermochemical water-splitting (Appendix A), a chemical process that accomplishes the decomposition of water into hydrogen and oxygen using only heat or, in the case of a hybrid thermochemical process, by a combination of heat and electrolysis, could meet these goals.

Hydrogen produced from fossil fuels has trace contaminants (primarily carbon monoxide) that are detrimental to precious metal catalyzed fuel cells, as is now recognized by many of the world's largest automobile companies. Thermochemical hydrogen will not contain carbon monoxide as an impurity at any level. Electrolysis, the alternative process for producing hydrogen using nuclear energy, suffers from thermodynamic inefficiencies in both the production of electricity and in electrolytic parts of the process. The efficiency of electrolysis (electricity to hydrogen) is currently about 80%. Electric power generation efficiency would have to exceed 65% (thermal to electrical) for the combined efficiency to exceed the 52% (thermal to hydrogen) calculated for one thermochemical cycle.

Thermochemical water-splitting cycles have been studied, at various levels of effort, for the past 35 years. They were extensively studied in the late 70s and early 80s but have received little attention in the past 10 years, particularly in the U.S. While there is no question about the technical feasibility and the potential for high efficiency, cycles with

proven low cost and high efficiency have yet to be developed commercially. Over 100 cycles have been proposed, but substantial research has been executed on only a few.

This report describes work accomplished during a three-year project whose objective is to "define an economically feasible concept for production of hydrogen, by nuclear means, using an advanced high temperature nuclear reactor as the energy source." This work was performed as a collaborative effort between General Atomics (GA), the University of Kentucky (UK) and Sandia National Laboratories (SNL) under the Department of Energy under Nuclear Energy Research Initiative (NERI) Grant Nos. DE-FG03-99SF21888 (GA/UK) and DE-FG03-99SF0238 (SNL)

The work was divided into several tasks. All of the collaborators were involved in every task but one organization had responsibility for the task.

The emphasis of the first phase was to evaluate thermochemical processes which offer the potential for efficient, cost-effective, large-scale production of hydrogen from water in which the primary energy input is high temperature heat from an advanced nuclear reactor and to select one (or, at most three) for further detailed consideration.

During Phase 1, an exhaustive literature search was performed to locate all cycles previously proposed. The cycles located were screened using objective criteria to determine which could benefit, in terms of efficiency and cost, from the high-temperature capabilities of advanced nuclear reactors. The more promising cycles were then analyzed in depth as to their adaptability to advanced high-temperature nuclear reactors. As a result, the Sulfur-Iodine (S-I) cycle was selected for integration into the advanced nuclear reactor system.

In Phases 2 and 3, alternative flowsheets were developed and compared. This effort entailed a considerable effort into developing the solution thermodynamics pertinent to the S-I cycle. From each flowsheet, we derived the thermal efficiency of hydrogen production and made preliminary engineering estimates of size and cost for major pieces of equipment and estimates of the operating cost of the chemical plant. The efficiency, capital cost, and operating cost were combined for similar information for a high temperature nuclear reactor to calculate the cost of nuclear produced hydrogen.

The work of Phases 1 and 2 have been previously reported, but are covered briefly, the emphasis being on Phase 3.

2. PHASE 1: EVALUATION OF POTENTIAL NUCLEAR HYDROGEN PROCESSES

The purpose of Phase 1 was to evaluate the potential for efficient and economic thermochemical production of hydrogen based on nuclear energy and, if warranted, select a thermochemical cycle for detailed examination in Phases 2 and 3. The initial of Phase 1 was oriented toward the efficient manipulation and evaluation of a large amount of data. The later stages of Phase 1 required a more in depth evaluation of promising thermochemical cycles and ultimately the selection of one cycle for detailed evaluation in subsequent phases.

The Phase 1 effort is summarized here but also attached as Attachment.

2.1. LITERATURE SEARCH

Our first task was to survey the technical literature for all references to thermochemical water-splitting cycles and to abstract from each pertinent article a complete description of the thermochemical cycle discussed. Two major subtasks were determining efficient search strategies and developing database structures and procedures that maximized our ability to correlate the data and eliminated duplicate cycle entries due to variations in cycle definition by the various authors. These subtasks are described in detail in Attachment.

The literature search resulted in over 800 citations to 115 different cycles. Figure 2–1 shows the high interest in thermochemical water-splitting in the period 1975–1985. Since that time there has been a low level of ongoing interest, almost exclusively from Japan.

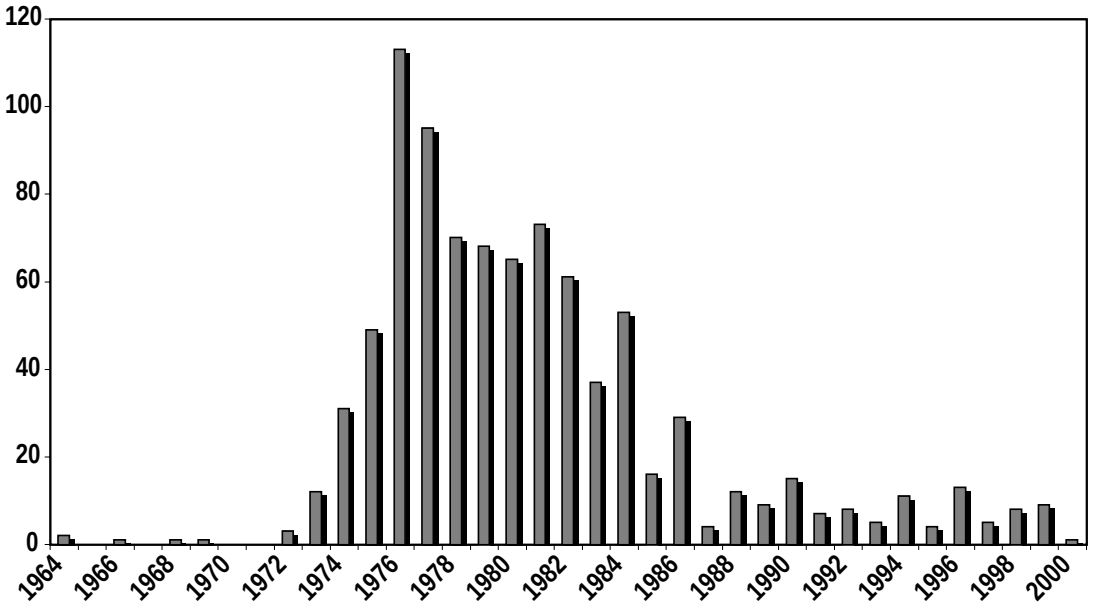

Fig. 2–1. Publications by year of issue.

This was far too many cycles to analyze in depth so; a set of objective criteria was established and used as the basis for reducing the number of cycles for which an in-depth analysis would be made. The purpose of the preliminary screening was not to develop an absolute ranking to the better cycles; rather it was to eliminate from further consideration the cycles least likely to be practical.

2.2. PRELIMINARY SCREENING

The criteria presented in the original proposal were refined and metrics were established by which each proposed cycle could be evaluated according to each criterion. Insofar as possible, the metrics were objectively defined so as to make the ranking independent of the person doing the ranking. Where subjective evaluations were necessary, a consensus ranking was determined among the three principal investigators. It should be emphasized that the purpose of the ranking was not to give an absolute ranking to the most promising cycles, rather it was to make sure that all promising cycles were ranked above the cut-off point while eliminating most defective cycles. Table 2–1 gives each criterion, the rational for the criterion and the metric based on the criterion. Table 2–2 indicates how the numerical score is obtained from each criterion.

One criterion, maximum process temperature, is not monotonic and deserves further explanation. The maximum process temperature can either be too high or too low to be useful. If the temperature is too low, the process cannot be efficient. If the maximum process temperature is too high, materials of construction will not be found. The maximum temperature for conventional heat transfer materials, 750–850°C was given the highest score. Higher temperatures can be accommodated using exotic materials of construction, thus getting a lower score. Low temperature processes are scored low, as they will be inefficient.

There was a significant correlation between the scores from the last three metrics and the total score. Leaving these metrics out of the scoring had little effect on which cycles scored best. This is probably because previous work has concentrated on cycles with few reactions, simple separations, available materials, which have minimal solids flow problems and which have their heat input requirements at reasonable temperatures.

Table 2–1
Rational for Development of First Round Screening Criteria

	Desirable Characteristic	Rational	Metric
1	Higher ranked cycles will have a minimum number of chemical reactions steps in the cycle.	A smaller number of chemical reactions indicates a simpler process and lower costs.	Score is based on number of chemical reactions.
2	Higher ranked cycles will have a minimum number of separation steps in the cycle.	A smaller number of chemical separations indicates a simpler process and lower costs.	Score is based on number of chemical separations, excluding simple phase separation.
3	Higher ranked cycles will have a minimum number of elements in the cycle.	A smaller number of chemical elements indicates a simpler process and lower costs.	Score is based on number of elements, excluding oxygen and hydrogen
4	Higher ranked cycles will employ elements which are abundant in the earth's crust, oceans and atmosphere.	Use of abundant elements will lower the cost and permit the chosen technology to be implemented on a large scale. There may be strategic availability issues.	Score is based on least abundant element in cycle.
5	Higher ranked cycles will minimize the use of expensive materials of construction by avoiding corrosive chemical systems, particularly in heat exchangers.	Improved materials of construction may allow consideration of processes previously dismissed yet the effect of materials cost on hydrogen production efficiency and cost must be considered.	Score is based on the relative corrosiveness of the process solutions.
6	Higher ranked cycles will minimize the flow of solids.	Chemical plant costs are considerably higher for solids processing plants. Flow of solid materials also corresponds to increased maintenance costs due to wear and to increased downtime due to blockage and unscheduled equipment failure.	Score is based on minimization of solid flow problems.
7	Higher ranked cycles will have maximum heat input temperature compatible with high temperature heat transfer materials.	High thermal efficiency cannot be realized without a high temperature heat input to the water-splitting process. The limit on temperature will be the thermal and mechanical performance of the heat transfer material separating the reactor coolant from the process stream requiring the highest temperature.	Score is based on the high temperature heat input to the process being close to that delivered by an advanced nuclear reactor.
8	Higher ranked cycles will have been the subject of many papers from many authors and institutions.	Cycles that have been thoroughly studied in the literature have a lower probability of having undiagnosed flaws.	Score will be based on the number of papers published dealing with the cycle.
9	Higher ranked cycles will have been tested at a moderate or large scale,	Relatively mature processes will have had their unit operations tested at relatively large scale. Processes for which the basic chemistry has not been verified are suspect.	Score will be based on the degree to which the chemistry of the cycle has been actually demonstrated and not just postulated.
10	Higher ranked cycles will have good efficiency and cost data available.	A significant amount of engineering design work is necessary to estimate process efficiencies and production costs. Note: cost estimates in the absence of efficiency calculations are meaningless and will not be considered.	Score will be based on the degree to which efficiencies and cost have been estimated.

Table 2–2
Metrics Used to Score Processes. For Each Metric, the Process Receives the Score Indicated. The Process Score is the Sum of the Individual Scores.

Metric ⇓ Score ⇒	0	1	2	3	4	5	6	7	8	9	10
1. Number of chemical reactions	6	—	—	5	—	—	4	—	—	3	2
2. Number of chemical separation steps	10	9	8	7	6	5	4	3	2	1	0
3. Number of elements – 2	7		6	—	5	—	4	—	3	2	1
4. Least abundant element in process	Ir	Rh, Te, Os, Ru, Re, Au	Pt, Bi, Pd, Hg, Se	Ag, In, Cd, Sb Tm, Tl, Lu	I, Tb, W, Ho, U, Ta, Mo, Eu, Cs, Yb, Er, Hf, Sn, Ge	Th, As, Gd, Dy, Sm, Pb, Pr	Nb, Be, Nd, La, Ga, Y, Ce, Co, Sc, Rb	Cu, Zn, Zr, Ni, B, Ba, Li, Br, Cr, V, Sr	Mn, F, P	S, Ti, C, K, N	Ca, Mg, Cl, Na, Al, Fe, Si
5. Relative corrosiveness of process solutions†	Very corrosive, e.g. aqua regia				Moderately corrosive, e.g. sulfuric acid						Not corrosive
6. Degree to which processis continuous and flowof solids is minimized	batch flow of solids			continuous flowof solids		flow of gases or liquids through packed beds				continuous flow of liquids and gases	
7. Maximum temperature in process	<300 C or <1300 C	300-350 C or 1250-1300 C	350-400 C or 1200-1250 C	400-450 C or 1150-1200 C	450-500 C or 1100-1150 C	500-550 C or 1050-1100 C	550-600 C or 1000-1050 C	600-650 C or 950-1000 C	650-700 C or 900-950 C	700-750C or 850-900C	750-850 C
8. Number of published references to cycle†	1 paper		A few papers			many papers			extensive literature base		
9. Degree to which chemistry of cycle has been demonstrated†	no laboratory work			test tube scale testing			bench scale testing				pilot plant scale testing
10. Degree to which good efficiency and cost data are available†	No efficiency estimate available		Thermodynamic efficiency estimated from elementary reactions.		Thermodynamic efficiency estimate based on rough flowsheet		Thermodynamic efficiency calculation based on detailed flowsheet		Detailed cost calculations, based on detailed flowsheets available from one or more independent sources.		

†Interpolate scores between defined scale points.

The screening criteria were applied to all 115 cycles and the results were sorted according to the total number of screening points awarded to each process. We used 50 out of the total possible of 100 points as the cut-off score leaving 40 cycles. We then applied environmental, safety and health (ES&H) considerations as well as well as other "sanity checks" reducing the number to 25. Two cycles were eliminated for ES&H reasons in that they are based on mercury and we do not believe that it would be possible to license such a plant. Three cycles were eliminated because they require temperatures in excess of 1600°C, which places them outside the scope of processes that are compatible with advanced nuclear reactors contemplated in the next 50 years. Seven cycles were eliminated because they had reactions that have large positive free energies that cannot be accomplished electrochemically. The final short list of 25 cycles is given in Table 2–3, along with their scores. Details for these cycles are given in Table 2–4.

2.3. SECOND STAGE SCREENING

The goal of the second stage screening was to reduce the number of cycles under consideration to three or less. Detailed investigations were made into the viability of each cycle. The most recent papers were obtained for each cycle and, when not available from the literature, preliminary block-flow diagrams were made to help gain an understanding of the process complexity. Thermodynamic calculations were made for each chemical reaction over a wide temperature range. Each chemical species was considered in each of its potential forms: gas, liquid, solid, and aqueous solution. Each of the principal investigators took responsibility for a part of the investigation and the results were shared.

Once all the background work was completed, the final selection was relatively easy. The three principal investigators independently rated the viability of each cycle. The 25 cycles were considered without reference to their original score and re-rated. Each principal investigator independently assigned a score to each cycle based on their rating of the cycle to be favorable (+1), acceptable (0), or unfavorable (–1). The scores of the three principal investigators (PIs) were summed, Table 2–5, and two cycles stood out from all the others with a score of +3. The most highly rated cycles are the adiabatic version of the UT-3 cycle and the Sulfur-Iodine cycle.

Table 2–3
Short List of Cycles and Their Scores

Ref. No.	Name	Class	Max Temp	Elements	#elem	#seps	#Rxns	1 Rxns	2 Seps	3 Elems	4 Abund	5 Corr	6 Solids	7 Temp	8 Pubs	9 Tests	10 Data	Total
1.	Westinghouse	H	850	S	1	2	2	10	8	10	9	5	10	9	10	6	8	85
2.	Ispra Mark 13	H	850	Br,S	2	3	3	9	7	9	7	5	10	9	10	6	8	80
3.	UT-3 Univ. of Tokyo	T	750	Br,Ca,Fe	3	3	4	6	7	8	7	5	6	10	10	10	10	79
4.	GA Sulfur-Iodine	T	800	I,S	2	3	3	9	7	9	4	5	10	10	10	6	8	78
5.	JulichCenter EOS	T	800	Fe,S	2	3	3	9	7	9	9	9	6	10	3	3	3	68
6.	Tokyo Inst. Tech. Ferrite	T	1000	Fe,Mn,Na	3	2	2	10	8	8	8	10	10	6	2	2	0	64
7.	HallettAir Products1965	H	800	Cl	1	3	2	10	7	10	10	5	10	10	0	0	0	62
8.	Gaz de France	T	825	K	1	3	3	9	7	10	9	5	6	10	2	2	2	62
9.	Nickel Ferrite	T	1000	Fe,Ni,Mn	3	0	2	10	10	8	7	10	6	6	0	3	0	60
10.	Aachen Univ Julich1972	T	800	Cr,Cl	2	3	3	9	7	9	7	5	6	10	2	2	2	59
11.	Ispra Mark 1C	T	900	Br,Ca,Cu	3	4	4	6	6	8	7	5	10	8	2	3	3	58
12.	LASL-U	T	700	C,U	2	3	3	9	7	9	4	10	6	9	1	3	0	58
13.	Ispra Mark 8	T	900	Cl,Mn	2	3	3	9	7	9	8	5	3	8	3	2	3	57
14.	Ispra Mark 6	T	800	Cl,Cr,Fe	3	4	4	6	6	8	7	5	6	10	2	3	3	56
15.	Ispra Mark 4	T	800	Cl,Fe	2	4	4	6	6	9	10	5	0	10	3	3	3	55
16.	Ispra Mark 3	T	800	Cl,V	2	3	3	9	7	9	7	5	0	10	2	3	3	55
17.	Ispra Mark 2 (1972)	T	800	C,Na,Mn	3	3	3	9	7	8	8	5	0	10	2	3	3	55
18.	CO/Mn3O4	T	977	C,Mn	2	3	3	9	7	9	8	9	6	7	0	0	0	55
19.	Ispra Mark 7B	T	1000	Cl,Fe	2	5	5	3	5	9	10	5	10	6	0	3	3	54
20.	Vanadium Chloride	T	700	Cl,V	3	5	4	6	5	8	7	5	6	9	3	2	2	53
21.	Ispra Mark 7A	T	1000	Cl,Fe	2	5	5	3	5	9	10	5	6	6	3	3	3	53
22.	GA Cycle 23	T	850	S	2	4	5	3	6	9	9	5	10	9	0	0	0	51
23.	US -Chlorine	T	993	Cl,Cu	2	3	3	9	7	9	7	6	5	7	0	0	0	50
24.	Ispra Mark 9	T	450	Cl,Fe	2	8	3	9	2	9	10	5	3	4	2	3	3	50
25.	Ispra Mark 6C	T	800	Cl,Cr,Cu,Fe	4	5	5	3	5	6	7	5	6	10	2	3	3	50

* T = Thermochemical, H = Hybrid Thermochemical/Electorchemical

Table 2–4
Reaction Details for Cycles

Cycle	Name	T/E*	T °C	Reaction	F†
1	Westinghouse [2–1]	T	850	$2H_2SO_4(g) \rightarrow 2SO_2(g) + 2H_2O(g) + O_2(g)$	$^1/_2$
		E	77	$SO_2(g) + 2H_2O(a) \rightarrow H_2SO_4(a) + H_2(g)$	1
2	Ispra Mark 13 [2–2]	T	850	$2H_2SO_4(g) \rightarrow 2SO_2(g) + 2H_2O(g) + O_2(g)$	$^1/_2$
		E	77	$2HBr(a) \rightarrow Br_2(a) + H_2(g)$	1
		T	77	$Br_2(l) + SO_2(g) + 2H_2O(l) \rightarrow 2HBr(g) + H_2SO_4(a)$	1
3	UT-3 Univ. of Tokyo [2–3]	T	600	$2Br_2(g) + 2CaO \rightarrow 2CaBr_2 + O_2(g)$	$^1/_2$
		T	600	$3FeBr_2 + 4H_2O \rightarrow Fe_3O_4 + 6HBr + H_2(g)$	1
		T	750	$CaBr_2 + H_2O \rightarrow CaO + 2HBr$	1
		T	300	$Fe_3O_4 + 8HBr \rightarrow Br_2 + 3FeBr_2 + 4H_2O$	1
4	Sulfur-Iodine [2–4]	T	850	$2H_2SO_4(g) \rightarrow 2SO_2(g) + 2H_2O(g) + O_2(g)$	$^1/_2$
		T	450	$2HI \rightarrow I_2(g) + H_2(g)$	1
		T	120	$I_2 + SO_2(a) + 2H_2O \rightarrow 2HI(a) + H_2SO_4(a)$	1
5	Jülich Center EOS [2–5]	T	800	$2Fe_3O_4 + 6FeSO_4 \rightarrow 6Fe_2O_3 + 6SO_2 + O_2(g)$	$^1/_2$
		T	700	$3FeO + H_2O \rightarrow Fe_3O_4 + H_2(g)$	1
		T	200	$Fe_2O_3 + SO_2 \rightarrow FeO + FeSO_4$	6
6	Tokyo Inst. Tech. Ferrite [2–6]	T	1000	$2MnFe_2O_4 + 3Na_2CO_3 + H_2O \rightarrow 2Na_3MnFe_2O_6 + 3CO_2(g) + H_2(g)$	1
		T	600	$4Na_3MnFe_2O_6 + 6CO_2(g) \rightarrow 4MnFe_2O_4 + 6Na_2CO_3 + O_2(g)$	$^1/_2$
7	Hallett Air Products 1965 [2–5]	T	800	$2Cl_2(g) + 2H_2O(g) \rightarrow 4HCl(g) + O_2(g)$	$^1/_2$
		E	25	$2HCl \rightarrow Cl_2(g) + H_2(g)$	1
8	Gaz de France [2–5]	T	725	$2K + 2KOH \rightarrow 2K_2O + H_2(g)$	1
		T	825	$2K_2O \rightarrow 2K + K_2O_2$	1
		T	125	$2K_2O_2 + 2H_2O \rightarrow 4KOH + O_2(g)$	$^1/_2$
9	Nickel Ferrite [2–7]	T	800	$NiMnFe_4O_6 + 2H_2O \rightarrow NiMnFe_4O_8 + 2H_2(g)$	1
		T	800	$NiMnFe_4O_8 \rightarrow NiMnFe_4O_6 + O_2(g)$	$^1/_2$
10	Aachen Univ Julich 1972 [2–5]	T	850	$2Cl_2(g) + 2H_2O(g) \rightarrow 4HCl(g) + O_2(g)$	$^1/_2$
		T	170	$2CrCl_2 + 2HCl \rightarrow 2CrCl_3 + H_2(g)$	1
		T	800	$2CrCl_3 \rightarrow 2CrCl_2 + Cl_2(g)$	1
11	Ispra Mark 1C [2–2]	T	100	$2CuBr_2 + Ca(OH)_2 \rightarrow 2CuO + 2CaBr_2 + H_2O$	1
		T	900	$4CuO(s) \rightarrow 2Cu_2O(s) + O_2(g)$	$^1/_2$
		T	730	$CaBr_2 + 2H_2O \rightarrow Ca(OH)_2 + 2HBr$	2
		T	100	$Cu_2O + 4HBr \rightarrow 2CuBr_2 + H_2(g) + H_2O$	1
12	LASL- U [2–5]	T	25	$3CO_2 + U_3O_8 + H_2O \rightarrow 3UO_2CO_3 + H_2(g)$	1
		T	250	$3UO_2CO_3 \rightarrow 3CO_2(g) + 3UO_3$	1
		T	700	$6UO_3(s) \rightarrow 2U_3O_8(s) + O_2(g)$	$^1/_2$

Table 2–4 (Cont.)

Cycle	Name	T/E*	T °C	Reaction	F†
13	Ispra Mark 8 [2–2]	T	700	$3MnCl_2 + 4H_2O \rightarrow Mn_3O_4 + 6HCl + H_2(g)$	1
		T	900	$3MnO_2 \rightarrow Mn_3O_4 + O_2(g)$	$^1/_2$
		T	100	$4HCl + Mn_3O_4 \rightarrow 2MnCl_2(a) + MnO_2 + 2H_2O$	$^3/_2$
14	Ispra Mark 6 [2–2]	T	850	$2Cl_2(g) + 2H_2O(g) \rightarrow 4HCl(g) + O_2(g)$	$^1/_2$
		T	170	$2CrCl_2 + 2HCl \rightarrow 2CrCl_3 + H_2(g)$	1
		T	700	$2CrCl_3 + 2FeCl_2 \rightarrow 2CrCl_2 + 2FeCl_3$	1
		T	420	$2FeCl_3 \rightarrow Cl_2(g) + 2FeCl_2$	1
15	Ispra Mark 4 [2–2]	T	850	$2Cl_2(g) + 2H_2O(g) \rightarrow 4HCl(g) + O_2(g)$	$^1/_2$
		T	100	$2FeCl_2 + 2HCl + S \rightarrow 2FeCl_3 + H_2S$	1
		T	420	$2FeCl_3 \rightarrow Cl_2(g) + 2FeCl_2$	1
		T	800	$H_2S \rightarrow S + H_2(g)$	1
16	Ispra Mark 3 [2–2]	T	850	$2Cl_2(g) + 2H_2O(g) \rightarrow 4HCl(g) + O_2(g)$	$^1/_2$
		T	170	$2VOCl_2 + 2HCl \rightarrow 2VOCl_3 + H_2(g)$	1
		T	200	$2VOCl_3 \rightarrow Cl_2(g) + 2VOCl_2$	1
17	Ispra Mark 2 (1972) [2–2]	T	100	$Na_2O.MnO_2 + H_2O \rightarrow 2NaOH(a) + MnO_2$	2
		T	487	$4MnO2(s) \rightarrow 2Mn_2O_3(s) + O_2(g)$	$^1/_2$
		T	800	$Mn_2O_3 + 4NaOH \rightarrow 2Na_2O.MnO_2 + H_2(g) + H_2O$	1
18	Ispra CO/Mn_3O_4 [2–8]	T	977	$6Mn_2O_3 \rightarrow 4Mn_3O_4 + O_2(g)$	$^1/_2$
		T	700	$C(s) + H_2O(g) \rightarrow CO(g) + H_2(g)$	1
		T	700	$CO(g) + 2Mn_3O_4 \rightarrow C + 3Mn_2O_3$	1
19	Ispra Mark 7B [2–2]	T	1000	$2Fe_2O_3 + 6Cl_2(g) \rightarrow 4FeCl_3 + 3O_2(g)$	$^3/_4$
		T	420	$2FeCl_3 \rightarrow Cl_2(g) + 2FeCl_2$	$^3/_2$
		T	650	$3FeCl_2 + 4H_2O \rightarrow Fe_3O_4 + 6HCl + H_2(g)$	1
		T	350	$4Fe_3O_4 + O_2(g) \rightarrow 6Fe_2O_3$	$^1/_4$
		T	400	$4HCl + O_2(g) \rightarrow 2Cl_2(g) + 2H_2O$	$^3/_2$
20	Vanadium Chloride [2–9]	T	850	$2Cl_2(g) + 2H_2O(g) \rightarrow 4HCl(g) + O_2(g)$	$^1/_2$
		T	25	$2HCl + 2VCl_2 \rightarrow 2VCl_3 + H_2(g)$	1
		T	700	$2VCl_3 \rightarrow VCl_4 + VCl_2$	2
		T	25	$2VCl_4 \rightarrow Cl_2(g) + 2VCl_3$	1
21	Mark 7A [2–2]	T	420	$2FeCl_3(l) \rightarrow Cl_2(g) + 2FeCl_2$	$^3/_2$
		T	650	$3FeCl_2 + 4H_2O(g) \rightarrow Fe_3O_4 + 6HCl(g) + H_2(g)$	1
		T	350	$4Fe_3O_4 + O_2(g) \rightarrow 6Fe_2O_3$	$^1/_4$
		T	1000	$6Cl_2(g) + 2Fe_2O_3 \rightarrow 4FeCl_3(g) + 3O_2(g)$	$^1/_4$
		T	120	$Fe_2O_3 + 6HCl(a) \rightarrow 2FeCl_3(a) + 3H_2O(l)$	1

Table 2–4 (Cont.)

Cycle	Name	T/E*	T °C	Reaction	F†
22	GA Cycle 23 [2–20]	T	800	$H_2S(g) \rightarrow S(g) + H_2(g)$	1
		T	850	$2H_2SO_4(g) \rightarrow 2SO_2(g) + 2H_2O(g) + O_2(g)$	$^1/_2$
		T	700	$3S + 2H_2O(g) \rightarrow 2H_2S(g) + SO_2(g)$	$^1/_2$
		T	25	$3SO_2(g) + 2H_2O(l) \rightarrow 2H_2SO_4(a) + S$	$^1/_2$
		T	25	$S(g) + O_2(g) \rightarrow SO_2(g)$	
23	US -Chlorine [2–5]	T	850	$2Cl_2(g) + 2H_2O(g) \rightarrow 4HCl(g) + O_2(g)$	$^1/_2$
		T	200	$2CuCl + 2HCl \rightarrow 2CuCl_2 + H_2(g)$	1
		T	500	$2CuCl_2 \rightarrow 2CuCl + Cl_2(g)$	1
24	Ispra Mark 9 [2–2]	T	420	$2FeCl_3 \rightarrow Cl_2(g) + 2FeCl_2$	$^3/_2$
		T	150	$3Cl_2(g) + 2Fe_3O_4 + 12HCl \rightarrow 6FeCl_3 + 6H_2O + O_2(g)$	$^1/_2$
		T	650	$3FeCl_2 + 4H_2O \rightarrow Fe_3O_4 + 6HCl + H_2(g)$	1
25	Ispra Mark 6C [2–2]	T	850	$2Cl_2(g) + 2H_2O(g) \rightarrow 4HCl(g) + O_2(g)$	$^1/_2$
		T	170	$2CrCl_2 + 2HCl \rightarrow 2CrCl_3 + H_2(g)$	1
		T	700	$2CrCl_3 + 2FeCl_2 \rightarrow 2CrCl_2 + 2FeCl_3$	1
		T	500	$2CuCl_2 \rightarrow 2CuCl + Cl_2(g)$	1
		T	300	$CuCl + FeCl_3 \rightarrow CuCl_2 + FeCl_2$	1

*T = thermochemical, E = electrochemical.

†Reactions are stored in database with minimum integer coefficients. Multiplier from reaction junction table converts the results to the basis of one mole of water decomposed.

After completing the rating, the rankings were discussed. Considerations mentioned by the various investigators for down-rating cycles include:

- A reaction of the cycle has a large positive Gibbs free energy, that cannot be performed electrochemically nor be shifted by pressure or concentration.
- The cycle requires the flow of solids.
- The cycle is excessively complex.
- The cycle includes an electrochemical step.

The degree to which each consideration affected the rating given by an investigator depended on his own analysis but there was a high degree of correlation in the rankings of each investigator with that of the group. The last consideration is not as obvious as the others and requires additional explanation.

Table 2–5
Second Stage Screening Scores

Cycle	Name	SNL	UK	GA	Score
1	Westinghouse [2–1]	1	0	0	1
2	Ispra Mark 13 [2–2]	0	0	0	0
3	UT-3 Univ. of Tokyo [2–3]	1	1	1	3
4	Sulfur-Iodine [2–4]	1	1	1	3
5	Julich Center EOS [2–5]	1	–1	–1	–1
6	Tokyo Inst. Tech. Ferrite [2–6]	–1	0	0	–1
7	Hallett Air Products 1965 [2–5]	1	–1	0	0
8	Gaz de France [2–5]	–1	–1	–1	–3
9	Nickel Ferrite [2–7]	–1	0	0	–1
10	Aachen Univ Julich 1972 [2–5]	0	–1	0	–1
11	Ispra Mark 1C [2–2]	–1	–1	–1	–3
12	LASL-U [2–5]	1	–1	–1	–1
13	Ispra Mark 8 [2–2]	0	–1	–1	–2
14	Ispra Mark 6 [2–2]	–1	–1	–1	–3
15	Ispra Mark 4 [2–2]	0	–1	–1	–2
16	Ispra Mark 3 [2–2]	0	–1	–1	–2
17	Ispra Mark 2 (1972) [2–2]	1	–1	–1	–1
18	Ispra CO/Mn_3O_4 [2–8]	–1	0	0	–1
19	Ispra Mark 7B [2–2]	–1	–1	–1	–3
20	Vanadium Chloride [2–9]	0	1	–1	0
21	Mark 7A [2–2]	–1	–1	–1	–3
22	GA Cycle 23 [2–20]	–1	–1	0	–2
23	US -Chlorine [2–5]	0	1	–1	0
24	Ispra Mark 9 [2–2]	0	–1	–1	–2
25	Ispra Mark 6C [2–2]	–1	–1	–1	–3

Hybrid cycles, those with an electrochemical step, have always attracted considerable interest in that they typically are simpler than pure thermochemical cycles. Never-the-less, they have one characteristic that tends to make them uneconomic at large scale. Energy efficient electrochemical processes require parallel electrodes, small gaps between electrodes and minimal mixing of the anodic and cathodic products – in short they require thin membranes between the anode and cathode. This basically limits efficient electrochemical processes to the small electrode areas that are consistent with thin membrane manufacture. This is not to say that there are not commercial electrochemical process but rather, that the commercial processes are efficient in an economic sense because they make valuable products and not that they are efficient in a thermodynamic sense.

Two cycles were rated far above the others in the second stage screening, the Adiabatic UT-3 and Sulfur-Iodine cycles.

2.3.1. Adiabatic UT-3 Cycle

The basic UT-3 cycle was first described at University of Tokyo [2–3] in the late 1970's and essentially all work on the cycle has been performed in Japan. Work has continued to this date with the latest publication last year. Over time the flowsheet has undergone several revisions the most recent, based on the adiabatic implementation of the cycle, was published in 1996. A simplified flow diagram of the Adiabatic UT-3 cycle matched to a nuclear reactor is shown in Fig. 2–2. The four chemical reactions take place in four adiabatic fixed packed bed chemical reactors that contain the solid reactants and products. The chemical reactors occur in pairs, one pair contains the calcium compounds and the other pair the iron compounds. The nuclear reactor transfers heat through a secondary heat exchanger into the gas stream that traverses through the four chemical reactors, three process heat exchangers, two membrane separators and the recycle compressor in sequence before the gases are recycled to the reactor secondary heat exchanger. The bulk of the stream is steam (H_2O) and although it may be either a react and or product in the various reactions, the large excess is required to provide the required entraples of reactor.

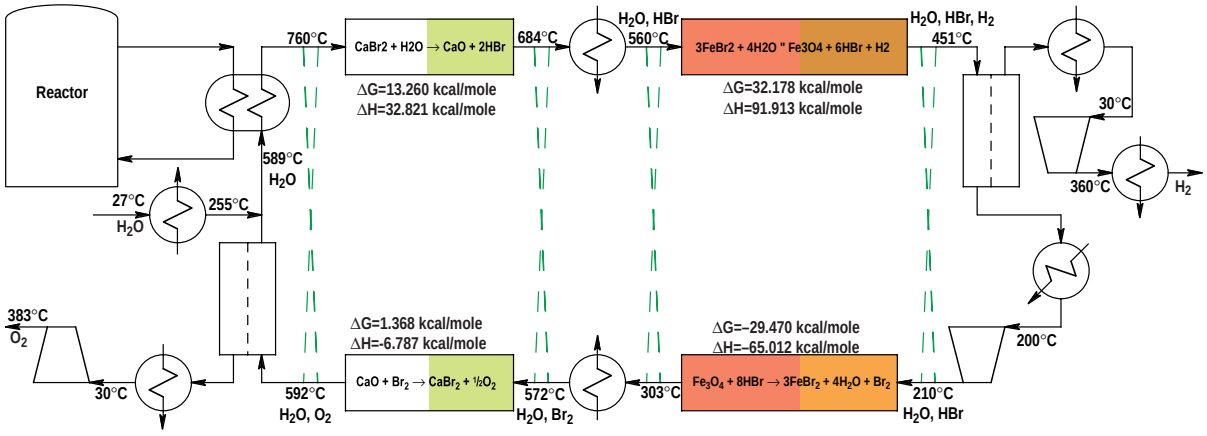

Fig. 2–2. Adiabatic UT-3 process flow diagram.

At each chemical reactor, the gaseous reactant passes through the bed of solid product until it reaches the reaction front where it is consumed, creating gaseous product and solid product. The gaseous product traverses through the unreacted solid and exits the chemical reactor. After some time, perhaps an hour, the reaction front has traveled from near the entrance of the reactor to near the exit. At this point, the flow paths are switched and the chemical reactors, in each pair, switch functions. The direction of flow through the reactor also switches so that the reaction front reverses direction and travels back toward the end that had previously been the entrance. The direction must be switched before the reaction front reaches the end of a reactor to prevent large temperature swings but it is desirable for the reaction front to approach the ends of the reactor to reduce the frequency of flow switching.

The gas stream is conditioned, either heated or cooled, before entering the chemical reactor. Since the gaseous reactant/product cannot carry sufficient heat to accomplish the reaction, a large quantity of inert material (steam) comprises the majority of the stream. The total stream pressure is 20 atmospheres and the minimum steam pressure is 18.5 atm. The inert flow provides the additional function of sweeping the products away from the reaction front and thus shifting the reaction equilibrium towards completion. This is necessary since the Gibbs free energy is positive for some of the reactions.

The operation of the semipermeable membranes is somewhat more involved than shown. The partial pressure of hydrogen and oxygen are 0.2 and 0.1 atm respectively. Each gas must be substantially removed from its stream so counter-current operation of the permeator is necessary. This is accomplished by flowing steam past the back side of the membrane. The steam is condensed and separated from the product gas before the product gas is compressed.

The efficiency of hydrogen generation, for a stand-alone plant, is predicted to be 36%–40%, depending upon the efficiency of the membrane separation processes. Higher overall efficiencies, 45%–49%, are predicted for a plant that co-generates both hydrogen and electricity. It is not evident from the published reports if these numbers are based on steady operation or if they take into account the additional inefficiencies associated with the transient operation which occurs when the flow paths are switched.

The chemistry of the cycle has been studied extensively. The basic thermodynamics are well documented. The overall cycle has been demonstrated first at the bench scale and finally in a pilot plant. The UT-3 cycle is the closest to commercial development of any cycle.

The major areas of ongoing research are in the stability of the solids and in the membrane separation processes. For the process to work, the solids must be chemically available to gas phase reactions yet physically stable while undergoing repeated cycling between the oxide and bromide forms. A considerable effort has gone into supporting the reactive solids in a form where they will not be transported by the gas flow. Membranes are being developed which are permeable to oxygen or hydrogen while not being permeable to hydrogen bromide or bromine. There still remains the problem of developing the membrane materials into a physical form that is suitable to large-scale economics.

The other questions that require analysis prior to full scale development have to do with the non-steady state operation of the cycle. The non-steady state operation will certainly affect hydrogen production efficiency. Of more concern is the effect of a non-steady state heat requirement on the reactor operation. This is not expected to be a serious problem as, for large-scale hydrogen production, the process will require several completely parallel process modules which can be operated such that, at any time, only a fraction of the chemical plant will be operating in a transient mode.

Overall, the process is in excellent shape for commercial exploitation. There is limited potential for future process improvements as the adiabatic implementation is already quite simple, as thermochemical processes go. There is little room for future efficiency improvements as the process is already operating at the physical limits of its constituents. The maximum $CaBr_2$ operating temperature is already slightly above the melting point. Any attempt to increase efficiency by increasing process temperature will result in migration of the $CaBr_2$.

2.3.2. Sulfur-Iodine Cycle

The Sulfur-Iodine cycle was first described in the mid 1970's. It was rejected by early workers due to difficulties encountered separating the hydrogen iodide and sulfuric acid produced in reaction 3. Attempts to use distillation were futile as sulfuric acid and hydrogen iodide react according to the reverse of reaction 3 when their mixture is heated. The key to successful implementation of the cycle was the recognition that using an excess of molten iodine would result in a two-phase solution, a light phase containing sulfuric acid and a heavy phase containing hydrogen iodide and iodine. Figure 2–3 shows a block flow diagram of the cycle based on this separation. The Sulfur-Iodine cycle has been studied by several investigators and while the process, as a whole is well defined, there is some uncertainty about the best way of accomplishing the hydrogen iodide decomposition step.

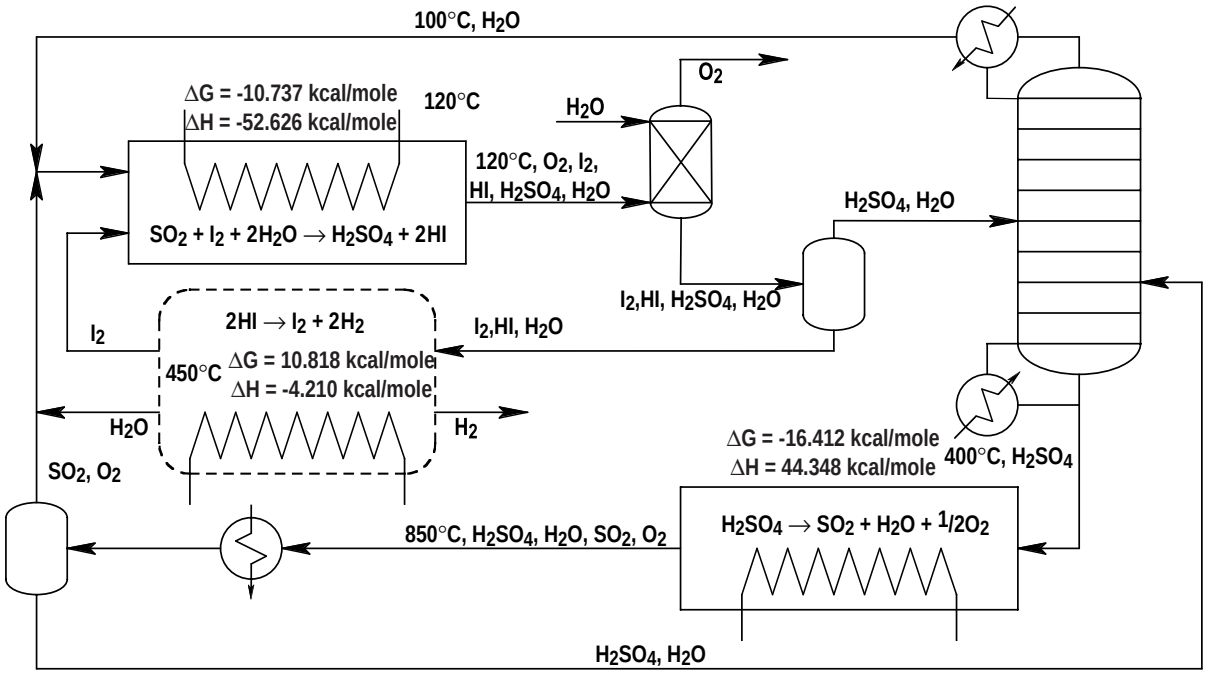

Fig. 2–3. Sulfur-iodine cycle process flow diagram.

All the early work on the cycle assumed it was necessary to separate the hydrogen iodide from the iodine and water of the heavy phase before performing reaction 4 to generate hydrogen. Bench scale experiments were made of the total process and the process was matched to a high-temperature nuclear reactor in 1978 and 1980. The early flowsheet, which was optimized for maximum efficiency, indicated that hydrogen could be produced at 47% efficiency. This is the highest efficiency reported for any water-splitting process, based on an integrated flowsheet. The later flowsheet employed as simplified flowsheet that had lower efficiency but also lower capital costs.

Subsequent to the cessation of development of the sulfur-iodine process in the U.S. in 1986, other workers have made several attempts to improve the efficiency of the cycle by modifying the hydrogen production section of the cycle. In particular, researchers at the University of Aachen demonstrated experimentally, that the hydrogen iodide need not be separated from iodine before the decomposition step. Based on their work, they predicted significant increases in efficiency and a 40% decrease in the cost of hydrogen compared with the standard flowsheet. The cost decreases not only because the efficiency increased, but also because the capital intensive heavy-phase separation was eliminated. These proposed improvements have never been incorporated into an integrated flowsheet of the sulfur-iodine hydrogen process with a nuclear reactor.

The Phase 1 conclusion was that the Sulfur-Iodine cycle should be matched to a nuclear reactor, incorporating the latest information and thinking. It is the cycle that is almost always used as the standard of comparison as to what can be done with a thermochemical cycle. It was the cycle chosen by Lawrence Livermore National Laboratory (LLNL) in their conceptual design of a plant to produce synthetic fuels from fusion energy. The Japanese consider the Sulfur-Iodine cycle to be a back-up for the UT-3 cycle and continue chemical investigations, although they have not published any flowsheets matching the cycle to a nuclear reactor. The cycle has never been matched to a nuclear reactor considering co-generation of electricity. The Japanese found that co-generation gave a 10% efficiency improvement (40% to 50%) for the Adiabatic UT-3 process.

3. PHASES 2 AND 3

The combined goal of Phases 2 and 3 was to determine the economic feasibility of producing thermochemical hydrogen using the heat from an advanced nuclear reactor. The sulfur-iodine (S-I) cycle was chosen during Phase 1 but the advanced nuclear reactor remained to be chosen.

The reactor selection task was carried out at Sandia National Laboratories (SNL). The reactor selection study, Appendix B, indicated that, although the heavy metal and molten salt-cooled reactor concepts could potentially be developed to the point that they could support hydrogen production, helium gas-cooled reactors had reached the point in development where nuclear hydrogen production is possible. This reactor selection screening study did not distinguish between the various types of helium-cooled high temperature reactors, (i.e., prismatic block or pebble bed).

The chemical process studies consisted of investigations of flowsheet configurations to determine a means of producing hydrogen at high efficiency and low cost. These studies began in Phase 2 and continued into Phase 3. A reactor configuration was selected and alternative integrated flowsheets were devised to investigate best use of the reactor thermal energy. Preliminary equipment sizing calculations were performed to form the basis of calculations of the capital and operating costs of the chemical plant.

A reactor model was developed which permitted the investigation of alternative reactor operating scenarios, including production of only hydrogen and co-generation of hydrogen and electricity. The model does not distinguish between pebble bed reactors and prismatic block reactors. Since pebble bed reactors are limited to sizes below the optimum size for thermochemical hydrogen production, the prismatic block reactor was chosen as the basis for the economic analysis.

3.1. FLOWSHEET DEVELOPMENT

The S-I cycle consists of three coupled chemical reactions as shown in Fig. 3–1. Sulfuric acid and hydrogen iodide are generated in the central low temperature reaction, the Bunsen reaction. Sulfuric acid is decomposed at high temperature and hydrogen iodide at lower temperatures. There are significant chemical separations associated with each chemical reaction. Water is the primary solvent in the system and iodine is also an important solvent in the Bunsen reaction.

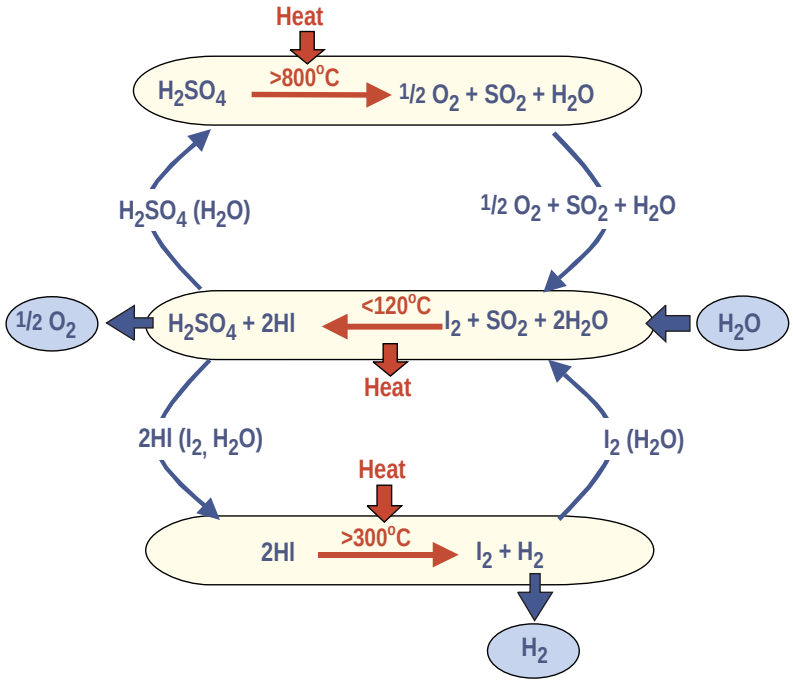

Fig. 3–1. Coupled chemical reactions of the S-I cycle.

The S-I cycle was studied extensively in the 1970s and 1980s. Two flowsheets were developed, the 1979 flowsheet [E–4], which matched the cycle to an advanced High Temperature Gas-cooled Reactor (HTGR) and a 1981 flowsheet [E–4] that was open ended, permitting the cycle to be matched to a number of thermal sources. Each flowsheet was separated, for descriptive purposes, into sections that correspond to the chemical reactions given in Fig. 3–1.

The 1981 flowsheet did not contain the sulfuric acid decomposition section as that section would need to be modified to match the heat source. The 1981 flowsheet was subsequently matched to a specific fusion heat source, the Tandem Mirror [3–1], and to a high temperature solar collector, but never to a nuclear reactor.

Both the 1979 and 1981 flowsheets are very similar from an overall standpoint but had different goals. The earlier flowsheet emphasized high efficiency but this was achieved at the expense of using some very non-standard process equipment such as a combination countercurrent gas-liquid contactor and heat exchanger. The latter flowsheet attempted to use more conventional equipment, though with a somewhat lower efficiency. Both flowsheets used phosphoric acid to extract the water from the HI_x ($HI/I_2/H_2O$) solution resulting from the Bunsen reaction. No hydrogen cost estimates were made using the 1979 flowsheet but the cost estimates for the 1981 flowsheet indicated that over 40% of the total capital cost of the process was associated with the phosphoric acid concentration step.

There have been a number of suggestions as to methods of modifying the process to reduce the capital cost. The methods proposed included the use of liquid hydrogen bromide, at elevated pressure, to extract the hydrogen iodide from the HI_x; and reactive distillation of the HI_x. At the time (1981), the vapor-liquid equilibrium (VLE) measurements required to evaluate the reactive distillation scheme had not been made. The analysis of the hydrogen bromide indicated some promise but the scheme was never evaluated in depth.

Subsequently, measurements of VLE for the system $HI/I_2/H_2O$ were made in Germany and German researchers produced a partial flowsheet [E–5] that indicated that reactive distillation could work.

During Phase 2, Task 2.1, we evaluated the possible flowsheet variations and decided to pursue the reactive distillation scenario as the primary effort but maintain the H_3PO_4 variation as a backup. The HBr variation also remains a potential alternative but thermodynamic data on the system $HI/HBr/I_2/H_2O$ is sparse and this project had insufficient resources to perform the laboratory investigations necessary to make an evaluation of the system.

The overall process naturally divides itself into process sections in which there is significant recycle and interconnection and which are connected to the other sections by a minimum number of streams. For the S-I cycle, these natural sections roughly correspond to the chemical reactions. The flowsheet associated with each chemical reaction and its attendant separation processes is numbered. Sections 1, 2 and 3 are used to designate the portions of the flowsheet associated with the Bunsen reaction (where the acids are formed,) the sulfuric acid decomposition reaction, and the hydrogen iodide decomposition reaction. The hydrogen iodide separation section of the phosphoric acid flowsheet is sufficiently complicated that the separation processes are called Section 3 and the decomposition reaction and hydrogen purification processes are called Section 4.

3.2. CHEMICAL FLOWSHEET SIMULATOR

The early flowsheets for the S-I cycle were all developed based on hand calculations. Attempts were made to use chemical flowsheet simulation programs but the programs available at that time were unable to handle extremely non-ideal systems such as those found in the S-I thermochemical water-splitting cycle. Significant advances have been made in understanding the thermodynamics of aqueous ionic systems since the time of the earlier flowsheeting efforts. It was our intent to develop thermodynamic models compatible with a modern chemical flowsheet simulator and perform extensive process optimization studies to best match the reactor to the thermochemical process.

The chemical process simulator with the best tools for handling non-ideal chemical systems is Aspen Plus®, Aspen Technology, Inc. (AspenTech.). Aspen Plus® incorporates

the capability of modeling electrolytes via several different modeling techniques including an electrolytic version of the non-random two liquid (NRTL) technique. An electrolytic NRTL (ELECNRTL) model can handle everything from concentrated electrolytes through dilute electrolytes to non-polar species, such as iodine, so it should be able to handle the chemistry of the S-I cycle. In fact, Aspen Plus® included an ELECNRTL model for sulfuric acid, good to 200°C, right out of the box. In addition, Aspen Plus® includes the capability of regressing model parameter simultaneously to several different types of experimental data in order to generate a thermodynamic model for a specific chemical system. Aspen Plus® was chosen as the process simulator for this work.

3.3. DEVELOPMENT OF THERMODYNAMIC MODELS

An NRTL model describes a chemical system in terms of the thermodynamic parameters for the pure components along with pair-wise parameters, which describe the interactions between each pair of pure components. The electrolytic variation (ELECNRTL) adds a description of the ionic associations and dissociations along with pure component and pair-wise parameters for the ionic species with each other and with the nonionic species present. Our plan of attack was to use the existing ELECNRTL model for sulfuric acid, describing the system H_2SO_4/H_2O, and use this model for developing the flowsheet for Section 2. Simultaneously, we would develop a new ELECNRTL model for the system $HI/I_2/H_2O$, which used the same pure component properties for water as used in the sulfuric acid model, and use this model to develop the flowsheet for Section 3. Finally, we would develop a model for the system $H_2SO_4/HI/I_2/H_2O$, using the pure component and pair-wise components of the earlier models along with pair-wise parameters that were undefined in the simpler models, for the Section 1 flowsheeting effort. The first two models would need to be valid over wide ranges of temperature and pressure, as operating conditions for Sections 2 and 3 may need to be varied widely in order to optimize the overall flowsheet. The final model would only need to be valid over the limited range of temperatures and pressures for which sulfuric acid and hydrogen iodide form separate condensed phases.

We soon found that we had been optimistic in our assumption that the existing ELECNRTL sulfuric acid model would be adequate for our needs. Although sulfuric acid is one of the most common industrial chemicals, it is almost never concentrated by thermal means. (Concentrated sulfuric acid is produced commercially at low temperatures by adsorbing SO_3 in dilute sulfuric acid.) Previous work had shown that optimal configurations for Section 2 involved performing some of the concentration steps at high pressure (and temperature) so that the condensing temperature of the distillate was high enough to reuse elsewhere in the process. The maximum temperature of the existing liquid sulfuric acid model was 200°C and we would require a model that was valid at temperatures on the order of 300°C.

Although we had access to sulfuric acid VLE data at the temperatures and pressures of interest, we were unsuccessful in our attempts to regress the data to generate a valid ELECNRTL model for sulfuric acid, using the regression capabilities found in Aspen Plus®. The number of parameters to be regressed was very large and, unless initial estimates of each parameter were very close to the "correct" values, the regression process would not converge to reasonable solution. Experts at Aspen Technologies have developed techniques that allow them to regress difficult systems. These are not "cookbook" techniques, rather interactive techniques which involve fixing most of the parameters and varying a few at a time using limited data sets until a "close parameter set" is obtained and a final global regression is performed. We elected to subcontract the regression task to Aspen Technologies in order to save cost. Their report is presented in Appendix C.

As we were unsuccessful in regressing the "simple" system H_2SO_4/H_2O, we did not even attempt to regress the more complicated systems $HI/I_2/H_2O$ and $H_2SO_4/HI/I_2/H_2O$. For the later systems, we did participate actively in the regression process by providing data and insights into the chemistry of the system.

Our ELECNRTL sulfuric acid model is a very good representation of the system and was used in our Section 2 flowsheet.

The $HI/I_2/H_2O$ regression was not as successful. The final model accurately describes the "iodine lean" liquid-liquid equilibrium (LLE) region, but its description of the "hydrogen iodide lean" LLE region is suspect. There are no data for this region, except for the hydrogen iodide free endpoints, but the shape of this LLE boundary is irregular. More telling is the fact that Aspen Plus® was unable to converge multistage VLE processes that are the basis for the reactive distillation flowsheet for Section 3.

We were unable to tell, even with the aid of experts from Aspen Technologies, whether the model was too complicated for Aspen Plus® or if there were physically unrealizable conditions predicted by the model. That the model might predict physically unrealizable conditions is not surprising as no vapor composition data were used in the regression that generated the model. In fact, the only VLE data available are total pressure data. These data are further confounded by the fact that the pressure measurement includes the equilibrium decomposition of hydrogen iodide into hydrogen and iodine. The model is able to converge for a single-stage VLE process, therefore, it is useful for predicting physical properties in a given state but not the rate of change of properties with change in state. Likewise, the overall model for $H_2SO_4/HI/I_2/H_2O$ could be used to predict physical properties, but was unable to predict chemical equilibrium due to the scarcity of thermal data for the system. These two models were used extensively in the equipment sizing calculations, which were the basis of the economic analysis, but were not used in generating the final flowsheets.

3.3.1. Reactive Distillation Flowsheet

A flowsheet for the reactive distillation scheme was developed based on the work of Roth and Knoche [E–5]. The results are presented in Figs. 3–2, 3–3 and 3–4 and in Tables 3–1 through 3–6. The streams are labeled in the figures, the temperature, pressure, and molar flow rate for each stream are given in Tables 3–1 through 3–3 and the mechanical and thermal duties are given in Tables 3–4 through 3–6. The flow rates presented in the tables are normalized to the production of one mole of hydrogen in the overall plant. On this basis, referring back to the reactions presented in Fig. 3–1, one mole of sulfuric acid and two moles of hydrogen iodide are produced in Section 1. The mole of sulfuric acid is decomposed in Section 2 producing half a mole of oxygen and the two moles of hydrogen iodide are decomposed in Section 3 producing one mole of hydrogen. Figure 3–1 indicates most of the major recycled components but does not indicate the recycle of hydrogen iodide between Sections 1 and 3 that is characteristic of the reactive distillation scheme but not of the phosphoric acid dehydration scheme.

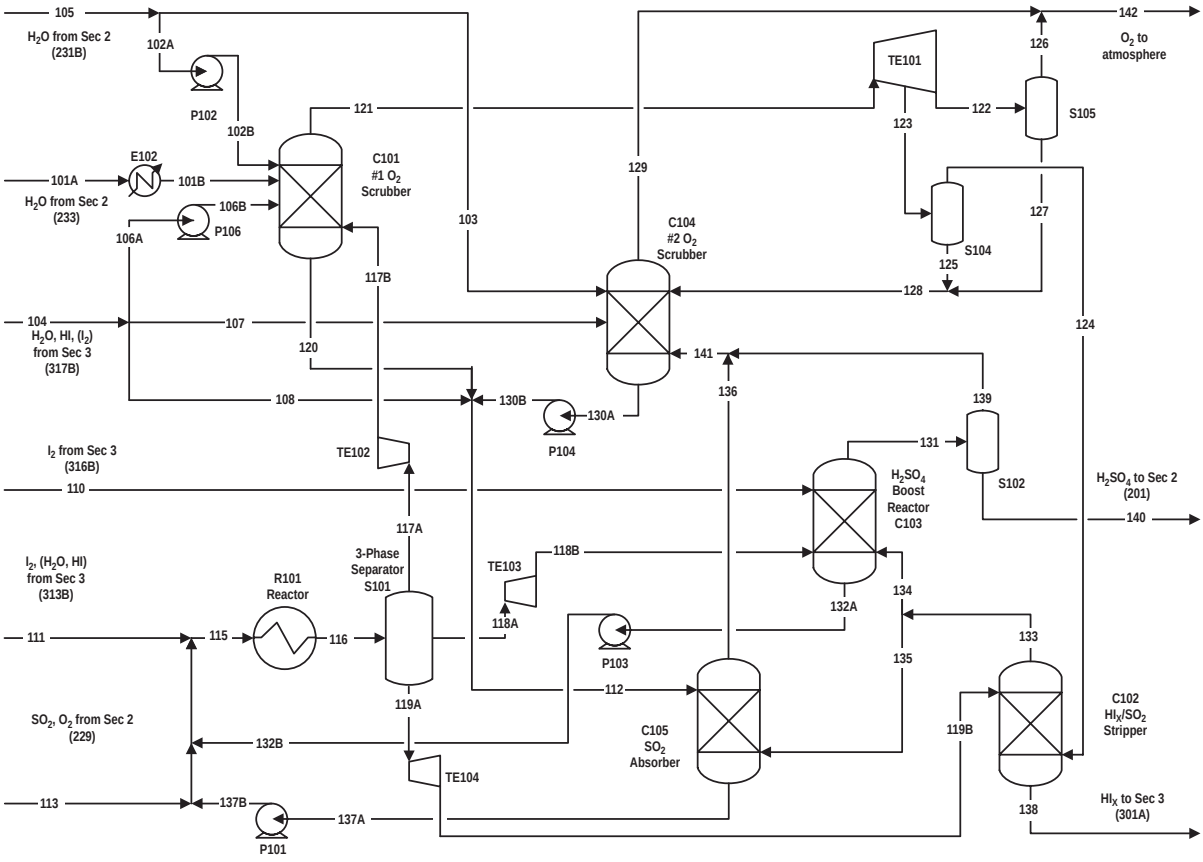

Fig. 3–2. Section 1 flowsheet.

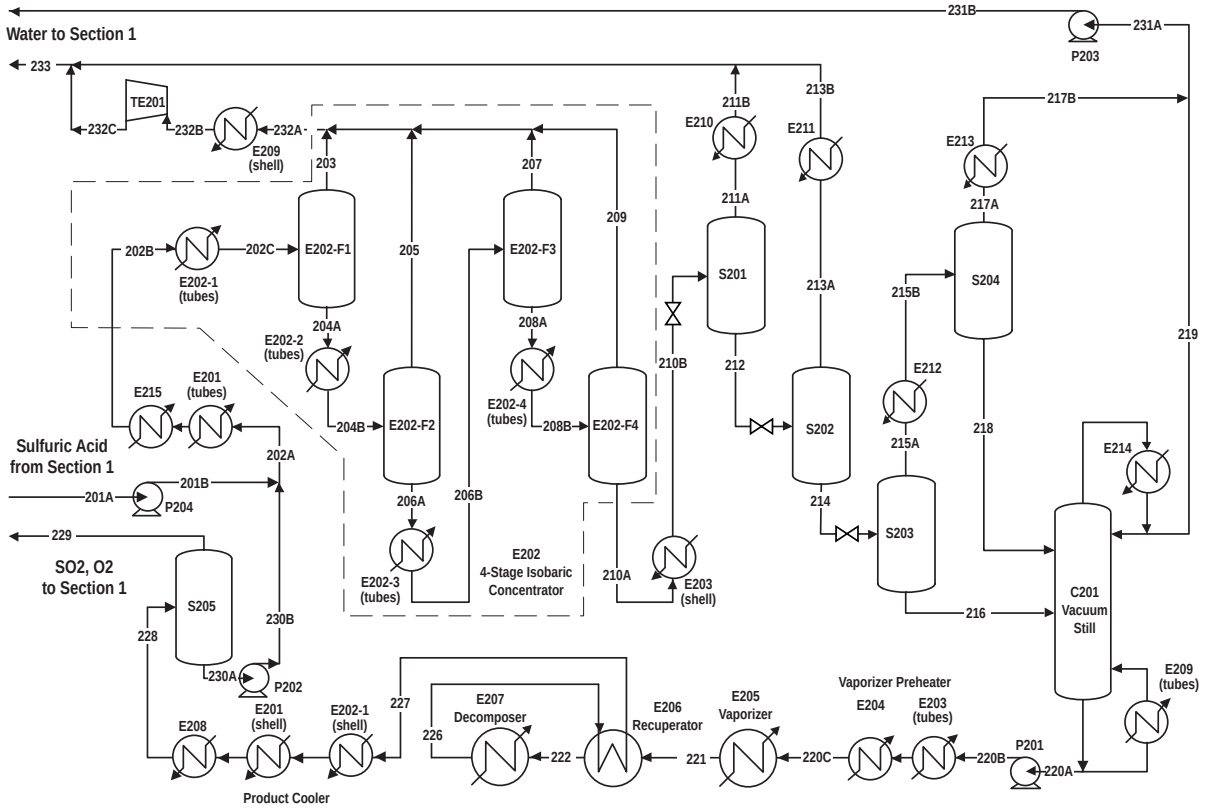

Fig. 3–3. Section 2 flowsheet.

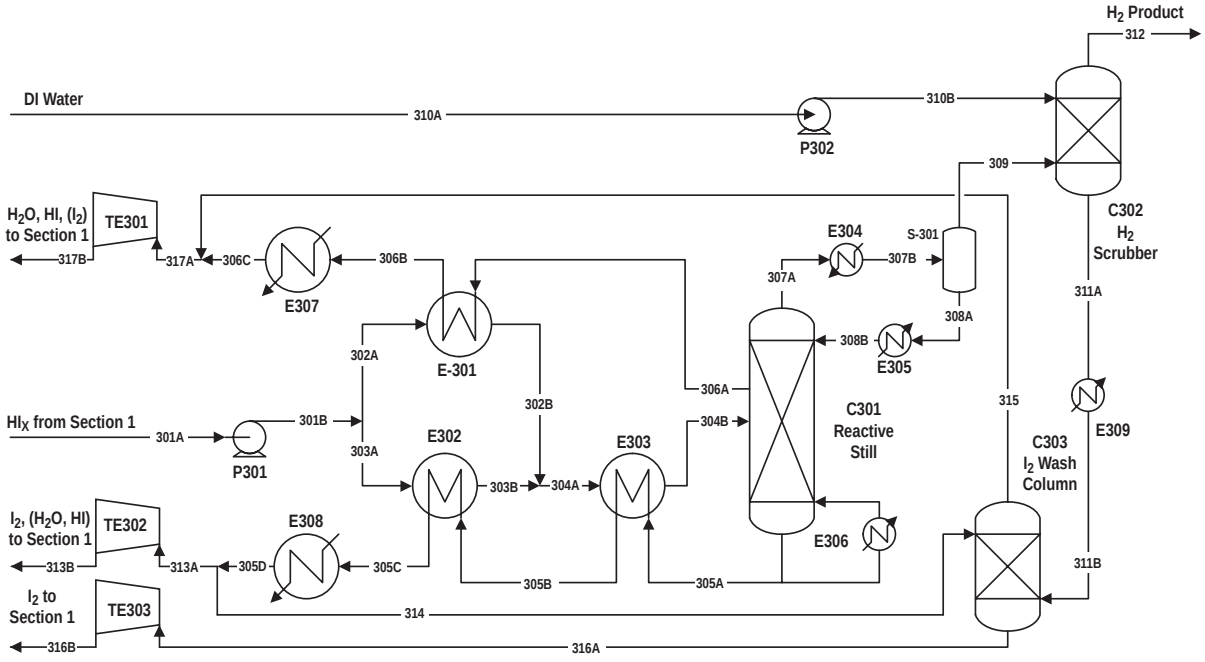

Fig. 3–4. Section 3 flowsheet.

Table 3–1
Material Balance Section 1 — Main Solution Reaction

Stream	H_2SO_4	HI	I_2	H_2O	SO_2	O_2	Total	Phase	P Bar	T K
101A	0.0222	0.0000	0.0000	3.4582	0.0078	0.0000	3.4882	L	4.2	393.15
101B	0.0222	0.0000	0.0000	3.4582	0.0078	0.0000	3.4882	L	4.2	359.6
102A	0.0002	0.0000	0.0000	0.3186	0.0000	0.0000	0.3188	L	1.01	311.15
102B	0.0002	0.0000	0.0000	0.3186	0.0000	0.0000	0.3188	L	4.4	311.15
103	0.0010	0.0000	0.0000	1.2847	0.0000	0.0000	1.2857	L	1.01	311.15
104	0.0000	9.5997	5.6840	62.4940	0.0000	0.0000	77.7777	L	4.2	368.51
105	0.0012	0.0000	0.0000	1.6033	0.0000	0.0000	1.6045	L	1.01	311.15
106	0.0000	0.2880	0.1705	1.8742	0.0000	0.0000	2.3327	L	1.85	311.15
107	0.0000	0.0806	0.0477	0.5248	0.0000	0.0000	0.6531	L	1.01	368.51
108	0.0000	9.2311	5.4658	60.0950	0.0000	0.0000	74.7919	L	4.2	368.51
110	0.0000	0.0011	0.8810	0.0170	0.0000	0.0000	0.8991	L	1.85	393
111	0.0000	0.8582	42.4423	4.2056	0.0000	0.0000	47.5061	L	1.85	393
112	0.2173	9.9875	5.5163	67.2589	0.0000	0.0000	82.9800	L	1.85	
113	0.0000	0.0000	0.0000	0.0328	0.9961	0.5000	1.5289	V	7	393
115	0.2173	10.9846	48.7791	72.7279	2.2660	0.5000	135.4749	V+L	7	
116	0.9545	12.4590	48.0419	71.2535	1.5288	0.5000	134.7377	V+L	7	393
117A	0.0000	0.0000	0.0075	0.0338	0.1424	0.5000	0.6837	V	7	393
117B	0.0000	0.0000	0.0075	0.0338	0.1424	0.5000	0.6837	V	4.2	354.2
118A	0.9545	0.0000	0.0000	5.1520	0.0154	0.0000	6.1219	L	7	393
118B	0.9545	0.0000	0.0000	5.1520	0.0154	0.0000	6.1219	L	1.85	393
119A	0.0000	12.4590	48.0344	66.0677	1.3710	0.0000	127.9321	L	7	393
119B	0.0000	12.4590	48.0344	66.0677	1.3710	0.0000	127.9321	L	1.85	393
120	0.1726	0.5884	0.0278	5.3694	0.0000	0.0000	6.1582	L	4.2	384.4
121	0.0000	0.0000	0.0000	0.0150	0.0000	0.5000	0.5150	V	4.2	384.4
122	0.0000	0.0000	0.0000	0.0095	0.0000	0.3175	0.3270	L+V	1.01	-
123	0.0000	0.0000	0.0000	0.0055	0.0000	0.1825	0.1880	L+V	1.85	289
124	0.0000	0.0000	0.0000	0.0027	0.0000	0.1825	0.1852	V	1.85	289
125	0.0000	0.0000	0.0000	0.0028	0.0000	0.0000	0.0028	L	1.85	289
126	0.0000	0.0000	0.0000	0.0051	0.0000	0.3175	0.3226	V	1.01	-
127	0.0000	0.0000	0.0000	0.0044	0.0000	0.0000	0.0044	L	1.01	-
128	0.0000	0.0000	0.0000	0.0072	0.0000	0.0000	0.0072	L	1.01	-
129	0.0000	0.0000	0.0000	0.0142	0.0000	0.1825	0.1967	V	1.01	313
130A	0.0447	0.1680	0.0227	1.7945	0.0000	0.0000	2.0299	L	1.01	393
130B	0.0447	0.1680	0.0227	1.7945	0.0000	0.0000	2.0299	L	1.85	393

Table 3–1 (Cont.)

Stream	H_2SO_4	HI	I_2	H_2O	SO_2	O_2	Total	Phase	P Bar	T K
131	1.0234	0.0000	0.0184	4.1377	0.0475	0.0155	5.2425	L	1.85	384.5
132A	0.0000	0.1389	0.7960	0.9252	0.0155	0.0000	1.8756	L	1.85	384.5
132B	0.0000	0.1389	0.7960	0.9252	0.0155	0.0000	1.8756	L	7	384.5
133	0.0000	0.0000	0.0271	0.3731	1.3710	0.1825	1.9537	V	1.85	393
134	0.0000	0.0000	0.0023	0.0317	0.1165	0.0155	0.1660	V	1.85	393
135	0.0000	0.0000	0.0248	0.3414	1.2545	0.1670	1.7877	V	1.85	393
136	0.0000	0.0000	0.0003	0.0360	0.0001	0.1670	0.2034	V	1.85	369.6
137A	0.2173	9.9875	5.5408	67.5643	1.2544	0.0000	84.5643	L	1.85	369.6
137B	0.2173	9.9875	5.5408	67.5643	1.2544	0.0000	84.5643	L	7	369.6
138	0.0000	12.4590	48.0073	65.6973	0.0000	0.0000	126.1636	L	1.85	393
139	0.0000	0.0000	0.0184	0.0434	0.0436	0.0155	0.1209	V	1.85	384.5
140	1.0234	0.0000	0.0000	4.0943	0.0039	0.0000	5.1216	L	1.85	384.5
141	0.0000	0.0000	0.0187	0.0794	0.0437	0.1825	0.3243	V	1.85	375.15
142	0.0000	0.0000	0.0000	0.0193	0.0000	0.5000	0.5193	V	1.01	—

Table 3–2
Material Balance for Section 2, Sulfuric Acid Decomposition

Stream	H_2O	H_2SO_4	SO_3	O_2	SO_2	Total	Phase	Press. Bar	Temp K
201A	4.0943	1.0234	0	0	0.0039	5.1216	L	1.85	393.15
201B	4.0943	1.0234	0	0	0.0039	5.1216	L	35.46	393.15
202A	5.2361	1.6298	0	0	0.0078	6.8737	L	35.46	393.98
202B	5.2361	1.6298	0	0	0.0078	6.8737	L + V	35.46	572.15
202C	5.2361	1.6298	0	0	0.0078	6.8737	L + V	35.46	603.15
203	1.0007	0.0018	0	0	0.0052	1.0077	V	35.46	603.15
204A	4.2354	1.628	0	0	0.0026	5.866	L	35.46	603.15
204B	4.2354	1.628	0	0	0.0026	5.866	L + V	35.46	619.15
205	0.8661	0.0038	0	0	0.0019	0.8718	V	35.46	619.15
206A	3.3693	1.6242	0	0	0.0007	4.9942	V	35.46	619.15
206B	3.3693	1.6242	0	0	0.0007	4.9942	L + V	35.46	631.15
207	0.5037	0.0039	0	0	0.0004	0.508	V	35.46	631.15
208A	2.8656	1.6203	0	0	0.0003	4.4862	L	35.46	631.15
208B	2.8656	1.6203	0	0	0.0003	4.4862	L + V	35.46	644.15
209	0.433	0.0056	0	0	0.0002	0.4388	V	35.46	644.15
210A	2.4326	1.6147	0	0	0.0001	4.0474	L	35.46	644.15
210B	2.4326	1.6147	0	0	0.0001	4.0474	L	35.46	581.15

Table 3–2 (Cont.)

Stream	H_2O	H_2SO_4	SO_3	O_2	SO_2	Total	Phase	Press. Bar	Temp K
211A	0.273	0.002	0	0	0.0001	0.2751	V	8.11	562.85
211B	0.273	0.002	0	0	0.0001	0.2751	L	8.11	393.15
212	2.1596	1.6127	0	0	0	3.7723	L	8.11	562.85
213A	0.3817	0.0051	0	0	0	0.3868	V	2.03	517.05
213B	0.3817	0.0051	0	0	0	0.3868	L	2.03	393.15
214	1.7779	1.6076	0	0	0	3.3855	L	2.03	517.05
215A	0.5471	0.0134	0	0	0	0.5605	V	0.07	432.85
215B	0.5471	0.0134	0	0	0	0.5605	V + L	0.07	408.15
216	1.2308	1.5942	0	0	0	2.825	L	0.07	432.85
217A	0.5335	0.0012	0	0	0	0.5347	V	0.07	408.15
217B	0.5335	0.0012	0	0	0	0.5347	L	0.07	311.15
218	0.0136	0.0122	0	0	0	0.0258	L	0.07	408.15
219	1.0698	0	0	0	0	1.0698	L	0.07	311.15
220A	0.1746	1.6064	0	0	0	1.781	L	0.07	485.25
220B	0.1746	1.6064	0	0	0	1.781	L	7.09	486.05
220C	0.1746	1.6064	0	0	0	1.781	L	7.09	684.15
221	0.6174	1.1636	0.4428	0	0	2.2238	L + V	7.09	684.15
222	1.4899	0.2911	1.3153	0	0	3.0963	V	7.09	796.85
223	1.7	0.081	1.261	0.1322	0.2644	3.4386	V	7.09	875.05
224	1.757	0.024	1.0776	0.2524	0.5048	3.6158	V	7.09	955.05
225	1.7725	0.0085	0.8405	0.3787	0.7574	3.7576	V	7.09	1027.05
226	1.7777	0.0033	0.6031	0.5	1	3.8841	V	7.09	1100.15
227	1.4456	0.3354	0.271	0.5	1	3.552	V	7.09	704.15
228	1.1746	0.6064	0	0.5	1	3.281	L + V	7.09	393.15
229	0.0328	0	0	0.5	0.9961	1.5289	V	7.09	393.15
230A	1.1418	0.6064	0	0	0.0039	1.7521	L	7.09	393.15
230B	1.1418	0.6064	0	0	0.0039	1.7521	L	35.46	396.05
231A	1.6033	0.0012	0	0	0	1.6045	L	0.07	311.15
231B	1.6033	0.0012	0	0	0	1.6045	L	1.02	311.25
232A	2.8035	0.0151	0	0	0.0077	2.8263	V	35.46	621.35
232B	2.788	0	0	0	0.0038	2.7918	L	35.46	393.15
232C	2.788	0	0	0	0.0038	2.7918	L	5.27	393.15
233	3.4582	0.0222	0	0	0.0078	3.4882	L	5.27	393.15

Table 3–3
Material Balance Section III HI Decomposition

Stream	HI	I_2	H_2O	H_2	Total	Phase	Press. Bar	Temp K
301A	12.4590	48.0073	65.6973	0.0000	126.1636	L	1.85	393.15
301B	12.4590	48.0073	65.6973	0.0000	126.1636	L	22	393.15
302A	7.7869	30.0046	41.0608	0.0000	78.8523	L	22	393.15
302B	7.7869	30.0046	41.0608	0.0000	78.8523	L	22	511.04
303A	4.6721	18.0027	24.6365	0.0000	47.3113	L	22	393.15
303B	4.6721	18.0027	24.6365	0.0000	47.3113	L	22	511.04
304A	12.4590	48.0073	65.6973	0.0000	126.1636	L	22	511.04
304B	12.4590	48.0073	65.6973	0.0000	126.1636	L	22	535.15
305A	0.8763	43.3367	4.2941	0.0000	48.5071	L	22	583.15
305B	0.8763	43.3367	4.2941	0.0000	48.5071	L	22	521.44
305C	0.8763	43.3367	4.2941	0.0000	48.5071	L	22	401.05
305D	0.8763	43.3367	4.2941	0.0000	48.5071	L	22	393.15
306A	9.5787	5.6706	61.3805	0.0000	76.6298	L	22	524.15
306B	9.5787	5.6706	61.3805	0.0000	76.6298	L	22	403.15
306C	9.5787	5.6706	61.3805	0.0000	76.6298	L	22	368.15
307A	0.5333	0.0000	1.8000	1.0000	3.3333	V	22	494.15
307B	0.5333	0.0000	1.8000	1.0000	3.3333	V+L	22	298.15
308A	0.5293	0.0000	1.7773	0.0000	2.3066	L	22	298.15
308B	0.5293	0.0000	1.7773	0.0000	2.3066	L	22	494.15
309	0.0040	0.0000	0.0227	1.0000	1.0267	V	22	298.15
310A	0.0000	0.0000	1.0207	0.0000	1.0207	L	1.013	298.15
310B	0.0000	0.0000	1.0207	0.0000	1.0207	L	22	298.15
311A	0.0040	0.0000	1.0420	0.0000	1.0460	L	22	298.15
311B	0.0040	0.0000	1.0420	0.0000	1.0460	L	22	393.15
312	0.0000	0.0000	0.0014	1.0000	1.0014	V	22	298.15
313A	0.8582	42.4423	4.2056	0.0000	47.5061	L	22	393.15
313B	0.8582	42.4423	4.2056	0.0000	47.5061	L	7	393.15
314	0.0181	0.8944	0.0885	0.0000	1.0010	L	22	393.15
315	0.0210	0.0134	1.1135	0.0000	1.1479	L	22	393.15
316A	0.0011	0.8810	0.0170	0.0000	0.8991	L	22	393.15
316B	0.0011	0.8810	0.0170	0.0000	0.8991	L	7	393.15
317A	9.5997	5.6840	62.4940	0.0000	77.7777	L	22	368.51
317B	9.5997	5.6840	62.4940	0.0000	77.7777	L	4.2	368.51

Table 3–4
Power Devices

Power Device No.	Energy Load kJ	Inlet Stream No.	Inlet Pressure Bar	Outlet Stream No.	Outlet Pressure Bar
P101	1.3529	108A	1.850	108B	7.000
P102	0.1562	119A	4.200	119B	7.000
P103	0.0940	134A	1.850	134B	7.000
P104	0.0462	119C	1.000	119D	7.000
P201	0.2333	213	0.067	214	7.090
P202	0.4886	226	1.850	227	35.000
P203	0.0126	211B	7.090	211C	35.460
P204	0.0031	212BB	0.067	212BBB	1.010
P205	0.0450	213A	0.067	213B	7.090
P206	1.2343	137	1.850	200	35.000
P301	13.1102	301	1.850	302	22.000

Table 3–5
Power Recovery Devices

Power Device No.	Energy Load kJ	Inlet Stream No.	Inlet Pressure Bar	Outlet Stream No.	Outlet Pressure Bar
TE101	–1.0631	128A	4.200	128B	1.000
TE102	–0.0240	—	22.000	—	1.850
TE103A	–0.4793	115A	7.000	115B	1.850
TE103B	–0.6357	118A	7.000	118B	1.850
TE103C	–2.2576	117A	7.000	117B	1.850
TE201	–0.1079	201C	35.460	201D	7.090
TE301	–2.4679	319A	22.000	319B	1.850
TE302	–4.2495	320A	22.000	320B	7.000
TE303	–0.1414	316A	22.000	316B	7.000

Table 3–6
Heat Transfer Devices

Heat Exchange No.	Heat Load kJ	Hot Side In		Hot Side Out		Cold Side In		Cold Side Out	
		Stream No.	Temp deg K	Stream No.	Temp deg K	Stream No.	Temp deg K	Stream No.	Temp deg K
R101	109.600	115	~384.7	116	393.15	*	298.15	*	318.15
E102	8.856	101A	393.15	101B	359.6	*	298.15	*	318.15
E201	113.913	—	622.55	—	413	202A	393.89	—	548.76
E202-1	58.775	227	704.15	—	622.5	202B	572.15	202C	603.15
E202-2	46.387	—	699.15	—	635.15	204A	603.15	204B	619.15
E202-3	29.009	—	738.15	—	699.15	206A	619.15	206B	631.15
E202-4	27.782	—	778.15	—	738.15	208A	631.15	208B	644.15
E203	44.117	210A	644.15	210B	581.15	220B	486.05	—	634.15
E204	14.805	—	800.15	—	778.15	—	634.15	220C	684.15
E205	134.957	—	975.15	—	800.15	220C	684.15	221	684.15
E206	105.019	226	1100.15	227	704.15	221	684.15	222	796.85
E207	178.459	—	1123.15	—	975.15	222	796.85	226	1100.15
E208	6.231	—	413.15	228	393.15	*	298.15	*	318.15
E209	28.928	232A	621.35	232B	505.25	**	485.25	**	485.25
E210	14.838	211A	562.85	211B	393.15	*	298.15	*	318.15
E211	19.581	213A	517.05	213B	393.15	*	298.15	*	318.15
E212	6.231	215A	432.85	215B	408.15	*	298.15	*	318.15
E213	25.73	217A	408.15	217B	311.15	*	298.15	*	318.15
E214	26.500	**	311.18	**	311.18	*	293.15	*	303.15
E215	20.854	—	635	—	613	—	548.76	202B	572.15
E301	608.500	306A	524.15	306B	403.15	302A	393.15	302B	511.043
E302	405.200	305B	521.44	305C	401.05	303A	393.15	303B	511.043
E303	207.700	305A	583.15	305B	521.44	304A	511.043	304B	535.15
E304	78.000	307A	494.15	307B	298.15	*	293.15	*	318.15
E305	8.800	—	593.88	—	588.46	308A	298.15	308B	494.15
E306	237.000	—	740	—	593.88	**	583.15	**	583.15
E307	39.600	306B	403.15	306C	368.15	*	298.15	*	318.15
E308	26.600	305C	401.05	305D	393.15	*	298.15	*	318.15

*Cooling water stream.
**Stream is internal to equipment.

3.3.2. Sulfuric Acid and Hydriodic Acid Generation (Section 1)

Section 1 is central to the overall process but was the last section flowsheeted. The flowsheet for Section 1 is presented in Fig. 3–2 and Table 3–1. The composition of streams exiting Section 1 can be predicted from thermodynamic arguments but the properties of streams recycled back to Section 1 can only be determined after completing detailed flowsheeting of Sections 2 and 3. In particular, the Roth and Knoche [E–5] reactive distillation flowsheet results in a major recycle of moderately concentrated hydriodic acid, not seen in previous flowsheets. Since the reactive distillation only decomposes one-sixth of the hydrogen iodide fed to it, the flow rate of HI_x must be six times that of previous flowsheets for the same sulfuric acid flow rate. Otherwise, the flowsheet is similar to the flowsheet of the MARS [3–1] report.

The ELECNRTL thermodynamic model was insufficient to perform a strictly thermodynamic model so the Section 1 flowsheet was adapted from previous flowsheets. This restricted our ability to fully optimize the flowsheet. We based our flowsheet on the 1979 and 1981 flowsheets [E–4] but modified the flow rates to match the current versions of Sections 2 and 3. In particular, temperatures and liquid compositions were kept the same as the previous flowsheets to maintain constant activities of each species in the liquid phases and the total pressure was modified as necessary to maintain the same SO_2 partial pressure as the base flowsheet as required by Eq. (1).

$$K_{eq} = \frac{a_{H_2SO_4} a_{HI}^2}{P_{SO_2} a_{I_2} a_{H_2O}^2} \quad . \tag{1}$$

The majority of the Bunsen reaction: $SO_2 + I_2 + 2H_2O \rightarrow H_2SO_4 + 2HI$ takes place in the heat exchange reactor (R101) at 7 bar. This reaction also takes place in the primary oxygen scrubber (C101), the secondary oxygen scrubber (C104), and the H_2SO_4 boost reactor (C103). The pressure in R101 was raised from 4 bar to 7 bar for this flowsheet but the pressures of C101, C104 and C103 remain at 4 bar, 1 bar and 1.85 bar, as in the 1981 flowsheet.

The output from the heat exchange reactor consists of three phases, which are separated in S101 and processed separately. The gas phase contains residual SO_2 in O_2. The SO_2 is removed by chemical reaction in C101: most of the O_2 is vented but a portion is recycled and used to strip the SO_2 remaining in the dense HI_x liquid (119A). The SO_2, stripped from the HI_x in C102, is used to react water out of the light liquid phase (118A) in the H_2SO_4 boost reactor (C103). The sulfuric acid stream enters the boost reactor at 15 and exists at 20 mole %. The iodine stream (110) used in the boost reactor exits the bottom containing the HI formed in the boost reactor, along with the water required to solubilize the HI, and is

pumped (P103) to the heat exchanger reactor. The overhead liquid product of the boost reactor (131/140) passes to Section 2, where the H_2SO_4 is concentrated and decomposed. Any SO_2 remaining in the sulfuric acid is returned to Section 1, along with water flashed from the sulfuric acid (101A).

The gaseous product (131/139) of the boost reactor is scrubbed in the secondary scrubber, along with the exhaust (136) of the SO_2 Absorber (C105). The gaseous product (129) of the secondary O_2 scrubber exits the process along with the vent (126) from the primary O_2 scrubber. The combined vent (142) contains one-half mole of oxygen for every mole of hydrogen produced in the overall process. In a mature hydrogen economy, the oxygen will likely be vented to the atmosphere but for initial plants, the oxygen co-product may be sold.

The liquid products of the two oxygen scrubbers (120/130B) are combined with a portion (108) of the HI/H_2O recycled from Section 3 (104), and the combined stream (112) is used to adsorb much of the SO_2 stripped from the HI_x.

3.3.3. Sulfuric Acid Concentration and Decomposition (Section 2)

The purpose of Section 2 is to concentrate the sulfuric acid received from Section 1 and decompose the concentrated sulfuric acid, producing sulfur dioxide and oxygen. It is important to concentrate the sulfuric acid before decomposing it for several reasons. First, less material heated to high temperatures means less sensible heat must be supplied, which means smaller heat exchangers and less cost. Secondly, there is a thermodynamic loss associated with the differential temperature across heat exchangers and lower heat transfer means higher thermodynamic efficiency. Also, the heat of solvating sulfuric acid must be supplied at some point in the course of getting the sulfuric acid to the decomposition conditions. In concentrating the sulfuric acid, the pressures and, thus, the temperatures at which the water is removed from the sulfuric acid can be adjusted, permitting thermodynamic optimization of the overall concentration and decomposition process.

The sulfuric acid portion of the process is, to a large part, decoupled from the rest of the process. The flowsheet for Section 2 was developed at the University of Kentucky, largely independent of the other portions of the process. Once the ratio of sulfuric acid to water was defined, Section 2 could be optimized with minimal regard to the rest of the flowsheet. The final flowsheet for Section 2, generated using Aspen Plus®, is shown in Fig. 3–3 and Table 3–2. The streams are labeled in Fig. 3–3 and the temperature, pressure, and molar flow rate for each stream are given in Table 3–2.

3.4. CONCENTRATION OF SULFURIC ACID

The overall scheme for concentration and decomposition is based on the MARS report [3–1]. The inlet sulfuric acid, along with internally recycled sulfuric acid, is concentrated to

40 (40 mole %) in a high pressure four-stage isobaric concentrator (E202). The feed to Section 2 (201A) and the recycle stream (230A) are pumped up to the operating pressure of the isobaric concentrator (35 atm) and preheated together before entering the concentrator. The sulfuric acid solution flows through four connected and heated chambers. Water is boiled off in each chamber so that both the temperature and the acid concentration of the solution increase as the solution flows through the concentrator. The water vapor boiled off in each chamber is mixed above the chambers and leaves as a single stream. The small amount of sulfur dioxide remaining in the inlet sulfuric acid is also removed with the water. The sensible and latent heat in this stream will be used elsewhere in this section. Each of the four stages of the concentrator is modeled in Aspen Plus® as a heater followed by an adiabatic flash. The stream table gives values for intermediate streams within the isobaric concentrator but only the mixed vapor outlet and the concentrated liquid outlet are physically identifiable streams. The mixed vapor outlet is condensed and its sensible and latent heats are recovered via the reboiler of the vacuum distillation column (C201).

The liquid product of the isobaric concentrator (210A) is further concentrated in a series of three reduced pressure flashes at 8 bar, 2 bar and 50 Torr before entering the 50 Torr vacuum still. Prior to the first flash, some heat is removed for use later in the process, the subsequent flashes are adiabatic. The feed to the vacuum still (216) is 56 mole % sulfuric acid. The vapor from the final adiabatic flash passes through a partial condenser. The condensate from the partial condenser (218) is feed to the vacuum still at a position appropriate to its composition (47 mole % H_2SO_4).

The pressures of the distillation column and the isobaric concentrator were chosen such that the column reboiler temperature is low enough to utilize heat recovered upon condensing the isobaric concentrator vapor stream. That is, a balance must be struck between the pressure of the isobaric flash and the pressure of the distillation column in order to use this heat. As the pressure of the isobaric flash increases, the temperature of heat recovered from the vapor stream also increases. As the column pressure is decreased, the required temperature of heat required goes down. Figure 3–5 shows the required isobaric flash pressure as a function of the distillation column pressure, assuming a 20°C differential between the condenser and reboiler temperatures. All other considerations equal, the operating pressures should be as low as practical, although a higher helium temperature from the nuclear reactor might allow higher overall process efficiencies at higher pressures. A Japanese plant producing semiconductor grade sulfuric acid successfully operated at column pressure of 50 Torr [3–2], so this pressure was chosen for our vacuum still. The isobaric flash pressure correspondingly operates at 35 bar. This design point is shown in the figure.

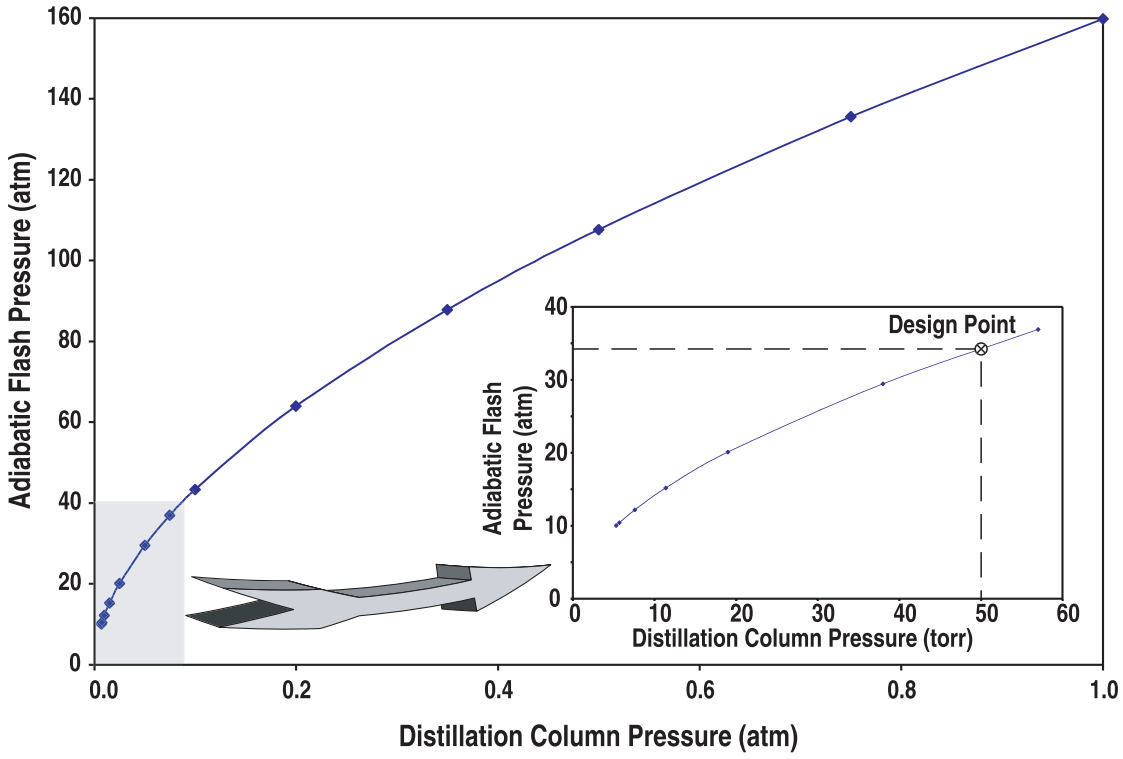

Fig. 3–5. Operating pressure of H_2SO_4 still when heated by the isobaric flash condensate with a 20°C temperature difference.

The overhead from the still, nearly pure water, is returned to Section 1. The bottom product of the distillation column (220A) is azeotropic sulfuric acid (~90 mole % H_2SO_4) liquid at 212°C. The concentrated sulfuric acid is pumped from the column pressure up to the 7 bar pressure used in the sulfuric acid decomposition portion of the process.

3.5. DECOMPOSITION REACTION

Before the sulfuric acid can be decomposed, it must first be heated to the vaporization temperature and vaporized. All of these steps occur at 7 bar. The first step in the reaction sequence is the vaporization of the concentrated sulfuric acid stream. Some of the heat required to preheat the stream prior to vaporization is recovered from the liquid product of the isobaric concentrator but the remainder of the heat required for heating, vaporizing, and decomposing the sulfuric acid is provided by the high temperature helium from the nuclear reactor. Some of the sulfuric acid decomposes into SO_3 and water as it is vaporized and this reaction proceeds further as the vaporized stream is heated in the recuperator.

The recuperator retrieves much of the heat remaining after sulfuric acid decomposition. Physically, the recuperator is similar to a shell and tube heat exchanger, with the hot fluid flows on the tube side and the cool fluid flows on the shell side, but in Aspen Plus® it is modeled as two Gibbs reactors coupled by a heat stream. Gibbs reactors are the modeling

block with the capability of rigorously predicting chemical equilibrium on the basis of the Gibbs-free energies of the components. Since SO_3 decomposition is slow in the absence of a catalyst, the Gibbs reactors are restricted to consider H_2SO_4 decomposition but not SO_3 decomposition. Most of the sulfuric acid has decomposed into SO_3 and water by the exit of the recuperator (222).

The catalytic decomposer is also modeled as a Gibbs reactor, but in this case the SO_3 is permitted to decompose into SO_2 and O_2. The stream table for Section 2 (Table 3–2) shows the effect of performing the decomposition in four stages, but the flow diagram (Fig. 3–3) only shows one piece of equipment. The MARS flowsheet, which was taken as a starting point for this flowsheet, performed the decomposition in a four-stage fluidized bed reactor. A fluidized bed reactor was initially chosen because of the large radial temperature drop associated with the traditional packed-bed reactor. The four-stage reactor was chosen to improve the process efficiency. As the number of stages is increased, more of the heat can be supplied to the reactor at lower temperatures. This four-stage reactor was modeled in Aspen as a series of four Gibbs reactors, where each stage reaches equilibrium.

Ultimately we elected to use an advanced technology, printed circuit heat exchanger (PCHE) with catalyst deposited on the wall of the exchanger on the process side in place of the multi-staged fluidized bed reactor. This same technology, without the catalyst, was selected for the intermediate heat exchanger interfacing the nuclear reactor coolant to the intermediate heat transfer loop. Figure 3–6 shows some details of the fabrication of a PCHE reactor. The catalytic wall reactor has the continuous temperature profile of the packed-bed reactor without the radial temperature gradient problem. Not only is the catalytic wall heat exchanger simpler to operate, it reduces the temperature difference between the hot helium and the decomposed acid compared with even a multi-staged fluidized bed. Figure 3–7 shows how catalytic wall reactor allows higher process temperatures, for a given helium temperature, than fluidized bed reactors. Alternatively, for a given process outlet temperature, the helium temperature can be lowered and thus the operating temperature of the nuclear reactor.

The reactor outlet stream (226) is cooled in the recuperator, transferring heat to the decomposer feed, as mentioned previously. Again a Gibbs reactor is used for the simulation, but as no catalyst is present, the equilibrium between SO_2, O_2 and SO_3 is frozen. The SO_3 is allowed to react, at equilibrium, with water reforming H_2SO_4. The reaction products are further cooled and the heat is recovered for use within this section in the product cooler. The product cooler is again modeled as a Gibbs reactor. The product cooler is physically divided into three heat exchangers. Part of the recovered heat is used for the first stage of the isobaric concentrator and the remainder is used to preheat the concentrator feed. Unrecoverable heat is lost to cooling water.

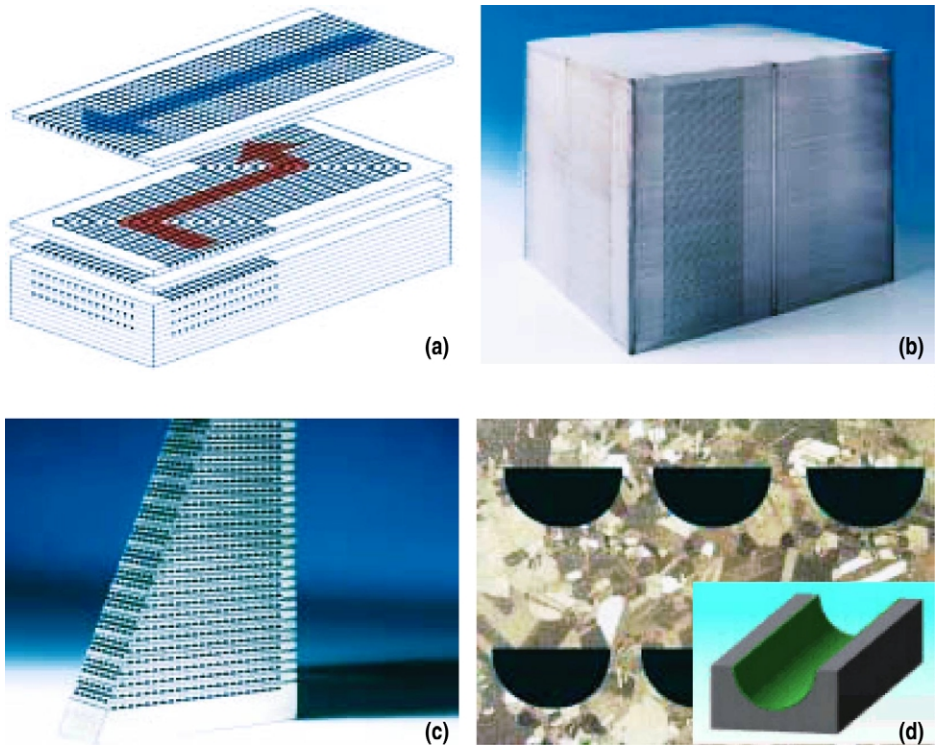

Fig. 3–6. PCHE reactor. (a) Plates with etched flow paths are stacked to form countercurrent flow paths in final exchanger and diffusion bonded to form monolithic heat exchanger. (b) PCHE prior to attachment of headers by welding. (c) Section of PCHE showing. (d) Metallographic section of PCHE showing extent of diffusion bonding with insert showing catalyst deposited on the wall of the flow channel. Note: The flow channel is approximately 3 mm wide.

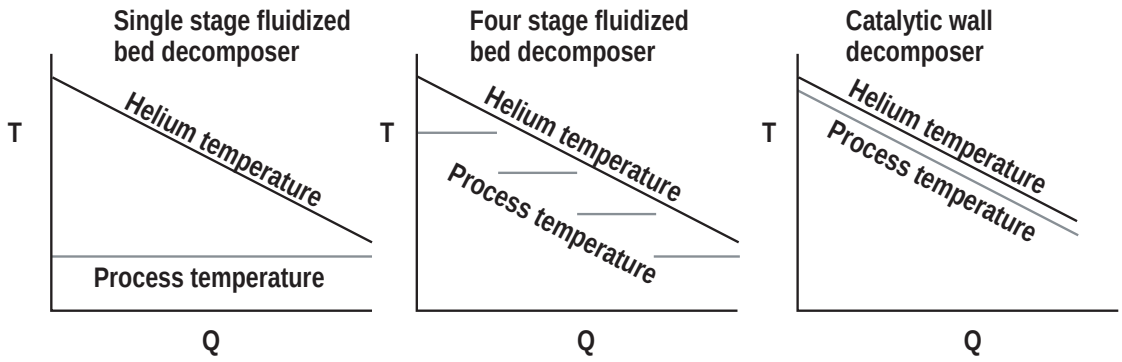

Fig. 3–7. Catalytic wall decomposer permits a higher process outlet temperature for a given helium temperature than fluidized bed decomposers.

The liquid condensed in the product cooler is recycled to the isobaric concentrator and the gas phase, consisting primarily of SO_2 and O_2 is recycled to Section 1.

3.5.1. Hydrogen Iodide Decomposition (Section 3)

The reactive distillation flowsheet was based on information presented by Roth and Knoche [E–5]. As in the case of sulfuric acid, we relied upon Aspen Technologies, Inc. to regress the vapor-liquid and LLE data for the system $HI/I_2/H_2O$. (We also had them to regress the system $HI/I_2/H_2O/H_2SO_4$ at the operating conditions of the Bunsen reaction.) To demonstrate the adequacy of the models we asked Aspen Technologies, Inc. to model the reactive distillation column under the conditions indicated by Roth and Knoche. The results of the regression and the modeling effort are presented in Appendix C.

Unfortunately, the results were not as useful as we had expected. The VLE data, which was available for regression, is incomplete. The available data gives the total vapor pressure above $HI/I_2/H_2O$ solutions, but not the vapor pressures of the individual components. Furthermore, as the hydrogen iodide was decomposing under the measurement conditions, the total vapor pressure measurements included the equilibrium hydrogen pressure. The result is a model that looks “reasonable” and which can be converged using Aspen Plus®, in the case of a single VLE stage, but which could be converged for a multistage VLE device such as the reactive still. We were unable to determine if the model was flawed, providing physically unrealizable results, or if the non-idealities of the system were extreme to the degree that the system was beyond the capabilities of Aspen Plus®. In the end, we were forced to abandon our attempts at optimizing the reactive distillation flowsheet and instead use the flowsheet presented by Roth and Knoche [E–5].

The reactive distillation Section 3 flowsheet is present in Fig. 3–4 and Table 3–3. The $HI/I_2/H_2O$ product of Section 1 is pumped up to 22 bar and recuperatively heated to the feed temperature of the reactive distillation column (C301) in a network of heat exchangers (E301/E302/E303). This heat is recovered from the two liquid products of the distillation column, the bottom stream (305A) containing most of the iodine, and the side outlet (306A) containing most of the water and undecomposed hydrogen iodide.

The overhead product of the column is scrubbed in a packed column (C302) with water to remove the residual hydrogen iodide from the hydrogen. The high pressure (22 bar) and low temperature (25°C) of the scrubber result in a relatively low water content (0.14 mole %) in the hydrogen product. Fresh deionized water, the overall water input to the process, is used to scrub the product hydrogen.

It is uneconomic and unnecessary to remove all of the water and hydrogen iodide from the still bottoms but it is necessary to provide a small amount of pure iodine for the boost reactor in Section 1. The scrub water (311A) is used to wash a portion of the bottoms in a packed column. The column was modeled as a single LLE stage using the model for $HI/I_2/H_2O$ previously discussed.

The still must have a side product to remove the water that accompanies the HI in the feed. The side product contains a significant amount of hydrogen iodide and some iodine. The total amount returned to Section 1, from the side product and still bottoms, is five/sixths of the HI fed to Section 3. For every mole of HI decomposed, five moles of HI are recycled unreacted and each mole of HI in the feed is accompanied by almost 4 moles of I_2 and over 5 moles of water. Even so, this version of the process is more efficient than the version using H_3PO_4 as it is not necessary to vaporize the water.

3.6. REACTOR MATCHING

The nuclear reactor must be matched to the chemical process such that high thermal efficiency is obtained, but not at the expense of sacrificing the operability of the combined plant. Provision must be made for startup and shutdown of both the nuclear reactor and the chemical process. Also, the matching must be done in a way that promotes operational stability of the chemical process. We chose to restrict thermal energy recovery to recovery within a section and to exclude recovery between sections in order to minimize the effect of flow or composition transients in one section on the operational stability of other sections. Section 1 requires no thermal energy; it is an exporter of heat to the environment. Temperatures are much higher in Section 2 than Section 3 and the theoretical energy requirements of Section 2 are much larger than Section 3, therefore, the major effect of this decision is to rule out transfer of waste heat from Section 2 to Section 3. This decision resulted in a lower thermal efficiency than could have otherwise been achieved, perhaps needlessly, as the coupling between sections is inherently very high because both Sections 2 and 3 are strongly coupled via flows to and from Section 1.

SNL modeled the coupling of the nuclear reactor with the chemical plant. The model, described in Appendix D, considers two approaches. For the simpler approach, high temperature helium from the reactor is split into two streams, which power Sections 2 and 3 in parallel. The helium flow is similar, for the alternative case, but instead of heating Section 3 directly, Section 3 is heated by the waste heat from a Brayton cycle. The Brayton cycle is powered in parallel with Section 3. For completeness, the model also describes a pure electricity production plant, but that part of the model was not used in this work. We found that the efficiency, using the reactive distillation flowsheet presented above, is 42%. This compares with a 38% efficiency found in the MARS [3–1] study. The H_3PO_4 flowsheet [E–4] used in the MARS study accomplished the removal of water from the H_3PO_4 in three stages of vapor-recompression-driven flash evaporation. Only the last stage required any heat input from the combined cycle, but all three stages required significant quantities of power for vapor recompression. The phosphoric acid concentration step is simple in concept, but capital costs of the turbine compressors and heat exchangers were significant in the overall hydrogen production costs. The shaft work required for vapor recompression was provided

by a combined cycle, consisting of a Brayton power-topping cycle and a Freon® Rankine bottoming cycle. The Brayton cycle worked with the energy being transferred to process, primarily Section 3. The Freon® Rankine cycle was powered with the waste heat from Section 1. Much effort has been directed at circumventing the capital-intensive vapor-recompression-driven flash evaporation in H_3PO_4 Section 3.

Early on we postulated that co-generation of hydrogen and electricity could result in higher efficiencies than production of hydrogen alone [E–1]. We investigated co-generation of hydrogen and electricity for both the reactive distillation version of the flowsheet and the H_3PO_4 dehydration version. We compared efficiencies for three cases in which hydrogen was produced without co-generation and then examined the effect of co-generation on two of these cases. The base case, that of the MARS [3–1] study, employed vapor recompression and the Freon® bottoming cycle as described above. The second case omitted the Freon® bottoming cycle and the third case substituted high temperature heat for vapor recompression in concentrating the H_3PO_4. We then interposed a Brayton cycle between the high temperature heat source and the vaporization stages and calculated the overall efficiency as a function of the energy split between hydrogen and electricity using the SNL model. Finally, we simulated a more complicated dual Brayton cycle, which could not be described by the SNL model, using Aspen Plus®. The dual Brayton cycle provided heat to the lower temperature portions of the heat load with the reject heat of a Brayton cycle, as above, but the high temperature loads were directly heated with part of the excess heat going to a Brayton bottoming cycle. The dual HTGR Brayton cycle is based on the current-state-of-the-art helium cycle which operates at an efficiency of 51% [3–3]. Figure 3–8 shows the results of these H_3PO_4 cases along with some results for reactive distillation. The reactive distillation cases are the “hydrogen only” case, which uses high temperature helium to drive the distillation column, and a co-generation version, where the SNL model is used to calculate the overall efficiency as a function of the split between hydrogen and electricity.

Design of the Brayton cycles entailed a tradeoff between overall efficiency and the proportion of hydrogen energy produced, to the quantity of electrical energy produced. A high proportion of hydrogen energy to electrical energy is desirable to support a hydrogen based economy but this comes at the expense of overall efficiency. The use of low helium flow rates in the power-topping cycle increases the proportion of hydrogen to electricity but decreases the overall efficiency. This is because the lower the helium flow rate for a given heat output, the greater the resulting helium temperature drop will be. The greater the helium temperature drop is, the lower the average helium temperature throughout the cycle. Everything else being the same, the overall efficiency of a heat engine decreases with decreasing input temperatures, i.e., the average helium temperature, as governed by Carnot’s equations. The maximum overall efficiency, for both the H_3PO_4 and reactive distillation scenarios, occurs at a hydrogen fraction significantly lower than needed for a fully developed

hydrogen economy. Thus, we did not pursue co-generation further for this study. In the interim, co-generation may be important as a bridge technology.

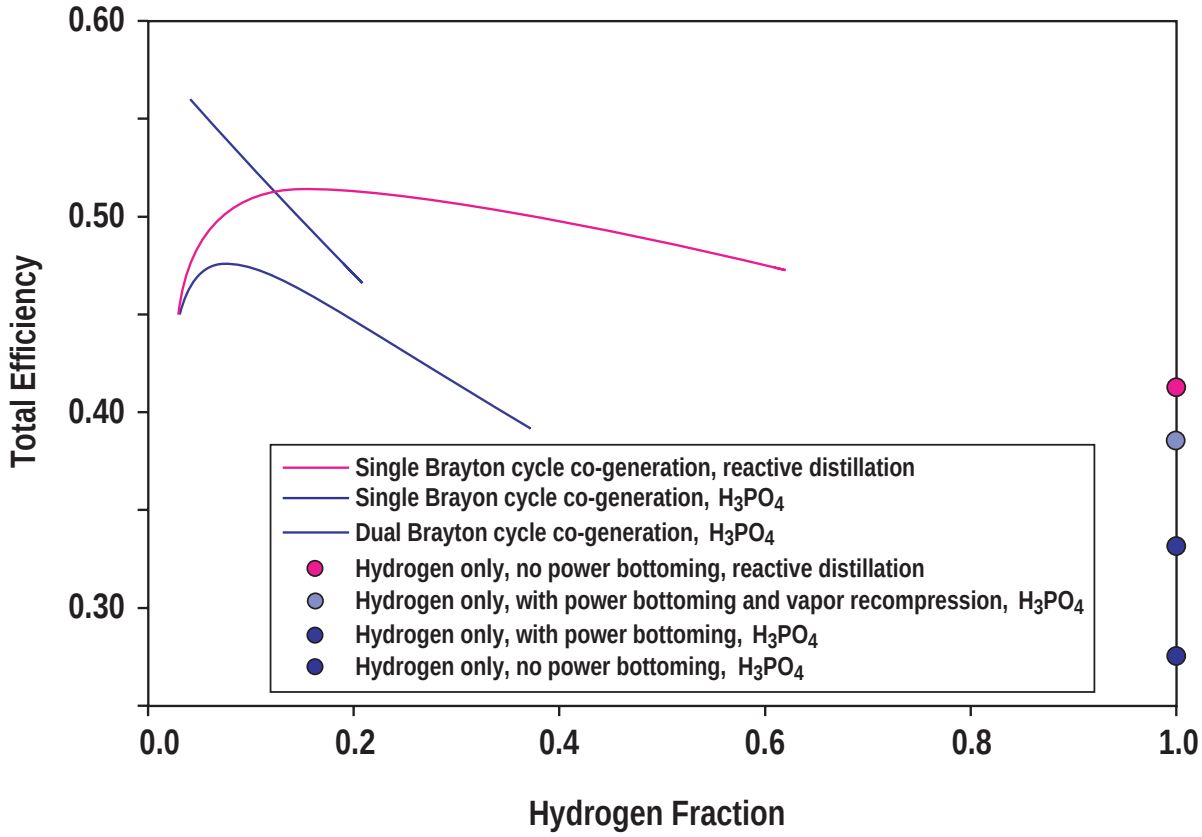

Fig. 3–8. Effect of co-generation on the overall efficiency of hydrogen and electricity production.

3.7. EFFECT OF REACTOR TEMPERATURE

The efficiency we obtained without co-generation, 42%, is less than we had hoped. In our work we assumed that the heat would be available at temperatures demonstrated in previous helium-cooled reactors. We assumed a peak temperature of 827°C in the process fluid, which might be obtained with 850°C reactor outlet temperature and an efficient PCHE. Since higher temperature helium cooled reactors are being developed, it is instructive to extrapolate the efficiency of the S-I process to higher temperatures. The efficiency is expected to increase with temperature for several reasons. First, the theoretical efficiency of thermochemical water-splitting increases with temperature: this is analogous to the increase in theoretical efficiency of heat engines as given by Carnot. Equation (2) indicates that the theoretical efficiency of a thermochemical process is composed of two factors — the Carnot efficiency and a thermochemical correction term — this is referred to as the “thermochemical Carnot efficiency”.

$$\varepsilon^0 = \left(1 - \frac{T_C}{T_H}\right)\left(\frac{\Delta G^0_{T_C}}{\Delta H^0_{T_C}}\right) \quad . \tag{2}$$

The efficiency of a thermochemical process will also increase with temperature as higher temperatures provide more opportunity for heat recuperation and reuse within the process. Finally, in the case of the S-I cycle, the equilibrium decomposition of sulfuric acid to sulfur trioxide and the equilibrium decomposition of sulfur trioxide both increase with temperature and the rate of sulfur dioxide decomposition is negligible below about 675°C.

We have used engineering judgment to extrapolate our results to higher process temperatures. Figure 3–9 extrapolates the efficiency of the S-I cycle to higher process temperatures, based on our efficiency of 42% at 827°C for the case of reactive distillation without co-generation. The extrapolation assumes that the efficiency is zero below the kinetic temperature limit of 650°C and that the efficiency exponentially approaches 80% of thermochemical Carnot as the temperature increases above the kinetic limit. If the extrapolation is correct, increasing the process temperature to 900°C will let the process operate at 52%.

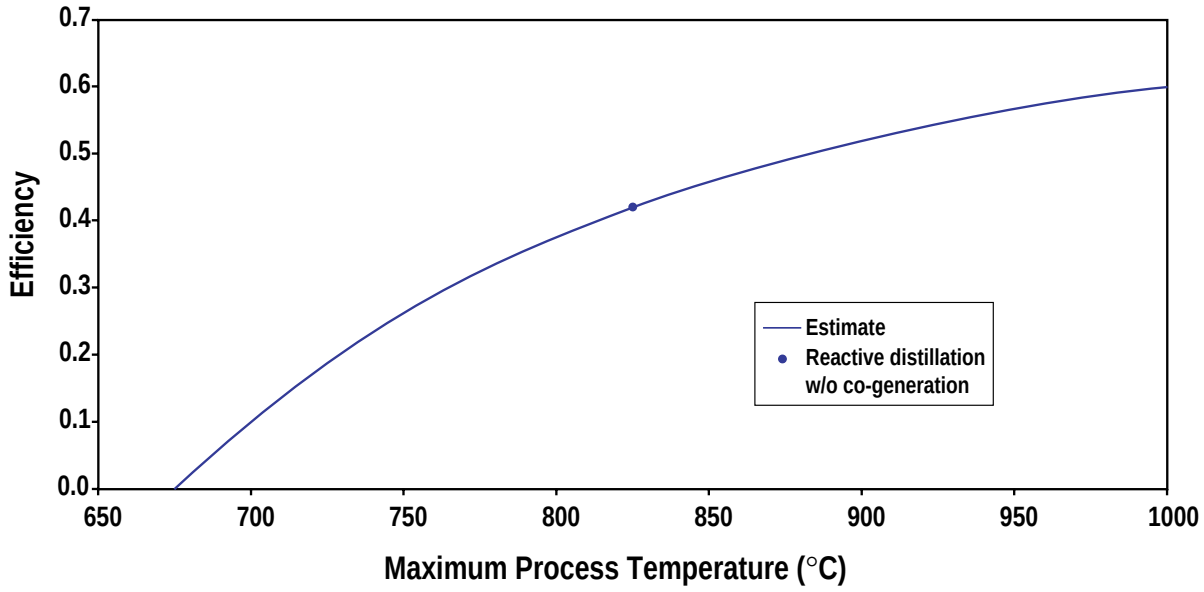

Fig. 3–9. Projected hydrogen generation efficiency at higher maximum process temperatures.

3.8. SIZING AND COSTING

We wished to evaluate the economic potential for hydrogen produced from nuclear energy in a mature hydrogen economy. The scenario chosen was that of a large hydrogen plant located on a major hydrogen pipeline. The largest gas-cooled reactor complex on the

drawing board is a cluster of four 600 MW_T GT-MHRs. Cost estimates for the GT-MHR are available and served as the basis of our estimate of an H_2-MHR. The four-reactor cluster makes sense from an availability basis because fueling can be staggered and the plant can be kept at a minimum of 75% capacity at all times. In the mature hydrogen economy, there would likely be several four-reactor complexes at various points along a single major pipeline. In addition, there would be interconnections between major hydrogen pipelines just as there are interties between various electric power providers to increase the overall availability. The optimal placement of the reactor complexes would be near the interconnection between pipelines so that hydrogen production would not be impacted by distribution considerations.

The chemical plant sizing and costing effort began simultaneously with the effort to match the process to the nuclear reactor. We assumed that the hydrogen plant would operate at 50% efficiency for the sizing and costing effort. On this basis, the hydrogen plant was sized and costed assuming a hydrogen production of 4200 moles/s. When the matching effort was completed, resulting in a 42% efficiency or 3525 moles/s, we revised the overall capital cost estimate assuming the capital cost is proportional to the hydrogen production rate.

3.9. COMPONENT SIZING

The sizes of major chemical plant components were calculated to the extent necessary for estimating the equipment capital cost. The sizing data is presented in Tables 3–7, 3–8 and 3–9 for the three sections of the process. Standard chemical engineering methods were used to size the chemical process equipment. The diameters of packed and tray columns were determined utilizing the Leva generalized pressure drop correlation (GPDC) [3–4] as presented by Seader [3–5]. For given fluid flow rates and properties, and a given packing material, the GPDC chart is used to compute the superficial gas velocity at flooding. The diameters were then calculated using the flooding velocity corrected to 70% of flooding.

Table 3–7
Section 1 Equipment Description

Item	Equipment Description	Adders and Other Factors
C101	Primary O_2 scrubber, 5 req'd., Vertical Vessel, 8 ft dia. x 24 ft tall, Carbon Steel	704 ft^2 Fluorocarbon liner, 1026 ft^3 2" ceramic Raschig ring packing, Fluorocarbon lined piping
C102	Lower phase SO_2 scrubber, 5 req'd., Vertical Vessel, 19.5 ft dia. x 40 ft tall, Carbon Steel	3048 ft^2 Fluorocarbon liner, 11946 ft^3 2" ceramic Raschig ring packing, Fluorocarbon lined piping
C103	H_2SO_4 boost reactor, 5 req'd., Vertical Vessel, 5 ft dia. x 20 ft tall, Carbon Steel	353 ft^2 Fluorocarbon liner, 393 ft^3 2" ceramic Raschig ring packing, Fluorocarbon lined piping

Table 3–7 (Cont.)

Item	Equipment Description	Adders and Other Factors
C104	Secondary O_2 scrubber, 5 req'd., Vertical Vessel, 3 ft dia. x 12 ft tall, Carbon Steel	127 ft^2 Fluorocarbon liner, 85 ft^3 2" ceramic Raschig ring packing, Fluorocarbon lined piping
C105	SO_2 absorber, 10 req'd., Vertical Vessel, 12 ft dia. x 57.5 ft tall, Carbon Steel	2394 ft^2 Fluorocarbon liner, 6503 ft^3 2" ceramic Raschig ring packing, Fluorocarbon lined piping
S101	3-Phase Cyclonic Knockout drum, 5 req'd., Vertical Vessel, 7 ft dia. x 45 ft tall, Carbon Steel	1067 ft^2 Fluorocarbon liner, Fluorocarbon lined piping
S102	Flash Drum, 5 req'd., Vertical Vessel, 4 ft dia. x 8 ft tall, Carbon Steel	126 ft^2 Fluorocarbon liner, Fluorocarbon lined piping
SS104	Primary O_2 water knockout drum, 5 req'd., Vertical Vessel, 3 ft dia. x 12 ft tall, Carbon Steel	
S105	Secondary O_2 water knockout drum, 5 req'd., Horizontal Vessel, 2 ft dia. x 6 ft long, Carbon Steel	
R101	Flow reactor w/ integral heat exchanger, 5 req'd., Shell and tube, fixed tube sheet heat exchanger, 7320 ft^2 area	Fluorocarbon lined piping, Fluorocarbon lined heads, Niobium tubes and niobium lined tube sheets
E102	H_2O to cooling water knockout drum, 1 req'd., Shell and tube, fixed tube sheet heat exchanger, 9706 ft^2 area, CS/Cu	
P101	C105 Effluent to R101, 6 req'd., Fluorocarbon lined centrifugal pump, 762 shaft hp	Fluorocarbon lined piping
P102	C101 Effluent to R101, 6 req'd., Fluorocarbon lined centrifugal pump, 176 shaft hp	Fluorocarbon lined piping
P103	Boost Reactor Centrifugal Pump, 6 req'd., 106 shaft hp, Fluorocarbon lined	Fluorocarbon lined piping
P104	C104 Effluent to R101, Fluorocarbon lined centrifugal pump, 6 req'd., 52 shaft hp	Fluorocarbon lined piping
TE101	O_2 Axial Gas Turbine, 1 req'd., 5987 shaft hp, Ni Alloy	
TE102	Water from H_2 Scrubber Liquid Expander, 1 req'd., 135 shaft hp, Carbon Steel	
TE103A	S101 Overhead Axial Gas Turbine Expander, 5 req'd., 540 shaft hp, Ni Alloy	Fluorocarbon lined piping
TE103B	S101 Side Liquid Expander, 5 req'd., 716 shaft hp, Ni Alloy	Fluorocarbon lined piping
TE103C	S101 Bottoms Liquid Expander, 5 req'd., 2543 shaft hp, Ni Alloy	Fluorocarbon lined piping

Table 3–8
Section 2 Equipment Description

Item	Equipment Description	Adders and Other Factors
E201	Feed preheater/Product cooler, 1 req'd., 3338 ft ^{2} area, CS/N alloy Shell and tube, fixed tube sheet heat exchanger	Nickel alloy piping
E202-1	Stage 1 of isobaric concentrator/product cooler, 4 req'd., 29045 ft ^{2} area, CS/SiC Shell and tube, fixed tube sheet heat exchanger	735 ft ^{2} Fluorocarbon liner, 345 ft ^{3}Acid brick liner, Nickel alloy piping, High pressure on tube side only
E202-2	Stage 2 Flash Heater/helium, 1 req'd., 9550 ft ^{2} area, CS/SiC, Shell and tube, fixed tube sheet heat exchanger	Nickel alloy piping
E202-3	Stage 3 Flash Heater/helium, 1 req'd., 2461 ft ^{2} area, CS/SiC, Shell and tube, fixed tube sheet heat exchanger	Nickel alloy piping
E202-4	Stage 4 Flash Heater/helium, 1 req'd., 1775 ft ^{2} area, CS/SiC, Shell and tube, fixed tube sheet heat exchanger	Nickel alloy piping
E202-V	Multi-stage isobaric flash vessel, 1 req'd., Costed as 4 Vertical Carbon Steel Vessels, 10 ft dia. x 33 ft tall, lined as indicated	1194 ft^2 Fluorocarbon liner, 253 ft ^{3} Acid brick liner, Nickel alloy piping
E203	S201 Flash Cooler/Vaporizer preheater, 1 req'd., 20026 ft ^{2} area, CS/Ni Shell and tube, fixed tube sheet heat exchanger	817 ft^2 Fluorocarbon liner, 580 ft ^{3} Acid brick liner, Nickel alloy piping, High pressure on tube side only
E204	Helium/2nd Vaporizer preheater, 1 req'd., 1393 ft ^{2} area, CS/Ni Shell and tube, fixed tube sheet heat exchanger	Nickel alloy piping, High pressure on tube side only
E205	Vaporizer, 1 req'd., 14562 ft ^{2} area, CS/SiC Shell and tube, fixed tube sheet heat exchanger	Nickel alloy piping, High pressure on tube side only
E206	Recuperator, 3 req'd., 28745 ft ^{2} area, CS/SiC, Shell and tube fixed tube sheet heat exchanger	1307 ft^2 Fluorocarbon liner, 700 ft ^{3} Acid brick liner, Nickel alloy piping
E207	Decomposer, 1 req'd., Diffusion bonded Alloy 800HT PCHE	Nickel alloy piping
E208	Product Cooler/cooling water, 1 req'd., 3829 ft ^{2} area, CS/Ni, Shell and tube, fixed tube sheet heat exchanger	Nickel alloy piping, High pressure on tube side only
E209	Column Reboiler/Condensate cooler, 3 req'd., 12233 ft ^{2} area CS/SiC Shell and tube, fixed tube sheet heat exchanger	Nickel alloy piping, High pressure on tube side only
E210	Condensate Cooler, 1 req'd., 1000 ft ^{2} area, CS/CS, Shell and tube, fixed tube sheet heat exchanger	
E211	Condensate Cooler, 1 req'd., 1480 ft ^{2} area, CS/CS, Shell and tube, fixed tube sheet heat exchanger	
E212	Partial Condenser for 2nd column feed, 1 req'd., 4825 ft ^{2} area, CS/SS Shell and tube, fixed tube sheet heat exchanger	Fluorocarbon lined piping, high pressure on tube side only
E213	Condensate Cooler, 1 req'd., 6724 ft ^{2} area, CS/CS, Shell and tube, fixed tube sheet heat exchanger	
E214	Column Condenser, 1 req'd., 25248 ft ^{2} area, CS/CS, Shell and tube, fixed tube sheet heat exchanger	High pressure on tube side only
E215	Feed preheater/helium, 4 req'd., 27211 ft ^{2} area, CS/SiC, Shell and tube, fixed tube sheet heat exchanger	1055 ft^2 Fluorocarbon liner, 485 ft ^{3} Acid brick liner, Fluorocarbon lined process piping

Table 3–8 (Cont.)

Item	Equipment Description	Adders and Other Factors
S201	Flash Separator, 1 req'd., Carbon Steel Vertical Vessel, 8.25 ft dia. x 36 ft tall,	1040 ft^2 Fluorocarbon liner, 226 ft^3 Acid brick liner, Nickel alloy piping
S202	Flash Separator, 1 req'd., Carbon Steel, Vertical Vessel, 8 ft dia. x 32 ft tall	905 ft^2 Fluorocarbon liner, 195 ft^3 Acid brick liner, Nickel alloy piping
S203	Flash Separator, 1 req'd., Carbon Steel, Horizontal Vessel, 9 ft dia. x 19.2 ft long,	670 ft^2 Fluorocarbon liner, Fluorocarbon lined piping
S204	Column Partial Condenser Knockout, 1 req'd., Carbon Steel, Horizontal Vessel, 9 ft dia. x 19.2 ft long,	410 ft^2 Fluorocarbon liner, Fluorocarbon lined piping
S205	Flash Separator, 1 req'd., Carbon Steel, Vertical Vessel, 9 ft dia. x 10 ft tall,	670 ft^2 Fluorocarbon liner, Fluorocarbon lined piping
P201	Vaporizer feed Pump, 1 req'd., 1314 shaft hp, Ni Alloy, Centrifugal Pump	Fluorocarbon lined piping
P202	Recycle Pump, 1 req'd., 2752 shaft hp, Epoxy lined, Centrifugal Pump	Fluorocarbon lined piping
P203	Water pump to Sec. 1, 1 req'd., 44 shaft hp, Epoxy Lined, Centrifugal Pump	
P204	Feed Pump, 1 req'd., 6952 shaft hp, Plastic Lined, Centrifugal Pump	Fluorocarbon lined piping
TE201	Flash Water Expander, 1 req'd., 608 shaft hp, Carbon Steel, Liquid Expander	
C201	Column Vessel, 3 req'd., Carbon Steel Vertical Vessel, 12.8 ft dia. x 40 ft tall,	1866 ft^2 Fluorocarbon liner, , Nickel alloy piping
C201i	Column Internals, 3 sets req'd., Sieve Trays, 12.8 ft dia. x 48" spacing, Costed as Monel	

Table 3–9
Section 3 Equipment Description

Item	Equipment Description	Adders and Other Factors
E301	Recuperator, Shell and tube, fixed tube sheet heat exchanger, 9392 ft^2 area, CS/CS	193 ft^2 Fluorocarbon liner, 95 ft^3 Acid brick liner, Nickel alloy piping, Niobium Tubes and Lined Tube Sheets
E302	Recuperator, Shell and tube, fixed tube sheet heat exchanger, 12295 ft^2 area, CS/CS	283 ft^2 Fluorocarbon liner, 138 ft^3 Acid brick liner, Nickel alloy piping, Niobium Tubes and Lined Tube Sheets
E303	Recuperator, Shell and tube, fixed tube sheet heat exchanger, 3667 ft^2 area, CS/CS	82 ft^2 Fluorocarbon liner, 39 ft^3 Acid brick liner Nickel alloy piping, Niobium Tubes and Lined Tube Sheets
E304	Condenser, Shell and tube, fixed tube sheet heat exchanger, 2417 ft^2 area, CS/Karbate	PVC piping, High pressure on tube side only

Table 3–9 (Cont.)

Item	Equipment Description	Adders and Other Factors
E305	Condensate Reheater, Shell and tube, fixed tube sheet heat exchanger, 10 ft ^{2} area, CS/SiC	PVC piping
E306	Reboiler, Shell and tube, fixed tube sheet heat exchanger, 1805 ft^2 area, CS/SiC	Nickel alloy piping
E307A	Water Recycle heat exchanger to Sec I, Shell and tube, fixed tube sheet heat exchanger, 2089 ft ^{2} area, CS/Karbate	PVC piping, High pressure on tube side only
E307B	Water Recycle heat exchanger/C303 Heater, Shell and tube, fixed tube sheet heat exchanger, 6836 ft ^{2} area, CS/Karbate	266 ft^2 Fluorocarbon liner, PVC piping
E308	Iodine Recycle heat exchanger to Sec I, Shell and tube, fixed tube sheet heat exchanger, 2037 ft ^{2} area, CS/Karbate	PVC piping, High pressure on tube side only
S301	Condenser Drum, Vertical Vessel, 2.25 ft dia. x 13 ft tall, Carbon Steel	92 ft^2 Fluorocarbon liner, PVC piping
C301	Reactive distillation column, 17.5 ft dia. x 40 ft tall, Carbon Steel	2199 ft^2 Fluorocarbon liner, 219 ft ^{3} Acid brick liner, PVC piping
C301i	Column Internals, Sieve Trays, , 10 ft dia. x 48” spacing, Monel	
C302	H2 Scrubber, Vertical Vessel, 4 ft dia. x 10 ft tall, Carbon Steel	151 ft^2 Fluorocarbon liner, 2” ceramic Raschig rings, 126 ft^3, PVC piping packing,
C303	I2 Scrubber for Sec. I Boost Reactor, Vertical Vessel, 5.5 ft dia. x 8 ft tall, Carbon Steel	186 ft^2 Fluorocarbon liner, 190 ft ^{3} 2” ceramic Raschig rings packing, PVC piping
P301	Feed Centrifugal Pump, 1846 shaft hp, Stainless Steel	Fluorocarbon lined piping
TE301	Recycle Water Liquid Expander, 2780 shaft hp, Ni Alloy	PVC piping
TE302	Recycle Iodine Liquid Expander, 4787 shaft hp, Ni Alloy	Fluorocarbon lined piping
TE303	Iodine to Sec. I Boost reactor liquid expander, 812 shaft hp, Ni Alloy	Fluorocarbon lined piping

The minimum interfacial area for process vessels was determined such that vapor velocities were insufficient to entrain macroscopic liquid droplets. The methodology used to determine the interfacial area is presented by Seader [3–5]. This procedure utilizes Fair’s [3–6] general correlation for entrainment flooding capacity in tray towers for 24-in. tray spacing and vapor hole area to tray active area correction factor of 1 as a basis. For vertical vessels, the minimum diameter is calculated directly from the minimum interfacial area and the height is determined on the basis of residence time. For horizontal vessels, the minimum diameter is calculated by adjusting the L/D ratio to obtain the desired residence time. The residence time for each vessel was determined on a case-by-case basis via engineering judgment.

The heights of tray columns were calculated by determining the number of trays via the Fenske-Underwood-Gilliland shortcut method as presented by Seader [3–5] and specifying the tray-spacing via engineering judgement. The heights of packed columns were calculated

using the Chilton and Colburn method [3–7] in which the packed height is the product of the overall height of a transfer unit (H_{OG}) and the overall number of transfer units (N_{OG}).

The method used for sizing heat exchangers is presented in Perry's Chemical Engineers' Handbook [3–8]. This technique is based on the Delaware Method developed using extensive experimental and analytical research program carried on in the Department of Chemical Engineering a the University of Delaware [3–9].

All fluid properties used in the sizing calculations were determined using Aspen Plus® 10.2 software, the same software used in the flowsheet modeling. In addition, the power requirement for pumps, compressors, and turbines were all sized using Aspen Plus®.

3.10. COMPONENT COSTING

Capital cost estimates were generated using the Guthrie method [3–10] as modified by Ulrich [3–11]. The costing data was obtained from Turton [3–12], Ulrich [3–11], and Guthrie [3–10]. The Guthrie method is based on the cost of equipment constructed from carbon steel. Graphs or equations are presented which give the cost of equipment as a function of capacity or size. Generally, the cost per unit of capacity or size decreases with size until some maximum size is reached. If the maximum size or capacity is reached, multiple parallel units are required. Multiplicative factors are supplied by the various authors for common alternative materials. Factors for other materials used in the S-I process were originally developed for the MARS study [3–1]. The Guthrie method also modifies the basic equipment cost through the use of "adders." The use of adders is particularly applicable in the case of coatings, linings and packings where the cost is linear with area or volume and does not decrease with capacity or size. Older cost data were scaled to 2001 using the Chemical Engineering Plant Cost Index (CEPCI) [3–13].

Most of the chemical plant equipment is at the maximum size suggested by the costing algorithms. Under these conditions the majority of the economies of scale have diminished as the plant capacity is set by the number of parallel units. When multiple identical units are purchased, the cost per unit is less than the cost of one unit. This decrease in cost due to multiple units is often described in terms of a learning curve. We did not take credit for multiple units.

3.11. CHEMICAL PLANT CAPITAL AND OPERATING COSTS

The recovery of the total chemical plant investment is a major component of the cost of hydrogen. The total chemical plant investment is also one of the major inputs in calculating the operating cost of the chemical plant.

The Guthrie method provides a methodology for deriving the total investment cost from the bare equipment cost. The installed equipment cost, or bare module cost, is obtained from

the equipment by applying a factor appropriate to the equipment type. This factor considers costs such as piping, instrumentation and electrical equipment. Tables 3–10, 3–11 and 3–12 present the costs of the equipment for the three sections and Table 3–13 accumulates the costs of the three sections and calculates the total capital investment.

Table 3–10
Preliminary Capital Cost Estimate for Section 1 — 4200 mole/s

Item	Description	Parallel Units	Equiv CS FOB Cost ($)	Bare Module Cost ($)	Bare Module Cost plus Adders ($)
C101	Primary O_2 Scrubbing RXR	5	199,012	848,866	2,263,043
C102	Lower Phase SO_2 Scrubber	5	815,543	3,478,617	9,983,147
C103	H_2SO_4Boost RXR	5	102,021	435,162	1,133,723
C104	Secondary O_2 Scrubbing RXR	5	41,683	177,793	428,845
C105	SO_2 Absorber	10	1,352,165	5,767,526	15,679,119
S101	HP 3-Phase Cyclonic Knockout	5	310,215	1,476,057	3,513,646
S102	LP Flash Drum	5	41,290	176,117	419,059
S104	Primary O2 Water Knockout Drum	5	41,683	177,793	177,793
S105	Secondary O2 Water Knockout Drum	5	12,514	53,379	53,379
R101	Flow RXR w/ Integral HX	5	257,085	823,467	7,469,074
E102	H_2O to CW HX	1	63,168	215,749	215,749
P101	C-105 Effluent to R-101	10	597,552	2,674,198	2,856,451
P102	C-101 Effluent to R-101	6	182,799	1,347,860	1,403,614
P103	Boost Reactor Pump	6	146,598	1,080,933	1,125,646
P104	C-104 Effluent to R-101	6	108,685	653,798	686,947
TE101	O_2 Turbine	1	571,416	4,571,328	4,571,328
TE102	Water from Section 3.	1	39,636	118,909	118,909
TE103A	S-101 Overhead Expander	5	694,338	5,554,704	5,554,704
TE103B	S-101 Side Expander	5	629,054	3,774,326	3,774,326
TE103C	S-101 Bottoms Expander	5	1,512,783	9,076,701	9,076,701
Subtotals for Section 1			7,720,304	42,491,924	70,505,203

Table 3–11
Preliminary capital cost estimate for Section 2 — 4200 mole/s

Item	Description	Parallel Units	Equiv CS FOB Cost ($)	Bare Module Cost ($)	Bare Module Cost plus Adders ($)
E201	Feed Preheater/Product Cooler	1	29,846	198,524	253,562
E202-1	Stage 1 Flash Heater	4	592,285	10,417,084	12,608,099
E202-2	Stage 2 Flash Heater	1	62,417	1,193,820	1,308,916
E202-3	Stage 3 Flash Heater	1	24,445	467,558	512,635
E202-4	Stage 4 Flash Heater	1	19,877	380,178	416,831
E-202-V	Multi-stage isobaric flash vessel	1	271,704	3,219,328	5,591,980
E203	Stage 5 Flash Cooler/Vaporizer Preheat	1	109,882	683,535	1,202,646
E204	Helium/2nd Vaporizer Preheat	1	17,131	107,720	139,310
E205	Vaporizer	1	85,747	1,528,754	1,686,872
E206	Recuperator	3	440,472	7,152,981	9,445,211
E207	Decomposer	1	3,299,646	65,204,258	65,204,258
E208	Product Cooler/Cooling Water	1	32,722	193,531	253,871
E209	Column Reboiler/Condensate Cooler	3	225,278	3,962,173	4,377,585
E210	Condensate Cooler	1	14,071	51,339	51,339
E211	Condensate Cooler	1	17,773	62,303	62,303
E212	Partial Condenser for Column	1	38,320	142,432	160,097
E213	Condensate Cooler	1	48,380	155,276	155,276
E214	Column Condenser	9	1,189,635	3,482,785	3,482,785
E215	Feed Pre-heater/Helium	1	516,701	9,879,178	12,490,129
S201	Flash Separator	1	60,189	298,046	817,580
S202	Flash Separator	1	52,255	222,890	674,509
S203	Flash Separator	1	24,382	103,997	346,649
S204	Column Partial Condenser Knockout	1	22,997	109,425	265,555
S205	Flash Separator	1	24,382	103,997	346,649
P201	Vaporizer Feed Pump	1	77,811	573,735	597,467
P202	Recycle Pump	1	112,644	956,584	990,941
P203	Water pump to Sec. 1	1	16,854	115,858	115,858
P204	Feed Pump	1	182,566	2,873,912	2,929,594
TE201	Flash Water Expander	1	112,346	337,039	337,039
C201	Column Vessel	3	314,906	1,343,199	4,047,940
C201i	Column Internals	3	83,418	7473,314	743,314
Subtotals for Section 2			8,121,082	122,994,753	131,616,800

Table 3–12
Preliminary Capital Cost Estimate for Section 3 — 4200 mole/s

Item	Description	Parallel Units	Equiv CS FOB Cost ($)	Bare Module Cost ($)	Bare Module Cost plus Adders ($)
E301	Recuperator	40	2,466,127	8,382,131	33,515,067
E302	Recuperator	40	3,015,275	10,248,635	43,635,623
E303	Recuperator	40	1,271,329	4,321,127	30,394,257
E304	Condenser	40	966,523	4,731,362	4,731,362
E305	Condensate Reheater	40	80,266	1,535,227	1,535,227
E306	Reboiler	40	229,912	4,397,451	4,821,409
E307A	Water Recycle HX to Sec I	5	110,079	538,863	538,863
E307B/E309	Water Recycle HX to Sec I	1	48,956	244,674	337,059
E308	Iodine Recycle HX to Sec I	5	108,338	530,343	530,343
S101	Condenser Drum	40	261,255	2,122,423	3,507,579
C301	Reactive Distillation Column	40	5,825,477	47,325,886	85,749,055
C301i	Reactive Distillation Column Internals	40	1,007,012	8,962,403	8,962,403
C302	Hydrogen Scrubber	1	9,839	79,930	133,756
C303	Iodine Wash Column	1	11,526	93,636	160,366
P301	Feed Pump	40	3,683,448	26,434,398	27,557,849
TE301	Recycle Water Expander	5	1,608,956	9,653,733	9,653,733
TE302	Recycle Iodine Expander	5	2,343,904	14,063,421	14,063,421
TE303	Recycle Iodine Expander	1	137,214	823,286	823,286
Subtotals for Section 3			23,185,436	144,488,929	270,650,658

Table 3–13
Preliminary Capital Cost Estimate Summary — 4200 mole/s

Description		Equiv CS FOB Cost ($)	Bare Module Cost ($)	Bare Module Cost plus Adders ($)
Subtotals for Section 1	($)	7,720,304	42,491,924	70,505,203
Subtotals for Section 2	($)	8,121,082	122,994,753	131,616,800
Subtotals for Section 3	($)	23,185,436	144,488,929	270,650,658
Total CS FOB Cost	($)	39,026,822		
Total Bare Module Cost	($)		309,975,606	
Total Bare Module Cost with Adders	($)			472,772,661
Contingency and Fee	($)			85,099,079
Total Module Cost	($)			557,871,740

Table 3–13 (Cont.)

Description		Equiv CS FOB Cost ($)	Bare Module Cost ($)	Bare Module Cost plus Adders ($)
Auxiliary Facilities Cost	($)			13,659,388
Fixed Capital Investment	($)			571,531,128
Initial Chemical Inventory Cost	($)			114,802,000
Overnight Capital Investment	($)			686,333,128
Interest during construction (7% APR)	($)			79,340,110
Total Capital Investment	($)			765,673,238

Standard factors are used in Table 3–13 to calculate the total capital investment from the Total Installed Equipment Cost (Total Bare Module Cost with Adders). The Contingency and Fee are 18% of the Installed Equipment Cost. The Auxiliary Facilities cost is 35% of the FOB equipment cost based and carbon steel construction. The Initial Chemical Inventory is discussed below. Interest during Construction is calculated assuming that the construction funds will be borrowed linearly over the three years of construction and the 7% cost of construction funds is compounded monthly.

The Initial Chemical Inventory Cost requires additional discussion. The initial chemical inventory is almost exclusively iodine. The iodine is a major cost item because there is such a large recycle of HI_x between Sections 1 and 3 for the reactive distillation flowsheet. Analysis of the iodine inventory of the system indicates that it is almost entirely within the heat exchangers of Section 3. The volume of the heat exchangers has been minimized by using the PCHX concept as employed in the sulfuric acid decomposer. The PCHX requires both a heat exchange area than an equivalent shell and tube heat exchanger and a much smaller internal volume per unit heat exchange area. The cost per pound of exchanger is higher for a PCHX but these exchangers is so much smaller that the costs, for a given duty, are assumed to be the same as for the shell and tube heat exchangers initially specified and used in the capital cost estimate. The cost of the iodine inventory was valued at $13/kg, slightly more than the $2002 import cost.

The operating cost of a chemical plant is based on many factors, some of which can be estimated based on the total chemical plant investment and others on the design philosophy of the plant. Where applicable, we used the factors given by Peters and Timmerhaus [3–14] to estimate the operating cost of the hydrogen plant, as indicated in Table 3–14. Other factors are based on engineering estimates for a highly automated plant.

Table 3–14
Annual Operating Cost Estimate — 4200 mole/s

Cost Item	Basis	Annual Cost ($)
Operating Labor	15 operators per shift on 4 rotating shifts at $80,000/person year.	4,800,000
Supervisory and Clerical Labor	15% of operating labor	720,000
Maintenance and Repairs	6% of fixed capital investment	34,291,868
Operating Supplies	15% of maintenance and repairs	5,143,780
Laboratory Charges	15% of operating labor	720,000
Patents and Royalties	None	0
Taxes	2% of fixed capital investment	11,430,623
Administrative Costs	20% of operating labor	960,000
Total Operating Costs		58,066,271

As indicated earlier, the sizing and costing of the chemical plant was carried out concurrently with matching of the plant to the reactor. The hydrogen plant was assumed to operate at 50% efficiency or 4200 moles/s but the matching effort indicated that, for the process conditions chosen, the efficiency is 42%. Rather than increase the number of nuclear reactors to match the larger energy requirements of the chemical plant we have costed, we will scale back the size of the chemical plant. Since the cost of a piece of chemical equipment tends to scale with the size to a power varying between 0.6 and 1.0, the cost of process equipment, on a per unit throughput basis, will increase as the throughput is decreased. For this hydrogen plant, much of the decrease in throughput will be obtained by decreasing the number of parallel units. In a few cases, the equipment will be smaller and in others the equipment size will actually increase because in reducing the number of parallel items, the size of each item will be increased. We will assume that, for the range of throughputs contemplated, the capital and operating costs are proportional to the throughput. We will also cost a plant operating at 52% efficiency on the same basis.

3.12. Reactor Costing

A considerable effort has been made by the GA Reactor Group to develop the capital costs for Modular Helium Reactors that produces electricity by means of a gas turbine in the primary helium coolant circuit. Table 3–15 gives their capital cost of an Nth of a kind Gas Turbine Modular Helium Reactor (GT-MHR) as well as the cost of a Process Heat Turbine Modular Helium Reactor (PH-MHR) operating with the same helium outlet temperature. In Table 3–15 we have broken out the costs of Intermediate Heat Exchanger (IHX) and Primary Circulator from the Reactor Plant Equipment, so that they are more obvious, and added our estimates of the cost of the Secondary Circulator and the Secondary Helium Duct (SHD), which connects the reactor to the process. The Secondary Circulator is estimated at

Table 3–15
Nth-of-a-Kind Plant Capital Cost (2002 K$) for Four 600 MWt Gas Turbine (GT-MHR), Process Heat (PH-MHR) or Hydrogen (H_2-MHR) Modular Helium Reactors at a Single U.S. Site

Account	Account Description	GT-MHR (850°C)	PH-MHR (850°C)	H2-MHR (950°C)
	Direct Costs			
20	Land and Land Rights	0	0	0
21	Structures and Improvements	132,360	132,133	132,133
22	Reactor Plant Equipment	442,586	254,226	311,427
23	Turbine Plant Equipment	91,474	0	0
24	Electric Plant Equipment	61,510	49,582	49,582
25	Miscellaneous Plant Equipment	28,043	28,043	28,043
26	Heat Rejection System	32,614	0	0
	Intermediate Heat Exchanger	0	56,000	68,600
	Primary Circulator	0	33,000	40,425
	IHX Circulator	0	22,000	26,950
	Reactor-Process Ducting	0	38,070	38,070
	Total Direct Cost	788,587	613,054	695,230
	Indirect Costs			
91	Construction Services	82,959	64,493	73,138
92	Home Office Engr. and Services	25,393	19,740	22,386
93	Field Office Engr. And Services	28,310	22,009	24,959
94	Owner's Cost	138,003	107,284	121,665
	Total Indirect Costs	274,665	213,526	242,148
	Base Construction Cost	1,063,252	826,580	937,378
	Contingency	53,163	41,329	46,869
	Overnight Plant Construction Cost	1,116,415	867,909	984,247
	Interest During Construction	129,058	100,330	113,779
	Total Capital Investment	1,245,473	968,239	1,098,026
	MWe @ 47.7% eff.	1,145		
	$/kWe @ 47.7% eff.	975		
	MW-H_2 @ 42% eff.		1008	
	$/kW-$H_2$ @ 42% eff.		861	
	MW-H_2 @ 52% eff.			1,248
	$/kW-$H_2$ @ 52% eff.			760

two/thirds the cost of the Primary Circulator as it is not in the primary coolant system and does not require provision for remote maintenance. We calculated the cost of the SHD assuming it is a coaxial duct similar to that used to connect the reactor to the reactor to the power conversion vessel of the GT-MHR. Assuming that the SHD is 100 m long and the fabricated cost ($3.87/lb) is the same as for a large horizontal vessel made from Alloy 20. Using this method, the cost is the same for four ducts, one from each reactor, as for a single duct of twice the diameter but four times the capacity.

Table 3–15 also estimates the cost of a higher temperature reactor more suited for hydrogen production. Costs for this Hydrogen Modular Helium Reactor (H2-MHR) were derived from the PH-MHR by assuming that the high temperature portions of the H2-MHR cost 22.5% more than the same portions of the PH-MHR. Note that this factor was not applied to the Secondary Helium Duct. The helium return temperature is the same for both the H2-MHR and the PH-MHR and the inside of the inner pipe and the outside of the outer pipe of the SHD are insulated so that both walls run at the return helium temperature.

The operating cost of the nuclear reactor is composed of several factors. These were provided by the GA Reactor Group in the form of a fuel cycle cost of 7.4 mil/kWh and an operating and maintenance cost of 3 mil/kWh, for a GT-MHR operating at 47.7% efficiency. The fuel cycle cost corresponds to a cost of $74,260,000 per year for four 600 MW reactors operating at 100% availability. The operating and maintenance cost of the GT-MHR is $30,110,000 per year but, as the process heat reactors have less equipment, their O&M costs will be less. Assuming the O&M costs scale as the capital cost, the O&M cost is $23,400,000 per year for the PH-MHR and $26,540,000 for the H2-MHR.

3.12.1. Cost of Hydrogen

We have estimated the capital and operating costs of the nuclear plant and the chemical plant but the ultimate cost of hydrogen also depends on the operating scenario and the cost of money. Table 3–16 indicates the cost of hydrogen for both the PH-MHR and H_2-MHR. We assume, for our calculations, that the overall availability of the chemical and nuclear plant is 90%. Currently, nuclear reactors operate at availabilities of greater than 90% as do modern chemical plants. Periodic maintenance of the chemical plant components can be scheduled to coincide with refueling of the nuclear reactors. To the extent that the chemical plant is modular, a portion of the chemical plant can be shut down for maintenance while the parallel components remain online.

Both the nuclear reactor and chemical plant are capital intensive so the hydrogen cost is a strong function of interest rates. The table presents results for 10.5%, 12.5% and 16.5% capital recovery factors. The 10.5% factor may be typical of current interest rates whereas the 12.5% value in more typical of historic rates required by regulated utilities and the 16.5% is for unregulated utilities.

Table 3–16
Cost of Nuclear Hydrogen Using Sulfur-Iodine Process

Reactor		PH-MHR	H2-MHR	PH-MHR	H2-MHR	PH-MHR	H2-MHR
Hydrogen production efficiency		42%	52%	42%	52%	42%	52%
Overall Availability		90%	90%	90%	90%	90%	90%
Capital Recovery Factor		10.5%	10.5%	12.5%	12.5%	16.5%	16.5%
Water Cost	($/cubic meter)	1.00	1.00	1.00	1.00	1.00	1.00
Annual Reactor Capital Cost	(K$)	101,665	115,293	121,030	137,253	159,759	181,174
Annual Chemical Plant Capital Cost	(K$)	67,532	83,612	80,396	99,538	106,122	131,390
Annual Reactor O&M Cost	(K$)	23,400	26,540	23,400	26,540	23,400	26,540
Annual Chemical plant O&M Cost	(K$)	48,776	60,389	48,776	60,389	48,776	60,389
Annual Reactor Fuel Cycle Costs	(K$)	66,834	66,834	66,834	66,834	66,834	66,834
Annual water cost	(K$)	1,805	2,235	1,805	2,235	1,805	2,235
Total Annual Cost	(K$)	310,012	354,902	342,240	392,789	406,697	468,562
Annual Production	(tonne)	201,982	250,073	201,982	250,073	201,982	250,073
Cost	($/kg)	1.53	1.42	1.69	1.57	2.01	1.87

4. UNCERTAINTIES AND RISK REDUCTION

The sulfur-iodine cycle, coupled to a high temperature nuclear reactor, shows promise of economic hydrogen production in the future. Before nuclear hydrogen becomes commercial, the current uncertainties must be reduced. The technical uncertainties lie in several areas: chemistry, solution thermodynamics, chemical kinetics, and materials science. The economic uncertainties lie in the areas of capital and operating cost estimates, future costs of alternative clean (and dirty) hydrogen sources and the politics of global warming.

4.1. TECHNICAL UNCERTAINTIES

4.1.1. Chemistry

The chemistry of the Sulfur-Iodine (S-I) process is well understood and there are few potential side reactions. The side reactions, which could be problematic, are the formation of sulfur or hydrogen sulfide in Section 1. Sulfur dioxide can be disproportionate to form either elemental sulfur or hydrogen sulfide along with sulfuric acid. These reactions are in competition with the much more rapid Bunsen reaction but are energetically more favorable. Any hydrogen sulfide that is formed will eventually be recycled back to the oxygen scrubbers in Section 1 where conditions are favorable to the formation of elemental sulfur from hydrogen sulfide and sulfur dioxide. Thus the ultimate questions concerning side reactions are how much sulfur, if any, will be formed, where will it go and what will happen to it? Elemental sulfur is molten at the exit temperatures of Section 1. Any sulfur accompanying the sulfuric acid to Section 2 would accumulate in the H_2SO_4 vaporizer where it would react with the SO_3 forming SO_2. More likely, any elemental sulfur formed will accumulate in the iodine recycle stream.

Sulfur should be easily removed from iodine. If sulfur accumulates in the iodine, the sulfur removal will need to be demonstrated. Sulfur and iodine should be easily separable by distillation as their boiling points of differ by over 250°C. The sulfur would then be fed to the outlet of the sulfuric acid decomposer where the sulfur would be oxidized to SO_2 by O_2. Alternatively, the sulfur might be removed from the iodine by electrochemical oxidation. In either case, the maximum permissible concentration of sulfur in the iodine must be determined.

4.1.2. Solution Thermodynamics

The reactive distillation process for generating hydrogen appears to be viable but the current flowsheet is uncertain to the extent that the vapor-liquid equilibria of the system

$HI/I_2/H_2O$ are based on models and not experimentally determined. There is also some uncertainty in the enthalpy of solution of this system. The missing data can either be determined by specific experiments or in integral form from operation of prototypical process steps.

The liquid-liquid equilibria for $HI/I_2/H_2O/H_2SO_4$ are also very limited. Additional data would allow extrapolation to operating conditions outside the current operating envelope. Alternatively, one could simply extend the operating range through operation of prototypical process equipment.

4.1.3. Chemical Kinetics

The chemical kinetics of HI decomposition under the conditions of the reactive distillation column are unknown. If the kinetics are too slow for economic operation, a catalyst may be needed. The kinetics need to be examined in the absence of catalyst and in the presence of supported catalysts in both gas and liquid phases and liquid phase solution catalysts.

4.1.4. Material Science

Significant headway has been made at determining applicable materials of construction for the sulfur-iodine process [4–1]. Materials applicable to Sections 1 and 2 have been, for the most part, adequately researched. The one area of Section 2 that presents some concerns is that of boiling heat transfer. The only materials resistant to concentrated sulfuric acid at the gas-liquid interface tend to be brittle materials such as siliconized cast iron and silicon carbide. Small heat exchangers have been made from such materials but such exchangers must be developed in the required sizes.

The containment materials for Section 3 will be similar to those in Section 1. The higher temperatures of Section 3 will be accommodated by the use of corrosion resistant insulating materials inside the chemical containment boundary. The heat transfer materials used in Section 1 may also be usable at the higher temperatures encountered in Section 3 but this needs to be verified.

4.2. ECONOMIC UNCERTAINTIES

The economic uncertainties are twofold: the projection of future hydrogen costs from alternative sources and the uncertainties in the capital cost of the nuclear hydrogen plant. We have no control over the future cost of hydrogen from alternative sources. The future cost of hydrogen from fossil sources will certainly increase. The increase may be dramatic if carbon sequestration is mandated or a carbon tax is imposed.

The uncertainties in the capital cost of the reactor and chemical plant are manageable. The cost estimate for the GT-MHR was performed very recently, with the aid of an A&E firm. The cost of the PH-MHR was derived from the GT-MHR cost by eliminating systems and should be equally firm. The cost presented for the H_2-MHR was extrapolated from the PH-MHR cost and should be updated during the current DOE effort at defining a Very High Temperature Reactor (VHTR) as part of their Generation IV effort. The uncertainties in the cost of the chemical plant will be reduced as the chemical uncertainties are reduced and a pilot plant is designed.

4.3. RECOMMENDATIONS FOR RISK REDUCTION

There are two possible approaches to obtaining the data necessary to implement large-scale production of hydrogen using the sulfur-iodine process and thus overcome the technical uncertainties indicated. The first is a science based approach utilizing a systematic and methodical examination of each area of uncertainty before proceeding further. The second is an engineering approach that builds on previous work in the area to provide specific targeted technology demonstrations. The science-based approach has the least risk but will delay the potential benefits to the nation of reduced pollution and increased reliability of the national energy supply. The engineering approach will provide clean hydrogen from nuclear energy in the shortest time frame and at the lowest overall development cost, but has some risks. We believe that a combination of the two approaches is optimal. We recommend that the engineering development be carried out in five phases: (1) demonstration of the complete process chemistry in an integrated laboratory scale flow loop, (2) design, fabrication, and operation of an engineering demonstration loop, (3) design, fabrication, and operation of a small nuclear hydrogen production demonstration plant, (4) design, fabrication, and operation of the first commercial nuclear hydrogen demonstration plant based on a single reactor module, and (5) design, fabrication, and operation of the first full scale nuclear hydrogen production demonstration plant powered by multiple reactor modules. The first three phases will probably require government participation but, assuming the demonstration plant is a success, the last two phases should be financed by industry. Laboratory studies, especially solution thermodynamics and material science investigations, should be carried out simultaneously with the engineering development, particularly during two demonstration phases. The material sciences investigations, in particular, can be “piggy backed” on to the operation of the demonstration loops at a minimal cost. During each phase engineering models of the process should be updated based on the latest scientific information and on operational data from the previous phase of scaleup. Table 4–1 gives the recommended scaleup steps and the degree to which process conditions and equipment construction would be typical of the final full-scale production plant. The efficiency will increase as the scale is increased due to the increased thermal integration possible with larger plants, the decrease in

heat losses from larger equipment, and the concurrent development of higher temperature nuclear reactors.

Table 4–1
Recommended Scaleup Steps

	Materials	Heat Source	Heat Integration	Efficiency	Hydrogen (kg/day)
Laboratory demonstration loop	Primarily glass/quarts with selected prototypical components	Electrical	None	Nil	0.2
Engineering demonstration loop	Prototypical	0.5 MW Electrical	Minimal	20%	60
Pilot plant	Prototypical	5 MW Electrical	Moderate	30%	900
Demonstration plant	Prototypical	50 MW_t Nuclear	Full	40%	12000
Commercial demonstration	Commercial	600 MW_t Nuclear	Full	42%	150000
Commercial production	Commercial	2400 MW_t Nuclear	Full	52%	760000

5. CONCLUSIONS

We have completed the task we set out to accomplish. We investigated the open literature for thermochemical cycles compatible with the efficient production of clean hydrogen from water using nuclear energy. We selected the Sulfur-Iodine (S-I) cycle as the cycle most likely to produce hydrogen efficiently and economically. We developed a chemical process flowsheet for the S-I cycle, suitable for a conservatively designed helium cooled reactor, operating at an 850°C helium outlet temperature (827°C maximum process temperature), and estimated the capital and operating costs for the reactor and chemical plant. The cost of the resulting hydrogen is highly dependent upon the cost of capital, but assuming public utility financing (10.5% capital recovery factor) the resulting hydrogen cost is $1.53/kg. Assuming a higher temperature reactor, 950°C helium outlet temperature and 950°C process temperature, we extrapolate a hydrogen cost of $1.42/kg.

At current long-term contract costs for natural gas, the projected costs of thermochemical hydrogen produced from water and nuclear energy are greater than those of the current process of choice, steam reforming of natural gas. The cost of hydrogen from steam reformation of natural gas are very sensitive to the cost of natural gas and, at the peak spot prices, nuclear hydrogen is very competitive. If natural gas costs continue to rise, as they have over the past few years, nuclear hydrogen will become competitive, even without a carbon tax or a CO_2 sequestration requirement.

The development of the flowsheet, and thus estimating the cost of hydrogen, was not without complications. The chemical systems of interest are very non-ideal and their thermodynamic descriptions are not simple. Table 5–1 indicates the chemical systems of the S-I process and their ranges of applicability. The thermodynamic description of the sulfuric acid water is adequate, but even it is suspect at the highest temperatures of interest. Fortunately, the highest temperature region is of little overall importance as the only process occurring at these temperatures is the total vaporization of the sulfuric acid stream and the vapor phase thermodynamic description is good. The thermodynamics of the iodine containing systems is questionable due to a lack of good experimental data over the total range of interest. The flowsheets presented are largely based on points data and extrapolation to conditions away from these conditions are tenuous. This is particularly the case for the vapor liquid equilibria for hydrogen iodide-iodine-water, where there are only total vapor pressure data (no vapor composition data), and those data are confounded by the hydrogen iodide decomposition equilibria. The flowsheet for the hydrogen iodide decomposition section relied heavily on the results or Roth and Knoche [E–5] and their model remains to be verified.

Table 5–1
Thermodynamic Models of Chemical Systems for Sulfur-Iodine Process

System	Section	Temperature (°C)	Pressure (bar)	Comments
$H_2SO_4/HI/I_2/H_2O$	1	25–150	1–10	Present model adequately describes phase equilibria but not chemical equilibria
H_2SO_4/H_2O	2	25–350	0.01–35	Model is good
$HI/I_2/H_2O$	3	25–350	1–80	Present model represents phase equilibria at a point but cannot describe phase equilibria of multistage processes

The results of this study represent our best estimate of the cost of hydrogen from an nth of a kind plant nuclear powered thermochemical hydrogen plant at today's capital costs. The uncertainties in the thermodynamics need to be resolved in the course of developing the process but current indications are that the process will soon become economically competitive. The recommended steps to demonstration of the S-I cycle were presented in Table 3–16. In short, they are (1) demonstrate the closed loop process at the intended temperatures and pressures to verify the chemistry of all process steps, (2) demonstrate operation, at a scale sufficient to verify projected efficiency, in a pilot plant employing actual materials of construction, and (3) demonstrate the commercial feasibility of the process using nuclear heat and a full scale helium-cooled nuclear reactor.

6. REFERENCES

[E–1] Brown, L.C., J.F. Funk and S.K. Showalter, "High Efficiency Generation of Hydrogen Fuels Using Nuclear Power, Annual Report, August 1, 1999 through July 31, 2000," General Atomics report GA–A23451 (2000).

[E–2] Brown, L.C., J.F. Funk and A.C. Marshall "High Efficiency Generation of Hydrogen Fuels Using Nuclear Power, Annual Report, August 1, 2000 through July 31, 2001," General Atomics report GA–A24187 (2002).

[E–3] Brown, L.C., J.F. Funk and S.K. Showalter, "Initial Screening of Thermochemical Water-Splitting Cycles for High Efficiency Generation of Hydrogen Fuels Using Nuclear Power," General Atomics Report GA–A23373 (2000).

[E–4] Norman, J.H., G.E. Besenbruch, D.R. O'Keefe and C.L. Allen, "Thermochemical Water-Splitting Cycle, Bench-Scale Investigations, and Process Engineering, Final Report for the Period February 1977 through December 31, 1981," General Atomics Report GA–A16713, DOE Report DOE/ET/26225-1.

[E–5] Roth, M., and K.F. Knoche, "Thermochemical Water-Splitting through Direct HI-Decomposition from $H_2O/HI/I_2$ Solutions," Int. J. Hydrogen Energy, **14**, 545 (1989).

[1–1] International Energy Outlook 2000: DOE/EIA-0484(2000)], The Energy Information Administration of the Department of Energy (www.eia.doe.gov).

[1–2] Annual Energy Outlook 2000 with Projections to 2020: DOE/EIA-0383(2000), The Energy Information Administration of the Department of Energy (www.eia.doe.gov).

[1–3] Analysis of the Impacts of an Early Start for Compliance with the Kyoto Protocol: SR/OIAF/99-02, The Energy Information Administration of the Department of Energy (www.eia.doe.gov).

[1–4] Impacts of the Kyoto Protocol on U.S. Energy Markets and Economic Activity: SR/OIAF/98-03, The Energy Information Administration of the Department of Energy (www.eia.doe.gov).

[2–1] Brecher, L.E., S. Spewock, et al., "Westinghouse Sulfur Cycle for the Thermochemical Decomposition of Water," Int. J. Hydrogen Energy **21**, 7 (1977).

[2–2] Beghi, G.E., "A Decade of Research on Thermochemical Hydrogen at the Joint Research Center, Ispra," Int. J. Hydrogen Energy **11**, 761 (1986).

[2–3] Yoshida, K., H. Kameyama, et al., "A Simulation Study of the UT-3 Thermochemical Hydrogen Production Process," Int. J. Hydrogen Energy **15**, 171 (1990).

[2–4] Besenbruch, G.E., "General Atomic Sulfur-Iodine Thermochemical Water-Splitting Process," Am. Chem. Soc., Div. Pet. Chem., Prepr. **271**, 48 (1982).

[2–5] Williams, L.O., Hydrogen Power (Pergamon Press, 1980).

[2–6] Ueda, R., H. Tagawa, et al., "Production of Hydrogen from Water Using Nuclear Energy," A review, Japan At. Energy Res. Inst., Tokyo, Japan (1974) p. 69.

[2–7] Tamaura, Y., A. Steinfeld, et al., "Production of Solar Hydrogen by a Novel, 2-Step, Water-Splitting Thermochemical Cycle," Energy (Oxford) **20**, 325 (1995).

[2–8] Bamberger, C.E., "Hydrogen Production from Water by Thermochemical Cycles; a 1977 Update," Cryogenics **18**, 170 (1978).

[2–9] Knoche, K.F., and P. Schuster, "Thermochemical Production of Hydrogen by a Vanadium/Chlorine Cycle. Part 1: An Energy and Energy Analysis of the Process," Int. J. Hydrogen Energy **9**, 457 (1984).

[2–10] Russell, J., and J. Porter, "Production of Hydrogen from Water," General Atomics Report GA–A12889 (1974).

[3–1] "Synfuels from Fusion — Using the Tandem Mirror Reactor and a Thermochemical Cycle to produce Hydrogen," R.H. Werner, ed., Lawrence Livermore Laboratory Report UCID-19609 (1982).

[3–2] Annon, "Sulfuric Acid Concentration System," Kimura Chemical Plants Co., LTD. 1-2 Kuise-Terajima 2-Chome, Amagasaki, Hyogo 660, Oki Technical Review **63** (1998).

[3–3] Leva, M., Chem. Eng. Prog. **88**, 65 (1992).

[3–4] Schleicher, R.W., A.R. Raffray, C.P. Wong, "An assessment of the Brayton Cycle for High Performance Power Plants," General Atomics Report GA–A23550 (2000).

[3–5] Seader, J.D., E.J. Henley, Separation Process Principles, (Wiley, New York, 1998).

[3–6] Fair, J.R., Petro/Chem. Eng., **33**, 211 (1961).

[3–7] Chilton, T.H., and A.P. Colburn, Ind. Eng. Chem., 27, 255-260, 904 (1935).

[3–8] Perry's Chemical Engineers' Handbook, D.W. Green, ed., Seventh Ed. (McGraw Hill, New York, 1997).

[3–9] Bell, K.J., "Final Report of the Cooperative Research Program on Shell and Tube Heat Exchangers," Bulletin No. 5, University of Delaware, Engineering Experiment Station (1963).

[3–10] Guthrie, K.M., "Data and Techniques for Preliminary Capital Cost Estimating," Chem. Eng. Prog., 114–142 (1969).

[3–11] Ulrich, G.D., A Guide to Chemical Engineering Process Design and Economics (Wiley, New York, 1984).

[3–12] Turton, et al., Analysis, Synthesis, and Design of Chemical Processes (Prentice Hall, New Jersey, 1998).

[3–13] Chemical Engineering, (McGraw-Hill, last page of every issue).

[3–14] Peters, M.S., and K.D. Timmerhaus, Plant Design and Economics for Chemical Engineers (McGraw Hill, New York, 1980).

[4–1] Trester, P.W., and H.G. Staley, "Assessment and Investigation of Containment Materials for the Sulfur-Iodine Thermochemical Water-Splitting Process for Hydrogen Production: Final Report, July 1979 — December 1980," General Atomics Report GA–A16328, Gas Research Institute Report GRI-80/0081 (1981).

7. ACKNOWLEDGMENTS

This work was performed as a collaborative effort between General Atomics, the University of Kentucky and Sandia National Laboratories. Work at General Atomics and the University of Kentucky was supported by the Department of Energy under Nuclear Energy Research Initiative (NERI) Grant No. DE-FG03-99SF21888. Work at Sandia National Laboratories, a multiprogram laboratory operated by Sandia Corporation, a Lockheed Martin Company, was funded by the Department of Energy through contract No. DE-AC04-94AL85000 under NERI Award No. DE-FG03-99SF023.

ATTACHMENT
GENERAL ATOMICS REPORT GA–A23451

GA–A23451

HIGH EFFICIENCY GENERATION OF HYDROGEN FUELS USING NUCLEAR POWER

ANNUAL REPORT TO THE U.S. DEPARTMENT OF ENERGY

AUGUST 1, 1999 THROUGH JULY 31, 2000

by
L.C. BROWN, J.F. FUNK, and S.K. SHOWALTER

Prepared under
Nuclear Energy Research Initiative (NERI)
Grant No. DE-FG03-99SF21888
for the U.S. Department of Energy

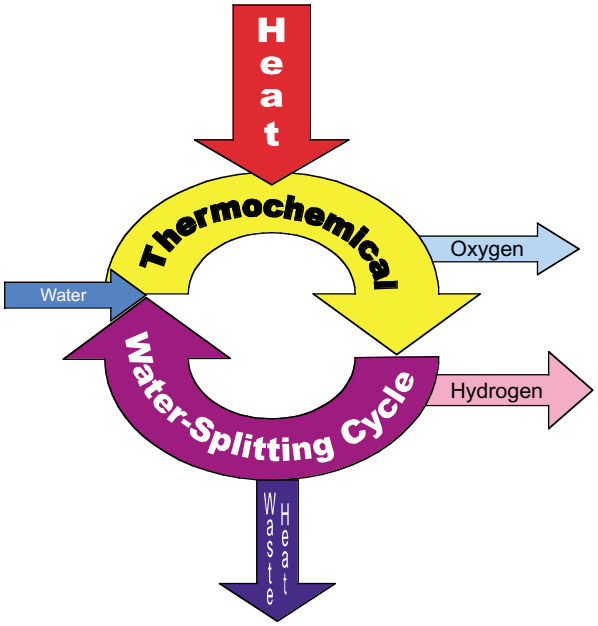

DATE PUBLISHED: JULY 2000

DISCLAIMER

This report was prepared as an account of work sponsored by an agency of the United States Government. Neither the United States Government nor any agency thereof, nor any of their employees, makes any warranty, express or implied, or assumes any legal liability or responsibility for the accuracy, completeness, or usefulness of any information, apparatus, product, or process disclosed, or represents that its use would not infringe privately owned rights. Reference herein to any specific commercial product, process, or service by trade name, trademark, manufacturer, or otherwise, does not necessarily constitute or imply its endorsement, recommendation, or favoring by the United States Government or any agency thereof. The views and opinions of authors expressed herein do not necessarily state or reflect those of the United States Government or any agency thereof.

GA–A23451

HIGH EFFICIENCY GENERATION OF HYDROGEN FUELS USING NUCLEAR POWER

ANNUAL REPORT TO THE U.S. DEPARTMENT OF ENERGY

AUGUST 1, 1999 THROUGH JULY 31, 2000

by
L.C. BROWN, J.F. FUNK,* and S.K. SHOWALTER†

*University of Kentucky, Lexington, Kentucky.
†Sandia National Laboratories, Albuquerque, New Mexico.

Prepared under
Nuclear Energy Research Initiative (NERI)
Grant No. DE-FG03-99SF21888
for the U.S. Department of Energy

GENERAL ATOMICS PROJECT 30047
DATE PUBLISHED: JULY 2000

EXECUTIVE SUMMARY

Currently no large scale, cost-effective, environmentally attractive hydrogen production process is available for commercialization nor has such a process been identified. Hydrogen is a promising energy carrier, which potentially could replace the fossil fuels used in the transportation sector of our economy. Fossil fuels are polluting and carbon dioxide emissions from their combustion are thought to be responsible for global warming.

The purpose of this work is to determine the potential for efficient, cost-effective, large-scale production of hydrogen utilizing high temperature heat from an advanced nuclear power station. The benefits of this work will include generation of a low-polluting transportable energy feedstock in a highly efficient method that has little or no implication for greenhouse gas emissions from an energy source whose availability and sources are domestically controlled. This will help to ensure energy surety to a future transportation/energy infrastructure that is not influenced/controlled by foreign governments.

This report describes work accomplished during the first year (Phase 1) of a three year project whose objective is to "define an economically feasible concept for production of hydrogen, by nuclear means, using an advanced high temperature nuclear reactor as the energy source." The emphasis of the first phase was to evaluate thermochemical processes which offer the potential for efficient, cost-effective, large-scale production of hydrogen from water, in which the primary energy input is high temperature heat from an advanced nuclear reactor and to select one (or, at most three) for further detailed consideration.

The main elements comprising Phase 1 are:

- A detailed literature search to develop a database of all published thermochemical cycles.
- Develop a rough screening criteria to rate each cycle.
- Perform a first round of screening reducing initial list to 20–30 cycles.
- Report on the results of the first round.
- Perform a second round of screening using refined criteria and reducing the number of cycles under consideration to 3 or less.
- Report on the results of Phase 1.

Ten databases were searched (e.g., Chemical Abstracts, NTIS, etc.), and over 800 literature references were located which pertain to thermochemical production of hydrogen from water. The references were organized in a computerized literature database. Over 100 thermochemical water-splitting cycles were identified. The cycle data was also organized into a computer searchable database.

The first round of screening, using defined screening criteria and quantifiable metrics, yielded 25 cycles for more detailed study. The second round of screening, using refined criteria reduced the 25 to 2.

The two cycles selected for final consideration are the UT-3 cycle and the sulfur-iodine cycle. The UT-3 cycle was invented at the University of Tokyo and much of the early development was done there. This cycle has been studied extensively in Japan by a number of organizations, including Toyo Engineering and Japan Atomic Energy Research Institute (JAERI). After considering several different flowsheets making use of the UT-3 cycle, JAERI selected the so-called Adiabatic UT-3 process for further development. The predicted efficiency of the Adiabatic UT-3 process varies between 35% and 50% depending upon the efficiency of membrane separators, which are under development, and whether electricity is co-generated along with the hydrogen. A 10% overall efficiency increase is projected if co-generation is employed. Much of the type of work we contemplated, such as pilot plant operation, materials studies, and flow sheet development has already been performed for this cycle in Japan.

The sulfur-iodine cycle remains the cycle with the highest reported efficiency, based on an integrated flowsheet. Various researchers have pointed out improvements that should increase the already high efficiency (52%) of this cycle and, in addition, lower the capital cost. In Phases 2 and 3 we will investigate the improvements that have been proposed to the sulfur-iodine cycle and will generate an integrated flowsheet describing a thermochemical hydrogen production plant powered by a high-temperature nuclear reactor. The detailed flowsheet will allow us to size the process equipment and calculate the hydrogen production efficiency. We will finish by calculating the capital cost of the equipment and estimate the cost of the hydrogen produced as a function of nuclear power costs.

It would be advantageous, but not essential, if some form of joint collaboration can be established with the Japanese. In particular, we would like access to their latest experimental results on the chemistry of the sulfur-iodine cycle. Although we will concentrate our effort on the sulfur-iodine cycle, we retain an interest in the UT-3 cycle. The work we have proposed, and which we will carry out for the sulfur-iodine cycle has, to a large part, already been performed in Japan for the Adiabatic UT-3 process. We would encourage the Japanese to perform the required non-steady-state analysis of the

Adiabatic UT-3 process. After the Japanese and we have completed our respective tasks, we will have two processes from which to select a means of producing hydrogen using nuclear power.

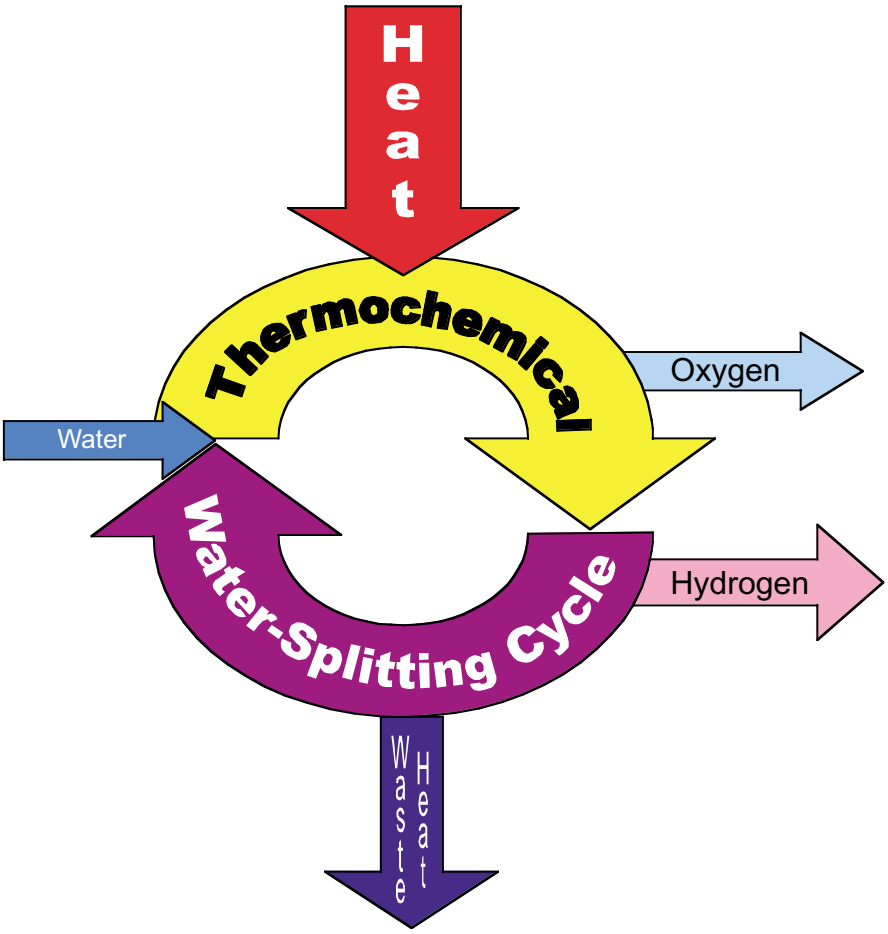

TABLE OF CONTENTS

LIST OF FIGURES

LIST OF TABLES

1. INTRODUCTION

Combustion of fossil fuels, used to power transportation, generate electricity, heat homes, and fuel industry, provides 86% of the world's energy [1, 2]. Drawbacks to fossil fuel utilization include limited supply, pollution, and carbon dioxide emissions. Carbon dioxide emissions, thought to be responsible for global warming, are now the subject of international treaties [3, 4]. Together, these drawbacks argue for the replacement of fossil fuels with a less-polluting potentially renewable primary energy such as nuclear energy. Conventional nuclear plants readily generate electric power but fossil fuels are firmly entrenched in the transportation sector. Hydrogen is an environmentally attractive transportation fuel that has the potential to displace fossil fuels. Hydrogen will be particularly advantageous when coupled with fuel cells. Fuel cells have higher efficiency than conventional battery/internal combustion engine combinations and do not produce nitrogen oxides during low-temperature operation. Contemporary hydrogen production is primarily based on fossil fuels and most specifically on natural gas. When hydrogen is produced using energy derived from fossil fuels, there is little or no environmental advantage.

There is currently no large scale, cost-effective, environmentally attractive hydrogen production process, available for commercialization, nor has such a process been identified. The objective of this work is to find an economically feasible process for the production of hydrogen, by nuclear means, using an advanced high-temperature nuclear reactor as the primary energy source. Hydrogen production by thermochemical water-splitting, a chemical process that accomplishes the decomposition of water into hydrogen and oxygen using only heat or, in the case of a hybrid thermochemical process, by a combination of heat and electrolysis, could meet these goals.

Hydrogen produced from fossil fuels has trace contaminants (primarily carbon monoxide) that are detrimental to precious metal fuel cells, as is now recognized by many of the world's largest automobile companies. Thermochemical hydrogen will not contain carbon monoxide as an impurity at any level. Electrolysis, the alternative process for producing hydrogen using nuclear energy, suffers from thermodynamic inefficiencies in both the production of electricity and in electrolytic parts of the process. The efficiency of electrolysis (electricity to hydrogen) is currently about 80%. Electric power generation efficiency would have to exceed 65% (thermal to electrical) for the combined efficiency to exceed the 52% (thermal to hydrogen) calculated for one thermochemical cycle.

Thermochemical water-splitting cycles have been studied, at various levels of effort, for the past 35 years. They were extensively studied in the late 70s and early 80s but received little attention in the past 10 years, particularly in the U.S. While there is no question about the technical feasibility and the potential for high efficiency, cycles with proven low cost and high efficiency have yet to be developed commercially. Over one hundred cycles have been proposed, but substantial research has been executed on only a few.

This report describes work accomplished during the first year (Phase 1) of a three-year project whose objective is to "define an economically feasible concept for production of hydrogen, by nuclear means, using an advanced high temperature nuclear reactor as the energy source." The emphasis of the first phase was to evaluate thermochemical processes which offer the potential for efficient, cost-effective, large-scale production of hydrogen from water in which the primary energy input is high temperature heat from an advanced nuclear reactor and to select one (or, at most three) for further detailed consideration.

This work is performed as a collaborative effort between General Atomics (GA), the University of Kentucky (UK) and Sandia National Laboratories (SNL) under the Department of Energy under Nuclear Energy Research Initiative (NERI) Grant No. (DE-FG03-99SF21888 (GA/UK).

The work was divided into several tasks. Each task was performed according to the predetermined schedule (Fig. 1) and all technical tasks were completed as scheduled. All of the collaborators were involved in every task but one organization had responsibility for the task. The Phase 1 tasks and the responsible organizations are:

Literature survey of new processes	UK
– Cycle database	SNL
Develop screening criteria	GA
Carry out first round screening	GA
Short report on conclusions	GA
Carry out second round screening	GA
Write Phase 1 report	GA

As reported here, an exhaustive literature search was performed to locate all cycles previously proposed. The cycles located have been screened using objective criteria, to determine which can benefit, in terms of efficiency and cost, from the high-temperature capabilities of advanced nuclear reactors. The literature search, the development of the screening criteria, the screening process and the results will be described in the following sections. Subsequently, the cycles were analyzed as to their adaptability to advanced

high-temperature nuclear reactors, considering among other things, the latest improvements in materials of construction and new membrane separation technologies. Guided by the results of the secondary screening process, one cycle was selected for integration into the advanced nuclear reactor system.

In Phases 2 and 3, which are to follow, the required flowsheets will be developed and preliminary engineering estimates of size and cost will be made for major pieces of equipment. From this information, a preliminary estimate of efficiency and cost of hydrogen will be made. This follow-on effort will perform the work scope and follow the schedule of the original proposal, as amended prior to contract award.

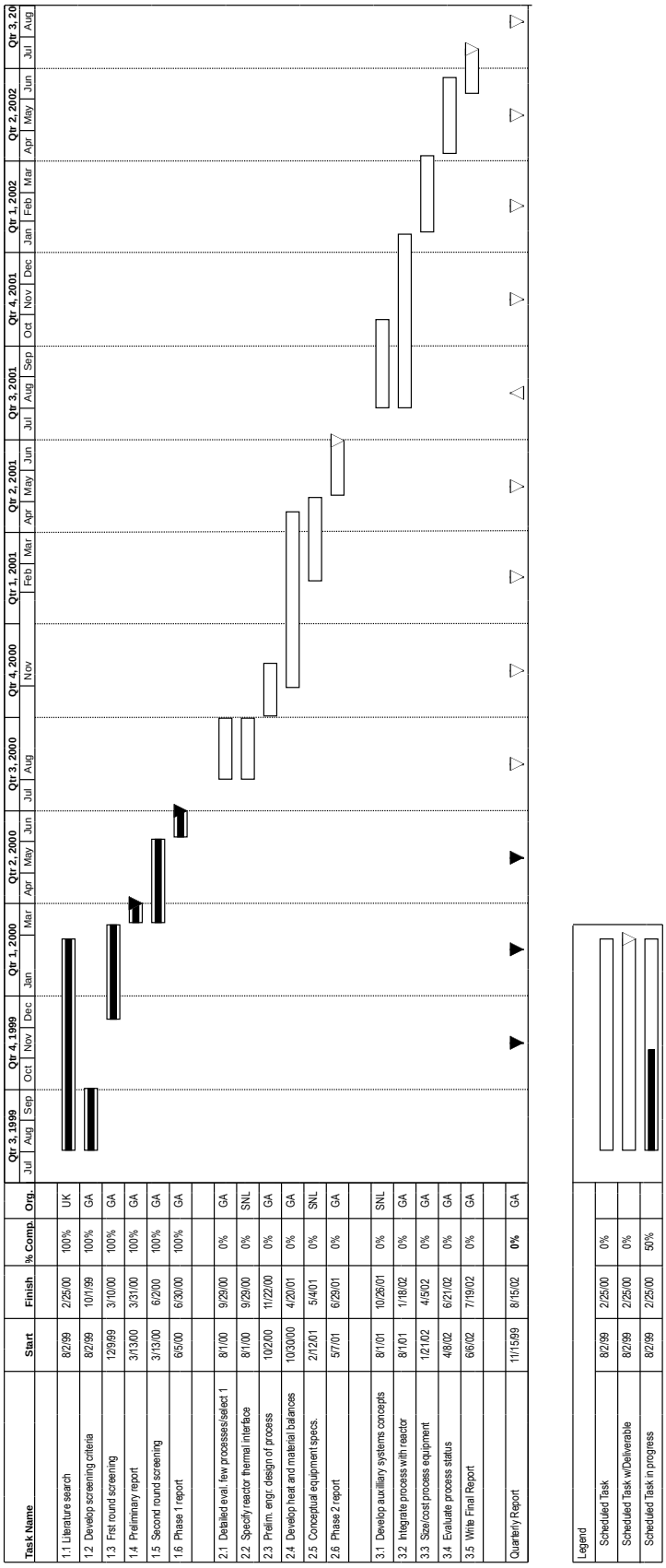

Fig. 1. Schedule of all three phases.

2. THERMOCHEMICAL WATER SPLITTING

Thermochemical water-splitting is the conversion of water into hydrogen and oxygen by a series of thermally driven chemical reactions. The direct thermolysis of water requires temperatures in excess of 2500°C for significant hydrogen generation.

(1*) $H_2O \rightarrow H_2 + {}^1/_2O_2$ (2500°C min)

At this temperature, 10% of the water is decomposed and 90% of the water would be recycled. In addition, a means of preventing the hydrogen and oxygen from recombining upon cooling must be provided or no net production would result. A thermochemical water-splitting cycle accomplishes the same overall result using much lower temperatures. The sulfur-iodine cycle is a prime example of a thermochemical cycle. It consists of three chemical reactions, which sum to the dissociation of water.

(2) $H_2SO_4 \rightarrow SO_2 + H_2O + {}^1/_2O_2$ (850°C)

(3) $I_2 + SO_2 + 2H_2O \rightarrow 2HI + H_2SO_4$ (120°C)

(4) $2HI \rightarrow I_2 + H_2$ (450°C)

(1) $H_2O \rightarrow H_2 + {}^1/_2O_2$

The thermochemical cycle has significant conversion at much lower temperatures. With a suitable catalyst, the high-temperature reaction (2) reaches 10% conversion at only 510°C, and 83% conversion at the indicated temperature of 850°C. Moreover, there is no need to perform a high temperature separation as the reaction ceases when the stream leaves the catalyst.

Energy, in the form of heat, is input to a thermochemical cycle via one or more endothermic high-temperature chemical reactions. Similar to the way that a heat engine must reject heat to a low temperature sink, a thermochemical cycle rejects heat via one or more exothermic low temperature chemical reactions. Finally, other thermally neutral chemical reaction may be required to complete the cycle so that all the reactants, other than water, are regenerated. In the case of the S-I, cycle most of the input heat goes into the oxygen generating reaction, the dissociation of sulfuric acid. Sulfuric acid and

*Note: Each chemical reaction retains a unique "reaction number" throughout this report.

hydrogen iodide are formed in the endothermic reaction of the S-I cycle and the hydrogen is generated in the mildly endothermic decomposition of hydrogen iodide.

The combination of high temperature endothermic reactions, low temperature exothermic reactions and energy neutral closing reactions are not sufficient for a cycle to be thermodynamically realizable. Each reaction must also have favorable ΔG (Gibbs free energy). The ΔG for a reaction is a measure of the concentrations of the reactants and products of the reaction at equilibrium. A reaction is favorable if ΔG is negative, or at least not too positive. A slightly positive ΔG does not mean that the reaction does not proceed, only that the reaction does not proceed far and high recycle may be required. It is possible to shift a reaction equilibrium by increasing the concentrations of the products or reducing the concentration of reactants. Each of the four chemical reactions of the UT-3 Cycle, in fact, has a slightly positive ΔG. The flow of gaseous reactant through the bed of solid reactants sweeps the gaseous products away resulting in total conversion of the solid reactants to solid products.

(5) $2Br_2(g) + 2CaO(s) \rightarrow 2CaBr_2(s) + {}^1/_2O_2(g)$ (672°C)

(6) $3FeBr_2(s) + 4H_2O(g) \rightarrow Fe_3O_4(s) + 6HBr(g) + H_2(g)$ 560°C)

(7) $CaBr_2(s) + H_2O(g) \rightarrow CaO(s) + 2HBr(g)$ (760°C)

(8) $Fe_3O_4(s) + 8HBr(g) \rightarrow Br_2(g) + 3FeBr_2(s) + 4H_2O(g)$ (210°C)

(1) $H_2O(g) \rightarrow H_2(g) + {}^1/_2O_2(g)$

Sometimes it is even possible to electrochemically force a non-spontaneous reaction: such a process is termed a hybrid thermochemical cycle to distinguish it from a pure thermochemical cycle. Hybrid cycles are often considered along with pure thermochemical cycles and we do so here. The hybrid sulfur cycle, also known as the Westinghouse cycle or as the Ispra Mark 11 cycle has the same high temperature endothermic reaction as the sulfur-iodine cycle. The hybrid cycle is closed by the electrochemical oxidation of sulfur dioxide to sulfuric acid.

(2) $H_2SO_4 \rightarrow SO_2 + H_2O + {}^1/_2O_2$ (850°C)

(9) $SO_2 + 2H_2O \rightarrow H_2SO_4 + H_2$ (80°C electrolysis)

(1) $H_2O \rightarrow H_2 + {}^1/_2O_2$

3. PROJECT DATABASES

An important part of the preliminary screening effort dealt with the details of organizing and presenting data in a easy to use form, i.e., the organization of project specific databases. There are many sources of compiled literature data. Each of these commercial databases uses its own method of organizing and presenting the same generic type of data. This makes it important that the data from the various sources be translated into a common format for comparison and duplicate removal. EndNote [5], a widely accepted and readily available database program designed to manage bibliographic information, is used to maintain the project literature database. EndNote provides the tools required for translating the output data from any of the various literature database search engines into a common format. Each EndNote entry includes the bibliographic entry, tracking information and, if available, an abstract.

A second database was required to keep track of all the thermochemical cycles. Here we had four main goals:

1. Inclusion of all the information required to screen the cycles
2. Ability to output reports with various parameters for the different cycles.
3. Ability to search for common threads among the various cycles and display the data electronically in alternative ways.
4. A means of preventing the same cycle from being entered multiple times.

Together, these indicated that we needed a relational database: we selected MS Access 2000 as the tool with which to organize the cycle data.

Figure 2 indicates the organization of the cycle database. A cycle represents a complete series of chemical reactions to produce water thermochemically (as in the University of Tokyo, UT-3 cycle). Reactions are the discreet reaction steps within a specific cycle. There are four main data table areas within the database: general, reactions, authors and references. Each of these tables was linked with a junction table that allowed a one-to-many relationship linked back to the general table. This allowed for a reference or reaction that was linked to multiple cycles to be represented only once in the database. The cycles were all uniquely identified by a primary identification (ID) number that was assigned automatically by the database in the order that they were entered. Some primary IDs are missing because, after entering cycles into the database and upon further examination, they were discovered to be duplicates of cycles already in

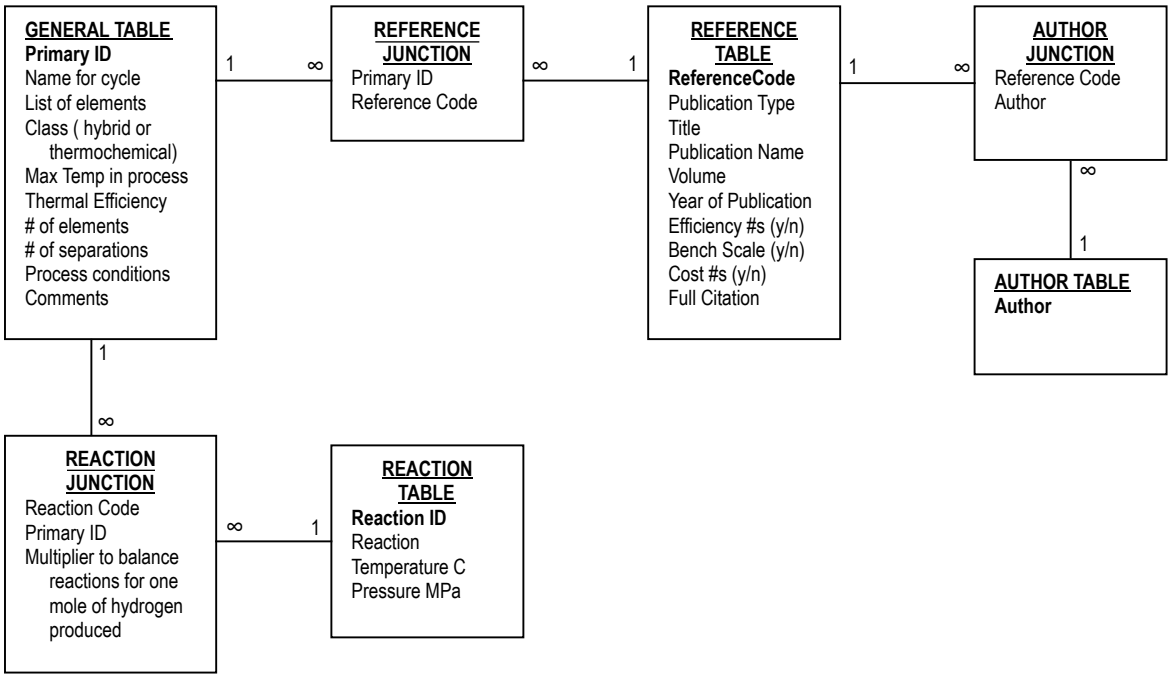

Fig. 2. Database structural relationship.

the database, or were not complete cycles. Names were assigned to ease reference in discussion when ranking the cycles. The names associated with the cycles were created from either given names in the references or names created from the compounds used in the cycle. The database format makes it easy to search for commonality between various cycles using a query (e.g. similar reactions, authors, compounds, etc.). The cycle database contains the details of the chemical reactions and process conditions for the process, as well as the abbreviated bibliographic information/literature references that describe or refer to the cycles. The start screen gives various choices to the researcher searching or entering data into the database (Fig. 3).

The first button takes you into the main database data entry area. The last two buttons generate reports for printing out lists of cycles and/or reactions. Pressing the first button takes you to the page represented by Fig. 4. The scroll bars and arrows at the bottom allow a user to “walk through” the database in sequential order. The raised buttons execute forms or queries to search or update the database.

Each of the junction tables needs a unique identifier to the attached data table to link with the primary ID and general table entry of the cycle. Therefore, there were identifiers for each reference, reaction and author independent of the primary ID identifier. Reference IDs were based on the initials of the first author of the reference followed by a number if needed to uniquely identify the reference. If only a company or institution was identified as the author, the uppercase initials are used to identify the reference. This

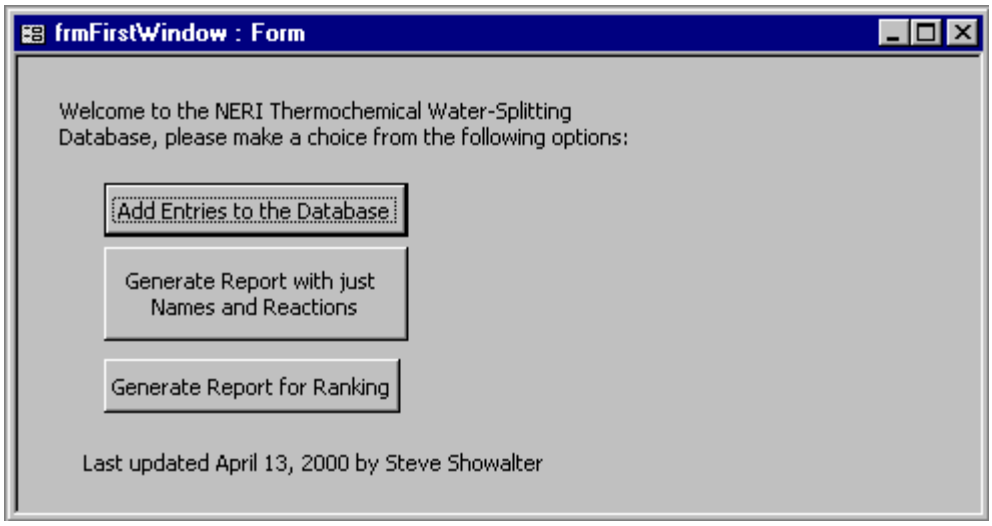

Fig. 3. Start page for thermochemical database.

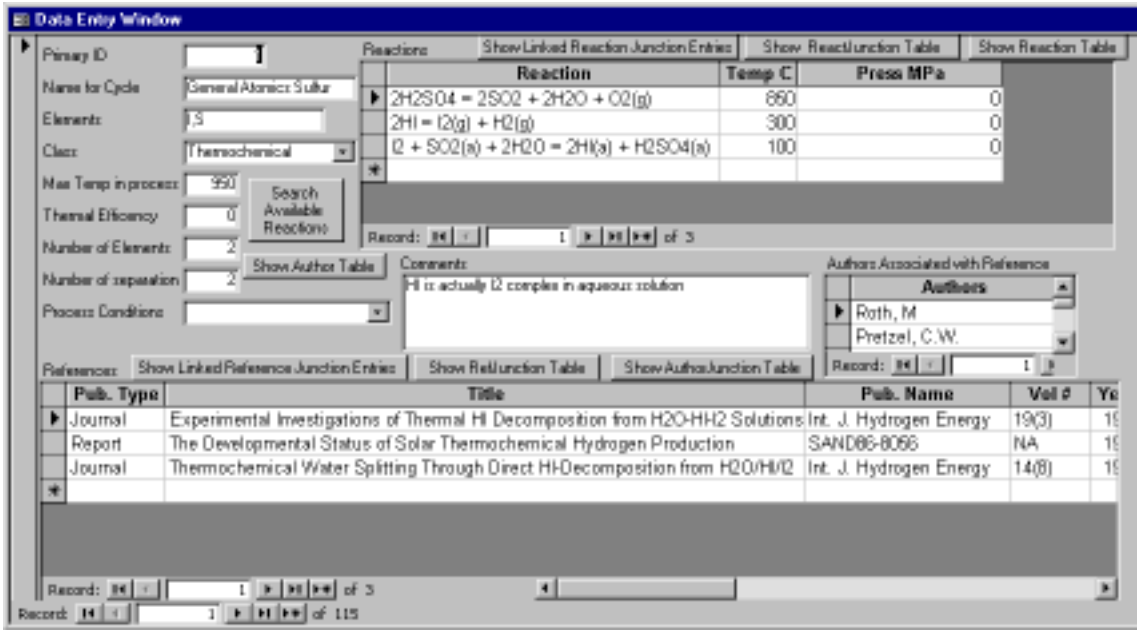

Fig. 4. Main data window for database.

allowed for papers, in which multiple cycles appeared, to be included in the database only once. Author IDs were simply the author's last name followed by the first two initials (Showalter, S.K.), this allowed for authors which appeared on multiple papers to be represented in the database uniquely. Rules were developed for addition of reactions to the database so that repetition could be easily identified. Reactants as well as products in each reaction were arranged in alphabetical order with H_2, H_2O and O_2 added to the end of the reactants or products in this order so as not to influence the naming convention

used for the reaction. The reaction ID consisted of the first compound in the reactants followed by a number if there were multiple reactions with the same starting compound. Therefore, all of the reactions were in a common format and it was simple to identify replicates by inspection. All data that was available to us was entered into the database however, many fields were left blank due to lack of information.

Many of the cycles have been the subjects of previous review articles. Data for these cycles was entered directly into the cycle database and, as the literature search identified additional cycles, they were added to the cycle database. Basic bibliographic data for each additional literature source, referring to a particular cycle, was added to the cycle database and linked to the cycle.

Data was entered into the database through the following procedure:

1. The cycle is first identified from a reference, compared with the general table database entries to determine if it is unique, then the general table information is entered (Fig. 5).

tblGeneral : Table

Primary ID	Name for Cycle	Elements	Class	Max Temp in process
1	General Atomics Sulfur	I,S	Thermochemical	950
2	NiFeMn Ferrite	Fe,Ni,Mn	Thermochemical	1000
3	Mark I-Oxide	Br,Ca,Hg	Thermochemical	750
4	Mark 9	Cl,Fe	Thermochemical	450
5	Cd/CdO	Cd	Hybrid	1200
6	Zn/ZnO	Zn	Thermochemical	2200
7	Iron Oxide	Fe	Thermochemical	2200
9	CO/Mn3O4	C,Mn	Thermochemical	977
10	Cl/Fe2O3	Cl,Fe	Thermochemical	739
11	Mark 1B	Br,Ca,Hg	Thermochemical	730
12	Mark 1C	Br,Ca,Cu	Thermochemical	900
13	Mark 1S	Br,Hg,Sr	Thermochemical	800
14	Mark 2 (1972)	C,Na,Mn	Thermochemical	800

Record: 1 of 115

Fig. 5. General table (not all fields shown).

2. Next the authors are compared to the available authors and if they are not represented then they are added to the authors table (Fig. 6).
3. Next the reference is added to the references table and assigned a unique reference ID (Fig. 7).
4. The author junction table is then used to join the author ID with the reference ID (Fig. 8).

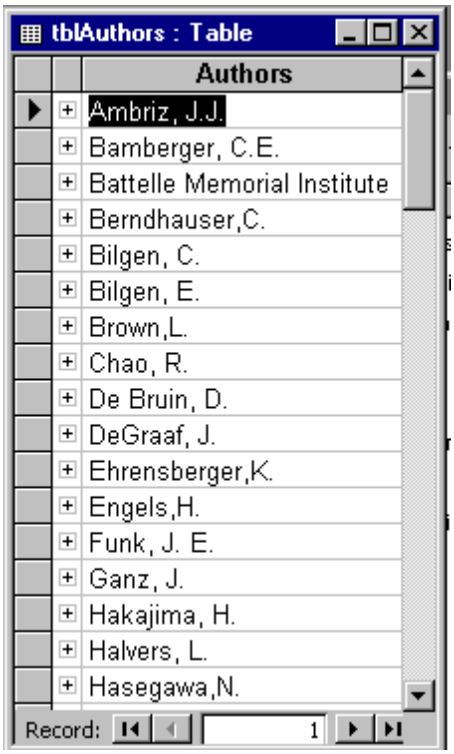

Fig. 6. Author table.

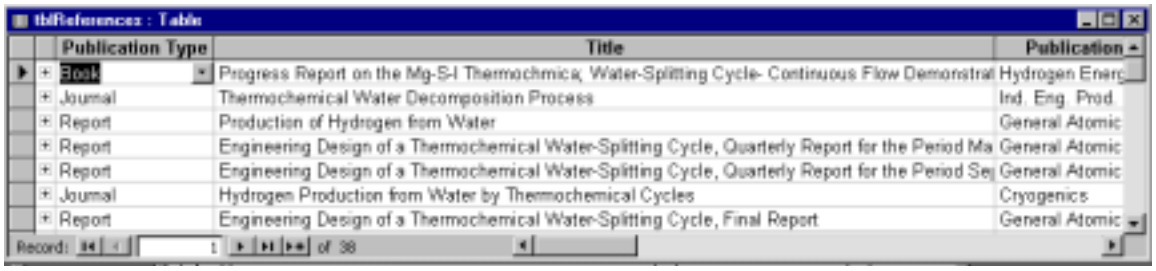

Fig. 7. Reference table (not all fields shown)

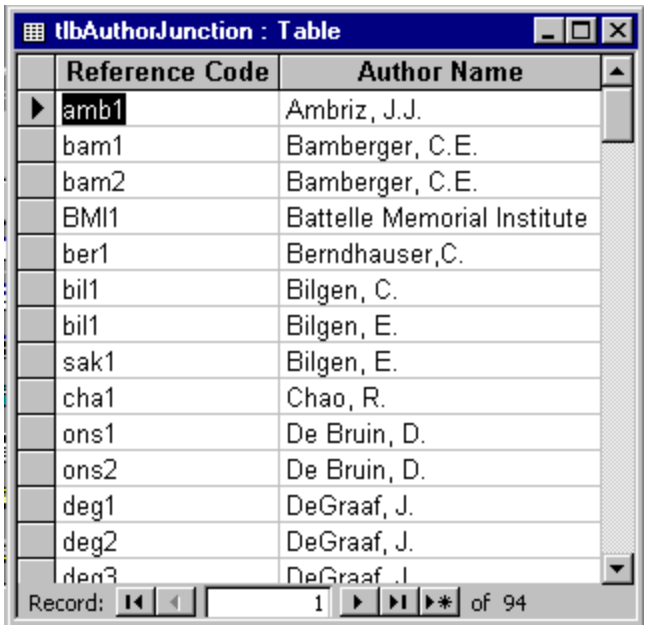

Fig. 8. Author junction to reference table.

5. The reference junction table is then used to join the reference ID to the general table (primary ID) entry (Fig. 9).
6. Finally the reactions in the cycle are rearranged to fit our format (as described previously), checked against the reaction table to determine if they are represented in the table, balanced, and finally normalized to remove all fractional exponents. If not present they are entered and assigned a reaction ID into the reaction table along with any temperature or pressure information (Fig. 10).
7. The reaction IDs are then joined to the general table through the reaction junction table.
8. The final step is to determine the fractional exponent that needs to be multiplied through each reaction in a cycle to normalize all of the reaction against the decomposition of one mole of water ($H_2O \rightarrow H_2(g) + {}^1/_2\ O_2(g)$). This number is then added to the reaction junction table (Fig. 11).

This procedure allowed us to generate a database of information that could be easily searched and updated allowing us to call up information on demand for our various selection requirements.

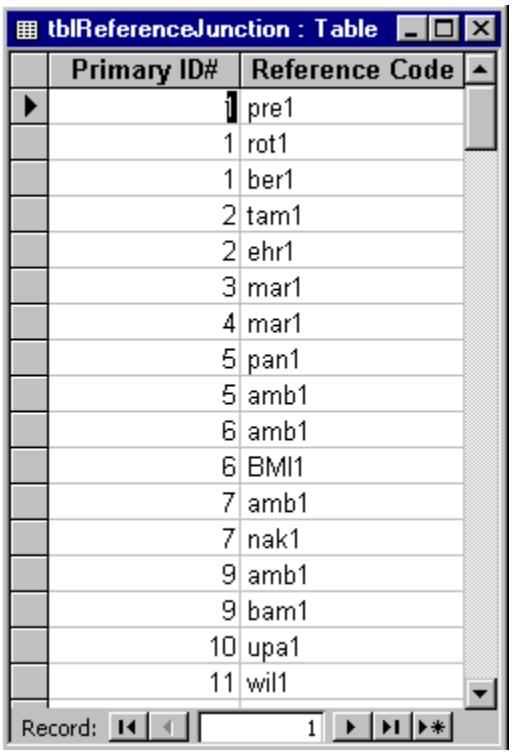

tblReferenceJunction : Table

Primary ID#	Reference Code
1	pre1
1	rot1
1	ber1
2	tam1
2	ehr1
3	mar1
4	mar1
5	pan1
5	amb1
6	amb1
6	BMI1
7	amb1
7	nak1
9	amb1
9	bam1
10	upa1
11	wil1

Record: 1

Fig. 9. Reference junction to general table.

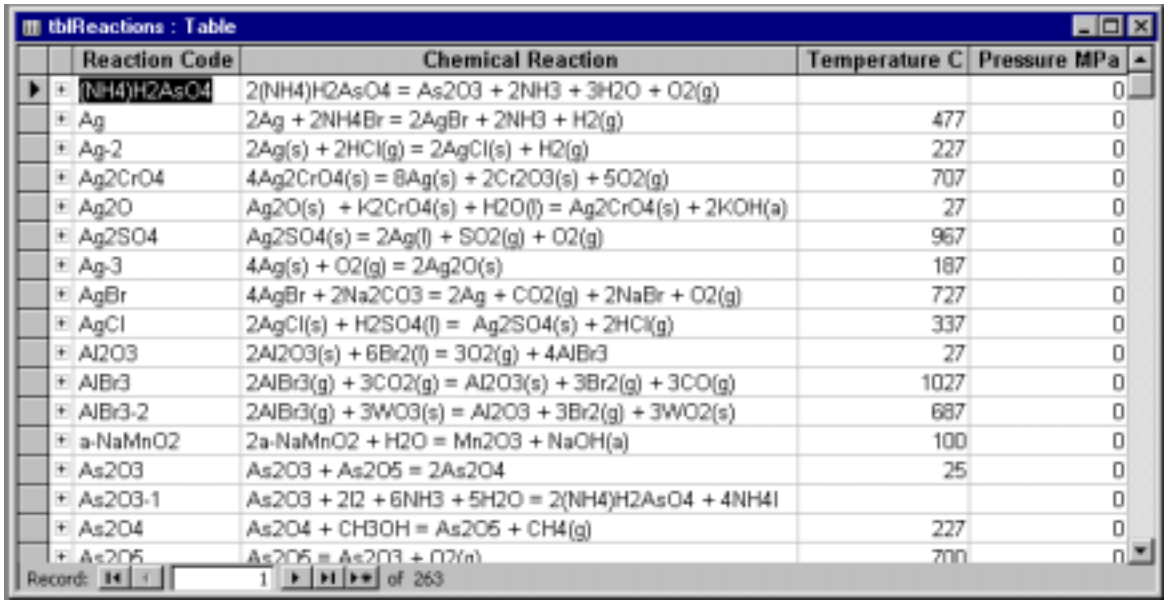

tblReactions : Table

Reaction Code	Chemical Reaction	Temperature C	Pressure MPa
(NH4)H2AsO4	2(NH4)H2AsO4 = As2O3 + 2NH3 + 3H2O + O2(g)		0
Ag	2Ag + 2NH4Br = 2AgBr + 2NH3 + H2(g)	477	0
Ag-2	2Ag(s) + 2HCl(g) = 2AgCl(s) + H2(g)	227	0
Ag2CrO4	4Ag2CrO4(s) = 8Ag(s) + 2Cr2O3(s) + 5O2(g)	707	0
Ag2O	Ag2O(s) + K2CrO4(s) + H2O(l) = Ag2CrO4(s) + 2KOH(a)	27	0
Ag2SO4	Ag2SO4(s) = 2Ag(l) + SO2(g) + O2(g)	967	0
Ag-3	4Ag(s) + O2(g) = 2Ag2O(s)	187	0
AgBr	4AgBr + 2Na2CO3 = 2Ag + CO2(g) + 2NaBr + O2(g)	727	0
AgCl	2AgCl(s) + H2SO4(l) = Ag2SO4(s) + 2HCl(g)	337	0
Al2O3	2Al2O3(s) + 6Br2(l) = 3O2(g) + 4AlBr3	27	0
AlBr3	2AlBr3(g) + 3CO2(g) = Al2O3(s) + 3Br2(g) + 3CO(g)	1027	0
AlBr3-2	2AlBr3(g) + 3WO3(s) = Al2O3 + 3Br2(g) + 3WO2(s)	687	0
a-NaMnO2	2a-NaMnO2 + H2O = Mn2O3 + NaOH(a)	100	0
As2O3	As2O3 + As2O5 = 2As2O4	25	0
As2O3-1	As2O3 + 2I2 + 6NH3 + 5H2O = 2(NH4)H2AsO4 + 4NH4I		0
As2O4	As2O4 + CH3OH = As2O5 + CH4(g)	227	0
As2O5	As2O5 = As2O3 + O2(g)	700	0

Record: 1 of 263

Fig. 10. Reaction table.

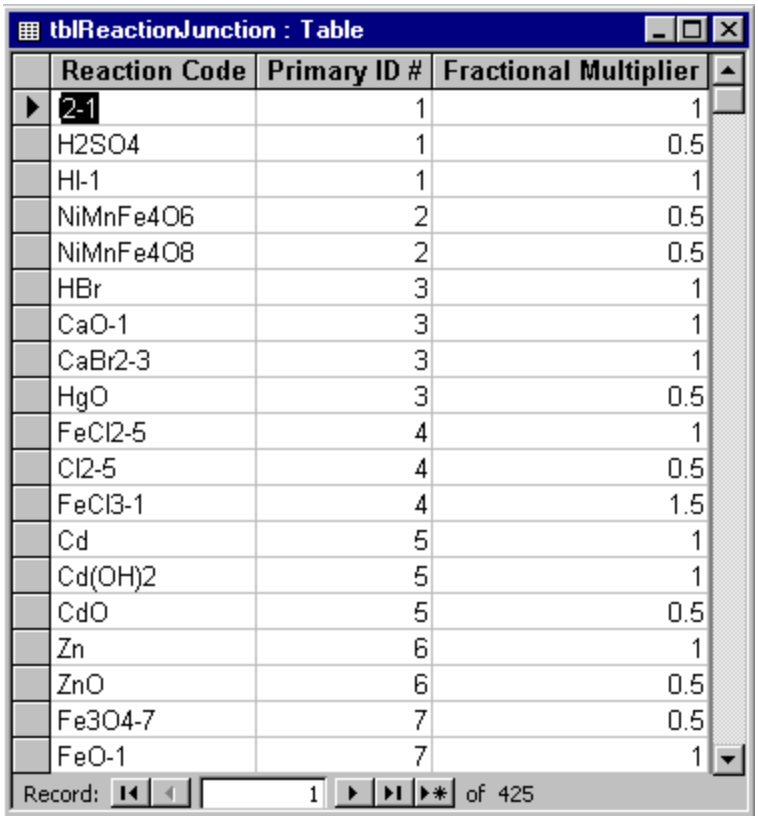

tblReactionJunction : Table

Reaction Code	Primary ID #	Fractional Multiplier
2-1	1	1
H2SO4	1	0.5
HI-1	1	1
NiMnFe4O6	2	0.5
NiMnFe4O8	2	0.5
HBr	3	1
CaO-1	3	1
CaBr2-3	3	1
HgO	3	0.5
FeCl2-5	4	1
Cl2-5	4	0.5
FeCl3-1	4	1.5
Cd	5	1
Cd(OH)2	5	1
CdO	5	0.5
Zn	6	1
ZnO	6	0.5
Fe3O4-7	7	0.5
FeO-1	7	1

Record: 1 of 425

Fig. 11. Reaction junction to general table.

4. LITERATURE SEARCH

The literature survey was designed to locate substantially all thermochemical water-splitting cycles that have been proposed in the open literature. Keywords were chosen and test searches were made using inexpensive databases as a means of testing search strategies. Thermochemical generation of hydrogen is usually referred to, by those who practice the art, as water-splitting. It was quickly determined that searches based upon water-splitting and "water splitting" lead to many thousands of hits — few of which were concerned with thermochemical water-splitting. Inspection of the titles showed a large number of biological, biochemical and photochemical articles and numerous titles dealing with corrosion and radiolysis. Moreover, some authors do not use the term water-splitting. Attempts to limit the search, by exclusion of biological and photochemical terms (Boolean NOT) exceeded the capabilities of the search engines before a significant reduction in number of hits was realized. It has proven to be much more profitable to build up a search criteria using inclusive criteria (Boolean AND/OR). The primary limit on the search has been the requirement of the inclusion of the term "thermochemical".

Chemical Abstracts Service (of the American Chemical Society) provides convenient access to many databases. Searching a large number of different databases can be very expensive and may produce a large number of redundant references to a single publication. The web site stnweb.cas.org allows one to simultaneously search a large number of databases at no cost, but the only results provided are the number of hits. This free search does allow one to quickly and inexpensively test various search strategies. Various Boolean searches were made of the CHEMENG cluster of databases in an attempt to optimize the search string and select the databases to be used for the "real" search. The search term ({water-splitting or water splitting or [(hydrogen or H_2) and (production or generation)]} and thermochemical) appeared to give very good results. The results from the databases showing a significant number of hits are given in Table 1.

The CAPLUS database was subjected to a full data retrieval search and over 50% of the hits are for papers related to thermochemical water-splitting. From the descriptors given for the various databases, it is likely that full searches of these databases, with the exception of NTIS, will result in hits that either duplicate hits resulting from the CAPLUS search or references previously entered into the EndNote literature database.

An example of an EndNote screen taken from our database is shown in Fig. 12. If additional information, such as an abstract is available it is displayed as shown in Fig. 13. More information about EndNote can be found at their website [5]. The formal search

TABLE 1
DATABASE HIT RESULTS

Hits	Databases	Description
905	CAPLUS	Chemical Abstracts Plus
448	COMPENDEX	COMPuterized ENgineering InDEX
440	NTIS	National Technical Information Service
322	INSPEC	The Database for Physics, Electronics and Computing. INSPEC corresponds to Physics Abstracts, Electrical & Electronics Abstracts, Computer & Control Abstracts, and Business Automation.
232	SCISEARCH	Science Citation Index Expanded
68	CEABA	Chemical Engineering And Biotechnology Abstracts
33	PROMT	Predicasts Overview of Markets and Technology — abstracts trade and business journals
28	INSPHYS	INSPHYS is a supplementary file to the INSPEC database. It contains those records from the former PHYS File from 1979 through 1994 that do not appear in INSPEC

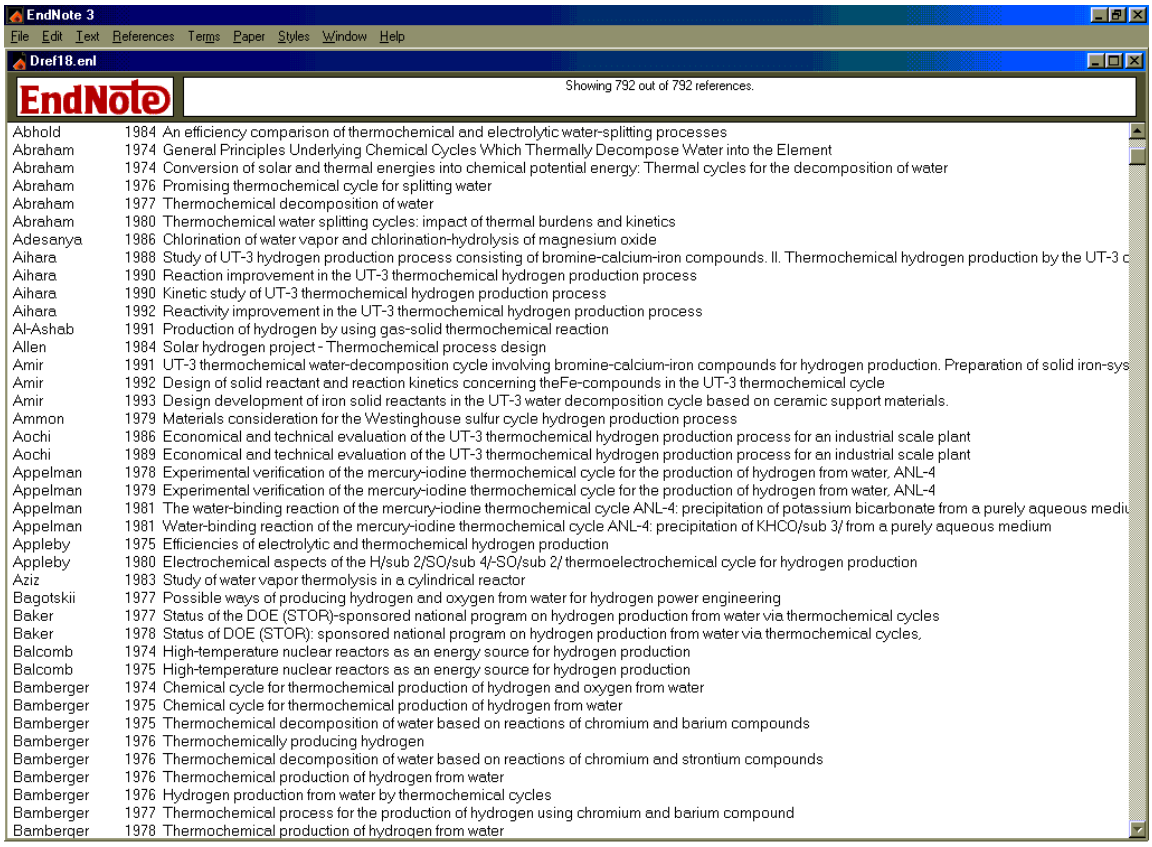

Fig. 12. Screen shot of EndNote database of literature survey results.

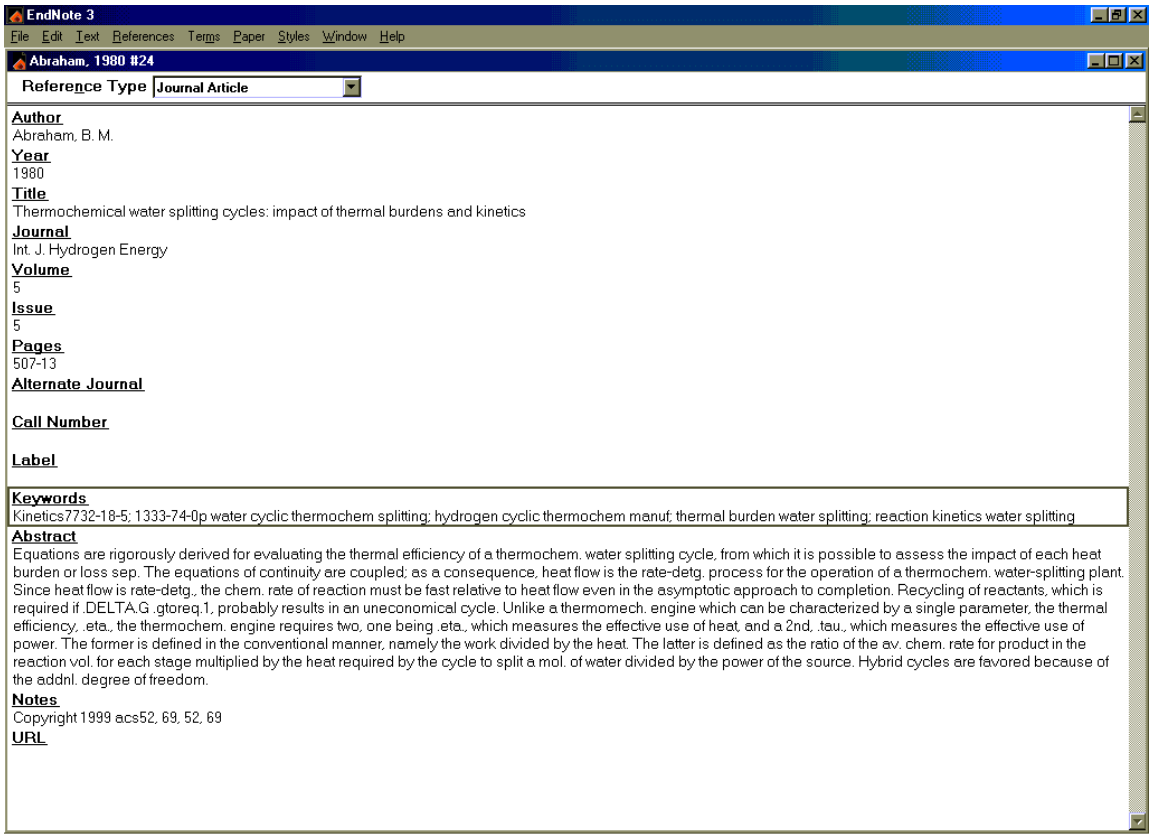

Fig. 13. Screen shot: Individual entry in EndNote database of literature survey results.

was completed by performing similar searches on the NTIS database, the DOE PubSCIENCE database [6] and the IBM Patent Server [7]. The results were added to the literature database. The EndNote database contains 822 entries, after purging duplicate and irrelevant entries.

Interest in thermochemical water splitting has varied greatly with time. Figure 14 indicates when the references in the database were published. The initial interest, in the early 1960s [8], was by the military, which was interested in the use of a portable nuclear reactor to provide logistical support, but interest quickly switched to civilian uses. Interest boomed in the 1970s at the time of the Arab Oil Crisis but petered out with the onset of cheap oil and plentiful natural gas. The last review of the subject was published in 1988 [9], just as the major funding in this area decreased worldwide. Since that time, about eight thermochemical water-splitting related papers have been published per year. Most of the continuing work takes place in Japan where dependence upon foreign energy sources continues to be of national concern.

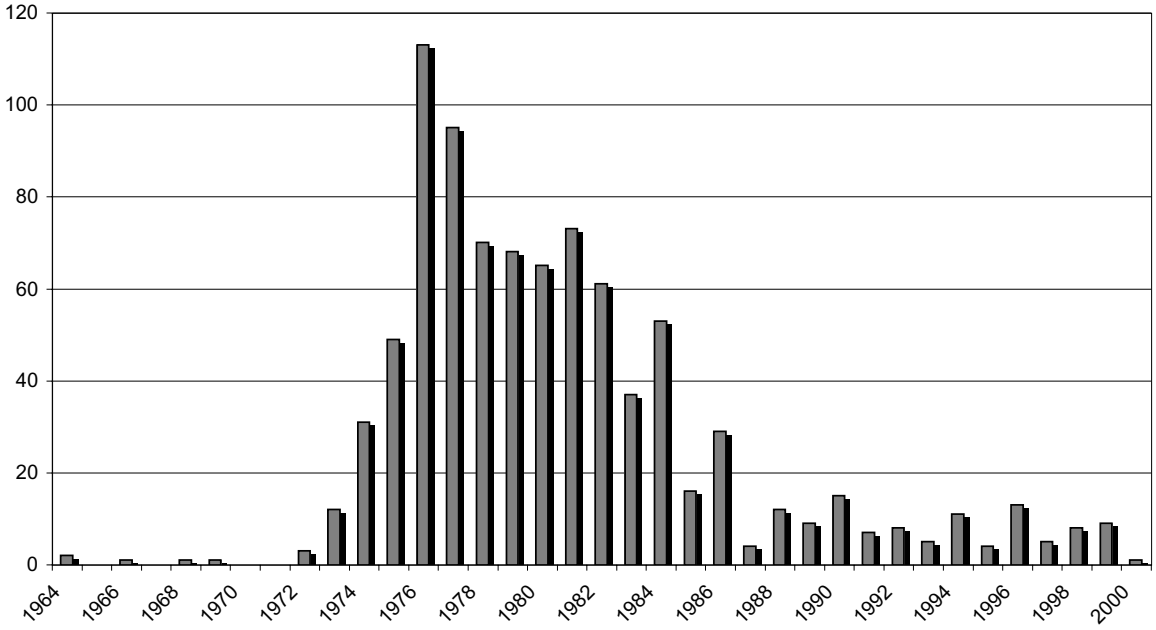

Fig. 14. Publications by year of issue.

5. PRELIMINARY SCREENING CRITERIA

As expected, the literature search turned up a large number of cycles (115), far too many to analyze in depth. In order to establish objective screening criteria, with which to reduce the number of cycles to a manageable number, it was necessary to establish meaningful and quantifiable criteria. The criteria given in Table 2 were presented in the original proposal. Our first task was to determine if, indeed, these were the appropriate criteria and if so, to establish metrics by which each proposed cycle could be evaluated according to each criterion. We also needed to establish weighing factors for each criterion with which to establish a final weighted score for each cycle.

TABLE 2
PROPOSED INITIAL SCREENING CRITERIA

Criteria	Impact
1. Number of reactions and/or separation steps in the cycle	Smaller number indicated reduces process complexity and cost
2. Number of elements in the cycle	Smaller number indicates less cost/complexity in element recovery
3. Cost and availability of process chemicals	There may be strategic availability issues
4. Corrosiveness of the process media and availability/cost of materials of construction and cost must be considered	Improved materials of construction may allow consideration of processes previously dismissed yet effect on hydrogen production efficiency
5. Are non-stationary solid reactants involved?	Bulk movement of solid reactants greatly increases processing difficulty and cost
6. Projected effect of higher temperatures on cost	This addresses the potential for higher hydrogen production cycle efficiency and temperatures in future nuclear reactors
7. Environmental, Safety and Health (ESH) considerations	Are there basic environmental safety and health issues with the cycle?
8. Amount of research done	Has the scientific basis of this cycle been verified or is it a new process?
9. Was at least a bench scale continuous flow model operated	Indicates the relative maturity of a process
10. Are efficiency and/or cost figures available? How good are they?	Indicates a significant amount of engineering design work

The criteria ultimately agreed upon are very similar to those originally proposed. Table 3 gives the basis for selecting the screening criteria and the metrics finally chosen. The translation of each metric, to a score based on the metric, is given in Table 4. Where possible the metrics are calculated from data, otherwise they are a consensus judgment of the principal investigators. Equal weighting was given to each criterion in calculating the final score for each process.

One of the original criteria was left out of the methodology because a simple metric could not be devised that would permit a score to be calculated from first principles. We decided that Environmental, Safety and Health (ES&H) concerns would be taken into account on a case by case basis after the list of cycles was limited using the numerical screening process.

TABLE 3
RATIONAL FOR DEVELOPMENT OF FIRST ROUND SCREENING CRITERIA

	Desirable Characteristic	Rational	Metric
1	Higher ranked cycles will have a minimum number of chemical reactions steps in the cycle.	A smaller number of chemical reactions indicates a simpler process and lower costs.	Score is based on number of chemical reactions.
2	Higher ranked cycles will have a minimum number of separation steps in the cycle.	A smaller number of chemical separations indicates a simpler process and lower costs.	Score is based on number of chemical separations, excluding simple phase separation.
3	Higher ranked cycles will have a minimum number of elements in the cycle.	A smaller number of chemical elements indicates a simpler process and lower costs.	Score is based on number of elements, excluding oxygen and hydrogen
4	Higher ranked cycles will employ elements which are abundant in the earth's crust, oceans and atmosphere.	Use of abundant elements will lower the cost and permit the chosen technology to be implemented on a large scale. There may be strategic availability issues.	Score is based on least abundant element in cycle.
5	Higher ranked cycles will minimize the use of expensive materials of construction by avoiding corrosive chemical systems, particularly in heat exchangers.	Improved materials of construction may allow consideration of processes previously dismissed yet the effect of materials cost on hydrogen production efficiency and cost must be considered.	Score is based on the relative corrosiveness of the process solutions.
6	Higher ranked cycles will minimize the flow of solids.	Chemical plant costs are considerably higher for solids processing plants. Flow of solid materials also corresponds to increased maintenance costs due to wear and to increased downtime due to blockage and unscheduled equipment failure.	Score is based on minimization of solid flow problems.
7	Higher ranked cycles will have maximum heat input temperature compatible with high temperature heat transfer materials.	High thermal efficiency cannot be realized without a high temperature heat input to the water-splitting process. The limit on temperature will be the thermal and mechanical performance of the heat transfer material separating the reactor coolant from the process stream requiring the highest temperature.	Score is based on the high temperature heat input to the process being close to that delivered by an advanced nuclear reactor.
8	Higher ranked cycles will have been the subject of many papers from many authors and institutions.	Cycles that have been thoroughly studied in the literature have a lower probability of having undiagnosed flaws.	Score will be based on the number of papers published dealing with the cycle.
9	Higher ranked cycles will have been tested at a moderate or large scale,	Relatively mature processes will have had their unit operations tested at relatively large scale. Processes for which the basic chemistry has not been verified are suspect.	Score will be based on the degree to which the chemistry of the cycle has been actually demonstrated and not just postulated.
10	Higher ranked cycles will have good efficiency and cost data available.	A significant amount of engineering design work is necessary to estimate process efficiencies and production costs. Note: cost estimates in the absence of efficiency calculations are meaningless and will not be considered.	Score will be based on the degree to which efficiencies and cost have been estimated.

TABLE 4
METRICS USED TO SCORE PROCESSES. FOR EACH METRIC, THE PROCESS RECEIVES THE SCORE INDICATED. THE PROCESS SCORE IS THE SUM OF THE INDIVIDUAL SCORES

Metric ⇓ Score ⇒	0	1	2	3	4	5	6	7	8	9	10
1. Number of chemical reactions	6	-	-	5	-	-	4	-	-	3	2
2. Number of chemical separation steps	10	9	8	7	6	5	4	3	2	1	0
3. Number of elements – 2	7		6	-	5	-	4	-	3	2	1
4. Least abundant element in process	Ir	Rh, Te, Os, Ru, Re, Au	Pt, Bi, Pd, Hg, Se	Ag, In, Cd, Sb, Tm, Tl, Lu	I, Tb, W, Ho, U, Ta, Mo, Eu, Cs, Yb, Er, Hf, Sn, Ge	Th, As, Gd, Dy, Sm, Pb, Pr	Nb, Be, Nd, La, Ga, Y, Ce Co, Sc, Rb	Cu, Zn, Zr, Ni, B, Ba, Li, Br, Cr, V, Sr	Mn, F, P	S, Ti, C, K, N	Ca, Mg, Cl, Na, Al, Fe, Si
5. Relative corrosiveness of process solutions†	Very corrosive, e.g. *aqua* regia				Moderately corrosive, e.g. sulfuric acid						Not corrosive
6. Degree to which process is continuous and flow of solids is minimized	Batch flow of solids			Continuous flow of solids		Flow of gases or liquids through packed beds				Continuous flow of liquids and gases	
7. Maximum temperature in process (°C)	<300 or <1300	300–350 or 1250–1300	350–400 or 1200–1250	400–450 or 1150–1200	450–500 or 1100–1150	500–550 or 1050–1100	550–600 or 1000–1050	600–650 or 950–1000	650–700 or 900–950	700–750 or 850–900	750–850
8. Number of published references to cycle†	1 paper	A few papers			Many papers				Extensive literature base		
9. Degree to which chemistry of cycle has been demonstrated†	No laboratory work			Test tube scale testing			Bench scale testing				Pilot plant scale testing
10. Degree to which good efficiency and cost data are available†	No efficiency estimate available		Thermodynamic efficiency estimated from elementary reactions.		Thermodynamic efficiency estimate based on rough flowsheet		Thermodynamic efficiency calculation based on detailed flow sheet		Detailed cost calculations, based on detailed flowsheets available from one or more independent sources.		

†Interpolate scores between defined scale points.

6. PRELIMINARY SCREENING PROCESS

The preliminary screening process consisted of applying the metrics to each process and summing the scores to get an overall score for each process. Some of the metrics can be easily calculated but for the others, value judgments are required. The three principal investigators jointly went over these aspects of all 115 cycles to generate a consensus score for each cycle and for each metrics requiring a judgment call. The scores for Metrics 1, 2, 3, 4 and 7 are readily evaluated with little subjective judgment required. The other metrics required a consensus judgment.

Metric 1 — Number of Chemical Reactions. Counting the number of chemical reactions is usually easy. An exception is when two or more chemical reactions occur sequentially in a single processing operation. In this case, we considered there to be just one reaction, for the purpose of calculating the score. This question arises primarily for cycles involving the decomposition of sulfuric acid. Most authors considered the reaction to be

(2) $$H_2SO_4 \rightarrow SO_2 + H_2O + {}^1/_2O_2$$

whereas others, attempting to be more precise, considered there to be two reactions

(2a) $$H_2SO_4 \rightarrow H_2O + SO_3$$

followed by

(2b) $$SO_3 \rightarrow SO_2 + {}^1/_2O_2 \quad .$$

Since both reactions occur sequentially in a single heat exchanger/reactor system, without any intermediate separations, we considered there to be one reaction, independent of the way the cycle was described in the literature.

Metric 2 — Number of Chemical Separation Steps. The number of separations for a cycle was determined from the number of separations required for each chemical reaction. Each chemical reaction is assumed to yield a mixture of its reactants and products. After phase separation, for each phase, there is one less separation than there are components, if the components must be separated before the next reaction. As an example, consider the reactions of the UT-3 cycle [10].

(5) $2Br_2(g) + 2CaO(s) \rightarrow 2CaBr_2(s) + {}^1/_2O_2(g)$ (672°C)

(6) $3FeBr_2(s) + 4H_2O(g) \rightarrow Fe_3O_4(s) + 6HBr + H_2(g)$ (560°C)

(7) $CaBr_2(s) + H_2O(g) \rightarrow CaO(s) + 2HBr(g)$ (760°C)

(8) $Fe_3O_4(s) + 8HBr(g) \rightarrow Br_2(g) + 3FeBr_2(s) + 4H_2O(g)$ (210°C)

For this cycle, the solid reactants remain in fixed beds with the gas flow cycled between the beds as the temperatures are changed. The solids are never separated, even if the reaction is not driven to completion, and so solid separations do not contribute to the score. Reaction (5) includes two gaseous species, bromine and oxygen, and therefore one separation. Reaction (6) has three gaseous species, water, hydrogen bromide and hydrogen, and thus two separations. Reactions (7) and (8) have two and three gaseous species and one and two separations giving a potential total of six separations for the process. We recognized that the hydrogen bromide/water mixtures from Reactions (6) and (7) could be fed to Reaction (8) without separation, leaving three separations for a score of seven for this metric. Similar analyses were made for each cycle.

Metric 3 — Number of Elements. Every element found in any reaction of the cycle was listed and counted. Oxygen and hydrogen, which occur in every cycle, were ignored. Catalysts, which are not indicated in the reaction equations, were also ignored.

Metric 4 — Elemental Abundance. Elements were ordered based on their atomic abundance in the earth's crust and separated into groups differing by roughly an order of magnitude in abundance. An exception is nitrogen, which, based on its abundance in the atmosphere, was grouped with more abundant elements. The score was then based on the least abundant element employed in the cycle.

Metric 5 — Corrosive Chemicals. Cycles were rated based on the most corrosive materials in the process. If no corrosive materials are involved the cycles were given a 10. No cycle was rated worse than 5, which was defined as equivalent to sulfuric acid.

Metric 6 — Solids Flow. Cycles were separated into four groups: (1) cycles involving only gases and liquids, (2) cycles in which solids remained in stationary beds, (3) cycles in which solids flow continuously and (4) cycles in which solids remain in stationary beds part of the time and are moved at other times. We assumed that solids could be processed in static beds if only gas solid reactions were involved and all solid reactants resulted in solid products. We assumed that batch flow of solids would be necessary if liquids were converted to solids. It might not be strictly necessary that there be batch flow of solids in this case but the complications would be equally onerous and the score would be the same.

Metric 7 — Maximum Cycle Temperature. The maximum cycle temperature was another parameter requiring analysis. The score was reduced if the maximum temperature was either above or below that deemed optimum for an advanced high-temperature nuclear reactor. We used the temperatures given by the cycle proponents except where that would lower the score or when the value suggested produced a large positive for a non-electrolytic reaction. As an example of the former, Reaction (1) is part of several different cycles. The temperature of this reaction is quoted anywhere between 700°C and 1100°C. This reaction actually represents the sequence of Reactions 2(a) and 2(b). The Gibbs free energy of Reaction 2(b) changes relatively little over the range from 700°C to 1100°C so the net result of changing the temperature is to shift the equilibrium towards the products. It is not reasonable to give different cycles different scores based on use of the same high-temperature chemical reaction. In cases like this, we gave the maximum reasonable score to all cycles. In cases where the cycle proponents gave a temperature for which the reaction was non-spontaneous, i.e., it has a very positive Gibbs free energy, we assigned the temperature where the free energy was near zero. We used the computer program HSC Chemistry 4.0 [11] to calculate the free energy of each reaction as a function of temperature.

Metric 8 — References. The number of publications was determined from the literature search. Most cycles had either very few publications or very many publications.

Metric 9 — Chemical Demonstration. The degree and scale to which the chemistry has been demonstrated was determined from the literature.

Metric 10 — Efficiency and Cost Data. The degree to which costs and efficiencies have been calculated was determined from the literature.

There was a significant correlation between the scores from the last three metrics. Leaving these metrics out of the scoring had little effect on which cycles scored best. This is probably because previous work has concentrated on cycles with few reactions, simple separations, available materials, which have minimal solids flow problems and which have their heat input requirements at reasonable temperatures.

7. FIRST STAGE SHORT LIST

The screening criteria were applied to all 115 cycles and the results were sorted according to the total number of screening points awarded to each process. We had hoped that the totals would cluster in to high scoring and low scoring cycles to make the down selection easy, but this was not the case. We therefore somewhat arbitrarily used 50 points (out of the total possible of 100) as the cut-off score. The original goal was to retain 20–30 cycles, after down selection, for more detailed evaluation. Using 50 points as the cut-off gave over 40 cycles, which allowed us room to apply ES&H considerations as well as well as other "sanity checks".

Three additional go/no-go tests were applied to the short list. Two cycles were eliminated for ES&H reasons in that they are based on mercury and we do not believe that it would be possible to license such a plant. Three cycles were eliminated because they require temperatures in excess of 1600°C, which places them outside the scope of processes that are compatible with advanced nuclear reactors contemplated in the next 50 years. Additionally, use of the program HSC Chemistry 4.0 [11] allowed us to analyze cycles for thermodynamic feasibility earlier in the screening process than we had originally foreseen. Seven cycles were eliminated because they had reactions that have large positive free energies that cannot be accomplished electrochemically. The final short list of 25 cycles is given in Table 5, along with their scores. One literature reference is included for each cycle. Details for these cycles are given in Table 6.

TABLE 5
SHORT LIST OF CYCLES AND THEIR SCORES

Cycle#	Name	Class	Max T	Elem	#elem	#seps	#Rxns	Rxns	Seps	Elems	Abund	Corr	Solids	Temp	Pubs	Tests	Data	Total
1	Westinghouse [12]	H	850	S	1	2	2	10	8	10	9	5	10	9	10	6	8	85
2	Ispra Mark 13 [13]	H	850	Br,S	2	3	3	9	7	9	7	5	10	9	10	6	8	80
3	UT-3 Univ. of Tokyo [8]	T	750	Br,Ca,Fe	3	3	4	6	7	8	7	5	6	10	10	10	10	79
4	Sulfur-Iodine [14]	T	800	I,S	2	3	3	9	7	9	4	5	10	10	10	6	8	78
5	Julich Center EOS [15]	T	800	Fe,S	2	3	3	9	7	9	9	9	6	10	3	3	3	68
6	Tokyo Inst. Tech. Ferrite [16]	T	1000	Fe,Mn,Na	3	2	2	10	8	8	8	10	10	6	2	2	0	64
7	Hallett Air Products 1965 [15]	H	800	Cl	1	3	2	10	7	10	10	5	10	10	0	0	0	62
8	Gaz de France [15]	T	825	K	1	3	3	9	7	10	9	5	6	10	2	2	2	62
9	Nickel Ferrite [17]	T	1000	Fe,Ni,Mn	3	0	2	10	10	8	7	10	6	6	0	3	0	60
10	Aachen Univ Julich 1972 [15]	T	800	Cr,Cl	2	3	3	9	7	9	7	5	6	10	2	2	2	59
11	Mark 1C [13]	T	900	Br,Ca,Cu	3	4	4	6	6	8	7	5	10	8	2	3	3	58
12	LASL- U [15]	T	700	C,U	2	3	3	9	7	9	4	10	6	9	1	3	0	58
13	Ispra Mark 8 [13]	T	900	Cl,Mn	2	3	3	9	7	9	8	5	3	8	3	2	3	57
14	Ispra Mark 6 [13]	T	800	Cl,Cr,Fe	3	4	4	6	6	8	7	5	6	10	2	3	3	56
15	Ispra Mark 4 [13]	T	800	Cl,Fe	2	4	4	6	6	9	10	5	0	10	3	3	3	55
16	Ispra Mark 3 [13]	T	800	Cl,V	2	3	3	9	7	9	7	5	0	10	2	3	3	55
17	Ispra Mark 2 (1972) [13]	T	800	C,Na,Mn	3	3	3	9	7	8	8	5	0	10	2	3	3	55
18	Ispra CO/Mn_3O_4 [18]	T	977	C,Mn	2	3	3	9	7	9	8	9	6	7	0	0	0	55
19	Ispra Mark 7B [13]	T	1000	Cl,Fe	2	5	5	3	5	9	10	5	10	6	0	3	3	54
20	Vanadium Chloride [19]	T	700	Cl,V	3	5	4	6	5	8	7	5	6	9	3	2	2	53
21	Ispra Mark 7A [13]	T	1000	Cl,Fe	2	5	5	3	5	9	10	5	6	6	3	3	3	53
22	GA Cycle 23 [20]	T	850	S	2	4	5	3	6	9	9	5	10	9	0	0	0	51
23	US –Chlorine [15]	T	993	Cl,Cu	2	3	3	9	7	9	7	6	5	7	0	0	0	50
24	Ispra Mark 9 [13]	T	450	Cl,Fe	2	8	3	9	2	9	10	5	3	4	2	3	3	50
25	Ispra Mark 6C [13]	T	800	Cl,Cr,Cu,Fe	4	5	5	3	5	6	7	5	6	10	2	3	3	50

TABLE 6
REACTION DETAILS FOR CYCLES

Cycle	Name	T/E*	T (°C)	Reaction	F†
1	Westinghouse [12]	T	850	$2H_2SO_4(g) \rightarrow 2SO_2(g) + 2H_2O(g) + O_2(g)$	$^1/_2$
		E	77	$SO_2(g) + 2H_2O(a) \rightarrow H_2SO_4(a) + H_2(g)$	1
2	Ispra Mark 13 [13]	T	850	$2H_2SO_4(g) \rightarrow 2SO_2(g) + 2H_2O(g) + O_2(g)$	$^1/_2$
		E	77	$2HBr(a) \rightarrow Br_2(a) + H_2(g)$	1
		T	77	$Br_2(l) + SO_2(g) + 2H_2O(l) \rightarrow 2HBr(g) + H_2SO_4(a)$	1
3	UT-3 Univ. of Tokyo [8]	T	600	$2Br_2(g) + 2CaO \rightarrow 2CaBr_2 + O_2(g)$	$^1/_2$
		T	600	$3FeBr_2 + 4H_2O \rightarrow Fe_3O_4 + 6HBr + H_2(g)$	1
		T	750	$CaBr_2 + H_2O \rightarrow CaO + 2HBr$	1
		T	300	$Fe_3O_4 + 8HBr \rightarrow Br_2 + 3FeBr_2 + 4H_2O$	1
4	Sulfur-Iodine [14]	T	850	$2H_2SO_4(g) \rightarrow 2SO_2(g) + 2H_2O(g) + O_2(g)$	$^1/_2$
		T	450	$2HI \rightarrow I_2(g) + H_2(g)$	1
		T	120	$I_2 + SO_2(a) + 2H_2O \rightarrow 2HI(a) + H_2SO_4(a)$	1
5	Julich Center EOS [15]	T	800	$2Fe_3O_4 + 6FeSO_4 \rightarrow 6Fe_2O_3 + 6SO_2 + O_2(g)$	$^1/_2$
		T	700	$3FeO + H_2O \rightarrow Fe_3O_4 + H_2(g)$	1
		T	200	$Fe_2O_3 + SO_2 \rightarrow FeO + FeSO_4$	6
6	Tokyo Inst. Tech. Ferrite [16]	T	1000	$2MnFe_2O_4 + 3Na_2CO_3 + H_2O \rightarrow 2Na_3MnFe_2O_6 + 3CO_2(g) + H_2(g)$	1
		T	600	$4Na_3MnFe_2O_6 + 6CO_2(g) \rightarrow 4MnFe_2O_4 + 6Na_2CO_3 + O_2(g)$	$^1/_2$
7	Hallett Air Products 1965 [15]	T	800	$2Cl_2(g) + 2H_2O(g) \rightarrow 4HCl(g) + O_2(g)$	$^1/_2$
		E	25	$2HCl \rightarrow Cl_2(g) + H_2(g)$	1
8	Gaz de France [15]	T	725	$2K + 2KOH \rightarrow 2K_2O + H_2(g)$	1
		T	825	$2K_2O \rightarrow 2K + K_2O_2$	1
		T	125	$2K_2O_2 + 2H_2O \rightarrow 4KOH + O_2(g)$	$^1/_2$
9	Nickel Ferrite [17]	T	800	$NiMnFe_4O_6 + 2H_2O \rightarrow NiMnFe_4O_8 + 2H_2(g)$	1
		T	800	$NiMnFe_4O_8 \rightarrow NiMnFe_4O_6 + O_2(g)$	$^1/_2$
10	Aachen Univ Julich 1972 [15]	T	850	$2Cl_2(g) + 2H_2O(g) \rightarrow 4HCl(g) + O_2(g)$	$^1/_2$
		T	170	$2CrCl_2 + 2HCl \rightarrow 2CrCl_3 + H_2(g)$	1
		T	800	$2CrCl_3 \rightarrow 2CrCl_2 + Cl_2(g)$	1
11	Ispra Mark 1C [13]	T	100	$2CuBr_2 + Ca(OH)_2 \rightarrow 2CuO + 2CaBr_2 + H_2O$	1
		T	900	$4CuO(s) \rightarrow 2Cu_2O(s) + O_2(g)$	$^1/_2$
		T	730	$CaBr_2 + 2H_2O \rightarrow Ca(OH)_2 + 2HBr$	2
		T	100	$Cu_2O + 4HBr \rightarrow 2CuBr_2 + H_2(g) + H_2O$	1
12	LASL- U [15]	T	25	$3CO_2 + U_3O_8 + H_2O \rightarrow 3UO_2CO_3 + H_2(g)$	1
		T	250	$3UO_2CO_3 \rightarrow 3CO_2(g) + 3UO_3$	1
		T	700	$6UO_3(s) \rightarrow 2U_3O_8(s) + O_2(g)$	$^1/_2$
13	Ispra Mark 8 [13]	T	700	$3MnCl_2 + 4H_2O \rightarrow Mn_3O_4 + 6HCl + H_2(g)$	1
		T	900	$3MnO_2 \rightarrow Mn_3O_4 + O_2(g)$	$^1/_2$
		T	100	$4HCl + Mn_3O_4 \rightarrow 2MnCl_2(a) + MnO_2 + 2H_2O$	$^3/_2$
14	Ispra Mark 6 [13]	T	850	$2Cl_2(g) + 2H_2O(g) \rightarrow 4HCl(g) + O_2(g)$	$^1/_2$
		T	170	$2CrCl_2 + 2HCl \rightarrow 2CrCl_3 + H_2(g)$	1
		T	700	$2CrCl_3 + 2FeCl_2 \rightarrow 2CrCl_2 + 2FeCl_3$	1
		T	420	$2FeCl_3 \rightarrow Cl_2(g) + 2FeCl_2$	1
15	Ispra Mark 4 [13]	T	850	$2Cl_2(g) + 2H_2O(g) \rightarrow 4HCl(g) + O_2(g)$	$^1/_2$
		T	100	$2FeCl_2 + 2HCl + S \rightarrow 2FeCl_3 + H_2S$	1
		T	420	$2FeCl_3 \rightarrow Cl_2(g) + 2FeCl_2$	1
		T	800	H_2S ™ $S + H_2(g)$	1

TABLE 6
REACTION DETAILS FOR CYCLES (Continued)

Cycle	Name	T/E*	T °C	Reaction	F†
16	Ispra Mark 3 [13]	T	850	$2Cl_2(g) + 2H_2O(g) \rightarrow 4HCl(g) + O_2(g)$	1/2
		T	170	$2VOCl_2 + 2HCl \rightarrow 2VOCl_3 + H_2(g)$	1
		T	200	$2VOCl_3 \rightarrow Cl_2(g) + 2VOCl_2$	1
17	Ispra Mark 2 (1972) [13]	T	100	$Na_2O.MnO_2 + H_2O \rightarrow 2NaOH(a) + MnO_2$	2
		T	487	$4MnO_2(s) \rightarrow 2Mn_2O_3(s) + O_2(g)$	1/2
		T	800	$Mn_2O_3 + 4NaOH \rightarrow 2Na_2O.MnO_2 + H_2(g) + H_2O$	1
18	Ispra CO/Mn_3O_4 [18]	T	977	$6Mn_2O_3 \rightarrow 4Mn_3O_4 + O_2(g)$	1/2
		T	700	$C(s) + H_2O(g) \rightarrow CO(g) + H_2(g)$	1
		T	700	$CO(g) + 2Mn_3O_4 \rightarrow C + 3Mn_2O_3$	1
19	Ispra Mark 7B [13]	T	1000	$2Fe_2O_3 + 6Cl_2(g) \rightarrow 4FeCl_3 + 3O_2(g)$	3/4
		T	420	$2FeCl_3 \rightarrow Cl_2(g) + 2FeCl_2$	3/2
		T	650	$3FeCl_2 + 4H_2O \rightarrow Fe_3O_4 + 6HCl + H_2(g)$	1
		T	350	$4Fe_3O_4 + O_2(g) \rightarrow 6Fe_2O_3$	1/4
		T	400	$4HCl + O_2(g) \rightarrow 2Cl_2(g) + 2H_2O$	3/2
20	Vanadium Chloride [19]	T	850	$2Cl_2(g) + 2H_2O(g) \rightarrow 4HCl(g) + O_2(g)$	1/2
		T	25	$2HCl + 2VCl_2 \rightarrow 2VCl_3 + H_2(g)$	1
		T	700	$2VCl_3 \rightarrow VCl_4 + VCl_2$	2
		T	25	$2VCl_4 \rightarrow Cl_2(g) + 2VCl_3$	1
21	Mark 7A [13]	T	420	$2FeCl_3(l) \rightarrow Cl_2(g) + 2FeCl_2$	3/2
		T	650	$3FeCl_2 + 4H_2O(g) \rightarrow Fe_3O_4 + 6HCl(g) + H_2(g)$	1
		T	350	$4Fe_3O_4 + O_2(g) \rightarrow 6Fe_2O_3$	1/4
		T	1000	$6Cl_2(g) + 2Fe_2O_3 \rightarrow 4FeCl_3(g) + 3O_2(g)$	1/4
		T	120	$Fe_2O_3 + 6HCl(a) \rightarrow 2FeCl_3(a) + 3H_2O(l)$	1
22	GA Cycle 23 [20]	T	800	$H_2S(g) \rightarrow S(g) + H_2(g)$	1
		T	850	$2H_2SO_4(g) \rightarrow 2SO_2(g) + 2H_2O(g) + O_2(g)$	1/2
		T	700	$3S + 2H_2O(g) \rightarrow 2H_2S(g) + SO_2(g)$	1/2
		T	25	$3SO_2(g) + 2H_2O(l) \rightarrow 2H_2SO_4(a) + S$	1/2
		T	25	$S(g) + O_2(g) \rightarrow SO_2(g)$	
23	US -Chlorine [15]	T	850	$2Cl_2(g) + 2H_2O(g) \rightarrow 4HCl(g) + O_2(g)$	1/2
		T	200	$2CuCl + 2HCl \rightarrow 2CuCl_2 + H_2(g)$	1
		T	500	$2CuCl_2 \rightarrow 2CuCl + Cl_2(g)$	1
24	Ispra Mark 9 [13]	T	420	$2FeCl_3 \rightarrow Cl_2(g) + 2FeCl_2$	3/2
		T	150	$3Cl_2(g) + 2Fe_3O_4 + 12HCl \rightarrow 6FeCl_3 + 6H_2O + O_2(g)$	1/2
		T	650	$3FeCl_2 + 4H_2O \rightarrow Fe_3O_4 + 6HCl + H_2(g)$	1
25	Ispra Mark 6C [13]	T	850	$2Cl_2(g) + 2H_2O(g) \rightarrow 4HCl(g) + O_2(g)$	1/2
		T	170	$2CrCl_2 + 2HCl \rightarrow 2CrCl_3 + H_2(g)$	1
		T	700	$2CrCl_3 + 2FeCl_2 \rightarrow 2CrCl_2 + 2FeCl_3$	1
		T	500	$2CuCl_2 \rightarrow 2CuCl + Cl_2(g)$	1
		T	300	$CuCl + FeCl_3 \rightarrow CuCl_2 + FeCl_2$	1

*T = thermochemical, E = electrochemical.

†Reactions are stored in database with minimum integer coefficients. Multiplier from reaction junction table converts the results to the basis of one mole of water decomposed.

8. SECOND STAGE SCREENING

The goal of the second stage screening was to reduce the number of cycles under consideration to three or less. Detailed investigations were made into the viability of each cycle. The most recent papers were obtained for each cycle and, when not available from the literature, preliminary block-flow diagrams were made to help gain an understanding of the process complexity. Thermodynamic calculations were made for each chemical reaction over a wide temperature range using HSC Chemistry 4.0 [11]. Each chemical species was considered in each of its potential forms: gas, liquid, solid, and aqueous solution. Each of the principal investigators took responsibility for a part of the investigation and the results were shared.

Once all the background work was completed, the final selection was relatively easy. The three principal investigators independently rated the viability of each cycle. The 25 cycles were considered without reference to their original score and re-rated. Each principal investigator independently assigned a score to each cycle based on their rating of the cycle to be favorable (+1), acceptable (0), or unfavorable (–1). The scores of the three principal investigators were summed, Table 7, and two cycles stood out from all the others with a score of +3. The most highly rated cycles are the adiabatic version of the UT-3 cycle and the sulfur-iodine cycle.

After completing the rating, the rankings were discussed. The rational for the scoring of each cycle is given in Appendix A. Cycles tended to be down-rated for the for the following reasons:

1. If any reaction has a large positive Gibbs free energy, that can not be performed electrochemically nor shifted by pressure or concentration.
2. If it requires the flow of solids.
3. If it is excessively complex.
4. If it can not be well matched to the characteristics of a high temperature reactor.
5. If it required an electrochemical step.

The last two considerations are not as obvious as the others and require additional explanation.

TABLE 7
SECOND STAGE SCREENING SCORES

Cycle	Name	SNL	UK	GA	Score
1	Westinghouse [12]	1	0	0	1
2	Ispra Mark 13 [13]	0	0	0	0
3	UT-3 Univ. of Tokyo [8]	1	1	1	3
4	Sulfur-Iodine [14]	1	1	1	3
5	Julich Center EOS [15]	1	-1	-1	-1
6	Tokyo Inst. Tech. Ferrite [16]	-1	0	0	-1
7	Hallett Air Products 1965 [15]	1	-1	0	0
8	Gaz de France [15]	-1	-1	-1	-3
9	Nickel Ferrite [17]	-1	0	0	-1
10	Aachen Univ Julich 1972 [15]	0	-1	0	-1
11	Ispra Mark 1C [13]	-1	-1	-1	-3
12	LASL- U [15]	1	-1	-1	-1
13	Ispra Mark 8 [13]	0	-1	-1	-2
14	Ispra Mark 6 [13]	-1	-1	-1	-3
15	Ispra Mark 4 [13]	0	-1	-1	-2
16	Ispra Mark 3 [13]	0	-1	-1	-2
17	Ispra Mark 2 (1972) [13]	1	-1	-1	-1
18	Ispra CO/Mn_3O_4 [18]	-1	0	0	-1
19	Ispra Mark 7B [13]	-1	-1	-1	-3
20	Vanadium Chloride [19]	0	1	-1	0
21	Mark 7A [13]	-1	-1	-1	-3
22	GA Cycle 23 [20]	-1	-1	0	-2
23	US -Chlorine [15]	0	1	-1	0
24	Ispra Mark 9 [13]	0	-1	-1	-2
25	Ispra Mark 6C [13]	-1	-1	-1	-3

The nuclear reactor to be used has not been defined except to the point that it will be a high temperature reactor. The coolant may be gas or liquid metal but it is unlikely that it will be water. Certainly, the chemical process will be isolated from the reactor coolant by an intermediate heat transfer loop. The flow rates of the intermediate heat transfer fluid and the reactor coolant will be excessive unless the intermediate heat transfer fluid is operated over a reasonably large temperature range. Thus, a cycle will be well matched to a reactor if it requires energy over a wide temperature range. Figure 15 shows temperature-enthalpy (T-H) curves for three processes matched to the same reactor coolant T-H curve and the same minimum approach temperature. A T-H curve shows the temperature

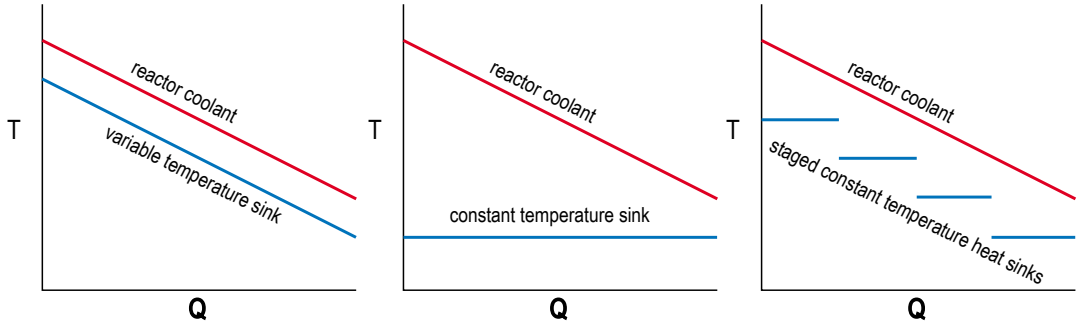

Fig. 15. Matching of thermochemical cycle to reactor.

of the coolant or the process as a function of the amount of heat transferred. As shown, the coolant and process are effectively in counter-current flow heat exchange. In each case, the temperature of the intermediate coolant loop (not shown) is between the reactor temperature and the process temperature.

The first process is well matched as the temperature-enthalpy curves of the process and reactor coolant are parallel. Since the coolant enthalpy is in the form of sensible heat (heat capacity), its temperature enthalpy curve is sloped and approximately linear. For a chemical reaction to have a sloped T-H curve, the reaction equilibria must shift with temperature: the reactants and products are in equilibria over the temperature range but as heat is input to the endothermic chemical reaction the concentration of reactants decreases and products increases. This is the type of T-H curve expected from homogeneous chemical reactions. It will also typify the sensible heat effects of heating or cooling of reactants and products.

The second process is poorly matched. The T-H curve for the process is horizontal, as typified by solid-solid chemical reaction or latent heat effects of phase changes of reactants or products. The third set of curves shows that the matching of processes with horizontal T-H curves can be improved if there is a way to break the process into horizontal segments that require heat at different temperatures. Examples of this would be to employ a number of chemical reactions that occur at different temperatures, or more reasonably, to perform latent heat operations (boiling) at different pressures and therefore at different temperatures.

Hybrid cycles have always attracted considerable interest in that they typically are simpler than pure thermochemical cycles. Never-the-less, they have one characteristic that renders them uneconomic at the scale required for hydrogen production using a nuclear heat source. Energy efficient electrochemical processes require parallel electrodes, small gaps between electrodes and minimal mixing of the anodic and cathodic

products — in short they require thin membranes between the anode and cathode. This basically limits efficient electrochemical processes to the small electrode areas that are consistent with thin membrane manufacture. This is not to say that there are not commercial electrochemical process but rather, that the commercial processes are efficient in an economic sense because they make valuable products and not that they are efficient in a thermodynamic sense.

9. SECOND STAGE SHORT LIST

Two cycles were rated far above the others in the second stage screening, the Adiabatic UT-3 and sulfur-iodine cycles.

Adiabatic UT-3 Cycle. The basic UT-3 cycle was first described at University of Tokyo in the late 1970s and essentially all work on the cycle has been performed in Japan. Work has continued to this date with the latest publication last year. Over time the flowsheet has undergone several revisions the most recent, based on the adiabatic implementation of the cycle, was published in 1996. A simplified flow diagram of the Adiabatic UT-3 cycle matched to a nuclear reactor is shown in Fig. 16. The four chemical reactions take place in four adiabatic fixed packed bed chemical reactors that contain the solid reactants and products. The chemical reactors occur in pairs, one pair contains the calcium compounds and the other pair the iron compounds. The nuclear reactor transfers heat through a secondary heat exchanger into the gas stream which traverses through the four chemical reactors, three process heat exchangers, two membrane separators and the recycle compressor in sequence before the gases are recycled to the reactor secondary heat exchanger.

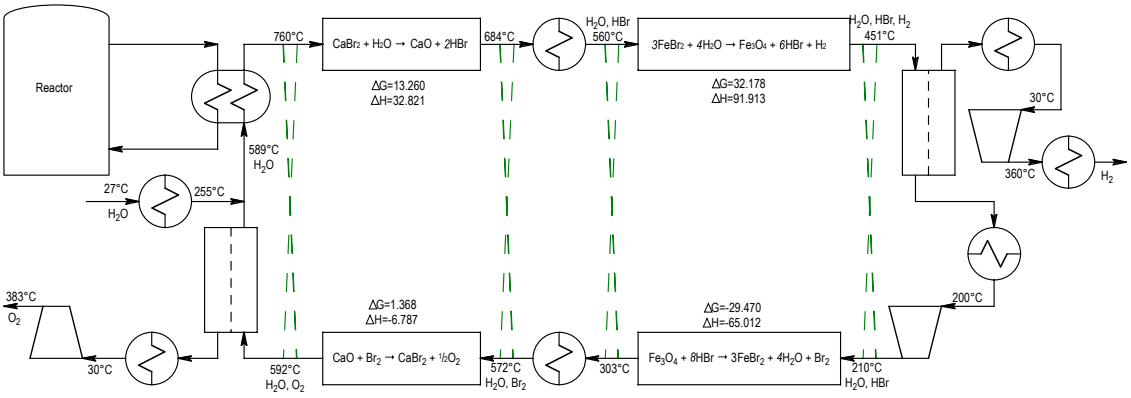

Fig. 16. Adiabatic UT-3 process flow diagram.

At each chemical reactor, the gaseous reactant passes through the bed of solid product until it reaches the reaction front where it is consumed creating gaseous product and solid product. The gaseous product traverses through the unreacted solid and exits the chemical reactor. After some time, perhaps an hour, the reaction front has traveled from near the entrance of the reactor to near the exit. At this point, the flow paths are switched and

chemical reactors, in each pair, switch functions. The direction of flow through the reactor also switches so that the reaction front reverses direction and travels back toward the end that had previously been the entrance. The direction must be switched before the reaction front reaches the end of a reactor to prevent large temperature swings but it is desirable for the reaction front to approach the ends of the reactor to reduce the frequency of flow switching.

The gas stream is conditioned, either heated or cooled, before entering the chemical reactor. Since the gaseous reactant/product cannot carry sufficient heat to accomplish the reaction, a large quantity of inert material (steam) comprises the majority of the stream. The total stream pressure is 20 atmospheres and the minimum steam pressure is 18.5 atmospheres. The inert flow provides the additional function of sweeping the products away from the reaction front and thus shifting the reaction equilibrium towards completion. This is necessary since the Gibbs free energy is positive for some of the reactions.

The operation of the semipermeable membranes is somewhat more involved than shown. The partial pressure of hydrogen and oxygen are 0.2 and 0.1 atmospheres respectively. Each gas must be substantially removed from its stream so counter-current operation of the permeator is necessary. This is accomplished by flowing steam past the back side of the membrane. The steam is condensed and separated from the product gas before the product gas is compressed.

The efficiency of hydrogen generation, for a stand-alone plant, is predicted to be 36%–40%, depending upon the efficiency of the membrane separation processes. Higher overall efficiencies, 45%–49%, are predicted for a plant that co-generates both hydrogen and electricity. It is not evident from the published reports if these numbers are based on steady operation or if they take into account the additional inefficiencies associated with the transient operation which occurs when the flow paths are switched.

The chemistry of the cycle has been studied extensively. The basic thermodynamics are well documented. The overall cycle has been demonstrated first at the bench scale and finally in a pilot plant. The UT-3 cycle is the closest to commercial development of any cycle.

The major areas of ongoing research are in the stability of the solids and in the membrane separation processes. For the process to work, the solids must be chemically available to gas phase reactions yet physically stable while undergoing repeated cycling between the oxide and bromide forms. A considerable effort has gone into supporting the reactive solids in a form where they will not be transported by the gas flow. Membranes are being developed which are permeable to oxygen or hydrogen while not being perme-

able to hydrogen bromide or bromine. There still remains the problem of developing the membrane materials into a physical form that is suitable to large scale economics.

The other questions that require analysis prior to full scale development have to do with the non-steady state operation of the cycle. The non-steady state operation will certainly affect hydrogen production efficiency. Of more concern is the effect of a non-steady-state heat requirement on the reactor operation. This is not expected to be a serious problem as, for large scale hydrogen production, the process will require several completely parallel process modules which can be operated such that, at any time, only a fraction of the chemical plant will be operating in a transient mode.

Overall, the process is in excellent shape for commercial exploitation. There is limited potential for future process improvements as the adiabatic implementation is already quite simple, as thermochemical processes go. There is little room for future efficiency improvements as the process is already operating at the physical limits of its constituents. The maximum $CaBr_2$ operating temperature is already slightly above the melting point. Any attempt to increase efficiency by increasing process temperature will result in migration of the $CaBr_2$.

Sulfur-Iodine Cycle. The sulfur-iodine cycle was first described in the mid 1970s. It was rejected by early workers due to difficulties encountered separating the hydrogen iodide and sulfuric acid produced in Reaction (3). Attempts to use distillation were futile as sulfuric acid and hydrogen iodide react according to the reverse of Reaction (3) when their mixture is heated. The key to successful implementation of the cycle was the recognition that using an excess of molten iodine would result in a two-phase solution, a light phase containing sulfuric acid and a heavy phase containing hydrogen iodide and iodine. Figure 17 shows a block flow diagram of the cycle based on this separation. The sulfur-iodine cycle has been studied by several investigators and while the process as a whole is well defined, there is some uncertainty about the best way of accomplishing the hydrogen iodide decomposition step.

All the early work on the cycle assumed it was necessary to separate the hydrogen iodide from the iodine and water of the heavy phase before performing Reaction (4) to generate hydrogen. Bench scale experiments were made of the total process and the process was matched to a high-temperature nuclear reactor in 1978 and 1980. The latter flowsheet, which was optimized for maximum efficiency, indicated that hydrogen could be produced at 52% efficiency. This is the highest efficiency reported for any water-splitting process, based on an integrated flowsheet.

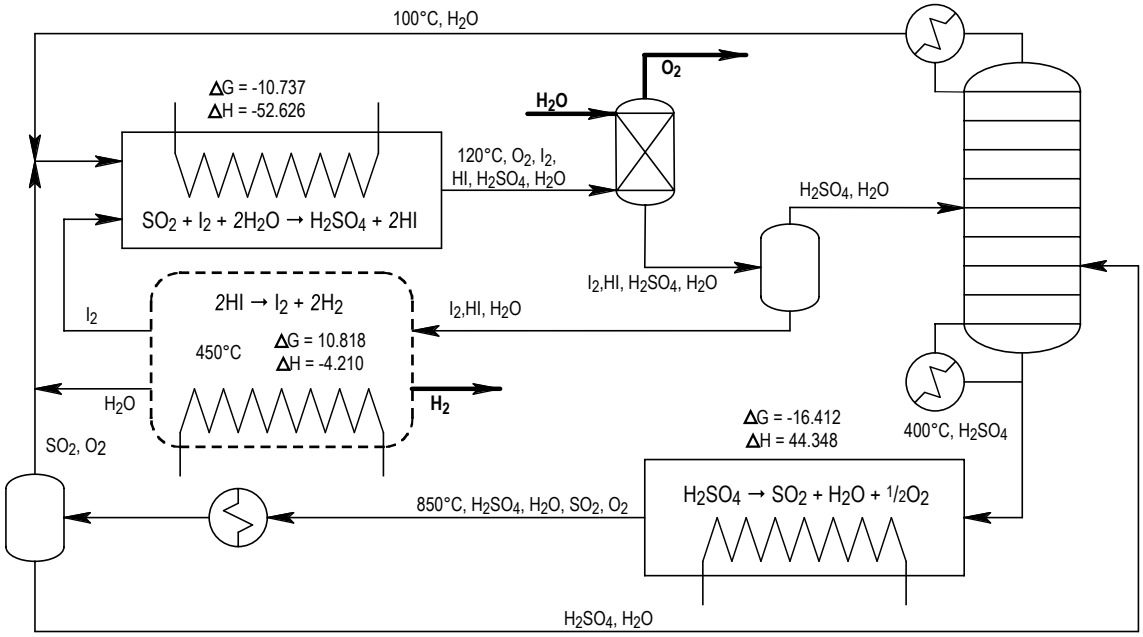

Fig. 17. Sulfur-iodine cycle process flow diagram.

Subsequent to the cessation of development of the sulfur-iodine process in the US, other workers have made several attempts to improve the efficiency of the cycle by modifying the hydrogen production section of the cycle. In particular, researchers at the University of Aachen demonstrated experimentally, that the hydrogen iodide need not be separated from iodine before the decomposition step. Based on their work, they predicted significant increases in efficiency and a 40% decrease in the cost of hydrogen compared with the standard flowsheet. The cost decreases not only because the efficiency increased, but also because the capital intensive heavy phase separation was eliminated. These proposed improvements have never been incorporated into an integrated flowsheet of the sulfur-iodine hydrogen process with a nuclear reactor.

The sulfur-iodine cycle should be matched to a nuclear reactor, incorporating the latest information and thinking. It is the cycle that is almost always used as the standard of comparison as to what can be done with a thermochemical cycle. It was the cycle chosen by LLNL in their conceptual design of a plant to produce synthetic fuels from fusion energy. The Japanese consider the sulfur-iodine cycle to be a back-up for the UT-3 cycle and continue chemical investigations, although they have not published any flowsheets matching the cycle to a nuclear reactor. The cycle has never been matched to a nuclear reactor considering co-generation of electricity. The Japanese found that co-generation gave a 10% efficiency improvement (40% to 50%) for the Adiabatic UT-3 process. If similar improvements are found with the sulfur-iodine cycle, and considering

the improvements projected by the University of Aachen, the sulfur-iodine cycle could co-produce hydrogen and electricity at over 60% efficiency.

10. PLANS FOR PHASE 2 AND 3

The sulfur-iodine cycle remains the cycle with the highest reported efficiency, based on an integrated flowsheet. Various researchers have pointed out improvements that should increase the already excellent efficiency of this cycle and, in addition, lower the capital cost significantly. In Phases 2 and 3 we will investigate the improvements that have been proposed to the sulfur-iodine cycle and generate an integrated flowsheet describing a thermochemical hydrogen production plant powered by a high-temperature nuclear reactor. The detailed flowsheet will allow us to size the process equipment and calculate the hydrogen production efficiency. We will finish by calculating the capital cost of the equipment and estimate the cost of the hydrogen produced as a function of nuclear power costs. The scope of work and schedule remain as originally proposed, see Table 8 and Fig. 1.

Phase 2 begins with a detailed process evaluation and a specification of the nuclear reactor thermal interface. The emphasis of Task 2.1, "Detailed Process Evaluation," will be upon the various methods of accomplishing the hydrogen iodide decomposition step as the down selection to one process has already been accomplished. The reactor will be specified (Task 2.2) only to the degree necessary to define the thermal characteristics of the stream(s) powering the thermochemical process.

The preliminary engineering design of the process (Task 2.3) defines the connectivity of the chemical flowsheet. Each piece of process equipment is indicated and each flowstream is specified as to chemical constituents and an initial estimate of composition, temperature and pressure. Where heating or cooling is indicated, appropriate streams will be paired in heat exchangers. Included in the pairing will be the heat input from the reactor coolant and waste heat to the cooling water flows as well as process-to-process recuperative pairings.

The major effort of Phase 2 will be in developing the material and energy balances for the process (Task 2.4). A chemical process simulator (e.g. AspenPlus) will be the primary tool used in this effort. The full process will be simulated and the flowsheet optimized, in so far as possible, to minimize hydrogen product cost. A process simulator can automatically optimized the process flowsheet to mimimize a specified cost function, but only for a given specification of process connectivity. The process connectivity will be modified progressively and the flowsheet re-optimized as time and funding permit.

TABLE 8
TASKS FOR ALL THREE PHASES

Task Number	Task Description
1.1	Literature survey of new processes
1.2	Develop screening criteria
1.3	Carry out first round screening
1.4	Short report on conclusions
1.5	Carry Out Second Round Screening
1.6	Write Phase 1 report
2.1	Carry out detailed evaluation of few processes to select one
2.2	Define reactor thermal interface
2.3	Preliminary engineering design of selected process
2.4	Develop flowsheet
2.5	Conceptual equipment specifications
2.6	Write Phase 2 Report
3.1	Develop concepts for auxiliary systems
3.2	Refine flowsheet
3.3	Size/cost process equipment
3.4	Evaluate process status
3.5	Write Final Report

As portions of the process design mature, we will define equipment specifications for the chemical process equipment (Task 2.5). These specifications will form the basis for the cost estimates to be made in Phase 3.

The result of Phase 3 will be an evaluation of the process and an estimate of the cost of hydrogen. A key to minimizing the hydrogen cost is to maximize the efficiency of energy utilization. Task 3.1, “Develop auxiliary system concepts,” will investigate the effects of power bottoming and power topping systems. These are the areas in which the Adiabatic UT-3 Process was able to significantly increase the overall efficiency of

hydrogen plus electricity co-generation. Meanwhile, the effort of flowsheet optimization will continue (Task 3.2) with an emphasis on incorporating the auxiliary systems.

The key components in estimating the hydrogen production costs are the capital costs of the chemical plant and the nuclear power costs. The capital equipment costs will be estimated using standard chemical engineering techniques based on process equipment sizes and materials (Task 3.3). All the information necessary to specify the process equipment, to this level of detail, will be available from the optimized mass and energy balance. Since the cost of the advanced nuclear reactor will not be available, the cost of hydrogen will be estimated as function of nuclear power costs.

Finally, the overall status of the process will be evaluated (Task 3.4). During the course of this investigation we will have evaluated all the available data on the cycle and its chemistry. We will be able to recommend the steps necessary to bring the process to the point of commercialization.

It would be advantageous, but not essential, if some form of joint collaboration can be established with the Japanese. In particular, we would like access to their latest experimental results on the chemistry of the sulfur-iodine cycle. Although we are concentrating our effort on the sulfur-iodine cycle, we retain our interest in the UT-3 cycle. The work we have proposed, and which we will carry out for the sulfur-iodine cycle has, to a large part, already been performed in Japan for the Adiabatic UT-3 process. We would encourage the Japanese to perform the required non-steady state analysis. After the Japanese and we have completed our respective tasks, we will have two processes from which to select a means of producing hydrogen using nuclear power.

REFERENCES

[1] International Energy Outlook 2000: DOE/EIA-0484(2000)], The Energy Information Administration of the Department of Energy (www.eia.doe.gov).

[2] Annual Energy Outlook 2000 with projections to 2020: DOE/EIA-0383(2000), The Energy Information Administration of the Department of Energy (www.eia.doe.gov).

[3] Analysis of the Impacts of an Early Start for Compliance with the Kyoto Protocol: SR/OIAF/99-02, The Energy Information Administration of the Department of Energy (www.eia.doe.gov).

[4] Impacts of the Kyoto Protocol on U.S. Energy Markets and Economic Activity: SR/OIAF/98-03, The Energy Information Administration of the Department of Energy (www.eia.doe.gov).

[5] EndNote 3.1.2, ISI Research Soft, Berkeley, California (1999). (www.endnote.com).

[6] DOE PubSCIENCE database (www.osti.gov/pubsci).

[7] The IBM Patent Server (www.ibm.com/patent).

[8] Funk, J.K., R.M. Reinstrom, "Energy requirements in the production of hydrogen from water," Ind. Eng. Chem. Proc. Des. Develop. **5**, 336 (1966).

[9] Yalcin, S., "A review of nuclear hydrogen production," Int. J. Hydrogen Energy **14**, 551 (1989).

[10] Yoshida, K., H. Kameyama, et al., "A simulation study of the UT-3 thermochemical hydrogen production process," Int. J. Hydrogen Energy **15,** 171 (1990).

[11] HSC Chemistry 4.0, Outokumpu research Oy, Pori, Finland (1999).

[12] Brecher, L.E., S. Spewock, et al., "Westinghouse sulfur cycle for the thermochemical decomposition of water," Int. J. Hydrogen Energy **21**, 7 (1977).

[13] Beghi, G.E., "A decade of research on thermochemical hydrogen at the joint research center, Ispra," Int. J. Hydrogen Energy **11**, 761 (1986).

[14] Besenbruch, G.E., "General Atomic sulfur-iodine thermochemical water-splitting process," Am. Chem. Soc., Div. Pet. Chem., Prepr. 271, 48 (1982).

[15] Williams, L.O., *Hydrogen Power,* Pergamon Press (1980).

[16] Ueda, R., H. Tagawa, et al., "Production of hydrogen from water using nuclear energy," A review, Japan At. Energy Res. Inst., Tokyo, Japan. (1974) 69.

[17] Tamaura, Y., A. Steinfeld, et al., "Production of solar hydrogen by a novel, 2-step, water-splitting thermochemical cycle," Energy (Oxford) **20**, 325 (1995).

[18] Bamberger, C.E., "Hydrogen production from water by thermochemical cycles; a 1977 update," Cryogenics **18**, 170 (1978).

[19] Knoche, K.F. and P. Schuster, "Thermochemical production of hydrogen by a vanadium/chlorine cycle. Part 1: An energy and exergy analysis of the process," Int. J. Hydrogen Energy **9**, 457 (1984).

[20] Russell, J., Porter, J., "Production of hydrogen from water," General Atomics Report GA–A12889 (1974).

ACKNOWLEDGMENTS

This work was performed as a collaborative effort between General Atomics, the University of Kentucky and Sandia National Laboratories. Work at General Atomics and the University of Kentucky was supported by the Department of Energy under Nuclear Energy Research Initiative (NERI) Grant No. DE-FG03-99SF21888.

APPENDIX A:
COMMENTS ON SCORING OF EACH CYCLE

Cycle 1 — Westinghouse, also Known as the Hybrid Sulfur, GA-22 or Ispra Mark 11 Cycle [12]

(2) $H_2SO_4(g) \rightarrow SO_2(g) + H_2O(g) + {}^1/_2O_2(g)$ (850°C)

(9) $SO_2(aq) + 2H_2O(\ell) \rightarrow H_2SO_4(aq) + H_2(g)$ (80°C electrolysis)

Advantages. This cycle is an all fluid process. There are only two reactions. The high temperature step (2), is actually a sequence of Reactions (2a) and (2b) that accept heat over a reasonably large temperature range and thus can be well matched to the sensible heat of a reactor coolant. The thermodynamic properties of the chemical species are well known. Side reactions are minimal. The cycle has been fully flow-sheeted. The cycle was operated at bench scale by Westinghouse and at the CRISTINA demonstration pilot plant scale by The Commission of the European Communities at their Ispra Research Establishment. The sulfuric acid decomposition step was also demonstrated using concentrated solar energy on a solar power tower.

Disadvantages. This cycle is a hybrid cycle and as such retains the scale-up problems inherent in electrochemical processes. Electrochemical process are limited by the surface area of the electrodes and can only be scaled-up, after the maximum practical electrode area is reached, by adding modules.

Comments. The cycle has been studied extensively by both Westinghouse and Ispra. The cycle was used by Ispra as part of the CRISTINA demonstration of sulfuric acid cracking step of the Mark 13 Cycle. Although not deemed as efficient as Mark 13 by Ispra, it was easier to use in the demonstration. There is probably little room for improvement since the last Westinghouse flowsheet.

Cycle 2 — Ispra Mark 13 [13]

(2) $H_2SO_4(g) \rightarrow SO_2(g) + H_2O(g) + {}^1/_2O_2(g)$ (850°C)

(10) $Br_2(aq) + SO_2(aq) + 2H_2O(\ell) \rightarrow 2HBr(g) + H_2SO_4(aq)$ (77°C)

(11) $2HBr(g) \rightarrow Br_2(\ell) + H_2(g)$ (77°C electrolysis)

Advantages. This cycle is an all fluid process. There are only three reactions. The high temperature step (2), is actually a sequence of Reactions (2a) and (2b) that adsorb heat over a reasonably large temperature range and thus can be well matched to the sensible heat of a reactor coolant. The thermodynamic properties of the chemical species are well known. Side reactions are minimal. The cycle has been fully flow-sheeted. The cycle was operated at the pilot plant scale by The Commission of the European Communities at their Ispra Research Establishment. The sulfuric acid decomposition step was also demonstrated using concentrated solar energy on a solar power tower. The electrolysis step has been operated at the pilot plant scale as part of a SO_2 recovery process at an oil refinery on Sardinia.

Disadvantages. This cycle is a hybrid cycle and as such retains the scale-up problems inherent in electrochemical processes. The electrode systems developed at Ispra for this cycle appear to be very difficult to scale-up.

Comments. The cycle has been extremely well studied and there is seems to be little room for improvement over the last CEC-Ispra designs.

Cycle 3 — University of Tokyo 3 (UT-3) [8]

(5) $2Br_2(g) + 2CaO(s) \rightarrow 2CaBr_2(s) + {}^1/_2O_2(g)$ (672°C)

(6) $3FeBr_2(s) + 4H_2O(g) \rightarrow Fe_3O_4(s) + 6HBr(g) + H_2(g)$ (560°C)

(7) $CaBr_2(s) + H_2O(g) \rightarrow CaO(s) + 2HBr(g)$ (760°C)

(8) $Fe_3O_4(s) + 8HBr(g) \rightarrow Br_2(g) + 3FeBr_2(s) + 4H_2O(g)$ (210°C)

Advantages. Although this cycle is based on solids, the solid materials remain in fixed beds and only gasses are transported. The cycle has been fully flow-sheeted. The reported efficiency is 40% in the adiabatic bed implementation. Efficiencies as high as 50% are claimed for a plant that co-produces hydrogen and electricity. The cycle has been operated at the pilot plant scale.

Disadvantages. The process involves solids. The cycle cannot be operated in steady-state mode without moving solids. Beds of solid material must be periodically transitioned from one temperature to another. The high temperature endothermic steps are operated under conditions in which the free energy of the reaction is positive. These reactions are forced to proceed by sweeping the reaction products out of the reaction

zone. These reactions are operated very near the melting point of the bromides and, if melting occurs, transport of the molten bromides could lead to blockage of the beds.

Comments. This cycle has been extensively studied in Japan. It is the only cycle presently being studied at large scale. There appear to be some parts of this reaction that are not discussed in the open literature, indicating that there may be some surprises that make this cycle more favorable than it appears. The reaction which consumes $CaBr_2$ is said to occur at 750°C but at this temperature $CaBr_2$ is liquid.

Cycle 4 — Sulfur-Iodine, Also Known as the Iodine-Sulfur, General Atomic or Ispra Mark 16 Cycle [14]

(2) $$H_2SO_4(g) \rightarrow SO_2(g) + H_2O(g) + {}^1/_2O_2(g) \qquad (850°C)$$

(3) $$I_2(\ell_2) + SO_2(aq) + 2H_2O(\ell_2) \rightarrow 2HI(\ell) + H_2SO_4(aq) \qquad (120°C)$$

(4) $$2HI(\ell) \rightarrow I_2(\ell) + H_2(g) \qquad (450°C)$$

Advantages. This cycle is an all fluid process. The high temperature step (2), is actually a sequence of Reactions (2a) and (2b) that adsorb heat over a reasonably large temperature range and thus can be well matched to the sensible heat of a reactor coolant. The thermodynamic properties of the chemical species are well known. Side reactions are minimal. The cycle has been fully flow sheeted. The cycle has been operated at the bench scale in the US and portions of it have been operated at bench scale in Japan. The sulfuric acid decomposition step was operated at the bench scale by General Atomics. This process has the highest quoted efficiency (52%) of any process that has been fully flow sheeted. The sulfuric acid decomposition step was also demonstrated using concentrated solar energy on a solar power tower. This cycle is unique in that the hydrogen is generated at high pressure (50 atmospheres) eliminating the necessity of compressing the hydrogen for pipeline transmission or other downstream processing. Compression of hydrogen is quite energy intensive and is to be avoided if possible.

Disadvantages. Separation of the dense liquid phase from the acid generating reaction into HI and I_2 is accomplished by extracting water into concentrated phosphoric acid in the standard flowsheet. There is a significant amount of water in the phase and the phosphoric acid is only effective at concentrations above 85% so there is a large recycle of phosphoric acid through the phosphoric acid dehydration system. The phosphoric acid dehydration system is thermodynamically efficient, but is capital intensive.

Comments. This cycle has been studied extensively by GA and more recently by other researchers. It was called Mark 16 by the researchers at Ispra. Much of the study by

other researchers has concentrated on the separation of HI and I_2 and several of the proposed alternative schemes look promising. Unfortunately, none of the alternative schemes have been integrated into a complete flowsheet so the integrated effect of the improved schemes cannot be ascertained.

Cycle 5 — Julich Center EOS [15]

(12) $Fe_3O_4(s) + 3FeSO_4(s) \rightarrow 3Fe_2O_3(s) + 3SO_2(g) + {}^1/_2O_2(g)$ 800°C

(13) $3Fe_2O_3(s) + 3SO_2(g) \rightarrow 3FeO(s) + 3FeSO_4$ 200°C

(14) $3FeO(s) + H_2O(g) \rightarrow Fe_3O_4(s) + H_2(g)$ 700°C

Advantages. There are only three reactions and the high temperature reaction occurs at a reasonable temperature.

Disadvantages. This process involves moving and separating solids. There does not appear to be any way to implement the process without moving solids. The solid-solid Reaction (12) between Fe_3O_4 and $FeSO_4$ probably requires a fluxing agent unless the two solids are finely ground together or occur in the same crystal. They could only occur in the same crystal if they are both present in the third Reaction (14), but it is not possible for hydrogen to be released in the presence of sulfate at 700°C without reducing the sulfate to SO_2. This means the FeO + $FeSO_4$ must be physically separated. The SO_2 and O_2 must be separated hot to keep from generating SO_3 while cooling.

Comments. May be able to separate and recombine solids with aqueous steps. This has severe negative impacts on the overall efficiency. This is one of the only $FeCl_x$ cycles that made it through our first cut that does not appear to have a high sensitivity to O_2 carry through.

Cycle 6 — Manganese Ferrite or Tokyo Institute of Technology Ferrite [16]

(15) $2MnFe_2O_4(s) + 3Na_2CO_3(\ell) + H_2O(s) \rightarrow 2\,Na_3MnFe_2O_6(s) + 3CO_2(g) + H_2\,(g)$ 1000°C

(16) $2Na_3MnFe_2O6(s) + 3CO_2\,(g) \rightarrow 2MnFe_2O_4(s) + 3Na_2CO_3(s) + {}^1/_2O_2\,(g)$ 600°C

Advantages. There are 2 reactions. The reactions involve solids but they don’t need to move.

Disadvantages. The process involves solids. Experimental results indicate that there is only 5% conversion per pass. Thermodynamic data are unavailable for the ferrites as pure phases, let alone as the solid solutions. Solid solutions must be important as the reaction does not form a new sold phase. If a new solid phase were formed, the reaction would proced to completion. The H_2 and CO_2 products will equilibrate to also form CO and H_2O. Sodium carbonate is molten in the high temperature Reaction (15) and could separate before reacting. The highest temperature required is higher than desired.

Comments. This is from class of cycles which could be interesting if the reactions proceeded to a significant extent. Such a small change in a large molecule indicates that the ΔG will not be largely influenced by ΔS. Overall efficiency in terms of thermal input is likely to be very low due to cycling of solid bed between temperatures.

Cycle 7 — Hallett Air Products 1965 [15]

(17) $Cl_2(g) + H_2O(g) \rightarrow 2HCl(g) + {}^1/_2O_2(g)$ 850°C

(18) $2HCl(aq) \rightarrow Cl_2(g) + H_2(g)$ 25°C electrolysis

Advantages. This cycle is an all fluid process. There are only two chemical reactions and only one element other than hydrogen and oxygen. There is little potential for side reactions.

Disadvantages. This cycle is a hybrid cycle and as such retains the scaling problems inherent in electrochemical processes. Electrochemical process are limited by the surface area of the electrodes and can only be scaled-up, after the maximum practical electrode area is reached, by adding modules. The reversible voltage for the electrolysis of HCl (18) is greater than that for water. ΔG is 62.676 kcal/mole (E_0 = 1.36 volts) for the reactants and products in their standard states as compared with 57.662 kcal/mole (E_0 = 1.25 volts) for water electrolysis. This will give a 10% penalty before any other considerations. In terms of the adiabatic voltage the situation is worse, 1.73 vs. 1.48 volts or a 15% penalty. At elevated temperatures the relative voltage difference improves for the isothermal case and gets worse for the adiabatic case.

Comments. If the HCl concentration was high the electrode voltage would be reduced. There is plenty of heat available so there should be no problem is supplying the heat necessary to operate the cell isothermally. The cycle might compete with electrolysis if the over voltage for chlorine production is low compared with the over voltage for oxygen production.

Cycle 8 — Gaz de France [15]

(19) $2K(\ell) + 2KOH(\ell) \rightarrow 2K_2O(s) + H_2(g)$ 750°C

(20) $2K_2O(s) \rightarrow 2K(\ell) + K_2O_2(\ell)$ 825°C

(21) $K_2O_2(s) + H_2O(g) \rightarrow 2KOH(aq) + {}^1/_2O_2(g)$ 125°C

Advantages. There are only three chemical reactions and only one element other than hydrogen and oxygen.

Disadvantages. The process involves moving solids and solids melting and solidifying. The hydrogen production Reaction (19) is not spontaneous at any temperature.

Comments. The hydrogen producing Reaction (19) might be forced by using a sweep gas or a vacuum to remove the hydrogen and shift the reaction. Recovery of the hydrogen from the vacuum or sweep gas will be energy intensive. There are some safety concerns in dealing with molten K and its oxides.

Cycle 9 — Nickel Ferrite [15]

(22) ${}^1/_2NiMnFe_4O_6(s) + H_2O(g) \rightarrow {}^1/_2NiMnFe_4O_8(s) + H_2(g)$ 800°C

(23) ${}^1/_2NiMnFe_4O_8(s) \rightarrow {}^1/_2NiMnFe_4O_6(s) + {}^1/_2O_2(g)$ 800°C

Advantages. Only two reactions and the solid reactants/products do not move.

Disadvantages. The process involves solids. Experimental work showed only very low conversion. Evacuation or a sweep gas would be require to remove the oxygen.

Comments. This is from class of cycles which could be interesting if the reactions proceeded to a significant extent. Such a small change in a large molecule indicates that the ΔG will not be largely influenced by ΔS. Overall efficiency in terms of thermal input is likely to be very low due to cycling of solid bed between temperatures. Theoretically there can be no cycle if there is no temperature difference between the reactions. There is very little information in the literature on this cycle.

Cycle 10 — Aachen Univ Julich 1972 [15]

(17)	$Cl_2(g) + H_2O(g) \rightarrow 2HCl(g) + {}^1/_2O_2(g)$	850°C
(24)	$2CrCl_2(s) + 2HCl(g) \rightarrow 2CrCl_3(s) + H_2(g)$	170°C
(25)	$2CrCl_3(s) \rightarrow 2CrCl_2(s) + Cl_2(g)$	800°C

Advantages. The solids could stay in fixed beds, they do not have to move or be separated. Only three reactions. The temperature range is good.

Disadvantages. The process involves solids. The chlorine production Reaction (25) is not favorable until above 1200°C. The only way to shift the reaction at the indicated temperature is to sweep the chlorine away with an inert gas or use a vacuum. The inert gas would end up mixed with the oxygen and either have to be separated or thrown away.

Comments. If the temperature is actually raised to the required temperature of Reaction (25) the $CrCl_2$ (mp 814°C) is liquid and could easily be separated from the $CrCl_3$. The University of Aachen decided to not continue work on this cycle.

Cycle 11 — Ispra Mark 1C [13]

(26)	$2CuBr_2(aq) + 2Ca(OH)_2(aq) \rightarrow 2CuO(s) + 2CaBr_2(aq) + 2H_2O$	100°C
(27)	$2CuO(s) \rightarrow Cu_2O(s) + {}^1/_2\, O_2(g)$	900°C
(7*)	$2CaBr_2(s) + 2H_2O(g) \rightarrow 2Ca(OH)_2(s) + 4HBr(g)$	730°C
(28)	$Cu_2O(s) + 4HBr(g) \rightarrow 2CuBr_2 + H_2(g) + H_2O(g)$	100°C

Advantages. Two high temperature reactions may indicated potential for a high efficiency.

Disadvantages. This process involves separating and moving solids. Thermodynamics for $CuBr_2(aq)$ are not well known.

Comments. This cycle was rejected by its initial proponent in favor of Mark 13.

*Multiple of standard reaction.

Cycle 12 — LASL-U [15]

(29) $3CO_2(g) + U_3O_8(s) + H_2O(\ell) \rightarrow 3UO_2CO_3(aq) + H_2(g)$ 25°C

(30) $3UO_2CO_3(s) \rightarrow 3CO_2(g) + 3UO_3(s)$ 250°C

(31) $3UO_3(s) \rightarrow U_3O_3(s) + {}^1/_2O_2(g)$ 700°C

Advantages. Only three reactions.

Disadvantages. The process involves moving solids and concentrating salt solutions to dry solids.

Comments. Public perception of a uranium process might be that it was a health hazard. Production of very fine particles of UO_x could be a problem for workers within the plant especially during down-time maintenance.

Cycle 13 — Ispra Mark 8 [13]

(32) $3MnCl_2(s) + 4H_2O(g) \rightarrow Mn_3O_4(s) + 6HCl(g) + H_2(g)$ 700°C

(33) $3MnO_2(s) \rightarrow Mn_3O_4(s) + {}^1/_2O_2(g)$ 900°C

(34) $6HCl(aq) + {}^3/_2Mn_3O_4(s) \rightarrow 3MnCl_2(aq) + {}^3/_2MnO_2(s) + 3H_2O(\ell)$ 100°C

Advantages. Only three reactions.

Disadvantages. The process involves moving solids and concentrating salt solutions to dry solids.

Comments. Manganese has numerous oxidation states/phases and intermediates that could be formed. Care would have to be taken to investigate all side products and be certain that there are no thermodynamic sinks that will form over time. This cycle was rejected by its initial proponent in favor of Mark 13.

Cycle 14 — Ispra Mark 6 [13]

(17) $Cl_2(g) + H_2O(g) \rightarrow 2HCl(g) + {}^1/_2O_2(g)$ 850°C

(24) $2CrCl_2(s) + 2HCl(g) \rightarrow 2CrCl_3(s) + H_2(g)$ 170°C

(35) $2CrCl_3(s) + 2FeCl_2(\ell) \rightarrow 2CrCl_2(s) + 2FeCl_3(g)$ 700°C

(36) $2FeCl_3(g) \rightarrow Cl_2(g) + 2FeCl_2(s)$ 420°C

Advantages. Good temperature match.

Disadvantages. The process involves melting, separating and moving solids. The proponents found experimentally that $FeCl_3$ decomposition and hydrolysis of $FeCl_2$ to iron oxides were critical problems for which no suitable solution could be found.

Comments. Reaction (35) is operated above the melting point of $FeCl_2$(mp 677°C) so that it acts as a flux and increases the reaction rate. This cycle was rejected by its initial proponent in favor of Mark 13.

Cycle 15 — Ispra Mark 4 [13]

(17) $Cl_2(g) + H_2O(g) \rightarrow 2HCl(g) + {}^1/_2O_2(g)$ 850°C

(37) $2FeCl_2(aq) + 2HCl(aq) + S(s) \rightarrow 2FeCl_3(aq) + H_2S(g)$ 100°C

(36) $2FeCl_3(g) \rightarrow Cl_2(g) + 2FeCl_2(s)$ 420°C

(38) $H_2S(g) \rightarrow S(g) + H_2(g)$ 800°C

Advantages. Two high temperature reactions may promote high efficiency.

Disadvantages. The process involves separating and moving solids. The proponents found experimentally that $FeCl_3$ decomposition and hydrolysis of $FeCl_2$ to iron oxides were critical problems for which no suitable solution could be found.

Comments. This cycle was rejected by its initial proponent in favor of Mark 13.

Cycle 16 — Ispra Mark 3 [13]

(17) $Cl_2(g) + H_2O(g) \rightarrow 2HCl(g) + {}^1/_2O_2(g)$ 850°C

(39) $2VOCl_2(s) + 2HCl(g) \rightarrow 2VOCl_3(g) + H_2(g)$ 170°C

(40) $2VOCl_3(g) \rightarrow Cl_2(g) + 2VOCl_2(s)$ 200°C

Advantages. Only three reactions. The temperature fit is good.

Disadvantages. Reactions (39) and (40) both have positive ΔGs. The equilibria of Reaction (39) can be shifted by purging but the equilibria of Reaction (40) cannot. The process involves moving of solids.

Comments. The boiling point of $VOCl_3$ is 127°C. Operating at lower temperature where $VOCl_3$ is liquid does not help the thermodynamics. This cycle was rejected by its initial proponent in favor of Mark 13.

Cycle 17 — Ispra Mark 2 (1972) [13]

(41) $2Na_2O.MnO_2(s) + 2H_2O(\ell) \rightarrow 4NaOH(aq) + 2MnO_2(s)$ 100°C

(42) $2MnO_2(s) \rightarrow Mn_2O_3(s) + {}^1/_2O_2(g)$ 487°C

(43) $Mn_2O_3(s) + 4NaOH(\ell) \rightarrow 2Na_2O.MnO_2(s) + H_2(g) + H_2O(g)$ 800°C

Advantages. Only three reactions. The upper temperature is a good match to a nuclear reactor.

Disadvantages. The process involves moving solids and concentrating salt solutions to dry solids.

Comments. Caution is required in cycles involving manganese due to the many possible oxidation states. This cycle was rejected by its initial proponent in favor of Mark 13.

Cycle 18 — Ispra CO/Mn_3O_4 [18]

(44) $3Mn_2O_3(s) \rightarrow 2Mn_3O_4(s) + {}^1/_2O_2(g)$ 977°C

(45) $C(s) + H_2O(g) \rightarrow CO(g) + H_2(g)$ 700°C

(46) $CO(g) + 2Mn_3O_4(s) \rightarrow C(s) + 3Mn_2O_3(s)$ 700°C

Advantages. Only three reactions. The solids do not need to move.

Disadvantages. The process involves moving and separating solids. The carbon generating Reaction (46) is thermodynamically unfavorable. The reaction could be shifted by raising the pressure but it would require in excess of 10^{13} atmospheres. Carbon would need to be separated from Mn_2O_3.

Comments. Caution is required in cycles involving manganese due to the many possible oxidation states. This cycle was rejected by its initial proponent in favor of Mark 13.

Cycle 19 — Ispra Mark 7B [13]

(47) $^{3}/_{2}Fe_2O_3(s) + {}^{9}/_{2}Cl_2(g) \rightarrow 3FeCl_3(g) + {}^{9}/_{4}O_2(g)$ 1000°C

(48) $3FeCl_3(g) \rightarrow {}^{3}/_{2}Cl_2(g) + 3FeCl_2(s)$ 420°C

(49) $3FeCl_2(s) + 4H_2O(g) \rightarrow Fe_3O_4(s) + 6HCl(g) + H_2(g)$ 650°C

(50) $Fe_3O_4(s) + 1/4O_2(g) \rightarrow {}^{3}/_{2}Fe_2O_3(s)$ 350°C

(51) $6HCl(g) + {}^{3}/_{2}O_2(g) \rightarrow 3Cl_2(g) + 3H_2O(g)$ 400°C

Advantages. No advantages over other cycles.

Disadvantages. The process involves five reactions. The process involves separating and moving solids. The proponents found experimentally that $FeCl_3$ decomposition and hydrolysis of $FeCl_2$ to iron oxides were critical problems for which no suitable solution could be found. Oxygen must be separated from gaseous ferric chloride at high temperature. The high temperature reaction is not favorable below 1200°C.

Comments. The process involves separating and moving solids. Reaction (47) appears to require 1200°C instead of the 1000°C indicated. The reaction can be shifted by sweeping the gaseous products away with chlorine gas. Reaction (49) requires purging with water to shift the reaction equilibria. This cycle was rejected by its initial proponent in favor of Mark 13.

Cycle 20 — Vanadium Chloride [19]

(17) $Cl_2(g) + H_2O(g) \rightarrow 2HCl(g) + {}^{1}/_{2}O_2(g)$ 850°C

(52) $2HCl(g) + 2VCl_2(s) \rightarrow 2VCl_3(s) + H_2(g)$ 25°C

(53) $4VCl_3(s) \rightarrow 2VCl_4(g) + 2VCl_2(s)$ 700°C

(54) $2VCl_4(\ell) \rightarrow Cl_2(g) + 2VCl_3(s)$ 25°C

Advantages. The cycle has a good temperature range. All process chemistry has been demonstrated.

Disadvantages. The process involves solids.

Comments. The HCl(*g*) and O_2(*g*) from Reaction (17) should be separated without the use of water as any water left in the HCl would produce VOCl as a byproduct of

Reaction (52). This process would be enhanced by the use of an oxygen permeable membrane. A variation of this process was fully flow-sheeted by the University of Aachen, with a resulting efficiency of 42.5%.

Cycle 21 — Mark 7A [13]

(55)	$3FeCl_3(\ell) \rightarrow {}^3/_2Cl_2(g) + 3FeCl_2(s)$	420°C
(17)	$Cl_2(g) + H_2O(g) \rightarrow 2HCl(g) + {}^1/_2O_2(g)$	850°C
(49)	$3FeCl_2(s) + 4H_2O(g) \rightarrow Fe_3O_4(s) + 6HCl(g) + H_2(g)$	650°C
(50)	$Fe_3O_4(s) + 1/4O_2(g) \rightarrow {}^3/_2Fe_2O_3(s)$	350°C
(51)	$^3/_2Cl_2(g) + {}^1/_2Fe_2O_3(s) \rightarrow FeCl_3(g) + {}^3/_4O_2(g)$	1000°C
(56)	$Fe_2O_3(s) + 6HCl(aq) \rightarrow 2FeCl_3(aq) + 3H_2O(\ell)$	120°C

Advantages. None compared with other cycles.

Disadvantages. Five chemical reactions. The maximum temperature is higher than desired. The process involves separating and moving solids. The proponents found experimentally that $FeCl_3$ decomposition and hydrolysis of $FeCl_2$ to iron oxides were critical problems for which no suitable solution could be found.

Comments. This cycle was rejected by its initial proponent in favor of Mark 13.

Cycle 22 — GA Cycle 23 [20]

(38)	$H_2S(g) \rightarrow S(g) + H_2(g)$	800°C
(2*)	$3H_2SO_4(g) \rightarrow 3SO_2(g) + 3H_2O(g) + {}^3/_2O_2(g)$	850°C
(57)	$^3/_2S(g) + H_2O(g) \rightarrow H_2S(g) + {}^1/_2SO_2(g)$	700°C
(58)	$^9/_2SO_2(g) + 3H_2O(l) \rightarrow 3H_2SO_4(aq) + {}^3/_2S(s)$	25°C
(59)	$S(g) + O_2(g) \rightarrow SO_2(g)$	850°C

Advantages. This cycle is an all fluid process.

*Multiple of standard reaction.

Disadvantages. The kinetics of the sulfur generating reaction may be slow.

Comments. This cycle was rejected by its initial proponent in favor of another cycle. Reactions (59) and (2) can be combined with the sulfur being injected downstream of the heat input to boost the reaction temperature and the conversion of SO_2.

Cycle 23 — US-Chlorine [15]

(17)	$Cl_2(g) + H_2O(g) \rightarrow 2HCl(g) + {}^1/_2O_2(g)$	850°C
(60)	$2CuCl(s) + 2HCl \rightarrow 2CuCl_2(s) + H_2(g)$	200°C
(61)	$2CuCl_2(s) \rightarrow 2CuCl(\ell) + Cl_2(g)$	500°C

Advantages. Three reactions. The temperature range is appropriate.

Disadvantages. The process involves solids with phase changes. Reaction (60) has a positive ΔG but the equilibria can be shifted by purging.

Comments. Thermodynamic analysis indicated that Reaction (60) needs to be performed at room temperature.

Cycle 24 — Ispa Mark 9 [115]

(55)	$3FeCl_3(\ell) \rightarrow {}^3/_2Cl_2(g) + 3FeCl_2(s)$	420°C
(62)	${}^3/_2Cl_2(g) + Fe_3O_4 + 6HCl \rightarrow 3FeCl_3 + 3H_2O + {}^1/_2O_2(g)$	150°C
(49)	$3FeCl_2(s) + 4H_2O(g) \rightarrow Fe_3O_4(s) + 6HCl(g) + H_2(g)$	650°C

Advantages. Three reactions.

Disadvantages. The process involves separating and moving solids. The proponents found experimentally that $FeCl_3$ decomposition and hydrolysis of $FeCl_2$ to iron oxides were critical problems for which no suitable solution could be found.

Comments. This cycle was rejected by its initial proponent in favor of Mark 13.

Cycle 25 — Ispa Mark 6C [13]

(17)	$Cl_2(g) + H_2O(g) \rightarrow 2HCl(g) + {}^1/_2O_2(g)$	850°C
(24)	$2CrCl_2(s) + 2HCl(g) \rightarrow 2CrCl_3(s) + H_2(g)$	170°C
(35)	$2CrCl_3(s) + 2FeCl_2(\ell) \rightarrow 2CrCl_2(s) + 2FeCl_3(g)$	700°C
(61)	$2CuCl_2(s) \rightarrow 2CuCl(\ell) + Cl_2(g)$	500°C
(63)	$CuCl(s) + FeCl_3(s) \rightarrow CuCl_2(s) + FeCl_2(s)$	300°C

Advantages. None.

Disadvantages. Five chemical reactions. Reaction (63) is a solid-solid reaction that probably requires a flux. The process involves separating and moving solids. The proponents found experimentally that $FeCl_3$ decomposition and hydrolysis of $FeCl_2$ to iron oxides were critical problems for which no suitable solution could be found.

Comments. This cycle was rejected by its initial proponent in favor of Mark 13.

APPENDIX A
AN INTRODUCTION TO THERMOCHEMICAL WATER SPLITTING

AN INTRODUCTION TO THERMOCHEMICAL WATER SPLITTING

Thermochemical water-splitting is the conversion of water into hydrogen and oxygen by a series of thermally driven chemical reactions. The direct thermolysis of water requires temperatures in excess of 2500°C for significant hydrogen generation.

(1) $H_2O \rightarrow H_2 + {}^1/_2O_2$ (2500°C min)

At this temperature and one atmosphere pressure, 10% of the water is decomposed and 90% of the water would be recycled. In addition, a means of preventing the hydrogen and oxygen from recombining upon cooling must be provided or no net production would result. A thermochemical water-splitting cycle accomplishes the same overall result using much lower temperatures. The sulfur-iodine cycle is a prime example of a thermochemical cycle. It consists of three chemical reactions, which sum to the dissociation of water.

(2) $H_2SO_4 \rightarrow SO_2 + H_2O + {}^1/_2O_2$ (850°C)

(3) $I_2 + SO_2 + 2H_2O \rightarrow 2HI + H_2SO_4$ (120°C)

(4) $2HI \rightarrow I_2 + H_2$ (450°C)

(1) $H_2O \rightarrow H_2 + {}^1/_2O_2$

The thermochemical cycle has significant conversion at much lower temperatures. With a suitable catalyst at one atmosphere pressure, the high-temperature reaction (2) reaches 10% conversion at only 510°C, and 83% conversion at the indicated temperature of 850°C. Moreover, there is no need to perform a high temperature separation as the reaction ceases when the product stream leaves the catalyst.

Energy, in the form of heat, is input to a thermochemical cycle via one or more endothermic high-temperature chemical reactions. Similar to the way that a heat engine must reject heat to a low temperature sink, a thermochemical cycle rejects heat via one or more exothermic low temperature chemical reactions. Finally, other thermally neutral chemical reaction may be required to complete the cycle so that all the reactants, other than water, are regenerated. In the case of the S-I cycle, most of the input heat goes into the oxygen generating reaction, the dissociation of sulfuric acid. Sulfuric acid and hydrogen iodide are formed in the endothermic reaction of the S-I cycle and the hydrogen is generated in the mildly endothermic decomposition of hydrogen iodide.

The combination of high temperature endothermic reactions, low temperature exothermic reactions and energy neutral closing reactions are not sufficient for a cycle to be thermodynamically realizable. Each reaction must also have favorable ΔG (Gibbs-free

energy). The ΔG for a reaction is a measure of the concentrations of the reactants and products of the reaction at equilibrium. A reaction is favorable if ΔG is negative, or at least not too positive. A slightly positive ΔG does not mean that the reaction does not proceed, only that the reaction does not proceed far and high recycle may be required. If ΔG is slightly positive, it is also possible to shift a reaction equilibrium by increasing the concentrations of the products or reducing the concentration of reactants. Each of the four chemical reactions Eqs. (5)–(8) of the UT-3 Cycle, in fact, has a slightly positive ΔG. The flow of gaseous reactant through beds of solid reactants sweeps the gaseous products away resulting in almost total conversion of the solid reactants to solid products.

(5) $2Br_2(g) + 2CaO(s) \rightarrow 2CaBr_2(s) + {}^1/_2O_2(g)$ (672°C)

(6) $3FeBr_2(s) + 4H_2O(g) \rightarrow Fe_3O_4(s) + 6HBr(g) + H_2(g)$ 560°C)

(7) $CaBr_2(s) + H_2O(g) \rightarrow CaO(s) + 2HBr(g)$ (760°C)

(8) $\underline{Fe_3O_4(s) + 8HBr(g) \rightarrow Br_2(g) + 3FeBr_2(s) + 4H_2O(g)}$ (210°C)

(1) $H_2O(g) \rightarrow H_2(g) + {}^1/_2O_2(g)$

Sometimes it is even possible to electrochemically force a nonspontaneous reaction. A process which includes both thermochemical reactions and electrochemical reactions is termed a hybrid thermochemical cycle to distinguish it from a pure thermochemical cycle. The hybrid sulfuric acid cycle, also known as the Westinghouse cycle or as the Ispra Mark 11 cycle has the same high temperature endothermic reaction as the S-I cycle. This hybrid cycle is closed by the electrochemical oxidation of sulfur dioxide to sulfuric acid.

(2) $H_2SO_4 \rightarrow SO_2 + H_2O + {}^1/_2O_2$ (850°C)

(9) $\underline{SO_2 + 2H_2O \rightarrow H_2SO_4 + H_2}$ (80°C electrolysis)

(1) $H_2O \rightarrow H_2 + {}^1/_2O_2$

APPENDIX B
SANDIA NATIONAL LABORATORY REPORT SAND2002-0513

SAND2002-0513
Unlimited Release
February 2002

An Assessment of Reactor Types for Thermochemical Hydrogen Production

Albert C. Marshall

Prepared by
Sandia National Laboratories
Albuquerque, New Mexico 87185 and Livermore, CA 94550

Sandia is a multiprogram laboratory operated by Sandia Corporation
a Lockheed Martin Company, for the United States Department of
Energy under Contract DE-AC04-94AL85000.

Issued by Sandia National Laboratories, operated for the United States Department of Energy by Sandia Corporation.

NOTICE: This report was prepared as an account of work sponsored by an agency of the United States Government. Neither the United States Government nor any agency thereof, nor any of their employees, nor any of their contractors, subcontractors, or their employees, makes any warranty, express or implied, or assumes any legal liability or responsibility for the accuracy, completeness, or usefulness of any information, apparatus, product, or process disclosed, or represents that its use would not infringe privately owned rights. Reference herein to any specific commercial product, process, or service by trade name, trademark, manufacturer, or otherwise, does not necessarily constitute or imply its endorsement, recommendation, or favoring by the United States Government, any agency thereof, or any of their contractors or subcontractors. The views and opinions expressed herein do not necessarily state or reflect those of the United States Government, any agency thereof, or any of their contractors.

Printed in the United States of America. This report has been reproduced directly from the best available copy.

Available to DOE and DOE contractors from
Office of Scientific and Technical Information
P.O. Box 62
Oak Ridge, TN 37831

Prices available from (615) 576-8401, FTS 626-8401

Available to the public from
National Technical Information Service
U.S. Department of Commerce
5285 Port Royal Rd
Springfield, VA 22161

NTIS price codes
Printed copy: A03
Microfiche copy: A01

SAND2002-0513
Unlimited Release
February 2002

An Assessment of Reactor Types for Thermochemical Hydrogen Production

Albert C. Marshall
Advanced Nuclear Concepts Department
P.O. Box 5800
Sandia National Laboratories
Albuquerque, New Mexico 87185-0425

Abstract

Nuclear energy has been proposed as a heat source for producing hydrogen from water using a sulfur-iodine thermochemical cycle. This document presents an assessment of the suitability of various reactor types for this application. The basic requirement for the reactor is the delivery of 900 C heat to a process interface heat exchanger. Ideally, the reactor heat source should not in itself present any significant design, safety, operational, or economic issues. This study found that Pressurized and Boiling Water Reactors, Organic-Cooled Reactors, and Gas-Core Reactors were unsuitable for the intended application. Although Alkali Metal-Cooled and Liquid-Core Reactors are possible candidates, they present significant development risks for the required conditions. Heavy Metal-Cooled Reactors and Molten Salt-Cooled Reactors have the potential to meet requirements, however, the cost and time required for their development may be appreciable. Gas-Cooled Reactors (GCRs) have been successfully operated in the required 900 C coolant temperature range, and do not present any obvious design, safety, operational, or economic issues. Altogether, the GCRs approach appears to be very well suited as a heat source for the intended application, and no major development work is identified. This study recommends using the Gas-Cooled Reactor as the baseline reactor concept for a sulfur-iodine cycle for hydrogen generation.

Acknowledgments

This work was performed for and funded by the U.S. Department of Energy for DOE Nuclear Energy Research Project number 99-238. The author is grateful for the suggestions and guidance provided by Paul Pickard, Dana Powers, and Steve Showalter of Sandia National Laboratories, and Lloyd Brown from General Atomics.

Table of Contents

List of Figures

List of Tables

Nomenclature

AVR	Arbeitsgemeinschaft Versuchsreaktor
BWR	Boiling Water Reactor
CRBR	Clinch River Breeder Reactor
DOE	Department of Energy
ES&H	Environmental Safety and Health
FSV	Fort St. Vrain
GCR	Gas-Cooled Reactor
HMR	Heavy Metal-Cooled Reactor
HTGR	High Temperature Gas Cooled Reactor
HTGR	High Temperature Graphite Reactor (when used for a MSCR core design)
MSCR	Molten Salt-Cooled Reactor
NERI	Nuclear Energy Research Initiative
PBR	Pebble Bed Reactor
PWR	Pressurized Water Reactor

Executive Summary

A broad range of reactor categories was reviewed to assess the suitability of various concepts as a heat source for the sulfur-iodine thermochemical production of hydrogen from water. The principal requirement is that heat must be supplied at 900 C in order to dissociate sulfuric acid into SO_2, H_2O, and O_2. The assessment was carried out in four stages, as follows:

Stage 1: Status of reactor types

For this stage, nine basic types of reactors were identified and their development status was assessed. The basic reactor types include pressurized water-cooled reactors, boiling water-cooled reactors, organic-cooled reactors, alkali metal-cooled reactors, heavy metal-cooled reactors, gas-cooled reactors, molten salt-cooled reactors, liquid-core reactors, and gas-core reactors. Based on this review, gas-core reactors were eliminated from consideration because, given the objectives of the program, the development requirements for this reactor category is unacceptably high.

Stage 2: Coolant property assessment

For stage 2 the properties of reactor coolants were reviewed to determine their suitability for the proposed application. Pressurized water-cooled reactors were eliminated from consideration because the required system pressure would be extremely high, and boiling water-cooled reactors were eliminated due the severe corrosion issues associated with 900 C steam. Organic-cooled reactors were dropped from consideration because organic coolants dissociate at temperatures well below 900 C. During this stage, baseline coolants were selected for each reactor category. For example, lithium was selected as the baseline coolant for the alkali metal-cooled reactor category.

Stage 3: Attribute assessment

A list of five requirements and five criteria was developed and used to further assess the suitability of the various reactor types for the sulfur-iodine cycle. The five requirements included (1) materials compatibility, (2) coolant stability, (3) reasonable operating pressures, (4) nuclear compatibility, and (5) basic feasibility and development requirements. The five criteria were (1) safety, (2) operational issues, (3) capital costs, (4) intermediate loop compatibility, and (5) other merits and issues. Guidelines were then established for rating each reactor category for each requirement and criterion with a score of 0 through 4 (with 4 indicating best achievable and 0 indicating unacceptable). Based on this assessment, liquid-core and alkali metal-cooled reactors were identified as possibilities, but were judged to present significant technology development risks. The issues for the liquid-core approach focus on the radiological challenges presented by a circulating fuel in the primary loop. For alkali metals, the general corrosiveness of the

coolant and the potential impact on development cost were the principal issues. Gas-cooled, heavy metal-cooled, and molten salt-cooled reactors were identified as promising candidates.

Stage 4: Development COST requirements

A comparison of the relative development cost requirements was made for the top three candidate approaches from stage 3. Based on this assessment, helium gas-cooled reactors appear to require the least development work and present the lowest development risk. The underlying reasons for their suitability for the high temperature sulfur-iodine cycle are: (1) helium is chemically inert, and (2) gas cooled reactors have been successfully operated for a number of years in the required temperature range. Based on this assessment helium gas-cooled reactors are recommended as the baseline choice as a reactor heat source for a sulfur-iodine thermochemical cycle for hydrogen production.

An Assessment of Reactor Types for Thermochemical Hydrogen Production

1.0 Introduction

The Department of Energy has awarded a Nuclear Energy Research Initiative (NERI) Grant to General Atomics, the University of Kentucky, and Sandia National Laboratories to explore the possibility of using a reactor heat source combined with a thermochemical cycle for the production of hydrogen from water [1]. The sulfur-iodine thermochemical cycle was selected during the first phase of this project as the baseline approach. For this cycle, a heat supply temperature of 850 C permits optimum operation; however, temperatures as low as 750 C may be acceptable [2], and by operating at higher pressures, higher temperatures may be utilized. The cycle reactions and operating temperatures are:

(1) $H_2SO_4 \rightarrow SO_2 + H_2O + 1/2O_2$ 850 C

(2) $2HI \rightarrow I_2 + H_2$. 300 C

(3) $2H_2O + SO_2 + I_2 \rightarrow 2HI + H_2SO_4$ 100 C

The cyclical relationship of the chemical reactants is illustrated in Fig. 1, and a schematic illustration of a reactor based hydrogen production system is illustrated in Fig. 2. Reaction 1 is highly endothermic, requiring most of the heat input to the process. Reaction 2 is slightly endothermic and Reaction 3 is very exothermic.

For the second phase of this project, one of the tasks is to define the thermal characteristics of the advanced nuclear reactor heat source. This definition includes a specification of the reactor coolant/heat transfer medium. Several types of nuclear reactors are capable of producing process heat in the temperature range of interest. Sandia was tasked with analyzing the characteristics of the various types of reactors and recommending reactor concepts best suited as a heat source for a sulfur-iodine cycle. This report provides the findings of the Sandia study.

1.1 Objective

The objectives of this study are to identify the most promising reactor concepts for use as the heat source in a sulfur-iodine thermochemical system for producing hydrogen from water, and to select one reactor concept as the baseline design for Phase 3 of this project.

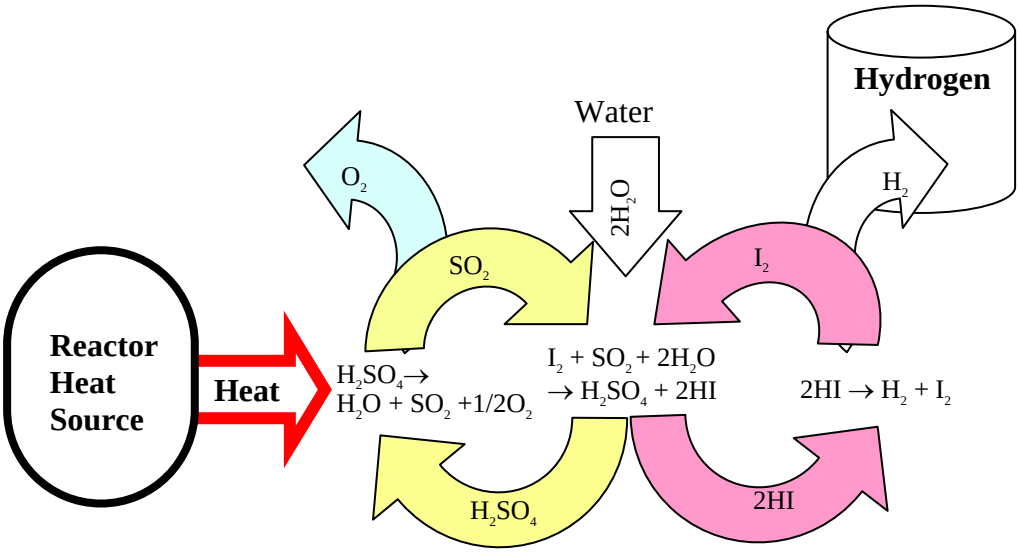

Figure 1 Sulfur-iodine thermochemical cycle for hydrogen production

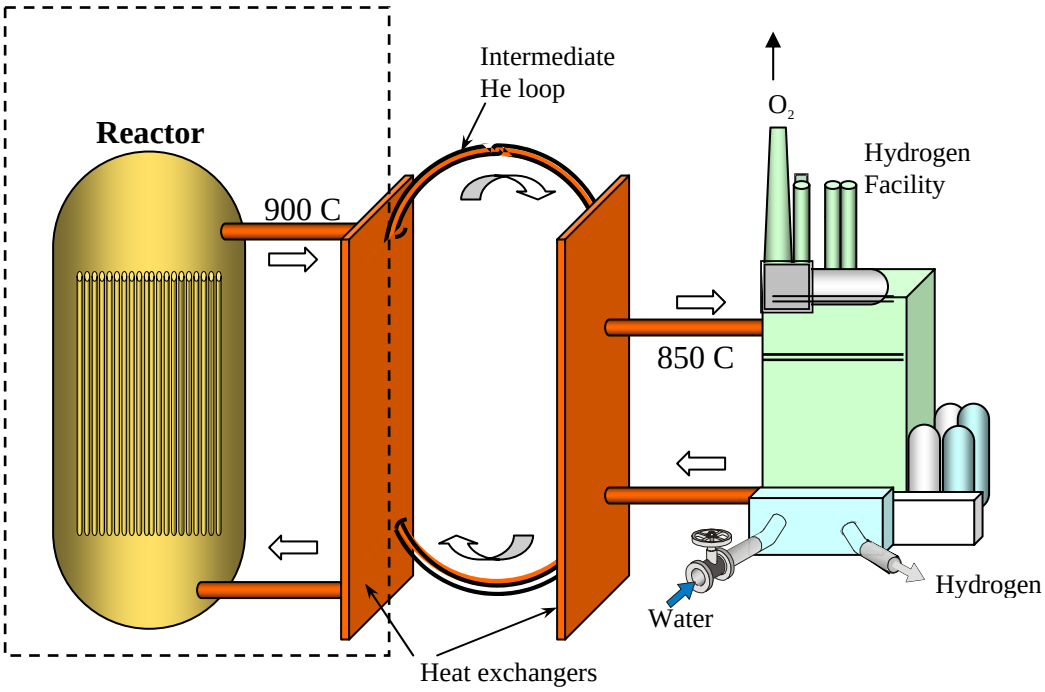

Figure 2 Schematic of nuclear reactor heat source with a water/thermochemical hydrogen production system.

1.2 Approach

The focus for this project is the integration of a reactor system with a chemical plant for the production of hydrogen from water. This challenging goal is in itself an innovative application of nuclear power. Ideally, the recommended reactor technology would require minimal technology development to meet the high temperature requirement. Furthermore, the reactor system should not present any significant design, safety, operational, or economic issues. In other words, the focus of this DOE project should be on the integration and development of a reactor-based hydrogen production plant, rather on a major development of the reactor itself.

The reactor heat source can be conceptually decoupled from the hydrogen production plant, with a heat exchanger providing the interface between the two systems. At present, the plan is to use an intermediate helium loop between the reactor coolant loop and the hydrogen production system. The intermediate helium loop assures that any leakage from the reactor coolant loop will not contaminate the hydrogen production system or expose plant personnel to radiation from the primary loop coolant. The intermediate helium loop also assures that corrosive process chemicals cannot enter the core of the nuclear reactor. Thus, the heat exchanger interface, to a large extent, sets the boundary conditions for selection of the reactor system. The principal requirement set by the interface is the temperature requirement for the decomposition of H_2SO_4. General Atomics estimates a 50 C drop from the core outlet to the point of application [2]; thus, in order to deliver 850 C to the hydrogen production system, the required core outlet temperature is 900 C.

The project objectives and reactor operational requirements suggest a logical approach for reviewing and assessing potentially applicable reactor system options. Given the basic requirements of coolant temperature, and the potential effect of leakage into the coolant loop, the reactor coolant becomes a primary consideration for determining which concepts are most appropriate. Furthermore, the basic reactor types are generally classified by the coolant type. Given these considerations, reactor categories can be delineated by nine basic coolant types identified in Table 1. In order to aid the discussion, a number of sub-categories are also defined in Table 1. The reactor/coolant types include pressurized water-cooled reactors, boiling water-cooled reactors, alkali liquid metal-cooled reactors, heavy liquid metal-cooled reactors, gas-cooled reactors, organic-cooled reactors, molten salt-cooled reactors, liquid-core reactors, and gas-core reactors.

Four assessment stages are used in this study:

STAGE 1: The basic reactor types are reviewed to provide perspective on the development level of candidate reactor systems. Speculative concepts with extreme developmental requirements may be eliminated at this stage. Coolant limitations and concept attributes are not assessed at this stage

STAGE 2: For the second stage, coolant properties are examined to identify merits, issues, and limitations. Fundamental limitations of coolant choices may result in the elimination of some reactor types. At this stage, specific coolant options for each reactor type are examined to select a baseline coolant option; e.g., Li may be selected from the options of Na, Li, NaK, and K for alkali metal-cooled reactors.

STAGE 3: For the third stage, the reactor types are subjectively assessed based on the five requirements and five important criteria given in Table 2. A subjective grade is given for each reactor type (0 through 4) for each assessment criterion.

STAGE 4: For the final stage, the relative development costs are reviewed for the top remaining candidates. A subjective score for development costs (0 through 4) are awarded to each reactor type for five development categories. Based on this analysis a baseline concept is recommended as a heat source for the sulfur-iodine cycle.

From the preceding discussion of the assessment approach, it should be clear that conclusions from this study are based on subjective assessments and the study is limited in both scope and detail. Nonetheless, for the purpose of selecting a baseline approach for system analysis of a sulfur-iodine hydrogen production facility, the conclusions from this study should provide adequate guidance.

Table 1 Reactor Types Considered in the Assessment

1. Pressurized Water Reactors
    - Pressurized Water Reactors (light and heavy water)
    - Supercritical-Phase Pressurized Water Reactors
2. Boiling Water Reactors
    - Boiling Water Reactors (light and heavy water)
    - Boiling Water Reactors with Superheat
3. Organic-Cooled Reactors
    - Diphenyl
    - Other organic coolants
4. Alkali Liquid Metal-Cooled reactors
    - Lithium-cooled
    - Other (Na, K, NaK)
5. Heavy Liquid Metal-Cooled Reactors
    - Lead-bismuth
    - Other (Pb, Bi, Sn, Hg)
6. Gas-Cooled Reactors
    - Noble gasses (He, Ar)
    - Other gasses (CO_2, H_2, N_2, Air, Ar, Steam)
7. Molten Salt-Cooled Reactors
    - $2LiF\text{-}BeF_2$
    - Other salts
8. Liquid-Core Reactors
    - Molten Salt-Core
    - Liquid Metal-Core
    - Aqueous-Core
9. Gas-Core Reactors
    - UF_6
    - Other gas/fuel (UF_4, U-plasma)

Table 2 Attribute Requirements and Criteria

(a) Basic Requirements

1. Chemical compatibility
    - Compatibility of coolant with primary loop materials and fuel.
2. Coolant Stability
    - Molecular stability of coolant at operating temperatures and in a radiation environment.
3. Pressure requirements
    - Pressure limitations for primary loop.
4. Nuclear requirements
    - Issues associated with nuclear aspects of the reactor type.
5. Feasibility
    - Basic feasibility, development requirements, and development risk.

(b) Important Criteria

1. Safety
2. Operational Issues
3. Capital Costs
4. Intermediate Loop Compatibility
5. Other merits and Issues

2.0 Stage 1: Status of Reactor Types

Before embarking on an in-depth study of a specific reactor concept for hydrogen production, an assessment of all possible reactor candidates should be carried out to determine the best choices. This study explores a broad range of reactor concepts and options, from the highly conventional to the highly speculative. The basic reactor types and the principal concepts in each category are briefly reviewed in this section. The principal reactor categories include pressurized water reactors, boiling water reactors, alkali liquid metal-cooled reactors, heavy liquid metal-cooled reactors, gas-cooled reactors, organic-cooled reactors, molten salt-cooled reactors, liquid-core reactors, and gas-core reactors.

2.1 Pressurized Water-Cooled Reactors

Pressurized water reactors (PWRs) are used extensively for commercial production of electricity. A typical PWR reactor system design is illustrated in Fig. 3. The basic design of a PWR core consists of bundles of approximately one cm in diameter, 3.6 m long zircaloy clad fuel rods. Each fuel rod contains stacks of UO_2 fuel pellets. The moderator/coolant/heat transfer medium is water. Water in the primary cooling loop is pressurized to about 15.5 MPa (2,250 psi) and remains in the liquid phase. A heat exchanger is used to transfer heat to a low-pressure secondary loop. The working fluid in the secondary loop is also water. Steam is formed in the secondary loop and used in a Rankine cycle to drive a turbine-generator. The core outlet coolant temperature is about 325 C. The nominal fuel centerline temperature and cladding temperature are 2280 C and 347 C, respectively. A typical large PWR produces 3,400 MW_{th} to provide 1,100 MW_e at 32% efficiency. The total coolant flow rate is about 1.7 x 10^4 kg/sec (19 tons/sec) [3].

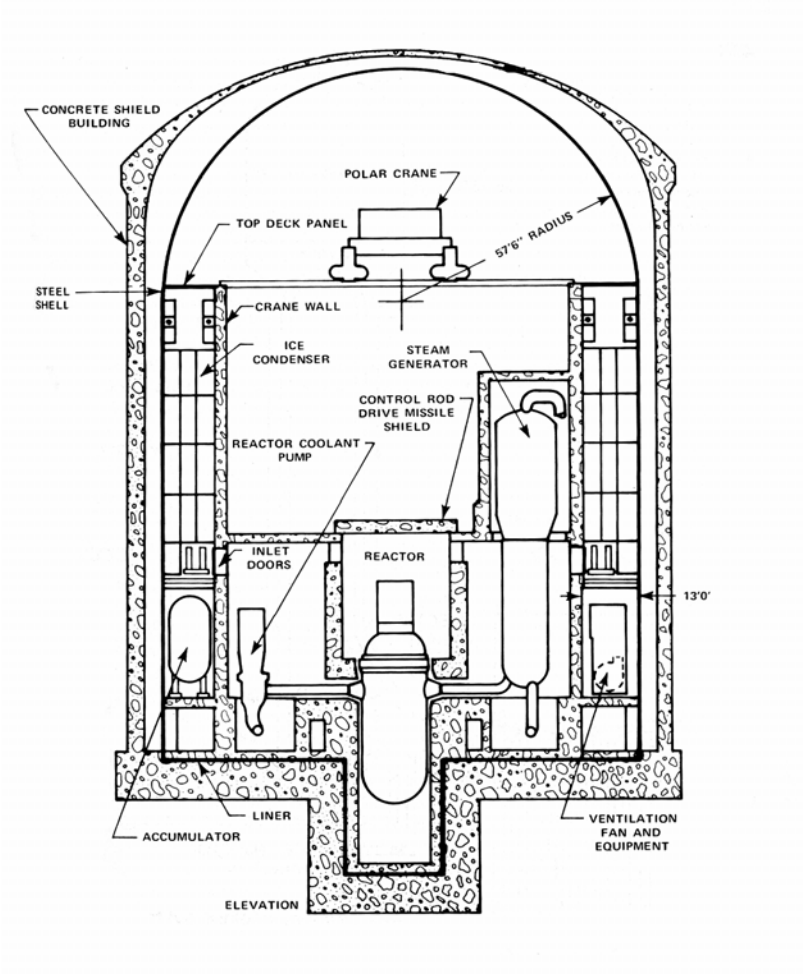

Figure 3 PWR containment building and system components

A number of variations on the basic pressurized water reactor design are available. The Canadian CANDU pressurized water reactors use heavy water, rather than light water, as the moderator. Heavy water (D_2O) absorbs fewer neutrons, thus permitting the use of natural uranium rather than enriched uranium. Advanced PWR concepts, including both evolutionary and revolutionary designs, are under development. These advanced designs are primarily focused on providing passive safety features [4]. Although PWRs are fully mature and they are among the most prolific reactor types, none of the PWRs described in the preceding discussion can achieve the temperature required for the sulfur-iodine cycle using liquid water. In order to provide thermal energy at 900 C with a pressurized water-cooled reactor, the water coolant must be in the supercritical state. The supercritical state of water refers to water above 374C; above this temperature water cannot exist in the liquid state (supercritical water is unrelated to neutronic supercriticality). So-called *supercritical* pressurized water-cooled reactors (high temperature water-cooled reactors in the supercritical phase) have been proposed [5].

2.2 Boiling Water-Cooled Reactors

In the United States, about one-third of operating water-cooled power reactors are boiling water reactors (BWRs). Fuel rods in BWRs are similar to PWR fuel rods. The coolant in a BWR, however, is maintained at lower pressure (7.2 MPa) and steam is formed in the primary loop. For the BWR, water in the primary loop serves as the moderator, coolant, and working fluid. This design eliminates the need for a secondary loop. The coolant temperature is 290 C, and the maximum fuel centerline temperature and average cladding temperatures are 1830 C and 300 C, respectively. A typical large BWR produces 3,579 MWth to provide 1,220 MWe at 34% efficiency. Current U.S. reactors provide steam at saturation conditions; consequently, current design BWRs are incapable of providing steam at the required temperature. If the reactor is used to superheat the steam, however, it may be possible to provide thermal energy at 900 C. BWRs employing nuclear superheat have been operated in the 1950s and 1960s, with reactor outlet steam temperatures up to 500 C. Nuclear Superheated BWRs present a number of problems, such as severe corrosion of fuel elements exposed to superheated steam and shutdown cooling of fuel zones used for superheating [3, 6, 7]. The British have developed boiling heavy water-cooled reactor designs [7].

2.3 Organic-Cooled Reactors

Organic liquid coolants, such as diphenyl, have been developed as an alternative to water coolants for power reactors. The principle advantages of organic coolants are the relatively low vapor pressure and low corrosion characteristics. The low vapor pressure leads to low pressure system designs, compared to water-cooled reactors, resulting in a potentially significant capital cost reduction. An experimental organic-cooled reactor was designed, built, and operated at Oak Ridge National Laboratories in the 1950s. A small U.S. organic-cooled reactor commercial power plant and a Soviet transportable organic-cooled reactor were built and operated in the 1960s. Coolant dissociation in radiation and high temperature environments resulted in virtual abandonment of the organic-cooled reactor option [6, 7].

2.4 Alkali Metal-Cooled Reactors

Alkali liquid metal-cooled Reactor development has focused on sodium-cooled breeder reactor systems. The French have built and operated a large-scale sodium-cooled breeder reactor. In the United States several breeder-prototype liquid metal-cooled reactors were developed. The United States also began construction (subsequently terminated) on a 975 MW_{th} Clinch River Breeder Reactor (CRBR). The CRBR basic design is presented in Fig. 4. Typical reactor outlet temperatures are about 530 C, and the coolant is maintained at a very low operating pressure. For the CRBR system, the flow rate of the sodium coolant was designed to be approximately 2.3×10^3 kg/sec (2.5 tons per sec). For liquid metal-cooled power reactors, heat from the primary liquid metal cooling loop is transferred to a water loop using a heat exchanger. Steam is generated in the secondary loop for use in Rankine cycle to produce electrical power [3]. Fast breeder reactor core designs usually consist of uranium and plutonium oxide pellets contained in steel-clad fuel pins. An advanced liquid metal cooled reactor concept has been proposed that uses a ternary metallic fuel consisting of uranium, plutonium, and zirconium [8]. Other fuel types have been studied and used in alkali liquid metal-cooled reactor designs. Most liquid metal-cooled reactors are fast reactors; however, some designs have been developed that utilize graphite or other materials to moderate (slow down) neutrons.

Although sodium is usually selected as the coolant for liquid metal-cooled breeder reactor system designs, space reactor systems have been developed in the United States and the former Soviet Union that utilize other liquid metal coolants. In the United States, sodium-potassium (NaK) eutectic, potassium, and lithium coolant technology have been developed for space reactors. For the proposed lithium-cooled SP-100 reactor, the fuel was uranium nitride and the design temperature of the coolant outlet was 1,120 C [8].

2.5 Heavy Metal-Cooled Reactors

Heavy liquid metals considered for both terrestrial and space reactors include mercury, bismuth, lead, tin, and lead-bismuth eutectics [7, 9, 10]. The United States developed and tested a small reactor with a mercury Rankine cycle in a secondary-side loop. Lead-bismuth reactors were developed and used in the Russian nuclear-powered submarine program [10]. Heavy metal-coolants are not fire or chemical explosive hazards, and exhibit very low vapor pressures. Furthermore, heavy metal cooled reactors have negative void coefficients of reactivity. For one proposed PbBi power reactor system, the coolant outlet temperature and pressure are 439 C and 0.5 MPa, respectively. For this design, the fuel is UO_2, and the core diameter and length are 1.65 m and 0.9 m, respectively [11]. A variety of other fuels have been proposed for heavy metal-cooled reactors; e.g., UZr, UPuZr, and UPuN.

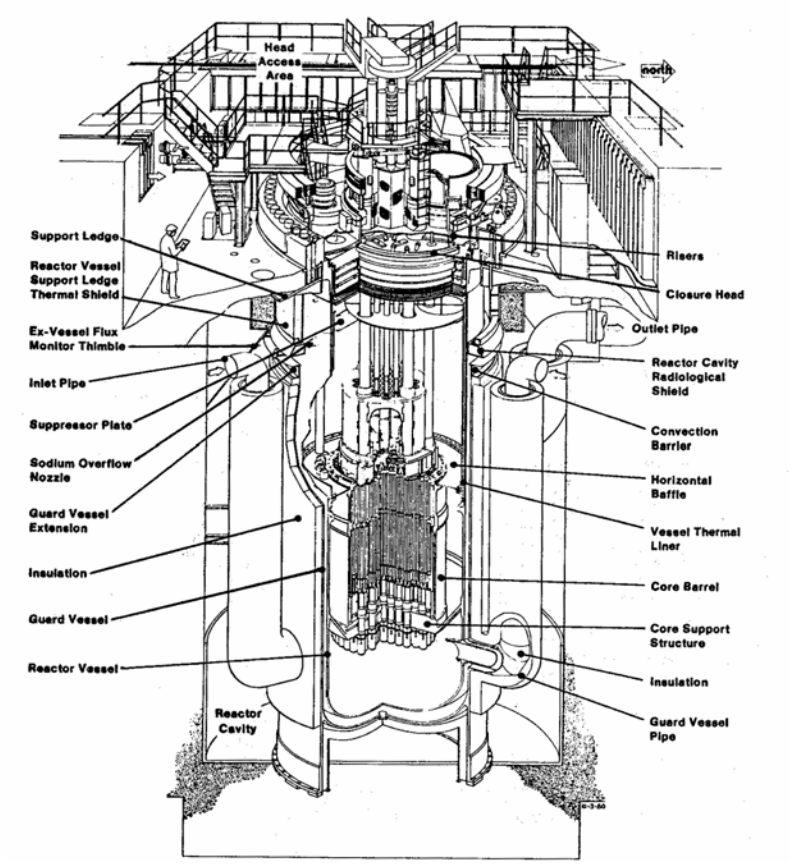

Figure 4 Clinch River Breeder Reactor liquid metal-cooled reactor.

2.6 Gas-Cooled Reactors

Potential gas coolants for reactors include hydrogen, helium, nitrogen, CO_2, argon, air, and steam. A number of large gas-cooled reactors (GCRs) have been developed and operated worldwide. Gas-cooled reactor designs are usually moderated, and graphite is commonly selected as the moderator. However, gas-cooled reactors have been studied and developed that employ other moderators or no moderator. A broad variety of fuel element geometries and fuel types have been used in gas-cooled reactors [6].

The first gas-cooled reactors developed in the United Kingdom were air-cooled reactors. By the late 1950s, gas-cooled reactor development in the United Kingdom and France was based on a CO_2 coolant. Oxidation and dissociation issues, however, have limited CO_2 coolant temperatures to less than 600 C. Fuel element designs for these reactors included uranium metal and uranium dioxide clad in magnesium alloy and other metals. The CO_2-cooled reactor approach proved successful, but these systems did not produce electricity as cheaply as PWRs. In 1979, Great Britain abandoned CO_2-cooled reactors in favor of the more economical PWR approach [6, 7]. In the United States, nitrogen-cooled reactors were once studied for remote power sources, and hydrogen-cooled reactors were developed for space applications. However, nitrogen and hydrogen-cooled reactors were never developed for commercial power applications. The use of steam as a coolant/working fluid has been limited to nuclear superheat in BWR reactors.

Developers in the United States, Germany, and Japan eventually selected helium as an attractive coolant for gas-cooled reactors. Helium is chemically inert, exhibits good heat transfer properties (among gasses), and has a very small neutron capture cross section. In the 1960s, a small high temperature, graphite moderated, helium-cooled reactor plant (Peach Bottom) was built and operated in the United States, and in the 1970s the Fort St. Vrain (FSV) commercial High Temperature Gas Cooled Reactor (HTGR) went into operation. The Fort St. Vrain system was a mid-sized power plant with the basic design features of current-design HTGRs. The FSV core consists of stacks of hexagonal graphite blocks. Each graphite block is 78.7 cm high and 35.6 cm across flats. Fuel rods are contained within the graphite blocks and helium flows through internal coolant channels in the blocks. The fuel rods consist of coated uranium carbide microspheres embedded in a graphitic binder. Maximum fuel temperatures were < 1260 C, and the coolant outlet temperature was 785 C. The primary system for an HTGR design is shown in Fig. 5. For a 2,900 MWth HTGR design, the coolant pressure and flow rate are about 4.8 MPa (700 psi) and 1.3×10^3 kg/sec (1.4 tons per sec), respectively [6, 7]. The recently completed Japanese 30 MWth test reactor, which uses HTGR technology, is designed to achieve an outlet temperature of about 900 C [1].

In the late 1960s, the Germans developed and operated the AVR helium-cooled Pebble Bed Reactor with coolant operating conditions similar to an HTGR, but with a radically different core configuration. Rather than hexagonal fuel elements, the AVR used

6-cm diameter graphite balls containing coated uranium carbide microparticles embedded in the graphite matrix of the ball. The AVR pebble bed reactor core, illustrated in Fig. 6, consists of several hundred thousand fuel balls and over one hundred thousand pure graphite moderator balls. The fuel and moderator balls are continuously recirculated through the core. "Spent" fuel balls are removed from the circulating loop and fresh fuel balls are added as needed to maintain criticality. The outlet coolant temperatures ranged between 850 and 950 C. The Germans also built a 746 MW_{th} prototype power plant pebble bed reactor system; the plant was operated from 1983 to 1988 [6, 7]. The maximum permitted fuel temperature for current generation PBRs (as for HTGRs) is 1260 C [2]. A pebble bed reactor is now under development in South Africa [12].

Currently, the United States has no operating Gas-Cooled Reactors but interest is growing worldwide. The U.S. GCR technology is being updated for use in burning plutonium in Russia. One utility has announced that they will build the Pebble Bed version of GCR in the United States. Development on GCRs is being carried out in the United States, Russia, Japan, China, Germany, and South Africa.

2.7 Molten Salt-Cooled Reactors

Molten Salt-Cooled Reactors have been recently proposed that combine features of the HTGR and Molten Salt Core Reactor concepts [13]. For this concept, the coolant is a molten salt, such as 2Li-BeF_2 and the core resembles the core of a prismatic HTGR. This approach can permit high temperature operation at low pressure, with the possibility of low corrosion. Molten salt-cooled reactors avoid most of the issues associated with the flowing fuel of the molten salt-core reactors (discussed subsequently). Molten salts exhibit very low vapor pressures and are stable in radiation and high temperature environments. Although the molten salt-cooled approach appears to be entirely feasible, it must be emphasized that this approach is only in the early conceptual stage.

2.8 Liquid-Core Reactors

One novel approach to reactor design uses reactor fuel in the liquid phase. The liquid fuel is pumped through the reactor system. Fuel entering the core region supports criticality and the liquid fuel is heated by nuclear fission of its fissile constituents. The hot liquid fuel then exits the core and passes through a heat exchanger, where heat is extracted for use in a power cycle. Liquid-core reactors offer a number of potential advantages. For example, because the fuel is also the fluid heat transfer medium, no thermodynamic losses result from temperature differences between the fuel and coolant. As a consequence, very high efficiencies are possible with liquid-core reactor systems. Furthermore, liquid-core reactors eliminate fuel fabrication costs and eliminate fuel damage concerns. Fluid cores also permit on-line refueling and removal of fission products. The low fission product inventory and low excess reactivity, made possible by on-line fuel processing and fuel re-supply, result in potential safety advantages.

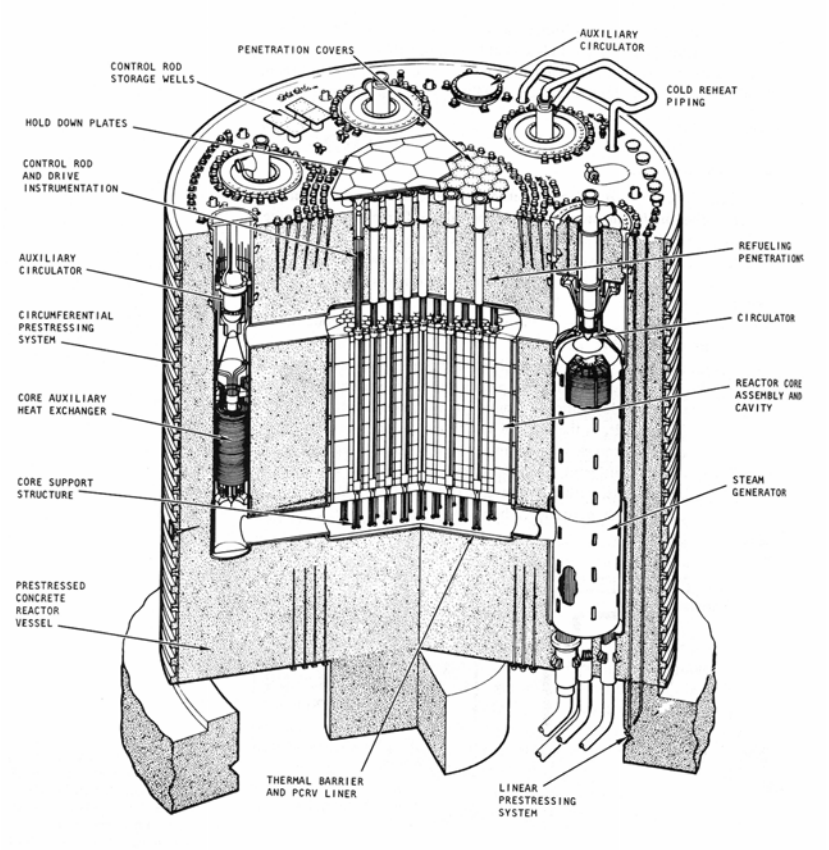

Figure 5 HTGR primary system cross section.

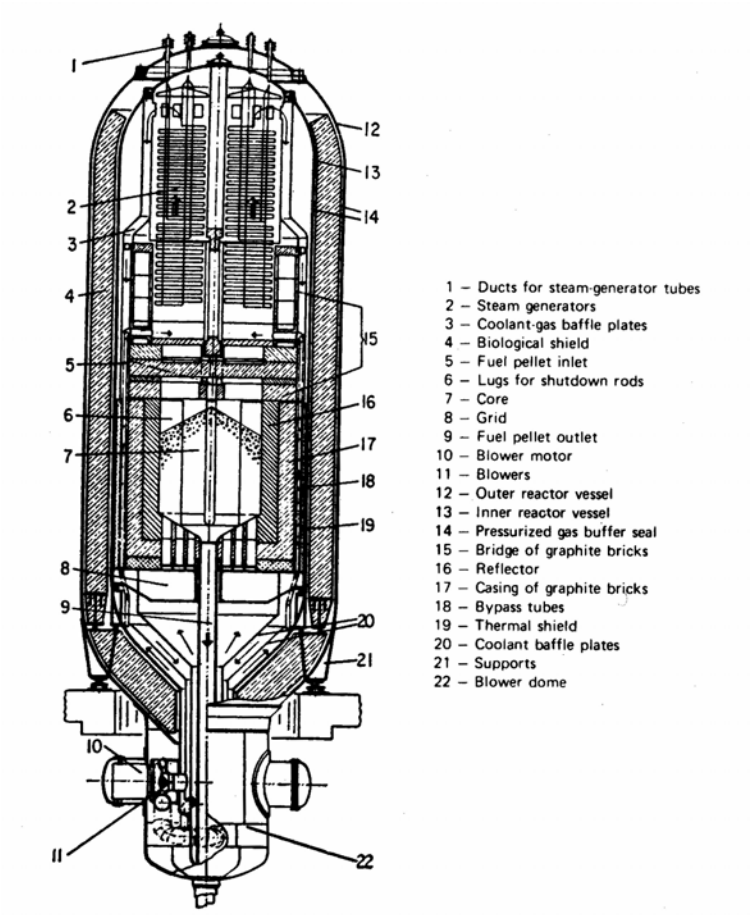

Figure 6 Pebble Bed Reactor vessel cross section.

Aqueous, liquid metal, and molten salt liquid-core reactors have been studied. Aqueous-core reactors include fuel solutions and slurries. Several uranium salts, such as uranyl sulfate (UO_2SO_4) have been studied for solution-type aqueous-core reactors. For slurry-type aqueous-core reactors, uranium compounds (e.g., UO2) are suspended in water. Aqueous-core reactor experiments were conducted in the United States in the 1950s [7].

Liquid metal-core reactors were extensively studied in the 1950s and early 1960s at Brookhaven and Los Alamos National Laboratories. As for aqueous fuel reactors, liquid-metal-fuel reactors include both fuel solutions and slurries. For this approach, uranium or plutonium is maintained in solution in a liquid metal, such as bismuth or lead, or in suspension in a liquid metal, such as sodium. Both moderated and unmoderated systems have been studied. Liquid metal core reactors are not limited by the high vapor pressure difficulties found in aqueous-fuel approaches. Fluid operating temperatures of > 500 C were planned for some designs [7].

Molten salt-core reactors have been more extensively developed than other liquid core concepts. For this approach, the reactor fluid consists of uranium tetrafluoride dissolved in a carrier salt, such as lithium fluoride and beryllium fluoride. Both moderated and unmoderated reactor systems have been designed. A test reactor was operated in the United States in the 1960s [6, 7], and commercial scale designs have been developed in the United States, Russia, and Japan. Molten salts are stable to both radiation and high temperature, and exhibit low vapor pressures. The fuel-fluid operating temperature for one molten salt reactor concept is 700 C [3]. The system pressure for this design is about 0.5 MPa. As for other liquid core designs, the use of a radioactive fluid in the primary loop presents a number of design and operational difficulties. The entire loop is a source of intense radiation fields, requiring shielding-exclusion areas, remote maintenance, containment, and decay-heat removal capability [6, 7, 14].

2.9 Gas-Core Reactors

Gas-core reactors are unquestionably the least developed of all the reactor types studied in this assessment. The fuel for this concept is typically a uranium compound in gaseous form, such as UF_6, UF_4, or uranium plasma. Similar to the liquid-core approach, the gaseous fuel is circulated through the reactor system. Fuel entering the core region supports criticality and the gaseous fuel is heated by nuclear fission. The principal advantage of this approach is that very high temperatures are possible. For gaseous fuel compounds, a typical design would provide gas outlet temperatures of several thousand C. Plasma core reactors are projected to produce gas exit temperatures in excess of 10,000 C. The very high temperature of the gaseous fuel presents serious materials and design challenges. One design approach for protection of core boundary materials includes cooling the pressure vessel and surrounding reflector by a flowing low temperature gas. Most of the work on gas core reactors has focused on nuclear rockets, where very high temperatures are an important advantage. Many operational and design issues must be resolved for gas-core reactors. Although some low power testing of gas core reactors was successfully carried out in the 1970s [15], the gas core approach is basically unproven technology. The required development work and the development risk for gas core reactors are too significant to merit further consideration for this study.

3.0 Stage 2: Coolant Properties

Reactor coolants and heat transport fluids should have low melting points, good heat transport properties, and low potential for chemical attack on vessels and piping. Reasonable operating pressures and compositional stability at operating temperature are also important characteristics. Other desirable properties include low toxicity and low fire and explosion hazard. Reactor coolants must also possess desirable nuclear properties, such as radiation stability and low neutron activation. For thermal reactors, low parasitic capture cross sections are required. If the coolant is to serve as a moderator, low atomic weight constituents are desirable. Property values and characteristics for potential reactor coolants are presented in Tables 3 and 4, and discussed in the following [7- 35]:

3.1 Pressurized Water

The low atomic weight constituents of water (hydrogen) and heavy water (deuterium) make these coolants desirable as moderators. Water has good heat transport properties and a low melting point, but its very low boiling point implies high vapor pressures at high temperatures. At only 327 C (600 K) the vapor pressure is 135 atm, requiring massive high-pressure coolant pipes and vessels. The critical point for water occurs at 374 C and a pressure of 22.1 MPa (218 atm) [14]. At the 900 C temperature required for the sulfur-iodine cycle, the coolant would be required to operate in a supercritical state. So-called *supercritical water-cooled reactors* have been proposed [5]; however, at only 500 C, operating pressures are 25 MPa. For the required cycle operating temperatures, pressures become extreme, and structural requirements are enormous. Furthermore, the potential energy stored in water at these temperatures and pressures is very large; safety issues associated with large breaks at these extreme pressures present additional concerns. Supercritical water is also highly corrosive and heat transfer capability is degraded relative to water in the purely liquid phase. Thus, at the required temperature for the sulfur-iodine cycle, pressurized water-cooled reactors are not feasible.

3.2 Boiling Water

Steam produced at saturation conditions in a BWR cannot provide heat at the high temperature required for the sulfur-iodine cycle. Water-cooled reactors producing superheated steam could, in principle, achieve the required 900 C operating temperature. Although boiling water reactors producing superheated steam at 537 C have been developed, nuclear superheated steam options are no longer actively pursued. High temperature oxidation in a superheated steam environment was one of the main reasons for abandoning this approach. At 900 C, the temperature required for the sulfur-iodine cycle, steam is highly corrosive; consequently, the boiling water-cooled reactor approach is not a feasible option.

Table 3 Reactor Coolant Basic Properties

Coolant	Molecular Weight	Density* (g/cc)	σ_{th}** parasitic (b)	Neutron activation	Radiolytic Decomposition	Hazards Toxic	Fire	Explosion
Water								
H_2O	18	1	0.66	Some	Some	N0	No	No
D_2O	20	1.1	0.001					
Organic								
Diphenyl	154	0.86	0.33	low	Yes	No	No	No
Alkali Metal								
(natural) Li	7	0.53	71	High	Stable	Yes	Yes	Yes
Na	23	0.82	0.525					
NaK	-	0.74	~0.5					
K	39	0.70	2.07					
Heavy Metal								
Sn	118	6.5	0.625	High	Stable	No	N0	No
Hg	200	13.6	380			High		
Pb	207	11.4	0.17			Yes		
Bi	209	9.75	0.034			No		
PbBi	-	~10	~0.1			Yes		
Gases								
H_2	2	0.00009	0.332	Low	Stable	No	High	High
He	4	0.00018	0.007	No	Stable	No	No	No
N_2	14	0.0013	1.88	No	Stable			
Ar	40	0.0018	0.66	Yes	Stable			
CO_2	44	0.0015	0.0038	Some				
Air	-	0.0013	~1.3	Yes				
Steam	18	0.00056	0.66	Some	Some			
Molten Salt								
$2LiF\text{-}BeF_2$	-	~2	-	Yes	Stable	Yes	No	No
Liquid Core								
Aqueous	-	~1	-	Fission products Very high	Some	Yes	No	No
Liquid Metal	-	~10	-		Stable	Yes	Yes	Yes
Molten Salt	-	~2.5	-		Stable	Yes	No	No

* @ ambient temperature

** neutron capture cross section in barns ($b = 10^{-24}$ cm^2)

Table 4 Reactor Coolant Thermal and Chemical Properties

Coolant	Melting Point (C)	Boiling Point (C)	Vapor Pressure (MPa)*	Heat transport properties	Thermal stability Limit (K)	Chemical attack @ 900 C
Water						
H_2O	0	100	13.7	Very good	Stable	Yes
D_2O	0	101	13.7		Stable	
Organic						
Diphenyl	69	255	0.2	Good	750	Yes
Alkali Metal						
Li	181	1331	$< 10^{-9}$	Excellent	Stable	Yes (Nb alloys may be suitable)
Na	98	881	5×10^{-6}			
NaK	-11	784	$\sim 10^{-4}$			
K	64	761	10^{-4}			
Heavy Metal						
Sn	232	2270	$< 10^{-9}$	Excellent	Stable	Some (Coolant additives may be suitable)
Hg	-38.5	358	0.07			
Pb	327	1740	$< 10^{-9}$			
Bi	271	1570	$< 10^{-9}$			
PbBi	125	1670	$< 10^{-9}$			
Gas						
H_2	-	-	-	Poor	Stable	Yes
He	-	-	-		Stable	No
N_2	-	-	-		Stable	Yes
Ar	-	-	-		Stable	No
CO_2	-	-	-		< 850	Yes
Air	-	-	-		< 850	Yes
Steam	0	100	-		-	High
Molten Salt						
$2LiF\text{-}BeF_2$	457	1397	$< 10^{-9}$	Excellent	Stable	Some
Liquid Core						
Aqueous	-	-	~10	Excellent	Some fuel precipitation	Yes
Liquid metal	~300	~1500	Low		Some fuel precipitation	Yes
Molten Salt	497		$< 10^{-9}$		Stable?	Yes

* @ saturation, 325 C

3.3 Organic Coolants

Organic coolants also contain hydrogen atoms and are good moderators. The vapor pressure for organic coolants, at comparable temperatures, is much lower than for water coolants. Although many organic coolants rapidly decompose in radiation environments, the decomposition of some organic coolants may be manageable [7]. Organic coolant heat transport properties are not as good as water, but the major limitation of organic coolants for high temperature applications is its thermal stability. Thermal decomposition limits organic coolant temperatures to a maximum of about 400 C [14, 16]; thus, organic-cooled reactors are not recommended for use as a heat source for the sodium-iodine thermochemical cycle.

3.4 Alkali-Metal Coolants

Most of the liquid metal-cooled reactor development in the United States has focused on alkali metal coolants such as sodium. Other possible alkali metal coolants include lithium, potassium, and NaK eutectic. Alkali metals are generally corrosive at high temperature, exhibit high neutron activation, are typically toxic, and present fire and explosion hazards. Some alkali metal-cooled reactor designs can exhibit positive void coefficients. In addition to sodium-cooled reactors, the United States developed a number of NaK-cooled reactors, mostly for space applications. Although NaK is liquid at ambient temperatures, the heat transport properties of NaK are not as good as Na. NaK is toxic, flammable, and can be highly explosive. All liquid metal cooled breeder reactor programs selected sodium rather than NaK; apparently NaK's ability to remain fluid at ambient temperatures was less important than economic and other benefits of sodium.

The United States carried out significant development work on a potassium-cooled reactor for space applications [15]. Like NaK, potassium is toxic, flammable, and can be highly explosive. For commercial terrestrial power applications, potassium-cooled reactors do not possess any significant advantages over sodium [7]. At the high temperatures of interest to this study, the vapor pressure of most alkali metals is fairly high; lithium, however, is an exception. The low vapor pressure and excellent heat transport properties of lithium are significant advantages. Lithium activation produces helium and radioactive tritium gases. The coolant activity and the quantity of gas produced by activation can be reduced by using depleted lithium. Lithium presents fire and severe chemical explosion hazards, and is solid at ambient temperatures. Life testing of Nb alloys with lithium coolants have been successful at temperatures above the desired cycle operating range; however, a long-term operational database has not been developed. Furthermore, the development cost and capital costs for candidate materials has not been determined. For this study, lithium is selected as the baseline coolant because it exhibits a low vapor pressure relative to other alkali metals.

3.5 Heavy-Metal Coolants

Possible heavy metal coolant options include tin, mercury, lead, bismuth, and lead-bismuth eutectic. Although tin appears to have a number of desirable features, no significant development work has been carried out for this option. In the United States, mercury was once considered as a working fluid for space reactors. Mercury has a relatively high vapor pressure, but its most significant drawback is its toxicity and a large thermal capture cross section. In the current ES&H environment, the health risk associated with mercury is too great to merit serious consideration of mercury as a coolant option.

Lead possess excellent heat transfer characteristics and does not present a fire or significant chemical explosion hazard. Lead also exhibits an extremely small vapor pressure, typically possesses a negative void coefficient, and may offer other safety advantages [17]. The Russians have developed and operated PbBi-cooled reactors for naval applications. Lead-bismuth coolants possess the advantage, relative to lead, of a 200 C lower melt temperature. A major disadvantage of PbBi coolants is the activation product ^{210}Po resulting from an n,γ reaction with ^{209}Bi and subsequent beta-decay to ^{210}Po. Polonium-210 is very toxic and difficult to contain [7]. Nonetheless, the former Soviet Union developed and used PbBi-cooled reactors, and the PbBi-cooled approach has been proposed by several laboratories as an advanced power production reactor [17-20]. Bismuth possesses a higher melt temperature than the PbBi eutectic and offers no significant advantages over PbBi-cooled reactors. Compared to the alkali metals, heavy metals may be more compatible with other core materials at very high temperatures. The issue has been raised of a loss of alloying agents in structural materials for high temperature flowing Pb or PbBi environments. Supplying appropriate additives to the cooling stream may eliminate this concern. For this study, PbBi was selected as the baseline heavy metal coolant because of its lower melt temperature, and because the Russians have accumulated significant experience with PbBi reactor technology.

3.6 Gas Coolants

Increasing the flow surface area, as well as operating at high temperatures, high pressures, and high flow rates can compensate for the generally poor heat transport characteristics of gas coolants. Gas coolant operating pressures, however, are far below that for water at required cycle temperatures, and for most gas coolants, no phase change occurs for any postulated accident sequence. Most importantly, noble gases are chemically inert. Gases are too diffuse to serve as effective moderators; consequently, thermal gas-cooled reactors require a separate moderator.

Reactive Gases

Although considerable CO_2-cooled nuclear power plant experience was accrued in the 1960s and 1970s in the UK, the economics of these systems proved unfavorable. More importantly to this study, the corrosiveness and thermal dissociation of CO_2 at > 600 C makes this coolant option unacceptable for the proposed cycle. Limited development work has been carried out for nitrogen reactors, and chemical incompatibility of materials with high temperatures nitrogen gas is an issue. In the pioneering days of nuclear power, once-through air-cooled reactors were developed and

operated (i.e., the air coolant passing through the reactor was released directly into the atmosphere). Air-cooled reactors suffer the same limitations as CO_2-cooled reactors and once-through cooling is no longer a viable approach.

Although water-cooled reactors with superheated steam have been developed, nuclear superheated steam options are no longer actively pursued. The high temperature oxidation of superheated steam was one of the main reasons for abandoning this approach. Furthermore, the heat transfer properties of steam are not as good as helium, and steam activation and dissociation are significant. Hydrogen-cooled reactors have been developed in the United States and Russia for nuclear rockets. Although hydrogen possesses the best heat transfer characteristics among gas coolants, the very high fire and explosion hazard of hydrogen rules out its use for terrestrial applications.

Noble Gasses

Little development has been carried out for argon-cooled reactors. Argon is chemically inert, but heat transfer characteristics for argon are not as good as helium and neutron activation and parasitic capture are disadvantages. Significant experience has been accumulated with helium-cooled reactors. Among gasses, helium exhibits good heat transport properties. Helium is neither a fire or explosion hazard, is non-toxic, is stable in radiation and high temperature environments, has a very small parasitic capture cross section, and neutron activation is extremely small. The most significant and pertinent advantage of helium is its chemical inertness. For these reasons, helium is selected as the baseline coolant for gas-cooled reactors.

3.7 Molten Salt Coolants

Molten salt-cooled reactors were recently proposed [13] that combine features of the HTGR and molten salt-core reactor concepts (here we assume that the "G" in HTGR refers to graphite, rather than gas). For this concept a molten salt coolant, such as 2Li-BeF_2 is used in place of helium in an HTGR. This approach permits high temperature operation at low pressure, with the possibility of low corrosion. The excellent heat transfer capabilities of molten salt should reduce fuel operating temperatures, relative to HTGR operation using a helium coolant. Molten salt-cooled reactors avoid most of the issues associated with flowing fuel for molten salt-core reactors (discussed subsequently). Molten salt coolants also offer the advantages of thermal and radiation stability, no fire or chemical explosion hazard, and a number of safety advantages. However, molten salts are solid at room temperatures, requiring a high-temperature auxiliary heating system for reactor startup. Depleted lithium (99.999% ^7Li) is required because the capture cross section of natural lithium is high. Another consideration is the generation of tritium and helium as a result of neutron capture by ^6Li.

3.8 Liquid Core Coolants

Heat transfer is excellent for liquid core coolants because the heat source (fuel) and coolant are embodied in the same fluid. The major disadvantage of liquid core coolants is that the primary loop contains radioactive fission products. Even with online fission product removal, the radiation environment of primary loop components is a major issue [7].

Aqueous Core

The corrosiveness of the uranium salt solutions, the inability to keep uranium compounds in suspension in slurry-type fuels, and a number of other difficulties resulted in a termination in the development of aqueous-fuel liquid core reactors [7]. Furthermore, the vapor pressure for aqueous-core reactors is too high for the required cycle temperature.

Liquid Metal Core

The vapor pressure for liquid metal core coolants is quite low, and the fluid is stable in high temperature and high radiation field environments. However, liquid metal core reactors have never been built. Furthermore, liquid metal core coolants are highly corrosive and mass transport is an issue for some liquid metal core concepts.

Molten Salt Core

Molten salt fuel/coolants possess a number of advantages; e.g., low vapor pressures, low corrosion at high temperature, thermal and radiation stability, no fire or chemical explosion hazard, a number of safety advantages, and the possibility of online refueling and fuel processing. Furthermore, a molten salt reactor was successfully operated in the United States in the 1960s. The issues associated with a circulating highly radioactive fuel and on-line fuel processing, however, are substantial. Although molten salt reactors generally exhibit low corrosion at high temperature, long term materials compatibility at the required 900 C cycle temperature has not been demonstrated. If a moderated molten salt-core is proposed, depleted Li must be used to reduce parasitic neutron capture by ^{6}Li. Nonetheless, molten salt core reactor technology is more developed and more promising than other liquid core coolants; consequently, molten salt core-coolants are selected as the baseline liquid core reactor category.

4.0 Stage 3:Attribute Assessments

Using the requirements and criteria presented in Table 2, a subjective grade was assessed for each of the remaining candidate reactor options. A brief discussion of the assessment basis is presented here, and a summary of the assessment grades for each requirement and criteria is provided in Table 5. For each consideration, reactor concepts were graded using the following rating scheme:

Grading basis for requirements

4: - Demonstrated to meet requirements

3: - Expected to meet requirements
2: - Promising, but entails a development risk
1: - Possible, but entails a significant development risk
0: - Not feasible (eliminate from consideration)

Grading basis for criteria

4: - Excellent
3: - Good, not optimum
2: - Acceptable
1: - Issues or poorly suited
0: - Unacceptable (eliminate from consideration)

Table 5 Assessment of Reactor Concepts for Sulfur-Iodine Thermochemical Cycle

Coolant	Gas	Salt	Heavy metal	Liquid core	Alkali metal	PWR	BWR	Org.	Gas core
1. Materials compatibility	4	3	3	3	2	-	0	-	-
2.Coolant stability	4	3	4	3	4	-	-	0	-
3. Operating Pressure	4	4	4	4	4	0	-	-	-
4.Nuclear issues	4	4	4	3	3	-	-	-	-
5. Feasibility	4	3	2	3	2	-	-	-	0
1. Safety	3	4	3	3	2	-	-	-	-
2. Operations	3	3	3	2	3	-	-	-	
3. Capital costs	2	3	3	1	1				
4. Intermediate loop compatibility	4	3	3	3	3	-	-	-	-
5. Other merits and issues	3	3	3	3	3	-	-	-	-
Unweighted Mean Score	3.5	3.3	3.2	2.8	2.7	N/A	N/A	N/A	N/A

4.1 Pressurized Water-Cooled Reactors

- **Pressure: 0**
  The extreme pressure requirements for PWRs eliminate this potential option.

4.2 Boiling Water-Cooled Reactors

- **Chemical compatibility: 0**
  Superheated steam at 900 C is highly corrosive; consequently, BWRs are eliminated from consideration.

4.3 Organic-Cooled Reactors

- **Coolant stability: 0**
  Thermal and radiation dissociation issues eliminate organic cooled reactors from consideration.

4.4 Alkali metal-Cooled Reactors

The low vapor pressure of lithium and the Li compatibility test data from the SP-100 program led to the selection of lithium as a representative coolant for alkali metal coolants.

Assessment:

- **Chemical compatibility: 2**

Alkali metals are generally corrosive at high temperatures; nonetheless, limited testing of liquid metals has been carried out at > 900 C. For example, the SP-100 space reactor program carried out successful compatibility testing of flowing Li in Nb alloy loops for several thousand hours at 1,077 C. Test data spanning many years of operation is lacking, and development and fabrication of corrosion resistant components may be very costly.

- **Coolant stability: 4**

Liquid metals are stable in high temperature and radiation environments.

- **Pressure requirements: 4**

The vapor pressure for lithium is very low.

- **Nuclear issues: 3**

Neutron capture in lithium-6 results in the formation of lithium-7 in an excited state. Subsequent decay produces tritium and helium.

$$Li^{6} + n \rightarrow (Li^{7})^{*} \rightarrow {}^{3}H + {}^{4}He$$

The design of lithium-cooled reactors must accommodate the production of tritium and helium. The use of depleted lithium can reduce tritium and helium production. Of greater concern is the potential for positive void coefficients and its effect on safety.

- **Feasibility: 2**

No reactor experience exists for lithium-cooled reactors (although experience exists for sodium cooled reactors, operating pressures for sodium are unacceptable). Compatibility testing of lithium coolants for the SP-100 program is promising; however, operational data for Li at 900 C was accrued for only a small fraction of the lifetime of a typical terrestrial reactor. Uranium nitride was selected as the fuel for the SP-100 reactor because UO_2 was found to dissolve in lithium (in the event of a cladding leak). Uranium nitride fuel, however, required specially designed fuel elements to deal with thermal dissociation and chemical incompatibility of the Nb alloy with UN fuel (a Re liner was used). The development requirements for a commercial scale lithium based system needs to be assessed.

- **Safety: 2**

Lithium's low vapor pressure should prevent rapid coolant evaporation following a postulated primary system breach. On the other hand, liquid metal-cooled reactors are typically fast reactors, raising some concerns relative to reactivity-induced accidents. These issues are more acute when positive void coefficients (coolant void induced reactivity increase) are possible. From the standpoint of positive void coefficients, lithium is probably worse than sodium. Although the United States and other nations have safely operated alkali metal cooled reactors, positive void coefficients, the potential for lithium fires and explosions, and tritium production are important safety considerations.

- **Operational issues: 3**

Lithium thaw requirements, fire and explosion safety precautions, and tritium management requirements may present operational issues.

- **Capital costs: 1**

High capital costs may result if special alloys and complex fuel element deigns are required (as for the SP-100 design). Low operating pressures may reduce some capital expenditures.

- **Intermediate loop compatibility: 3**

Possible reactivity effects of voids introduced by helium leakage from the intermediate loop must be considered. A liquid metal coolant could be used for the intermediate loop; however, compatibility with the thermochemical loop may then present issues for some postulated accidents.

- **Other issues and merits 3**

The development of high temperature alkali metal cooled reactors could provide the technology for highly efficient systems for electrical power. A fast reactor design could permit deep fuel-burn to render the fuel proliferation resistant.

4.5 Heavy Metal-Cooled Reactors

The lower melt temperature of PbBi, relative to lead, and the extensive Russian experience with PbBi reactors led to the selection of PbBi as the representative coolant for heavy metal-cooled reactors.

Assessment:

- **Materials compatibility 3**

Heavy metals are generally less corrosive than alkali metals. Nonetheless, extensive materials testing for liquid heavy metals at 900 C is lacking. Furthermore, issues have been raised concerning the possibility of leaching out alloying agents from structural materials containing very hot flowing lead or lead-bismuth. Coolant additives may result in acceptable materials compatibility at 900 C.

- **Coolant stability: 4**

Liquid metals are stable in high temperature and radiation environments.

- **Pressure requirements: 4**

The vapor pressure for lead-bismuth is very low.

- **Nuclear issues: 4**

The major nuclear disadvantage of PbBi coolants is the activation product ^{210}Po resulting from an n,γ reaction with ^{209}Bi (and beta decay). Although polonium-210 is very toxic and difficult to contain, Russian experience suggests that ^{210}Po can be safely managed.

- **Feasibility: 2**

The United States has little experience with heavy metal reactor coolants. Cooperation with Russian developers could be important if heavy metal cooled reactors are pursued. Reactor experience with heavy metal coolants is limited to temperatures far below 900 C. Although promising, this absence of materials and appropriate fuel data for these systems presents appreciable development risk.

- **Safety 3**

The low vapor pressure of heavy metal coolants provides the safety advantages of preventing loss of coolant accidents due to rapid coolant evaporation, and precluding explosive release of a high-pressure coolant. Heavy metal-cooled reactors are typically proposed as fast reactors. Reactivity induced accidents are generally more of a concern for fast reactors than for thermal reactors; however, heavy metal coolants possess an advantage over alkali metals in that they do not exhibit positive void coefficients.

Furthermore, PbBi does not present fire or chemical explosion hazards. On the other hand, the activation product ^{210}Po resulting from an n,γ reaction with ^{209}Bi, presents additional considerations.

- **Operational issues: 3**

Lead-bismuth thaw requirements may result in added operational complexity.

- **Capital costs: 3**

Lead-bismuth thaw requirements may result in additional capital expenditures. Low operating pressures may reduce some capital expenditures.

- **Intermediate loop compatibility: 3**

Possible reactivity effects of voids introduced by helium leakage from the intermediate loop must be considered. A liquid metal coolant could be used for the intermediate loop; however, compatibility with the thermochemical loop may then present issues for some postulated accidents.

- **Other issues and merits: 3**

The development of high temperature heavy metal-cooled reactors could provide the technology for highly efficient systems for electrical power. A fast reactor design could permit deep fuel-burn to render the fuel proliferation resistant.

4.6 Gas-Cooled Reactors

Although the coolant for PBRs and HTGRs is identical (He), the design characteristics of these approaches differ significantly. To simplify the grading of the helium-cooled approach, the HTGR design will be assumed as the representative approach for helium-cooled reactors.

Assessment:

- **Materials compatibility: 4**

Helium is an inert gas and, in its pure state, should be ideal for operation at the required temperature of 900 C. Although materials effects can result from impurities in the coolant, operational experience with Fort St. Vrain showed no significant materials issues related to impurities in the coolant. Some graphite transport materials problems were encountered that were associated with water entering the primary loop from the water bearings and Pelton wheel of the compressor. For new HTGR designs, these problems should not arise because the water bearings and Pelton wheels will be replaced by magnetic bearings and electric motors. Fort St. Vrain operated for 15 years at coolant temperatures of 750 C. The AVR operated for 21 years, including years of operation at 950 C; consequently, gas-cooled reactors have been successfully operated in the desired optimal temperature range. (The Japanese prismatic fuel HTTR will also operate at coolant temperatures > 900 C).

- **Coolant stability: 4**

Helium is stable in thermal and radiation environments.

- **Pressure requirements: 4**

Gas coolant operating pressures are high, but well within the operational envelope for gas cooled reactors. Although high pressure operation implies the possibility of rapid coolant loss, the high heat capacity of the graphite fuel elements mitigates the effects of these types of accidents.

- **Nuclear issues: 4**

Activation of He is insignificant.

- **Feasibility: 4**

In general little development work is identified for GCRs. The United States has considerable experience with gas-cooled reactor systems. U.S. industry is not directly engaged in gas-cooled reactor development at present, but U.S. technology is well documented. The U.S. HTGR technology is now being transferred to Russia for the purpose of building an HTGR to burn the plutonium from the Russian plutonium stockpile. Germany is no longer developing gas-cooled reactors but the German pebble bed technology is in the process of being transferred to the South African nuclear program. Japan is actively engaged in development of gas-cooled reactors. The required coolant temperature is a bit higher than the current experience base for U.S. designs; however, the current fuel form is expected to be acceptable for the somewhat higher operating temperatures. The German reactors have been successfully operated at a coolant outlet temperature 950C, and the Japanese are developing higher temperature zirconium carbide coated fuel. Although the United States has experience with zirconium carbide coated fuel, it may be expedient to license the Japanese technology. The U.S. facilities for gas-cooled reactor fuel fabrication have been decommissioned but the technology for making coated particle fuel still exists at facilities that produce Navy reactor fuel.

- **Safety: 3**

The high heat capacity of the core for graphite-moderated helium cooled concepts results in very gradual core heating in the event of a loss of flow accident. Furthermore, no coolant phase change occurs for any postulated accident sequence. The high fission product retention ability of the HTGR microsphere fuel provides another safety advantage. Helium is non-toxic and does not present a fire or explosion hazard.

The issue has been raised concerning the possibility of rapid oxidation of the graphite fuel elements in the event of accidental air ingress into the primary system. The proponents of gas-cooled reactors argue that the high-density, high-grade graphite used for the fuel elements does not undergo rapid oxidation for postulated loss-of-coolant accident conditions [36]. The possibility of significant water ingress seems highly improbable due to the absence of a high-pressure water interface with the primary loop. Furthermore, magnetic bearings and electric motors will be used for the compressor,

rather than using water bearings and steam-driven Pelton wheels (used for FSV). Nonetheless, independent study of the possibility of rapid oxidation is recommended. Gas cooled reactors, taking advantage of coated particle fuel technology, are sometimes designed without an external containment building. Here we have assumed adequate confinement by either the fuel particle coating, or by a confinement enclosure (reflected in somewhat higher capital costs, as discussed subsequently).

- **Operational issues: 3**

Other than the lack of a large base of operational experience (compared to PWRs and BWRs), no significant operational issues are identified. Nonetheless, very high temperature, high pressure operating conditions may present some operational considerations; thus, a score of (3) is awarded for operational issues.

- **Capital costs: 2**

The poor heat transfer characteristics of gasses and the large volumes of graphite required for effective moderation generally result is fairly large reactor systems. Furthermore, large reactor systems combined with the need for containing a high-temperature, high-pressure coolant may result in increased capital costs. Additional capital costs will result if a containment or confinement building is required. Given all of these considerations, a (2) was awarded for capital costs.

- **Intermediate loop compatibility: 4**

The helium coolant is entirely compatible with the intermediate loop.

- **Other issues and merits: 3**

The high temperature capability of the helium-cooled reactor can also be used to develop highly efficient systems for electrical power. The possibility of a direct Brayton cycle may result in significant efficiency improvements and reduced capital costs for the production of electricity. (If the PBR is used, online refueling, deep fuel burn, and low excess reactivity operation are feasible).

4.7 Molten Salt-Cooled Reactors

Fluoride salts were selected as the representative coolant for molten salt-cooled reactors.

Assessment:

- **Materials compatibility: 3**

Molten fluoride salts exhibit good corrosion resistance at high temperatures; however, the required temperatures are somewhat higher than the existing experience base. Although molten fluoride salts should be compatible with graphite, some evidence of mass transport has been obtained for systems using both metal and graphite components [37]. The possible issue of fission product effects for molten salt-core reactors does not apply to molten salt-cooled reactors.

- **Coolant stability: 3**

Molten salts are found to be stable in high temperature and radiation environments; however, long-term operation data is lacking.

- **Pressure requirements: 4**

The vapor pressure for molten salts is very low.

- **Nuclear issues: 4**

Activation of fluoride salts should be modest and the void coefficient is expected to be negative. Lithium fluoride salts will require the use of depleted lithium (99.999% ^{7}Li) to reduce parasitic neutron capture and the generation of tritium and helium.

- **Feasibility: 3**

The United States developed molten salt technology for the Molten Salt Reactor Experiment. The United States has also developed HTGR fuel and fuel elements (proposed to be used with a molten salt coolant). Furthermore, the excellent heat transfer capability of molten salts should reduce maximum fuel temperatures relative to gas-cooled reactors. On the other hand, the differences between molten salt and helium coolants will probably require modification of the core design. The lack of adequate long-term data in the desired temperature range also presents a development risk. MSCR is projected to be feasible, but undemonstrated (3).

- **Safety: 4**

Void coefficients for molten salts are expected to be negative. Molten salt coolants possess HTGR safety advantages as well as molten salt advantages. If the basic fuel form of the HTGR is not substantially altered, the high heat capacity of the graphite blocks result in very gradual core heating in the event of a loss of flow accident. The low pressure of molten salts provides the safety advantage of preventing loss-of-coolant accidents due to rapid coolant evaporation and explosive release of a high pressure coolant is precluded. Furthermore, the molten salt coolant can enhance passive heat transfer for some postulated accident conditions. The low-pressure coolant and passive heat removal capability may completely eliminate air ingress issues. The high fission product retention ability of the HTGR microsphere fuel provides another safety advantage. For postulated severe accidents, molten salts can react with some fission products, possibly reducing the source term. In addition, molten salts do not present fire or chemical explosion hazards. The toxicity of molten salts may present safety considerations, but on the whole, MSCRs appear to offer outstanding safety advantages. As a consequence, a score of (4) is awarded.

- **Operational issues: 3**

The very high melt temperature for molten salts may present some operational challenges.

- **Capital costs: 3**

Low operating pressures may reduce some capital expenditures, but the required high temperature thaw system may present additional capital expenditures.

- **Intermediate loop compatibility: 3**

Possible reactivity effects of voids introduced by helium leakage from the intermediate loop must be considered. A molten salt coolant could be used for the intermediate loop; however, compatibility with the thermochemical loop may then present issues for some postulated accidents.

- **Other issues and merits: 3**

The development of high temperature molten salt-cooled reactors could provide the technology for highly efficient systems for electrical power.

4.8 Liquid-Core Reactors

Liquid-core reactors possess a number of unique features and advantages. Aqueous liquid cores are not recommended, however, because operational pressures would be extreme. Liquid metal-core concepts are not as well developed as molten salt-core reactors and they present mass transport and corrosion issues. Molten salt-core reactors are selected as the lead candidate among molten-core approaches.

Assessment:

- **Materials compatibility: 3**

Molten fluoride salts exhibit good corrosion resistance at high temperatures; however, the required temperatures are somewhat higher than the existing experience base, and operational experience is much shorter than the required lifetime. Although fission products are removed from the coolant during operation, the effect of continued release of fission products into the coolant stream needs to be assessed.

- **Coolant stability: 3**

Molten salts are stable in high temperature and radiation environments, however, long-term operational data is lacking. Furthermore, the possibility of precipitation of fuel materials needs to be assessed.

- **Pressure requirements: 4**

The vapor pressure for a molten salt core is very low.

- **Nuclear issues: 3**

The circulation of hot fuel materials, actinides, and fission products can present significant operational challenges.

- **Feasibility: 3**

The United States has developed molten salt core technology with the Molten Salt Reactor Experiment. Nonetheless, long term operational data is lacking, and issues relating to a radiologically hot primary loop and on-line refueling and processing present significant challenges.

- **Safety: 3**

Molten core reactors offer significant safety advantages. Online refueling eliminates the need for high excess core reactivity and substantially reduces the risk from reactivity-induced accidents. The online removal of fission products reduces the potential source term for some postulated accidents and removes the decay heat source from the core and primary loop. Furthermore, the coolant is not a fire or chemical explosion hazard. On the other hand, the potentially high activity in the primary loop and the need for on-site fission product processing introduces some additional safety issues.

- **Operational issues: 2**

The high melt temperature for molten salts, the limitations on access due to a hot primary loop, and the need for online fuel/coolant processing presents operational challenges.

- **Capital costs: 1**

Low operating pressures may reduce some capital expenditures; however, the required high-temperature thaw system, online refueling system, and fission product removal and treatment systems could result in significant capital costs.

- **Intermediate loop compatibility: 3**

The radiologically-hot coolant could enter the secondary loop in the event of a heat exchanger leak. Furthermore, if helium is used in the intermediate loop, a leak of helium into the primary loop could create bubbles with possible effects on reactivity. A molten salt coolant could be used for the intermediate loop; however, compatibility with the thermochemical loop may then present issues for some postulated accidents.

- **Other issues and merits: 3**

The liquid-core reactor offers the advantages of online refueling, online waste treatment and storage, the ability to use a variety of fuel types (e.g., plutonium, uranium, MOX), and the potential for deep fuel-burn to render the fuel proliferation resistant. The high temperature capability could also be used to develop highly efficient systems for electrical power.

4.9 Gas-core Reactors

- **Feasibility: 0**

The required development work and the development risk for gas core reactors are too significant to merit further consideration for this study.

5.0 Stage 4: Development Costs

From the preceding analysis, the gas-cooled reactors (GCRs), molten salt-cooled reactors (MSCRs), and heavy metal-cooled reactors (HMRs) appear to be the most promising. A detailed economic analysis of development costs is beyond the scope of this study but an estimate of the relative development cost of the three concepts is instructive. For the purpose of selecting a baseline concept, a simple method for comparing development will be used.

5.1 Approach

Expected development cost trends for MSCR and HMR systems will be compared relative to GCR development costs. Gas cooled reactors are chosen as the baseline because GCRs are the most developed of the three promising concepts. If development costs are expected to be significantly greater than for GCRs, then selecting GCRs for the baseline is clearly recommended. The following simple indictors will be used:

4 Lower development cost than for gas-cooled reactors

3 Approximately the same development cost as for gas-cooled reactors

2 Higher development cost than for gas-cooled reactors

1 Significantly higher development costs

0 Prohibitive development costs (eliminate from consideration)

This numbering system is consistent with the numbering system in Section 5, in that higher numbers are favorable. Note that the reference GCR baseline score is always equal to (3).

The following development activities were identified:

- Materials development
- Fuel development
- Component development
- System design
- Fabrication facility development

The results of this assessment are presented in Table 6.

Table 6 Development Cost Scores Relative to GCRs.

Reactor Type	Materials develop	Fuel develop	Component develop	System develop	Fab. facility	Unweighted average
HMR	**1**	**1**	**2**	**3**	**1**	**1.6**
MSCR	**2**	**3**	**2**	**2**	**2**	**2.2**
GCR	**3**	**3**	**3**	**3**	**3**	**3.0**

5.2 Materials Development

Materials development refers to coolant compatibility issues. Gas-cooled reactors have demonstrated acceptable materials compatibility for more than a decade of operation (AVR) in the required temperature regime. Molten salt compatibility looks promising; however, demonstrated molten salt acceptable compatibility close to the desired temperature range was limited to about two years. Given this lack of long-term operational experience, additional materials development is most likely required for the MSCR (2), Heavy metal cooled reactors have not been operated anywhere near the required temperature range, and significant materials development is most likely required for the HMRs (1).

5.3 Fuel Development

The required coolant temperature is somewhat higher than that used in the U.S. HTGR program. The required higher coolant temperature could result in higher fuel temperatures than demonstrated for HTGR designs. If higher fuel temperatures are required to achieve 900 C coolant temperatures, fuel development work will be required. The Japanese HTTR, an HTGR-type reactor, is currently ramping up to the expected operating temperature of > 900C, and a significant effort in developing and demonstrating zirconium carbide coated fuel particles is underway in Japan.

The excellent heat transfer characteristics of molten salt cooled coolants may result in less demanding requirements on the fuel; optimistically, the fuel already developed for gas-cooled reactors may be used for the MSCR. The MSCR is a new and undeveloped concept and additional development work cannot be ruled out. At this stage, a significant difference in MSCR fuel development cost, relative to GCRs, is not clearly indicated (3).

Fuel performance for HMRs is totally lacking in the required operational range, and appreciable development work is projected for HMRs. As a consequence, the HMR is scored a (1).

5.4 Component Development

Some component development is required for all three concepts. No significant component development issues, relative to GCRs, are identified for the MSCR or the HMR. Nonetheless, the lack of experience with these systems in the required temperature range implies the possibility of unexpected component development costs. Both MSCRs and HMRs are scored a (2).

5.5 System Design Development

Full system designs for high temperature GCRs have been developed; whereas the MSCR is an entirely new concept and significant MSCR system design development is anticipated (2). The Russians have carried out appreciable design development work for a commercial HMR. If the higher temperature capability required for the sulfur-iodine cycle does not alter the HMR design significantly, it is possible that additional system design work will be minimal (3).

5.6 Fabrication Facility Development

Internationally, fuel fabrication facilities existed in Germany for the Pebble Bed reactor fuel, and the technology is being transferred to South Africa. Developmental fuel fabrication facilities exist in Japan and facilities are now under development in Russia. Fuel fabrication facilities for production of coated fuel particles that can be used in GCRs exist in the United States at (e.g., Babcock and Wilcox). These facilities have been in operation, producing fuel for the Navy, for more than twenty years. A complete fuel fabrication facility for the HTGR existed at General Atomics. Although the General Atomics fabrication facility has been dismantled, the technology is fully documented and recoverable. Fabrication processes for most major GCR components have been established.

If MSCRs use the same fuel as GCRs, no fabrication development will be necessary. The assumption that MSCRs can use GCR fuel is based on the documented resistance of graphite to $2LiF\text{-}BF_2$. Although the fuel elements and coated particles are fully graphitized, the fuel compacts are not. Nonetheless, a clear need for greater fuel fabrication development (relative to GCRs) is not identified. Fabrication technology may need to be developed, however, for other MSCR components that will be required to operate at higher temperatures than those required for the molten salt reactor experiment. The fabrication development cost for the MSCR is scored a (2).

Fuel fabrication facilities will need to be developed for the HMR. Some facilities capable of producing HMR fuel probably exist in Russia, but this fuel never operated at the required temperatures. Appreciable fuel fabrication technology development is expected, and other component fabrication technology development is expected as well (1).

5.7 Development Assessment

From Table 6 we observe that the GCR approach is expected to result in the lowest development cost and risk. The MSCR and, especially, the HMR approaches are expected to require significantly greater development costs.

6.0 Conclusions

Based on the forgoing discussion, the following preliminary conclusions and recommendations are made:

PWR, BWR, Organic-Cooled, and Gas-Core Reactors – Not Recommended

- From the preceding analysis we conclude that all PWR approaches are impractical in that enormous system pressures are required to obtain 900 C coolant temperatures.
- The highly corrosive nature of 900 C steam eliminates BWRs from consideration.
- Organic-cooled reactors are not recommended as a heat source for the sulfur-iodine thermochemical cycle because organic coolants dissociate at temperatures well below the required cycle temperature.
- Gas core reactors were not considered because the approach requires unproven technology at a fundamental level and the development risk is too great for the goals of this program.

Liquid-Core Reactors and Alkali Metal-Cooled Reactors
– Significant development risk

- Although the liquid-core reactor technology is promising for operation at the required temperatures, the circulation of radiologically hot fuel/coolant presents many operational and developmental issues, as well as high capital costs. At this stage the molten core is judged to be a possible approach, but it is not retained as a strong alternative.

- Alkali metal-cooled reactors are also possible candidates, but the general corrosiveness of alkali metals at very high temperatures is an important issue. At this stage, the technology risk and development cost are judged to be significant. Furthermore, if special alloys and complex fuel elements are required, the capital cost required to produce a system capable of meeting performance requirements may be significant. Positive void coefficients, fire and explosion hazards, coolant activation, and thaw requirements are additional undesirable features of alkali metal coolants. For these reasons, alkali metal-cooled reactors are considered as possibilities, but not a strong alternative.

Heavy Metal and Molten Salt-Cooled Reactors – Promising

- Both HMRs and MSCRs appear to be promising candidates, but relatively high development costs places these approaches in the promising alternative category.

Gas Cooled Reactors – Baseline choice

- Based on Table 5, helium gas cooled reactors appear to well suited for the proposed application. From Table 6, GCRs are projected to require substantially lower development costs then alternative approaches. The underlying reasons for the suitability of GCRs for the high temperature

sulfur-iodine cycle are: (1) helium is chemically inert, and (2) gas cooled reactors have been successfully operated for a number of years in the required temperature range. Altogether, the GCRs approach appears to be very well suited as a heat source for the intended application, and no major development work is identified. This study recommends using a Gas-Cooled Reactor as the baseline reactor concept for a sulfur-iodine cycle for hydrogen production.

- Although the GCR approach provides a number of important safety advantages, a possible safety issue has been raised associated with postulated accidents leading to air ingress. An independent review of this issue is recommended.

References:

1. L. C. Brown, *High efficiency Generation of Hydrogen Fuels Using Nuclear Power*, NERI Proposal, January 29 1999.
2. L. C. Brown, General Atomics, personal communication, November 2000.
3. A. V. Nero, Jr., *A Guidebook to Nuclear Reactors*, U. of Cal. Press, Berkeley, 1979.
4. C. W. Forsberg and A. M. Weinberg, "Advanced Reactors, Passive Safety, and Acceptance of Nuclear Safety," *Annu. Rev. Energy*, **15**, pp. 133-152
5. S. Koshizuka and Y. Oka, "Supercritical-Pressure, Light-Water-Cooled Reactors for Economical Nuclear Power Plants," *Prog. Nucl Ener*. **32**, pp. 547-554, 1998.
6. M. Simnad, *Fuel Element Experience in Nuclear Power Reactors*, Gordon and Breach Science Publ., NY, 1971.
7. S. Glasstone and A. Sesonske, *Nuclear Reactor Engineering*, Van Nostrand Reinhold Co., NY, 1967.
8. D. Bleuel, J. Scott, and L. Sevingy, *Introduction to the ALMR/PRISM*, http://www.nuc.berkeley.edu/~gav/almr/01.intro.html. November 2000.
9. M. S. El-Genk, *A Critical Review of Space Nuclear Power and Propulsion 1984-1993*, American Institute of Physics, NY, 1994.
10. M. I. Bugreev, et. Al., *Analysis of Risks Associated with Nuclear Submarine Decommissioning, Dismantling, and Disposals*, pp. 261-264, A. A. Sarkisov and A. Tournyol du (eds.), Kluver Academic Publishers, Netherlands, 1999.
11. A. V. Zrodnikov, O. G. Grigoriev, A. V. Dedoul, G. I. Toshinsky, V. I. Chitaykin, V. S. Stepanov, "Shore Small Power NPP with Lead-Bismuth cooled Reactor without on-site refueling", *International Workshop on Utilization of Nuc;ear Power in Oceans*, Tokyo, February, 2000.
12. K. Kemm, *Development of the South Africa Pebble Bed Modular Reactor System*, http:www.uilondon.org/sym/1999kemm.htm, November, 2000.
13. C. Forsberg and P. Pickard, *Advanced High-Temperature Reactor for Hydrgen and Electricity Production*, Oak Ridge National Laboratory view graph presentation, May, 2001.
14. M. M. El-Wakil, *Nuclear Power Engineering*, McGraw-Hill Book Co., NY, 1962.
15. J. A. Angelo and D. Buden, *Space Nuclear Power*, Orbit Book Co., Malabar, FL, 1985.
16. *Coolants for Nuclear Reactors*, http://www.nuc.berkeley.edu/thyd/ne161/rahmed/coolants.html. November, 2000.
17. V. V. Orlov and E. O. Adamov, "A radical approach is needed for a nuclear future in Russia," *Nucl. Engr. Inter.*, pp. 42-44, May, 1992.
18. B. F. Gromov, et al., "Inherently safe lead-bismuth-cooled reactors," *Atomic Energy*, **76** No. 4, 1984.
19. C. B. Davis and A. S. Shieh, *Overview of the use of ATHENA for thermal-hydraulic analysis of systems with lead-bismuth cooling*, INEEL/CON-2000-00127, April 2000.
20. H. Sekimoto and Z. Su'ud, "Design of lead and lead-bismuth cooled small long-life nuclear power reactors using metallic and nitride fuel," *Nucl. Tech.*, **109**, 307-313, March 1995.
21. J. A. Lane, H. G. MacPherson, and F. Maslan, *Fluid Fuel Reactors*, Addison-Wesley Publ. Co., Reading MS, 1958.

22. U. Gat and J. R. Engel, "Non-proliferation attributes of molten salt reactors," *Nucl. Engr. & Des.*, **201**, pp. 327-334, 2000.
23. K. Mitachi, T. Suzki, and K. Furakawa, "A preliminary design of a small molten salt reactor for effective use of thorium resource," proc. *7th International Conf. On Nucl. Engr.*, Tokyo, Japan, April 1999.
24. A. S. Shenoy, *Modular helium reactors for non electric applications of Nuclear energy*, GA-A22701, Nov. 1995.
25. K. Onuki, et al., "Studies on water splitting hydrogen production," *The third symposium on HTGR Technologies*, pp. 262-474, 2000.
26. *High temperature engineering test research*, http://www.jari.go.jp/nglish/temp, December 2000.
27. A. N. Nesmeyanov, *Vapor Pressure of the Chemical Elements*, Elsevier Publ. Co., Amsterdam, 1963.
28. B. M. Ma, *Nuclear Reactor Materials and Applications*, Van Nostrand Reinhold Co., NY, 1983.
29. M. M. El-Wakil, *Nuclear Energy Conversion*, International Textbook Co., La Grange Park, IL, 1982.
30. A. R. Foster, R. L. Right, *Basic Nuclear Engineering*, Allyn and Bacon, Inc. Boston, 1974.
31. J. E. Draley and J. R. Weeks, *Corrosion by Liquid Metals*, Plenum Press, NY, 1970.
32. D. W. Yaun, R. F. Yan, and G. Simkovich, "Rapid oxidation of liquid tin and its alloys at 600 to 800C," *Jour. Matls. Sc.*, **34**, pp. 2911-2920, 1999.
33. M. Broc, J. Sannier, and G. Santarini, "Behavior of ferritic steels in the presence of flowing purified liquid lead," proc. *Conf. Liquid Metal in Energy Applications*, Oxford UK, April 1984.
34. R. C. West, et al. (eds.) *CRC Handbook of Chemistry and Physics, 70th Edition*, CRC Press Inc., Boca Raton FL, 1989.
35. N. Brown and J. A. Hassberger, "New concept of small power reactor without on-site refueling for non-proliferation," IAEA advisory group meeting on propulsion reactor technologies for civilian applications," Obninsk, Russia, July 1998.
36. A. S. Shenoy, General Atomics, personal communication, September 2001.
37. J. Sannier and G. Santarini, "Studies of materials for molten salt nuclear operations", *International Symposium on Molten Salt Chemical and Tecnical*, Kyoto, Japan, April, 1983.

APPENDIX C
GA & SNL MODELING THE SULFUR-IODINE CYCLE
ASPEN PLUS® BUILDING BLOCKS AND SIMULATION MODELS

General Atomics and Sandia National Laboratories

MODELING THE SULFUR-IODINE CYCLE

Aspen Plus Building Blocks and Simulation Models

Name	**:**	**Sulfur-Iodine Water-Splitting Cycle**
Aspen Plus Files	**:**	**Section1-04.bkp** **Section2-01.bkp** **ReacDistLiqDraw.bkp** **ReacDistVapDraw.bkp**
AspenTech Author	**:**	**Paul M. Mathias**
Status	**:**	**Final**
Rev No.	**:**	**02**
Issue Date	**:**	**26-October-2002**

aspentech

process. to the power of e.

Contents

List of Figures

List of Tables

1 INTRODUCTION

AspenTech developed Aspen Plus® building blocks and simulation models related to the Sulfur-Iodine water-splitting cycle in a project sponsored by General Atomics and Sandia National Laboratories. This report describes the building blocks and simulation models.

Combustion of fossil fuels currently provides about 86% of the world's energy.[1,2] Drawbacks to fossil fuel utilization include limited supply, pollution and carbon dioxide emissions. Hydrogen is an environmentally attractive fuel that has the potential to displace fossil fuels, but contemporary hydrogen production is primarily based on fossil fuels. When hydrogen is produced from fossil fuels, there is little or no environmental advantage.

Hydrogen production by thermochemical water splitting, a process that accomplishes the decomposition of water into hydrogen and oxygen, is an attractive and environmentally-clean alternate to hydrogen production using fossil fuels. The high-temperature heat source for thermochemical water splitting is likely to be an advanced nuclear reactor.

The Sulfur-Iodine water-splitting cycle is a promising candidate for thermochemical hydrogen production.[3,4] The direct thermolysis of water requires temperatures in excess of 2,500°C for significant hydrogen generation.

Equation 1: $H_2O \rightarrow H_2 + \frac{1}{2}O_2$ (2,500°C)

At the temperature of 2,500°C only 10% of the water is decomposed. In addition, a means of preventing the hydrogen and oxygen from recombining upon cooling must be provided or no net production would result. A thermochemical water-splitting cycle accomplishes the same overall result more effectively while using much lower temperatures. The Sulfur-Iodine cycle is a prime example of a thermochemical water-splitting cycle. It consists of three chemical reactions that sum to the dissociation of water.

Equation 2: $H_2SO_4 \rightarrow SO_2 + H_2O + \frac{1}{2}O_2$ (850°C)

Equation 3: $I_2 + SO_2 + 2H_2O \rightarrow 2HI + H_2SO_4$ (120°C)

Equation 4: $2HI \rightarrow I_2 + H_2$ (450°C)

Equation 2-Equation 4 sum to the dissociation of water, or Equation 1. With a suitable catalyst, the high-temperature reaction (Equation 2) reaches 10% conversion at only 510°C and 83% conversion at 850°C. Moreover, there is no need to perform a high-temperature separation as the reaction ceases when the process stream leaves the catalyst.

A simple schematic for the Sulfur-Iodine cycle is shown in the figure below:

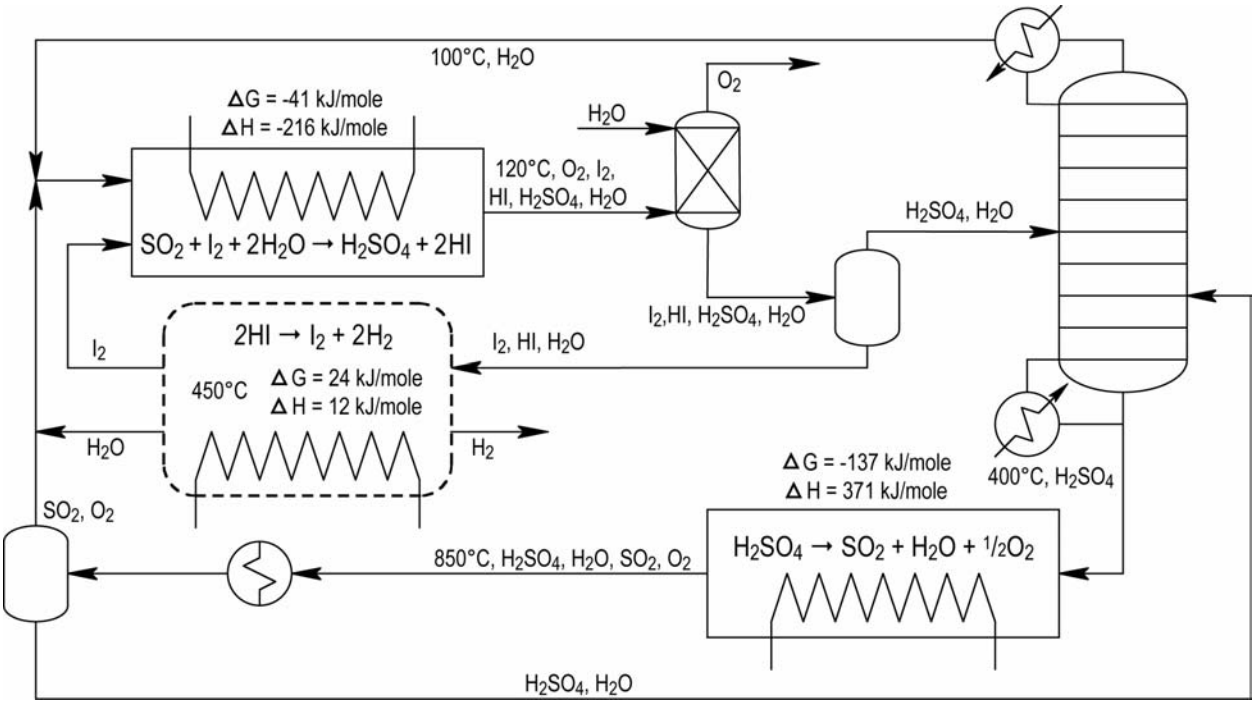

Figure 1 – Simple Schematic of the Sulfur-Iodine Water-Splitting Cycle

The chemistry of the Sulfur-Iodine cycle was demonstrated by General Atomics in 1974-1986.[3] As part of this project, a process flowsheet was generated in 1984. The HI concentration and decomposition originally proposed by General Atomics, which involved extraction with phosphoric acid, was the most expensive step of the entire process. A German project over the years 1984-1989 proposed a new reactive distillation scheme to achieve the twin objectives of HI concentration and decomposition. These process enhancements have been presented by Roth and Knoche.[5] The Sulfur-Iodine cycle modeled in this project is the General Atomics process together with the modifications proposed by Roth and Knoche.[5]

The process cycle has been divided into sections as presented in the figure below:

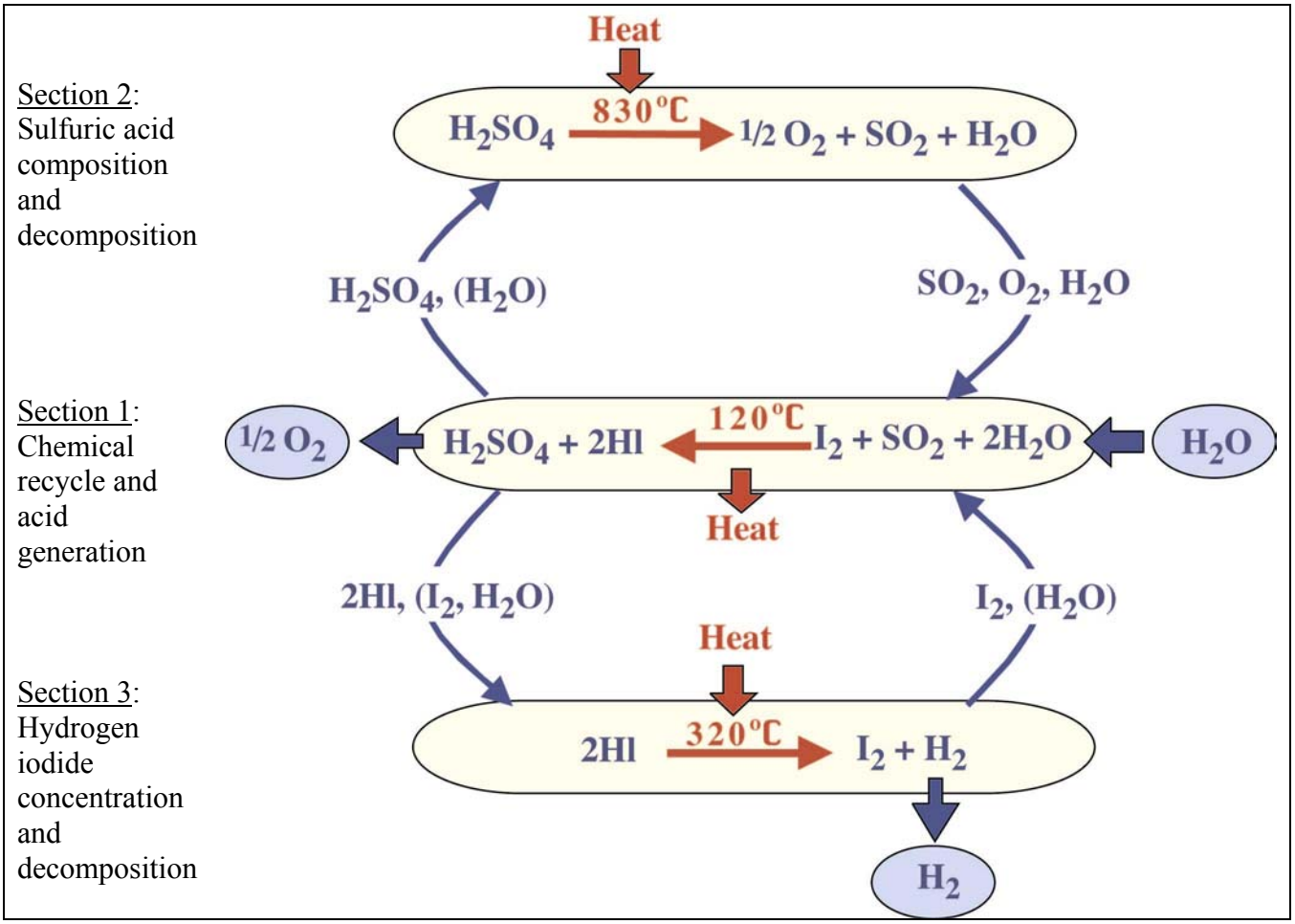

Figure 2 – Sections in the Sulfur-Iodine Water-Splitting Cycle

The sections referred to in this report correspond to those in Figure 2.

The work reported in this project is part of an effort by General Atomics to produce a simulation model of the Sulfur-Iodine cycle using the Aspen Plus® steady-state process simulator. The Sulfur-Iodine cycle poses many modeling challenges. The main challenges are listed below:

1. The chemical species include strong acids (H_2SO_4 and HI) that dissociate and thus an electrolytic model must be used for accurate and reliable modeling.
2. In Section 1, a two-phase solution occurs, with a light phase containing sulfuric acid and a heavy phase containing iodine and hydrogen iodide. This phase separation is key to successful implementation of the Sulfur-Iodide cycle and must be modeled accurately.
3. Section 2 has units that operate at very high temperatures that exceed the critical temperature of water (374°C). At these temperatures, ions tend to exist as pairs and this must be correctly accounted for in the model.

4. Section 3 exhibits complex behavior of the HI-I_2-H_2O system that includes multiple liquid phases. While the process conditions apparently do not include regions where multiple liquid phase behavior actually occurs, the model must correctly account for this behavior, if only to avoid these regions.
5. Even after the complex phase behavior is correctly modeled, the complexity of the nonideality causes serious convergence difficulties. These convergence difficulties must be overcome.

The key goal of the project is to develop practical and useful simulation models for the Sulfur-Iodine cycle.

While strenuous attempts have been made to overcome the modeling challenges, several areas of inadequacy remain in inadequate property data, physical-property modeling deficiencies and flowsheet convergence. These areas of inadequacy are identified in this report.

2 MODELING BACKGROUND

The goal of this project is to develop building blocks and flowsheet models for the Sulfur-Iodine cycle using the Aspen Plus® flowsheet simulator.

The physical properties model used is the ElecNRTL model.[6,7,8] This thermodynamic model captures the nonideality of the ionic liquid solutions, but needs to be coupled with "chemistry" models that describe the dissociation and complexation reactions (solution chemistry) that occur in solution. Because of the complexity and variety of phenomena that occur in various parts of the process, many chemistry models have been developed.

The physical-property models have been tuned based upon experimental data available in the literature. The data sources have been clearly identified. The areas where further data are needed are identified, as appropriate.

There are two ways to represent the composition of electrolyte systems in process simulation: apparent composition, which represents the system's composition in terms of molecular components prior to solving the solution chemistry; and true species composition, which represents the system's composition in terms of all species that exist at chemical equilibrium. Apparent component and true species approaches are interchangeable since they both give the same ultimate result. But one choice or another is usually preferred is a given simulation, for reasons of simulation effectiveness; for more discussion on this topic see the Aspen Plus Electrolytes Manual.[9] In the present project, the apparent-composition approach has been chosen. This approach leads to better model convergence and also permits combination of chemistry models with reactions models.

It is often effective simulation practice to combine "chemistry" models with "reactions" models. In Aspen Plus, reactions models contain a set of reactions that may be at equilibrium or kinetically controlled.

The flowsheet models have been developed using unit-operation models available in Aspen Plus®. In many cases, special approaches must be taken to improve the robustness of the flowsheet model. These special approaches have been identified in the report.

3 MODEL FILES AND SUPPORT FILES DELIVERED

The following Aspen Plus model files have been developed:

Section1-04.bkp	-	Section 1 model
Section2-01,bkp	-	Section 2 model
ReacDistLiqDraw.bkp	-	Section 3, reactive distillation, liquid draw
ReacDistVapDraw.bkp	-	Section 3, reactive distillation, vapor draw

The Section 1 and Section 2 models are reasonably complete simulations of their respective sections. The Section 3 models are mainly simulations of the reactive distillation columns. Due to convergence difficulties and time limitations, a complete simulation of this section was not completed.

The following project support files are also provided:

SulfurIodineReport-02.doc	-	Project documentation

4 COMPONENTS, CHEMISTRY AND REACTIONS

This section describes the components (chemical species), chemistry models (liquid-phase equilibrium reactions) and reactions models (equilibrium or kinetic models used together with chemistry models).

4.1 Components

The following pure components have been used in the Aspen Plus models:

Component ID	Formula	Description
H2O	H_2O	Water

H2SO4	H_2SO_4	Sulfuric acid
SO2	SO_2	Sulfur dioxide
SO3	HO_3	Sulfur trioxide
HI	HI	Hydrogen iodide
I2	I_2	Iodine
H2	H_2	Hydrogen
H3O+	H_3O^+	Hydrated hydronium ion
HSO4-	HSO_4^-	Bisulfate ion
SO4-2	SO_4^{-2}	Sulfate ion
I-	I^-	Iodide ion
SAIPAIR	$H_2S_{0.5}O_{2.5}$	Sulfuric acid-water ion pair
I2-S	I_2	Solid iodine
HIX	$H_3I_{1.5}O$	HIx complex
HE	He	Helium

Table 1 – Components in Sulfur-Iodide Cycle Simulations

4.2 Chemistry Models

Several chemistry models are used in various areas of the simulation. These are first summarized and then described in detail.

Name	Description
CH2SO4	Concentrated sulfuric acid
CH2SO4HT	Concentrated sulfuric acid – high temperature
H2SO4	Sulfuric acid
H2SO4HT	Sulfuric acid – high temperature
H2SO4-HI	Sulfuric acid and hydrogen iodide – Section 1
HI-FULL	Hydrogen iodide, including iodine precipitation
HI-H2	Hydrogen iodide – dissociation and decomposition
HI-I2	Hydrogen iodide - dissociation

Table 2 - Summary of Chemistry Models

4.2.1 CH2SO4 - Concentrated sulfuric acid

CH2SO4 covers the ionic dissociation of sulfuric acid as well as the molecular dissociation of sulfuric acid to form water and sulfur trioxide. CH2SO4 includes the following reactions:

Equation 5: $H_2SO_4 + H_2O \leftrightarrow H_3O^+ + HSO_4^-$

Equation 6: $HSO_4^- + H_2O \leftrightarrow H_3O^+ + SO_4^{-2}$

Equation 7: $H_2O + SO_3 \leftrightarrow H_2SO_4$

CH2SO4 is not used as a simulation model since simulations preferably use the dissociation of sulfuric acid as a Chemistry model (H2SO4) and treat the dissociation of sulfuric acid as a Reaction model. However, CH2SO4 is useful as a check of the simulation since the combination of chemistry model H2SO4 in the apparent mode and reactions model H2SO4D is equivalent to Chemistry model CH2SO4 in the true mode. As a rule, we generally use such internally consistency checks to ensure the correctness of the simulation model.

4.2.2 CH2SO4HT - Concentrated sulfuric acid – high temperature

CH2SO4HT is intended to describe the reactions that occur in aqueous solutions of sulfuric acid at high temperatures, above 300°C. At these temperatures sulfuric acid tends to form ion pairs or complexes as opposed to positive and negative ions. CH2SO4HT includes the following reactions:

Equation 8: $SO_3 + H_2O \leftrightarrow H_2SO_4$

Equation 9: $H_2O + H_2SO_4 \leftrightarrow$ 2. IONPAIR

The postulated complex "IonPair" has been assumed to be a molecular component with a very low boiling point. The model thus does not have any electrolytes. The equilibrium constant for Reaction 1a and NRTL parameters between IonPair and water and sulfuric acid have been fit to provide a good description of the vapor pressure data measured by Wüster.[10]

CH2SO4HT is not used as a simulation model since simulations preferably use the complexation of sulfuric acid as a Chemistry model (H2SO4HT) and treat the dissociation of sulfuric acid as a Reaction model. However, CH2SO4HT is useful as a check of the simulation since the combination of chemistry model H2SO4HT in the apparent mode and reactions model H2SO4D is equivalent to Chemistry model CH2SO4HT in the true mode.

4.2.3 H2SO4 - Sulfuric acid

H2SO4 describes the ionization of sulfuric acid and includes the following reactions:

Equation 10: $H_2SO_4 + H_2O \leftrightarrow H_3O^+ + HSO_4^-$

Equation 11: $HSO_4^- + H_2O \leftrightarrow H_3O^+ + SO_4^{-2}$

4.2.4 H2SO4HT - Sulfuric acid – high temperature

H2SO4HT describes the high-temperature complexation of sulfuric acid and includes the following reaction:

Equation 12: $H2O + H2SO4 \leftrightarrow 2.\ IONPAIR$

4.2.5 H2SO4-HI - Sulfuric acid and hydrogen iodide – Section 1

In Section 1, a two-phase solution occurs, with a light phase containing sulfuric acid and a heavy phase containing iodine and hydrogen iodide. This phase separation is key to successful implementation of the Sulfur-Iodide cycle and must be modeled accurately. H2SO4-HI provides a practical way to model this system by using the following reactions:

Equation 13: $H2SO4 + H2O \leftrightarrow H3O+ + HSO4-$

Equation 14: $HI + 0.25\ I2 + H2O \leftrightarrow HIX$

Equation 13 represents the acidic dissociation of sulfuric acid. For simplicity the dissociation of bisulfate ions to form sulfate ions has been neglected since it tends not to occur in concentrated solutions. Equation 14 captures the ionization of hydrogen iodide. In the concentration range that occurs in Section 1, the ions appear to complex with iodine and thus it has been included in the HIX complex.

4.2.6 HI-FULL - Hydrogen iodide, including iodine precipitation

HI-FULL represents the entire set of reactions that occur in aqueous hydrogen iodide solutions, including the decomposition of hydrogen iodide and the precipitation of solid iodine. HI-FULL includes the following reactions:

Equation 15: $HI + H2O \leftrightarrow H3O+ + I-$

Equation 16: $2.\ HI \leftrightarrow I2 + H2$

Equation 17: $I2\text{-}S \leftrightarrow I2$

This chemistry model is presented for the sake of completeness. It is not used in the plant simulations, but may be useful in simulations that study the composition ranges where iodine may precipitate.

4.2.7 HI-H2 - Hydrogen iodide - dissociation and decomposition

HI-H2 represents the dissociation of hydrogen iodide and the decomposition of hydrogen iodide to form iodine and hydrogen. HI-I2 includes the following reactions:

Equation 18: $HI + H2O \leftrightarrow H3O+ + I-$

Equation 19: $2.\ HI \leftrightarrow I2 + H2$

HI-H2 is not used as a simulation model since simulations preferably use the ionization of hydrogen iodide as a Chemistry model (HI-I2) and treat the dissociation of hydrogen iodide as a Reaction model. However, HI-H2 is useful as a check of the simulation since the combination of chemistry model HI-I2 in the apparent mode and reactions model H2-EQUIL is equivalent to Chemistry model HI-H2 in the true mode.

4.2.8 HI-I2 - Hydrogen iodide – dissociation

HI-I2 only describes the ionic dissociation of hydrogen iodide>

Equation 20: $HI + H2O \leftrightarrow H3O+ + I-$

The chemistry model HI-I2 has been used in the simulations of the reactive distillation columns in Section 3.

4.3 Reactions Models

Several reactions models have been used together with chemistry models to describe the process phenomena. These are first summarized and then described in detail.

Name	Description
H2SO4D	Sulfuric acid dissociation - distillation
H2SO4R	Sulfuric acid dissociation - reactor
ACIDP-CR	Bunsen reaction - distillation
BUNSEN	Bunsen reaction - reactor
H2-EQUIL	Hydrogen iodide dissociation - distillation

Table 3 - Summary of Reactions Models

4.3.1 H2SO4D - Sulfuric acid dissociation - distillation

H2SO4D describes the dissociation of sulfuric acid in distillation-column models.

Equation 21: $SO3 + H2O \leftrightarrow H2SO4$

H2SO4D models the dissociation of sulfuric acid as a vapor-phase equilibrium reaction and is used in distillation-column models. It is used in Section 2 models together with chemistry models H2SO4 and H2SO4HT.

4.3.2 H2SO4R - Sulfuric acid dissociation - reactor

H2SO4R describes the dissociation of sulfuric acid in reactor models.

Equation 22: $SO3 + H2O \leftrightarrow H2SO4$

H2SO4R models the dissociation of sulfuric acid as a vapor-phase equilibrium reaction and is used in reactor models. It is used in Section 2 models together with chemistry models H2SO4 and H2SO4HT.

4.3.3 ACIDP-CR - Bunsen reaction - distillation

ACID-CR describes the acid production (H_2SO_4 and HI) in Section 1 distillation-column models.

Equation 23: $2.\ H2O + SO2 + I2 \leftrightarrow H2SO4 + 2.\ HI$

ACID-PR models the acid production as a liquid-phase kinetic model and is used in distillation-column models. It is used in Section 1 models together with chemistry model H2SO4-HI.

4.3.4 BUNSEN - Bunsen reaction - reactor

BUNSEN describes the acid production (H_2SO_4 and HI or Bunsen reaction) in Section 1 reactor models.

Equation 24: $2.\ H2O + SO2 + I2 \leftrightarrow H2SO4 + 2.\ HI$

BUNSEN models the acid production as a liquid-phase kinetic model and is used in reactor models. It is used in Section 1 models together with chemistry model H2SO4-HI.

4.3.5 H2-EQUIL - Hydrogen iodide dissociation - distillation

H2-EQUIL models the hydrogen iodide dissociation in the Section 3 reactive distillation models.

Equation 25: $2.\ HI \leftrightarrow I2 + H2$

H2-EQUIL models the hydrogen iodide dissociation as a vapor-phase equilibrium reaction. It is used in section 3 models together with chemistry model HI-I2.

5 THERMOPHYSICAL PROPERTIES

While there are several chemistry and reactions models used in various parts of the Sulfur-Iodine process, only one universal set of thermodynamic parameters is used for the entire set of process models. This section summarizes how the thermodynamic parameters were fit and how well

they represent the equilibrium data. This section also serves to summarize the experimental data used to fit the model parameters.

This section is divided into three sub-sections:

1. The H_2SO_4-H_2O System
2. The HI-I_2-H_2O System
3. The H_2SO_4-HIx-H_2O System

This section also provides comments on the adequacy of the available experimental data.

5.1 The H_2SO_4-H_2O System

The model performance for the H_2SO_4-H_2O system, except for the high-temperature region, has been presented previously by Mathias et al.[11] and Randolph et al.[12] and thus only brief descriptions will be provided here. The chemistry model used is CH2SO4. This system is mainly relevant for the Section 2 model.

A reliable correlation for the vapor-liquid equilibrium of the sulfuric acid-water system has been developed by Gmitro and Vermeulen.[13] The following figure demonstrates that the present model has good agreement with the previously developed correlation of Gmitro and Vermeulen at moderate temperatures (up to 300°C).

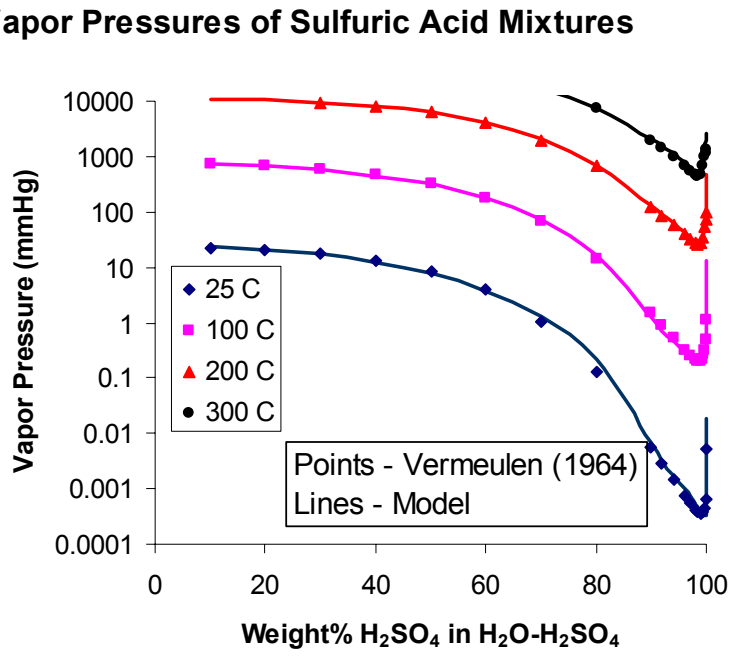

Figure 3 – Vapor Pressures of Sulfuric Acid Mixtures - Comparison with Correlation of Gmitro and Vermeulen

An accurate thermodynamic model must also provide a good description of thermodynamic properties such as enthalpy and heat capacity. The following two figures demonstrate that the model provides accurate properties for the excess enthalpy[14] and heat capacity[15] of sulfuric acid-water mixtures, again at moderate temperatures.

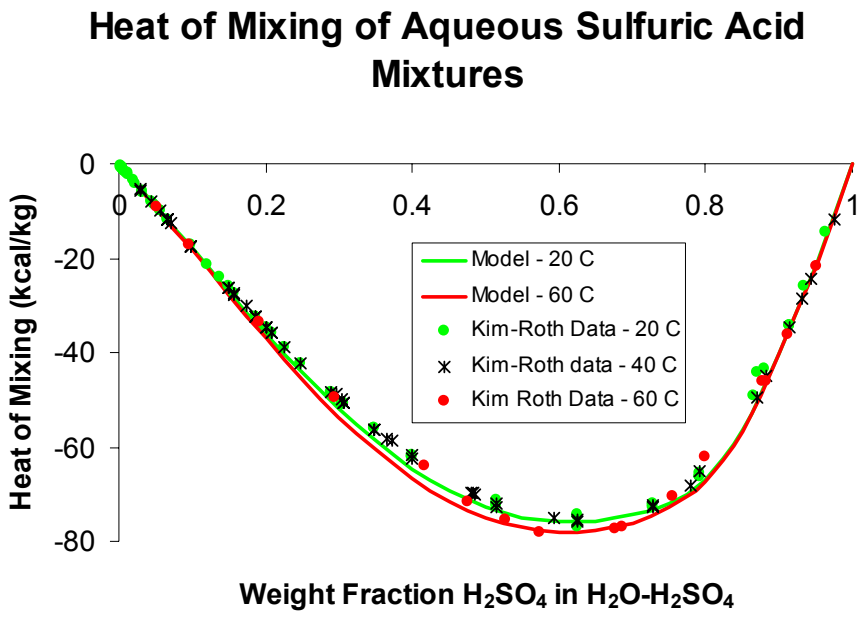

Figure 4 – Heat of Mixing of Sulfuric Acid Mixtures – Comparison with Data of Kim and Roth (2001).

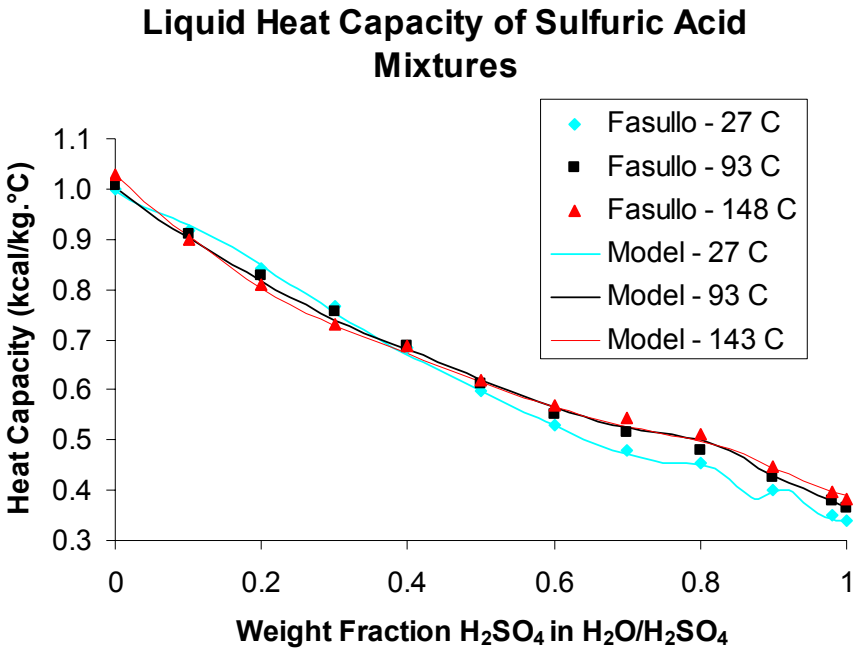

Figure 5 – Liquid Heat Capacity of Sulfuric Acid mixtures – Comparison with Data reported by Fasullo (1965).

The properties of high-temperature sulfuric acid mixtures are of critical importance to the Sulfur-Iodine cycle. As noted above, the model was developed by using the data of Wüster.[10] The following figure compares the model calculations (Chemistry model CH2SO4HT) with Wüster's data.

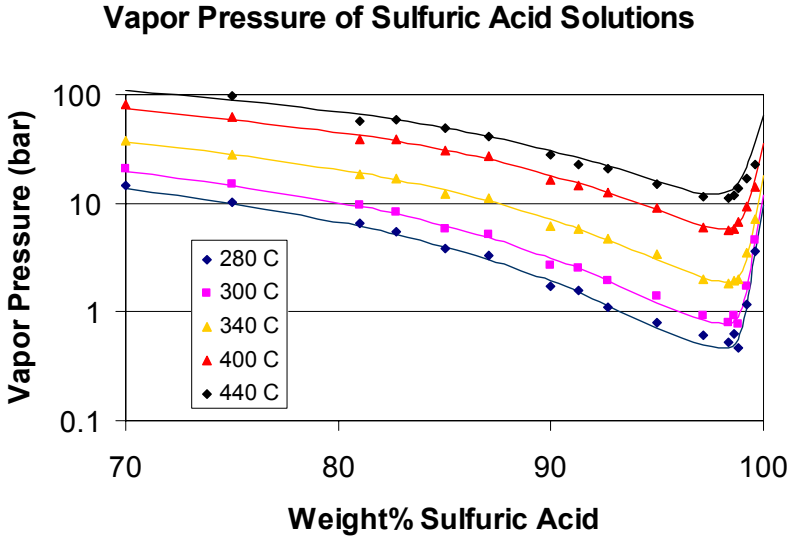

Figure 6 – Vapor Pressure of Sulfuric Acid Solutions at High Temperature – Comparison with Data of Wüster

The model is expected to provide a reliable description of the aqueous sulfuric acid mixture in Section 2 of the Sulfur-Iodine cycle.

5.2 The HI-I_2-H_2O System

The HI-I_2-H_2O system is relevant to Section 3 of the Sulfur-Iodine cycle. It is very complicated because of the various ionization and complexation phenomena that occur. In this work we have developed a phenomenologically reasonable model that provides a quantitative description of the known data for the system. The chemistry model used for this system is HI-I2.

The iodine-water binary mixture is highly nonideal. At the triple point of iodine (113.6°C) the solubility of iodine in water is about 0.05 mol% and the solubility of water in iodine is about 1.7 mol%. Kracek[16] has presented mutual solubility data for this system. The following two figures compare the model to Kracek's data.

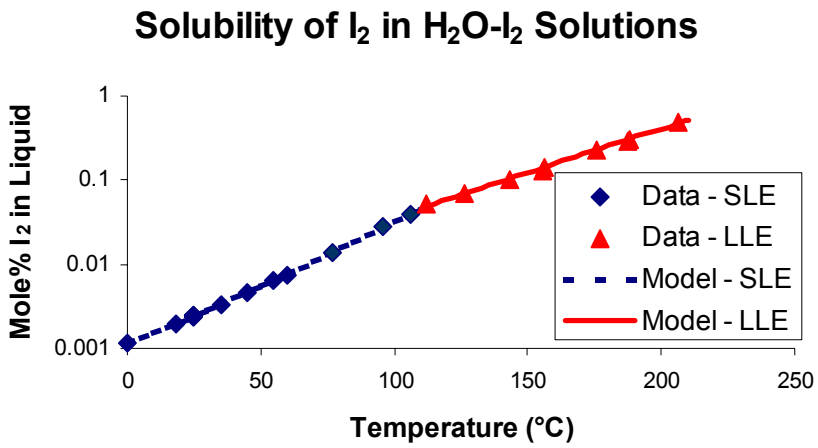

Figure 7 – Solubility of I_2 in Aqueous Iodine Solutions – Comparison to Data of Kracek (1931)

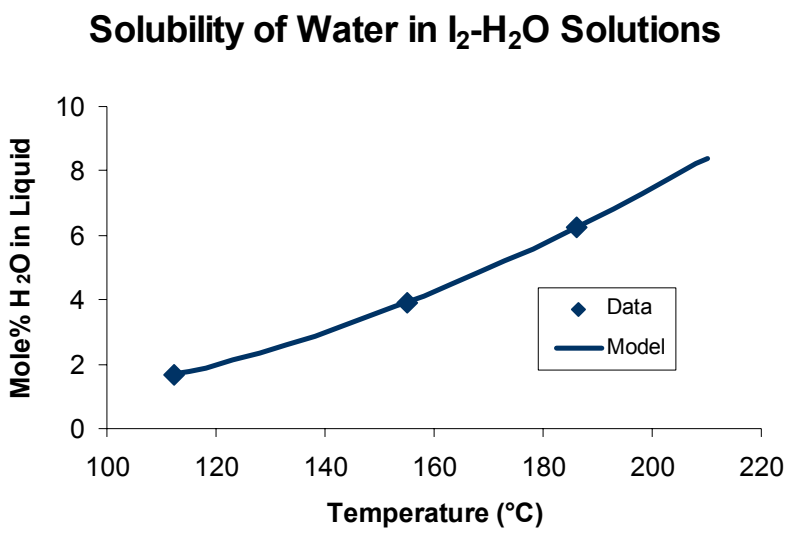

Figure 8 – Solubility of Water in Aqueous Iodine Solutions – Comparison to Data of Kracek (1931)

The hydrogen iodide-iodine system exhibits only small deviations from ideality. The solid-liquid equilibrium data for iodine in hydrogen iodide, presented by O'Keefe and Norman,[17] serve to develop a model for this binary system. The following figure provides a comparison between the model and experimental data.

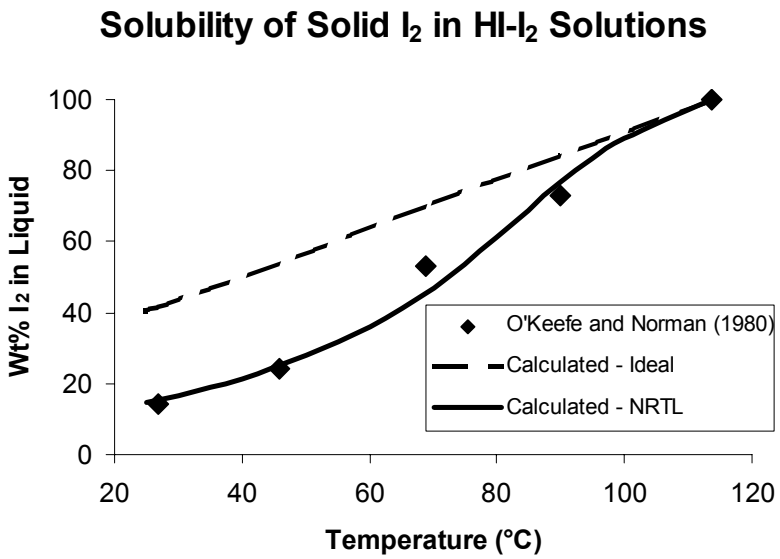

Figure 9 – Solubility of Solid I_2 in HI-I_2 solutions - Comparison with Data of O'Keefe and Norman (1988)

Aqueous solutions of hydrogen iodide must be modeled with an ionic model since HI is a very strong acid. Several sets of data are available for aqueous solutions of HI and for the HI-I2-H2O ternary system:

1. Total pressure vapor-liquid equilibrium data for the HI-H_2O binary (Neumann[18]).
2. 25°C vapor-liquid azeotrope for the HI-H_2O binary (CRC Handbook, 1975[19]).
3. 25°C liquid-liquid equilibrium data point for the HI-H_2O binary (Haase et al.[20]).
4. Total pressure vapor-liquid equilibrium data for the HI-I_2-H_2O ternary (Neumann[18]).
5. Liquid-liquid equilibrium data for the HI-I_2-H_2O ternary (Norman[21]).

The following chart presents the comparison between experimental data[20] and model predictions for the vapor-liquid equilibrium of HI-H_2O binary mixtures.

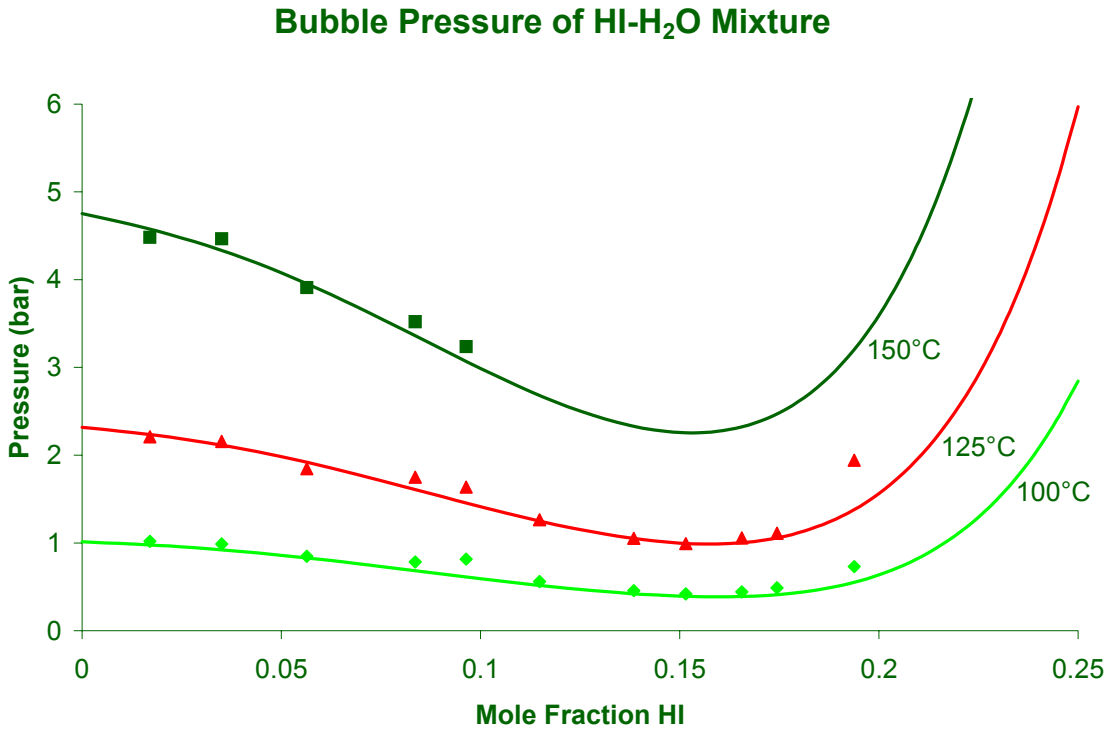

Figure 10 - VLE of HI-H2O mixtures

Figure 10 demonstrates that the model captures the azeotrope of the HI-H_2O binary, which is typical of aqueous mixtures containing a volatile component that is also a strong electrolyte.

The next four charts show how well the total pressure ternary data[18] has been represented, and provide an indication of the deviation as a function of temperature, pressure and composition.

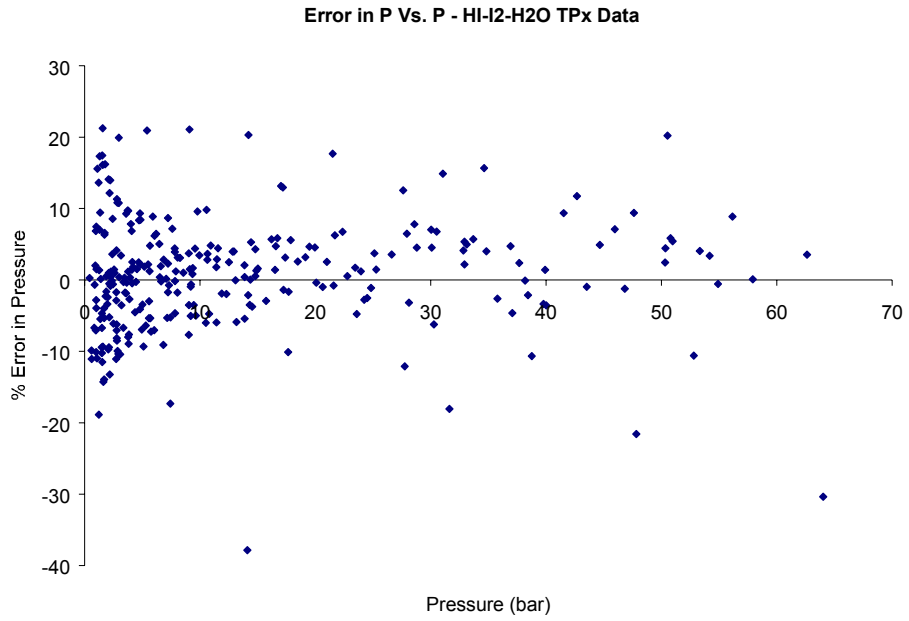

Figure 11 - Error in Pressure Vs. Pressure – HI-I2-H2O TPx Data

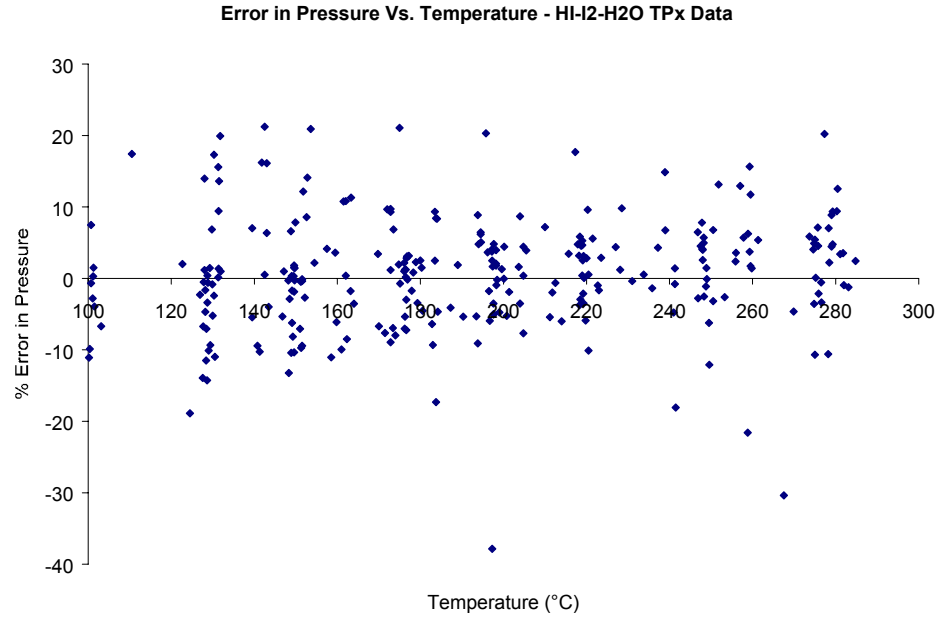

Figure 12 - Error in Pressure Vs. Temperature – HI-I2-H2O TPx Data

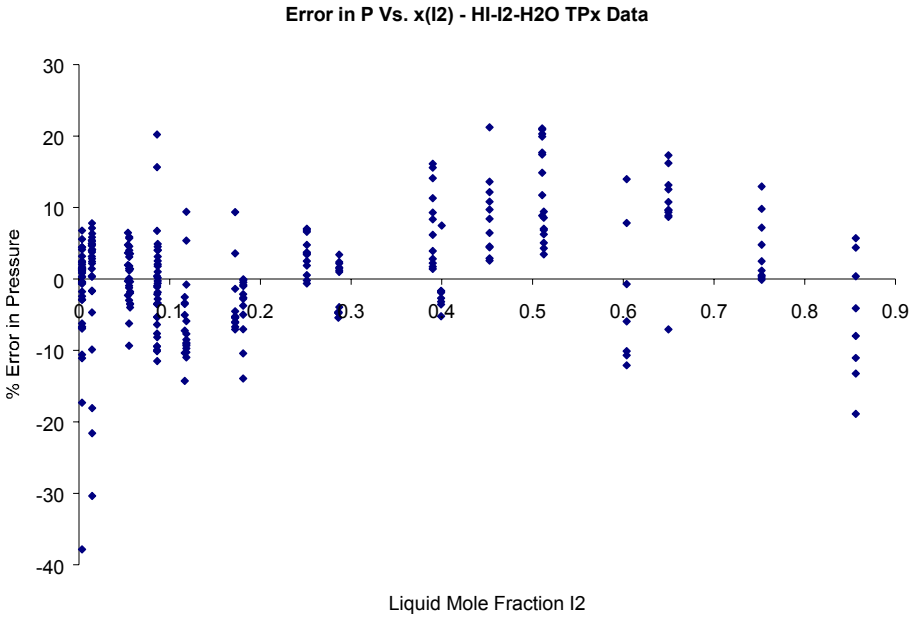

Figure 13 - Error in Pressure Vs x(I2) – HI-I2-H2O TPx Data

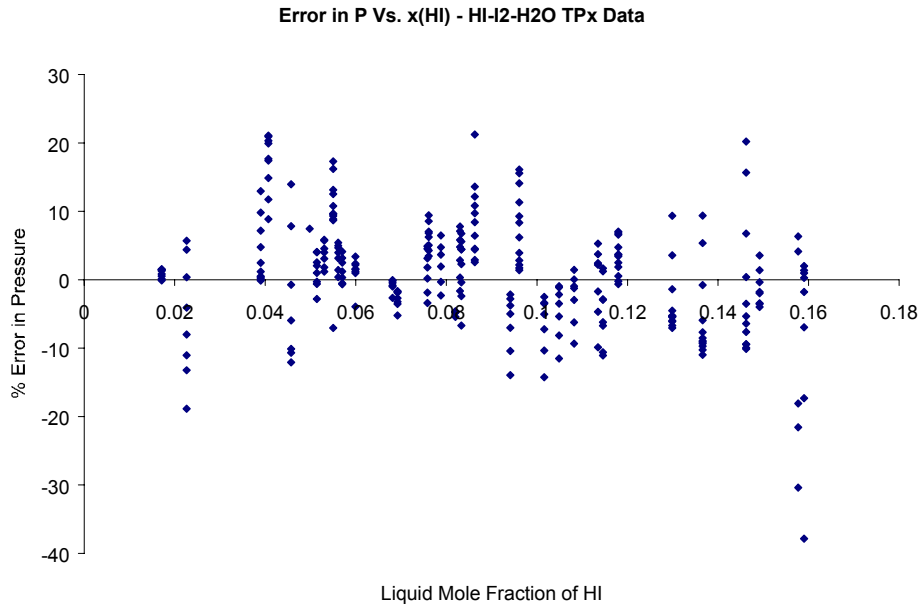

Figure 14 - Error in Pressure Vs x(HI) – HI-I2-H2O TPx Data

Examination of these four charts indicates that the total pressure data are generally fit to within 20%; the average absolute error is 5.9%. The largest errors (above 20%) occur at high HI

concentrations (above about 16 mole% HI) and at high temperature (above 200°C). Engels and Knoche[22] have observed that HI dissociates into hydrogen and iodine at these conditions and this is probably why the model calculations of the total pressure are biased low at high temperatures and high HI concentrations. The fit of the data is considered good since the dissociation of HI is modeled separately in the plant simulations.

The HI-I2-H2O system exhibits complex liquid-liquid equilibrium. Although the process attempts to avoid regions of liquid-liquid equilibrium, this behavior is important because the process engineer must have knowledge of the composition regions to be avoided and also because this behavior is an important aspect of the system that must be thoroughly understood for a reliable and confident process design. The next series of charts summarizes our current knowledge and lack of knowledge of the liquid-liquid behavior of this system.

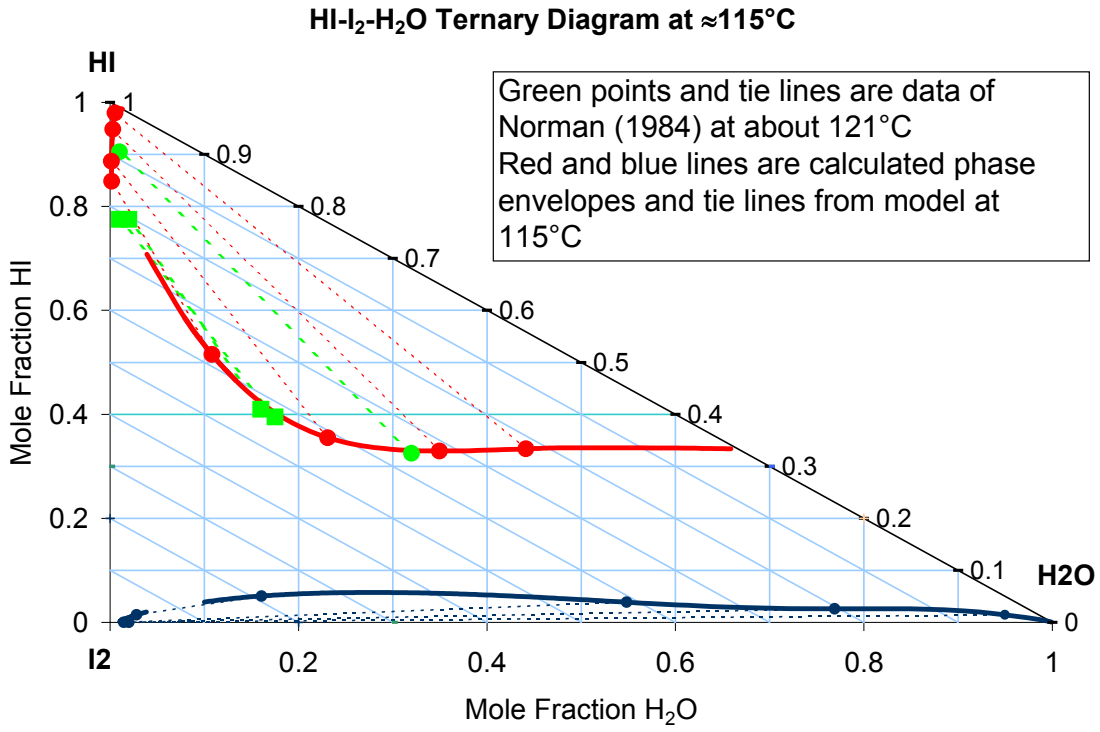

Figure 15 - HI-I2-H2O Ternary Diagram at ≈ 115°C

Figure 15 presents model calculations of the LL behavior of the ternary system at 115°C, at which some experimental data are available. The model qualitatively describes the two LL regions that were observed by GA researchers. The calculated tie lines for the I_2-lean mixture are in reasonable agreement with those presented by GA. There are no tie-line data presented by GA for the HI-lean region, but this region is predicted to be quite thin, again in agreement with the observations of GA researchers.

The phase boundary for the HI-lean region is not closed at low water concentrations. This is because of problems of flash convergence close to the critical point. Similarly, the phase boundary of the I_2-lean region is not closed in the critical region, again at low water concentrations.

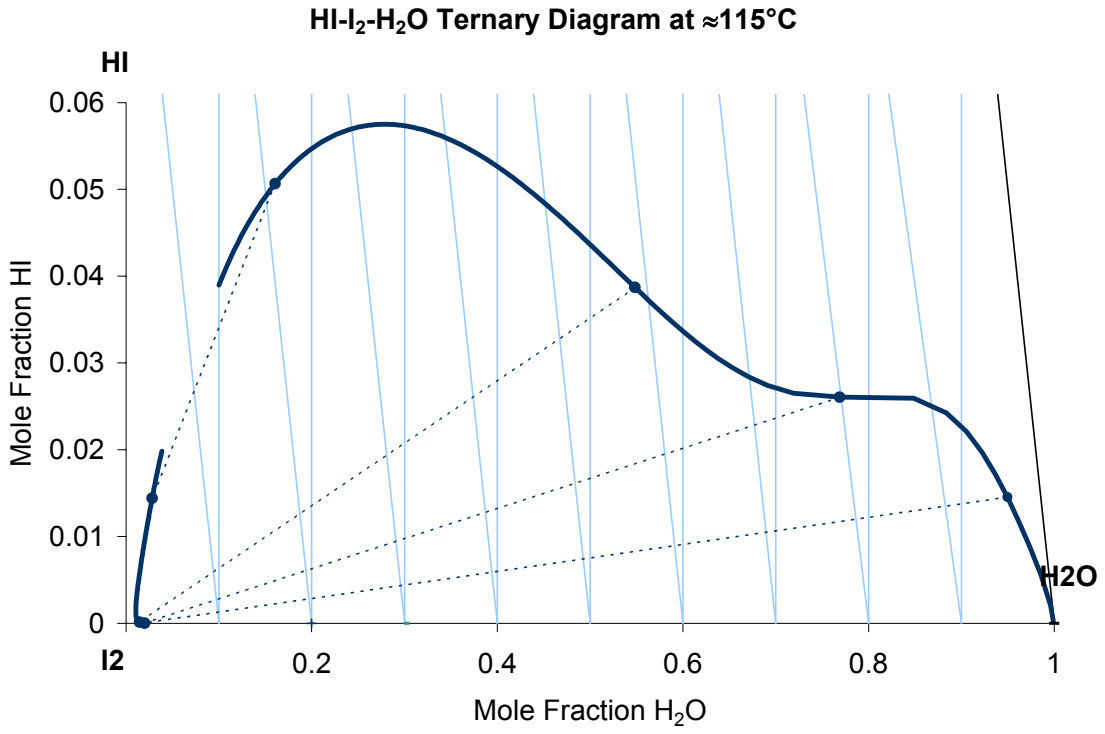

Figure 16 - HI-I2-H2O Ternary Diagram at ≈ 115°C – HI-Lean Region

Figure 16 magnifies the HI-lean region of Figure 15 (115°C). The predicted phase boundary has an unexpected "hump," but is not necessarily absurd. Figure 16 presents a few tie lines. The tie lines behave reasonably, i.e., they do not cross. While the behavior is reasonable, there is no experimental verification other than the tie lines and qualitative observations noted in relation to Figure 15.

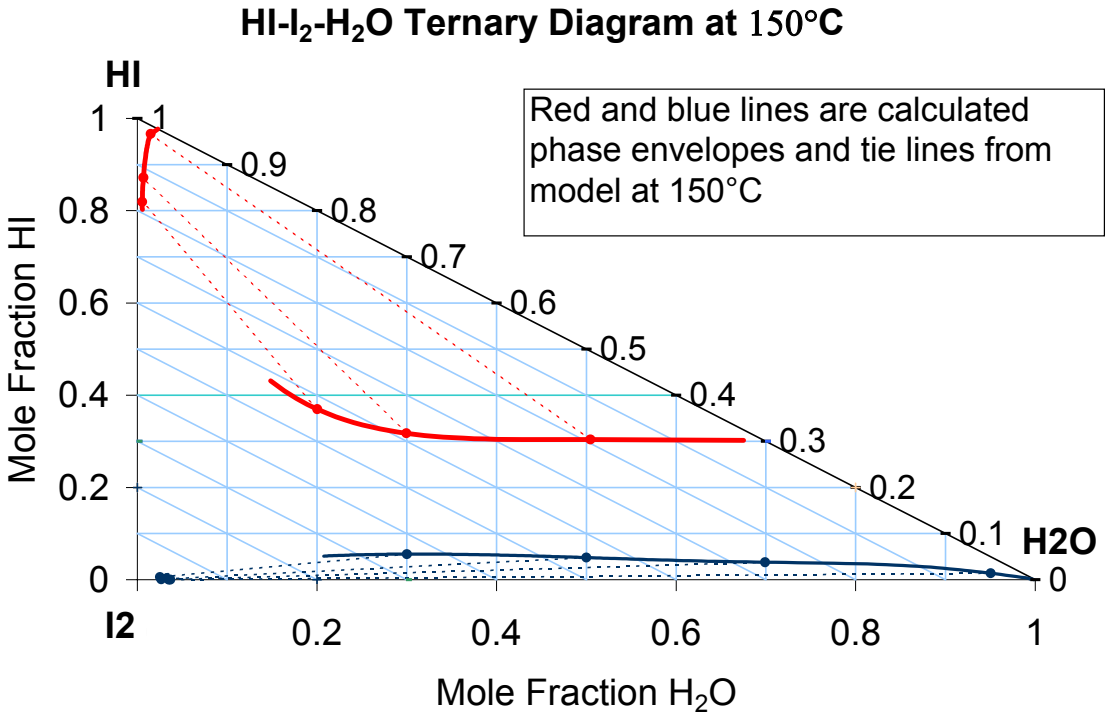

Figure 17 - HI-I2-H2O Ternary Diagram at ≈ 150°C

Figure 17 presents model calculations of the LL behavior of the ternary system at 150°C. The trend of the phase boundary of the I_2-lean region is reasonable because the physical solubility of water in HI increases with temperature, while the chemical solubility of HI in water decreases with temperature. But the trend is also unreasonable since we would not expect to predict liquid-liquid equilibrium at a temperature this close to the critical temperature of HI (T_c = 150.7°C). This is a fundamental deficiency of the activity-coefficient approach, which will predict formation of a liquid phase of a pure component at supercritical temperatures. However, this is unlikely to be a problem for the simulations since very high pressures will be necessary to form the HI-rich phase.

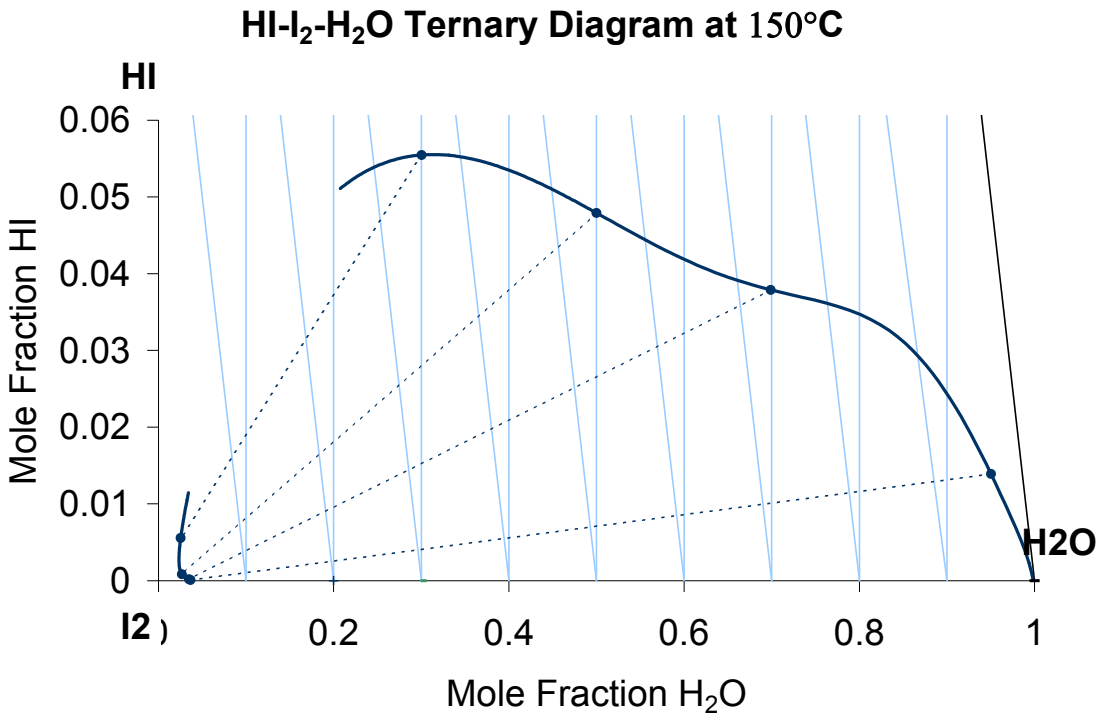

Figure 18 - HI-I2-H2O Ternary Diagram at ≈ 150°C – HI-Lean Region

It is of greater concern to monitor the liquid-liquid region in the HI-lean region since this region is relevant to the reactive distillation. This region is shown magnified in Figure 18. The "hump" observed at 115°C has lessened. Again, the predicted tie lines are reasonable, but there is no experimental verification.

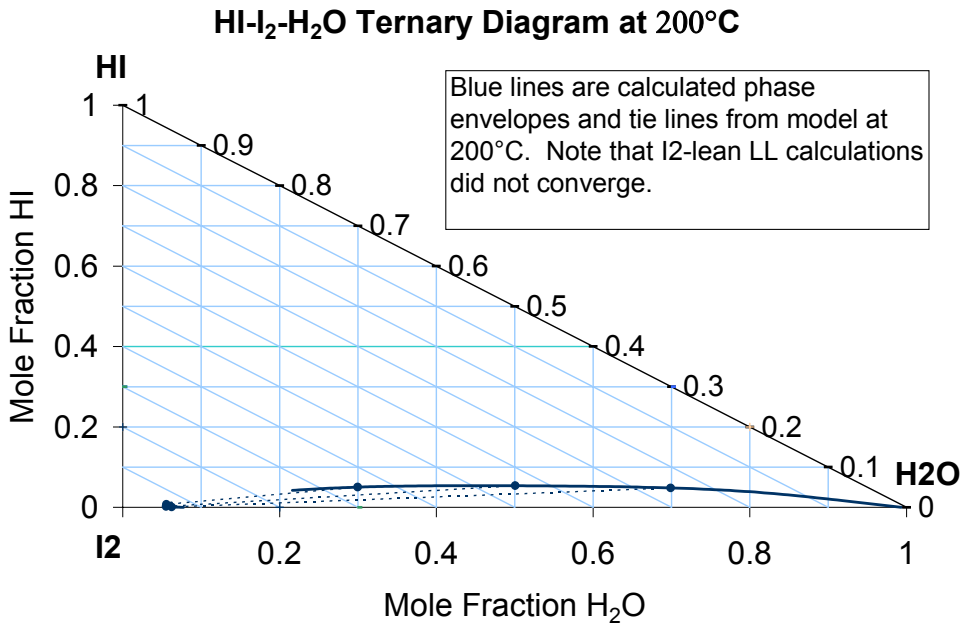

Figure 19 - HI-I2-H2O Ternary Diagram at ≈ 200°C

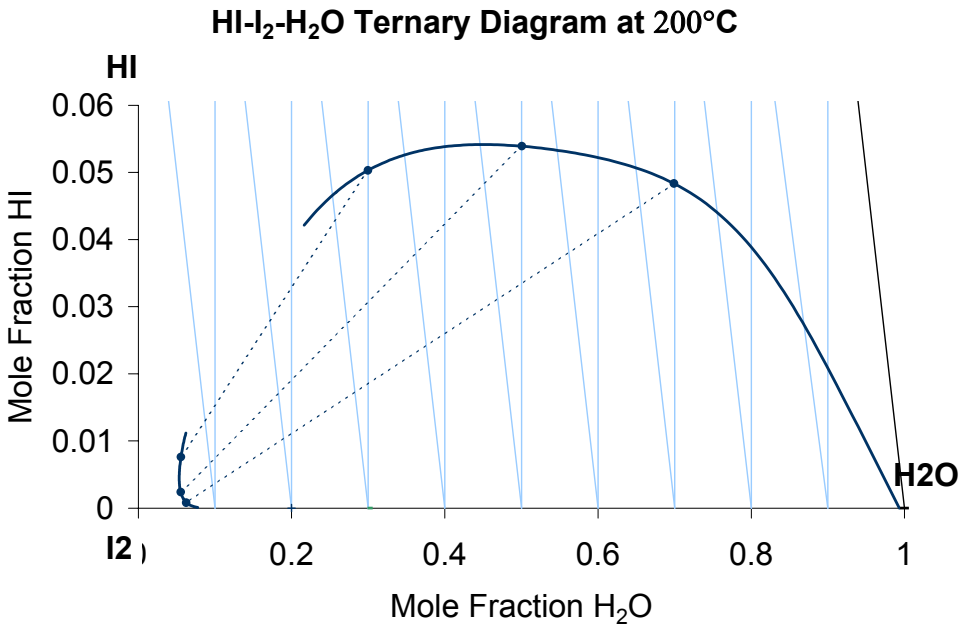

Figure 20 - HI-I2-H2O Ternary Diagram at ≈ 200°C – HI-Lean Region

Figure 19 and Figure 20 present the LL region for HI-lean mixtures at 200°C. The results are similar to those at 150°C. The LL calculations for the HI-rich region did not converge at 200°C.

It is highly unlikely that liquid-liquid immiscibility will occur for the HI-H_2O binary system at 200°C, since the temperature if far above the critical temperature of HI, but it is possible that LL behavior could occur if a small amount of I_2 is added to the HI-H_2O binary system.

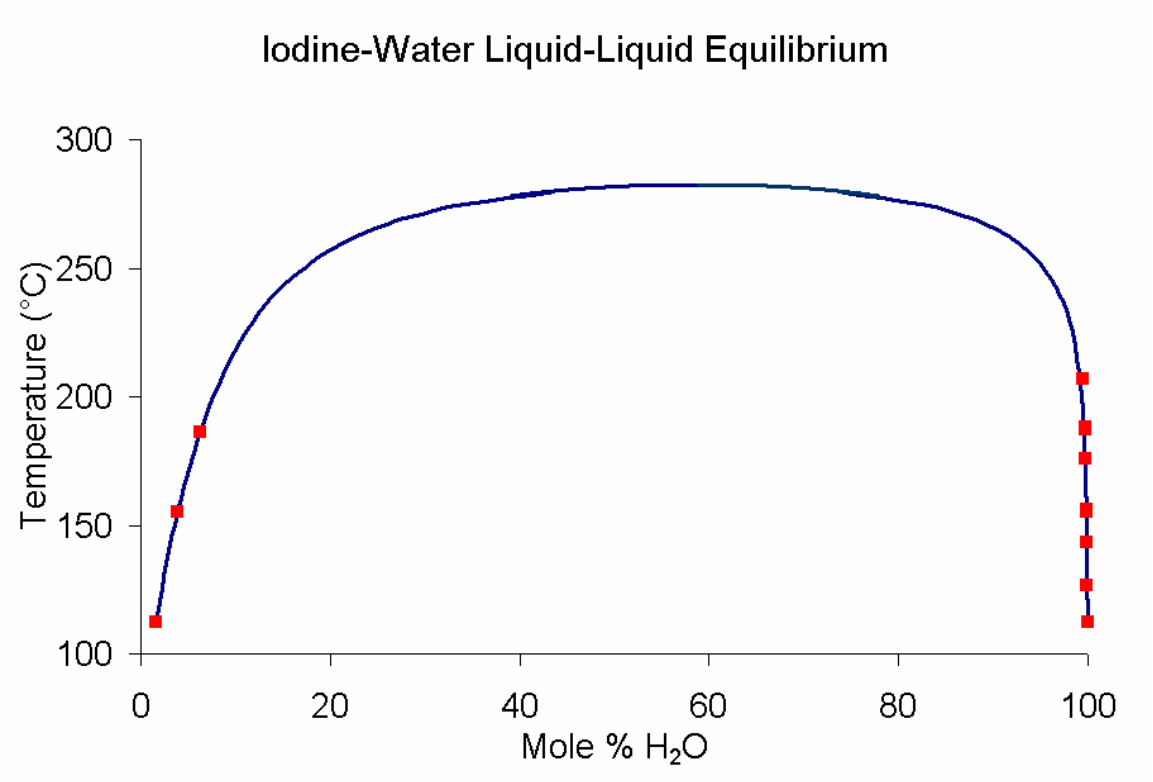

Figure 21 - Iodine-Water Liquid-Liquid equilibrium

We will next evaluate the predicted LL behavior of HI-lean mixtures over a range of temperatures, but first it is useful to examine the liquid-liquid equilibrium of the I_2-H_2O binary. The predicted LL behavior of the I_2-H_2O is presented in Figure 21. Note that experimental data are only available up to about 207°C, thus predictions above this temperature must be used with caution. The model predicts an upper consolute temperature of about 282.5°C. Above this temperature, I_2-H_2O binary mixtures will not exhibit LL behavior, but LLE may be induced by the addition of a small amount of HI.

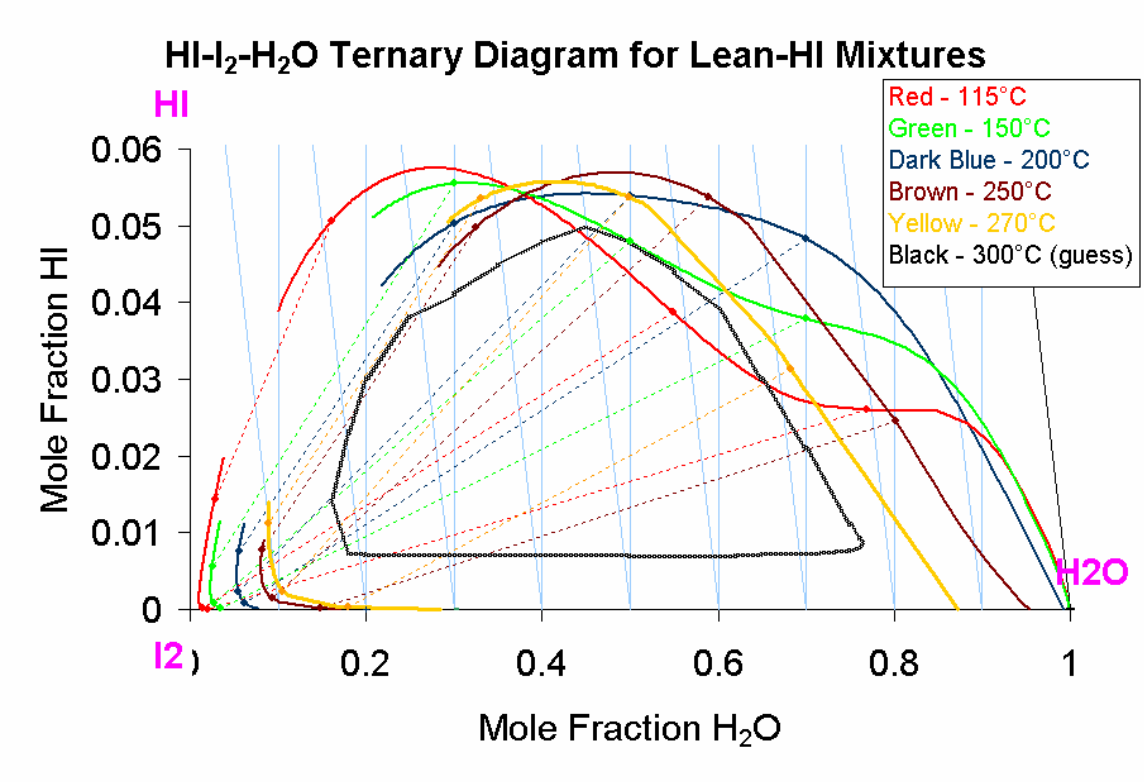

Figure 22 - HI-I2-H2O Ternary Diagram for HI-Lean Mixtures

Figure 22 evaluates the predicted LL behavior for the HI-lean region as a function of temperature. The variation with temperature is complex, but reasonable. As noted before, there are too few data to establish confidence in the model predictions. The calculations did not converge above 270°C, but it will be useful to anticipate the LL region at higher temperatures. Figure 8 presents a guess of the LL region at 300°C. The region is estimated to have both a lower and an upper critical point.

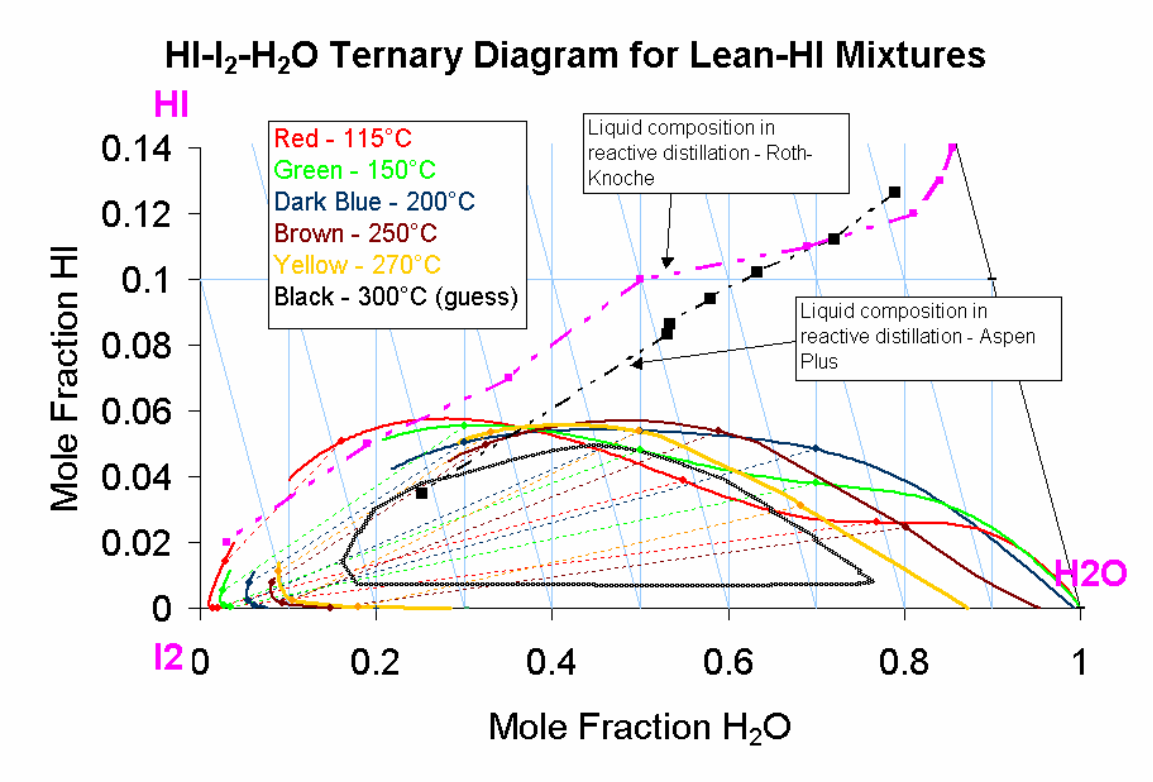

Figure 23 - HI-I2-H2O Ternary Diagram for HI-Lean Mixtures with Simulation Results

Figure 23 is the same as Figure 22, but the profiles from the reactive-distillation calculations of Roth and Knoche[23] and the Aspen Plus simulations in Section 6.3 have been added. Both sets of calculations assume only vapor-liquid equilibrium and thus should not intersect the liquid-liquid region. It appears that both sets of calculations are valid from this point of view. The Aspen Plus calculation is not able to attain the better separations of the Roth-Knoche scheme, but this is probably the result of different VLE predictions rather than the boundaries imposed by liquid-liquid equilibria.

This analysis suggests that the predicted phase behavior is reasonable and that the simulations of the reactive distillation are similarly reasonable.

The Roth and Knoche results similarly avoid the liquid-liquid region and give more favorable predicted results. It is currently unclear why the Roth and Knoche results are more favorable than the Aspen Plus simulations.

The Aspen Plus predictions are reasonable, but clearly need to be validated by lab and pilot-plant data.

5.3 The H_2SO_4-HIx-H_2O System

The H_2SO_4-HIx-H_2O system exhibits very favorable behavior from the viewpoint of the Sulfur-Iodine cycle since the liquid phase splits into two phases, one containing mainly the sulfuric acid and the second phase containing the HIx species (complexes containing HI and I_2). The water distribution does not strongly favor either phase. This phase behavior permits an effective separation of the two acid but is very difficult to model. We have developed a semi-empirical model based mainly upon the data of Sakurai et al.[24,25] The data reported by Sakurai et al. do not contain complete information. Dr. Sakurai kindly sent us the raw data on a spreadsheet.[26] Sakurai's data at 368 K, which were used to develop the model parameters are shown in the table below.

T = 368 K (HI/H2SO4/H2O = 0.070/0.048/0.882)					
No.	Sol.	f HI	f H2SO4	f I2	f H2O
1	Prep.	0.065	0.045	0.067	0.823
	S.A.	0.031	0.067	0.017	0.885
	HIx	0.073	0.031	0.094	0.803
2	Prep.	0.065	0.044	0.073	0.818
	S.A.	0.031	0.075	0.017	0.877
	HIx	0.077	0.028	0.101	0.794
3	Prep.	0.064	0.044	0.088	0.805
	S.A.	0.021	0.093	0.012	0.873
	HIx	0.083	0.015	0.130	0.772
4	Prep.	0.063	0.043	0.105	0.789
	S.A.	0.016	0.102	0.008	0.874
	HIx	0.089	0.009	0.162	0.739
5	Prep.	0.059	0.041	0.150	0.749
	S.A.	0.008	0.112	0.004	0.877
	HIx	0.090	0.005	0.237	0.668
6	Prep.	0.055	0.038	0.216	0.692
	S.A.	0.003	0.113	0.002	0.883
	HIx	0.080	0.003	0.318	0.599
7	Prep.	0.052	0.035	0.261	0.652
	S.A.	0.002	0.109	0.001	0.888
	HIx	0.065	0.004	0.322	0.609
8	Prep.	0.049	0.034	0.295	0.622
	S.A.	0.002	0.107	0.001	0.890
	HIx	0.068	0.002	0.379	0.552
9	Prep.	0.048	0.033	0.320	0.599
	S.A.	0.002	0.111	0.000	0.887
	HIx	0.065	0.004	0.366	0.564

Table 4 - H2SO4-HIx Liquid-Liquid Equilibrium at 368 K – Data of Sakurai et al.

In Table 4, the composition is in mole fraction and the row identifiers are as follows:

Prep. - Composition of the raw material (before separation)
S.A. - Composition of the sulfuric-acid phase
HIx - Composition of the HIx phase

The following chemistry model was used to describe the dominant features of the system:

Equation 26: $H_2SO_4 + H_2O \leftrightarrow H_3O^+ + HSO_4^-$

Equation 27: $HI + H_2O + 0.25I_2 \leftrightarrow HIx$

Equation 26 is the usual ionic dissociation of sulfuric acid. The parameters associated with Equation 26 have been fitted previously and this has been kept unchanged. It seems that I_2 and HI form a complex in aqueous solutions. The exact composition of this complex is not known. The particular formula of the complex, HIx, resulted from the trial of several different complexes to fit the data. Equation 27 is an attempt to capture the formation of this complex.

The thermodynamic model was developed by using the DRS system within Aspen Plus and Sakurai's data shown in Table 4. The fit of the data is good, but the range of the data is small and the results have not been used extensively and thus the present results should be treated with caution.

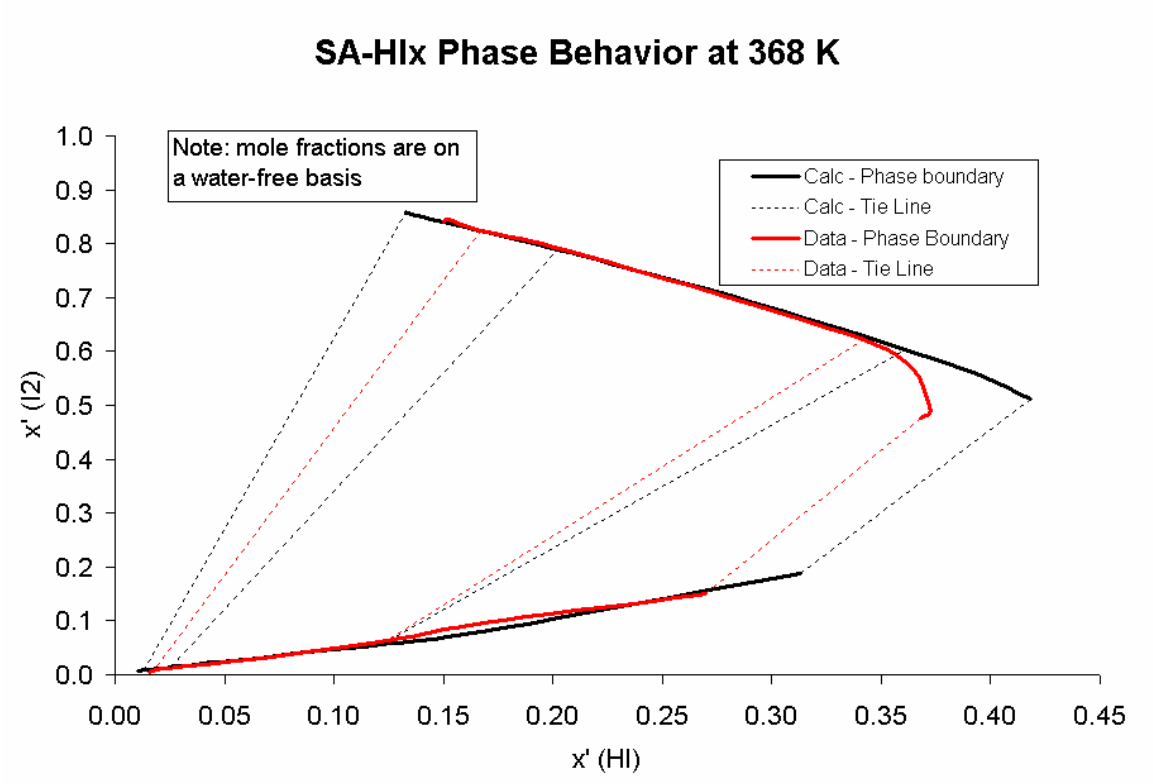

Figure 24 - SA-HIx Phase behavior at 368 K. Comparison of Model to Data of Sakurai et al.

Figure 24 compares model predictions to the data of Sakurai et al.[26] (Table 4). The fit appears to be good, but the results should be used with caution.

The fit attempted to force the sulfuric acid dissociation (Equation 26) to occur in the sulfuric-acid phase and the HIx complexation (Equation 27) to occur in the HIx phase. It has been observed that the present fit may allow Equation 27 to occur in the sulfuric acid phase, particularly for mixtures low in HI and with high concentrations of I_2, and this incorrect result should be watched for in the simulations. It seems that this incorrect behavior has a stronger tendency to occur at higher temperatures (80°C and above).

The model for the H_2SO_4-HIx-H_2O system is contained in the chemistry model H2SO4-HI.

The thermodynamic model developed for the H_2SO_4-HIx-H_2O system is a reasonable representation of this system, but much more testing and perhaps further development must be done before its results in process simulation can be trusted.

6 SIMULATION MODELS

This section provides descriptions of the Aspen Plus simulation models that have been developed for the Sulfur-Iodine Cycle. These models have been delivered as Aspen Plus bkp files and their input summaries are also provided as appendices in this report

6.1 Section 1 - Chemical Recycle and Acid Generation

The main purpose of Section I is to produce the two the acids (H_2SO_4 and HI) through the Bunsen reaction:

$$\text{Equation 28: } 2H_2O + I_2 + SO_2 \leftrightarrow 2HI + H_2SO_4$$

The Aspen Plus model PFD is presented in Appendix 1.

The Bunsen reaction (Equation 28) occurs in several pieces of equipment. The two reactive columns (C-101 and C-104) scrub process streams to remove costly iodine. They assume that the reaction can be described as a vapor-phase equilibrium reaction in Radfrac. The accurate description is not important since the reactions nearly go to completion.

The main reaction occurs in R-101. This is a rather complicated piece of equipment. We have assumed simply that the reaction is a kinetically-controlled liquid-phase reaction and the RCSTR model in Aspen Plus used to model the reactor. The kinetics-reactor sizes are currently set to reproduce the results provided in the GA flowsheet. It is expected that accurate modeling of this reactor will require laboratory or pilot-plant data.

The last reactor that must be modeled is C-103, which is a three-phase device in which the vapor and the light liquid phase (sulfuric-acid phase) move up the column and the heavy iodine phase move up the column. Aspen Plus does not have a standard model for this piece of equipment. Each stage has been modeled as a CSTR reactor (similar to R-101) and a FLASH3 block. Currently C-103 is assumed to have only two stages, but additional stages can be added if needed.

The other pieces of equipment in Section 1 have been described using standard models in Aspen Plus, i.e., FLASH2, FLASH3, MIXER, PUMP, COMPR, FSPLIT, RADFRAC, etc.

Section1-04.bkp provides a good description of the material balance presented by Norman et al.[3]

One important discrepancy between the GA flowsheet and the results from Section1-04.bkp is that a small, but significant, amount of I_2 is lost in the vapor streams from C-101 and C-104. In an attempt to reduce this loss, the flowsheet was modified to feed some of the vapor stream above the iodine feed. This change, which has been incorporated in Section1-04.bkp, caused some convergence difficulties. In an attempt to overcome these difficulties and also to provide a

more realistic simulation, the reactions models in C-101 and C-103 were made kinetic instead of equilibrium. The simulation results in Section1-04.bkp demonstrate that the modified scheme does reduce the I_2 loss in C-101. In C-103, the SO_3 in the inlet in not sufficient to react all the iodine and thus a change will have to be made in the flowsheet to attain this result.

However, it is clear that the Aspen Plus model is a valuable way to evaluate and improve the Section I flowsheet.

In summary, the following has been accomplished for the Section 1 flowsheet:

1. A thermodynamic model has been developed that captures the dominant effect, i.e., the favorable liquid-liquid between the sulfuric acid and HIx phases.
2. Equilibrium and kinetic building blocks have been developed to capture the main reactive processes in this section.
3. The thermodynamic and kinetic models have been used to develop two Aspen plus models for section 1.
4. While the results are preliminary, the Aspen Plus models promise to be useful to evaluate and improve the Section I flowsheet.

One aspect of the model that needs further analysis and perhaps development is the tendency of the thermodynamic model to (incorrectly?) allow HIx to form in the sulfuric acid phase.

6.2 Section 2 - Sulfuric Acid composition and Decomposition

The Section 2 Aspen Plus model for the Sulfur-Iodine cycle was developed by General Atomics and the University of Kentucky. AspenTech's role was to evaluate and improve the model. The main focus has been on equilibrium models that previously used the RGIBBS block.

The Section 2 flowsheet is presented in Appendix 2.

Section 1 accomplishes the decomposition of H_2SO_4 using high-temperature heat. The reactions that occur in this section are:

Equation 29: $H_2SO_4 + H_2O \leftrightarrow H_3O^+ + HSO_4^-$

Equation 30: $HSO_4^- + H_2O \leftrightarrow H_3O^+ + SO_4^=$

Equation 31: $H_2SO_4 + H_2O \leftrightarrow 2IonPair$

Equation 32: $H_2O + SO_3 \leftrightarrow H_2SO_4$

Equation 33: $SO_3 \leftrightarrow SO_2 + H_2O$

Equation 29 and Equation 30 describe the dissociation of sulfuric acid into ionic species. These reactions occur in the aqueous phase. Sulfuric acid will form complexes in aqueous solutions even at high temperatures approaching and exceeding the critical point of water (394°C). However, the electrolyte model tends to break down at temperatures in excess of about 300°C. Hence we have proposed Equation 31 as a practical high-temperature equivalent to Equation 29 and Equation 30. The decomposition of sulfuric acid (reverse of Equation 32) and the decomposition of SO_3 (Equation 33) tend to occur at high temperatures.

Equation 29-Equation 32 occur rapidly and therefore can be treated as equilibrium reactions. Equation 33 requires the use of a catalyst, but is treated in this simulation as an equilibrium reaction since this gives the most optimistic result. However, we do restrict Equation 33 to only occur in specific devices.

Reactions may be described through Chemistry or Reactions or both.

Chemistry refers to equilibrium reactions that go to equilibrium in the liquid phase. The power of the Chemistry feature is that it can be used with essentially all the unit operations in Aspen Plus, like flash blocks, reactors and distillation columns. Chemistry can be used in two modes: True and Apparent. In the True mode, the unit-operation model, the unit-operation block must solve the equations for chemical equilibrium together with other equations, such as equality of fugacities for phase equilibrium. In the Apparent mode, the property system solves the liquid-phase chemical equilibrium equations and provides artificial properties to the unit-operation model that will lead to the correct answer. It should be noted that the choice between True and Apparent will not and should not affect the simulation result; rather, the choice should be made based upon which approach improves the look-and-feel and the convergence characteristics of the simulation.

The Apparent mode should only be used for reactions where all the species on the right side are non-volatile. This is the case for Equation 29-Equation 31, but not for Equation 32 and Equation 33. The reason for this is that chemical equilibrium implies a relation between the fugacities of the species. This forced relationship among fugacities causes problems with the phase–equilibrium calculation where the fugacity of each species is set equal in the various phases in equilibrium. Problems result if every component in a reaction is involved with phase equilibrium calculations.

The Reactions system is very flexible. In this discussion, we will only consider the Power-Law model in the equilibrium mode. In the Power-Law model, sets of reactions can be defined to be at equilibrium. Reactions and Chemistry can be used together, but only if the Chemistry model is in the Apparent mode; if not, the (True) Chemistry model is ignored. Of course, the reaction sets in the combined Chemistry and Reactions models must be independent of one another; i.e., no one reaction in the union set may be a linear combination of the other reactions in the union set. The last point to be noted is that since a Chemistry model in the Apparent mode is being used, the liquid compositions seen by the unit-operation model are not strictly correct. For

example, for a Chemistry model using Equation 29 and Equation 30 (chemistry Model H2SO4), the apparent composition of the ionic species will be zero. Thus it is important to specify that the equilibrium in the Reactions model be calculated in the vapor phase where the composition of the nonvolatile species will be zero under any circumstances.

In the present simulation, two Reactions models have been set up, both describing the equilibrium constant of Equation 34. H2SO4D is used for Radfrac and H2SO4R is used for the CSTR model. The equilibrium constant, K, has been calculated, in a standard way, from the ideal-gas properties as:

Equation 34: $$\ln(K) = -\frac{1}{RT}\sum_i \nu_i G_i^0 + \ln\left(P^{ref}\right)\sum_i \gamma_i = -29.001873 + 11{,}677.3085/T$$

where,

R	-	Gas constant
T	-	Temperature, K
νi	-	Stoichiometric coefficient of component i
G_i^0	-	Ideal-gas Gibbs free energy of component i
P^{ref}	-	Reference pressure, 101,325 Pa (1 atm)

Reactions model H2SO4R has been used within the RCSTR model to describe Equation 32 together with a Chemistry model H2SO4 or the Chemistry model for the high-temperature complexation reaction (H2SO4HT). Similarly, the Reactions model H2SO4D can be combined with the Chemistry models H2SO4 and H2SO4HT to describe equilibrium reactions in Radfrac.

Another useful reactor model within Aspen Plus is RGIBBS, which calculates combines phase and chemical equilibrium for multicomponent systems by minimizing the system Gibbs free energy. RGIBBS is a valuable tool it handles all the possible reactions. RGIBBS should not be used together with chemistry. In the present simulation, RGIBBS has only been used for vapor-phase reactors where Equation 32 alone or both Equation 32 and Equation 33 occur.

The sub-simulation starting with feed 22T illustrates and tests the reaction scheme using the RCSTR model. COOLERA is simulated by block CLR-R, which uses the RCSTR model with Chemistry model H2SO4HT representing Equation 31 and Reaction model H2SO4R representing Equation 32. Flash2 block CLR-F simply separates the vapor and liquid products from CLR-R. CLR-TST is a vapor-phase RGIBBS block limited to Equation 32. As can be observed, CLR-TST does not cause further reaction, which proves that Equation 32 is at equilibrium upon entry to CLR.-TST.

With this background, we now provide a summary of the basis for properly simulating the various reaction devices in Section 2:

Unit	Chemistry Model	Reactions Model	Description of Simulation
COLUMN	H2SO4	H2SO4D	Distillation column to concentrate sulfuric acid. May possibly decompose some H_2SO_4 to form SO_3 and H_2O. Uses Radfrac
RECUP1	-	-	Obtain vapor-phase chemical equilibrium for Equation 32. Uses vapor-phase RGIBBS with products limited to H_2SO_4, SO_3 and H_2O.
DECOMP1	-	-	Obtain vapor-phase chemical equilibrium for Equation 32 and Equation 33. Uses vapor-phase RGIBBS with products limited to H_2SO_4, SO_3, H_2O, SO_2 and O_2.
DECOMP2	-	-	Same as DECOMP1
DECOMP3	-	-	Same as DECOMP1
DECOMP4	-	-	Same as DECOMP1
RECUP2			Obtain vapor-phase chemical equilibrium for Equation 32. Uses vapor-phase RGIBBS with products limited to H_2SO_4, SO_3, H_2O, SO_2 and O_2. Also, SO_2 and O_2 are treated as inerts.
COOLERA	H2SO4HT	H2SO4R	Condense H_2SO_4 and set Equation 32 to equilibrium. SO_2 and O_2 are treated as inerts. RCSTR model is used.
COOLERB	H2SO4	H2SO4R	Condense H_2SO_4 and set Equation 32 to equilibrium. SO_2 and O_2 are treated as inerts. RCSTR model is used.
COOLERC	H2SO4	H2SO4R	Condense H_2SO_4 and set Equation 32 to equilibrium. SO_2 and O_2 are treated as inerts. RCSTR model is used.

Table 5 - Summary of Section 2 Model Specifications

The Section 1 model is expected to provide an accurate simulation model.

6.3 Section 3 - Hydrogen Iodide Concentration and Decomposition

Two Aspen Plus bkp files representing simulations of hydrogen production by reactive distillation of HI-I2-H2O mixtures have been developed. The first bkp file (ReacDistLiqDraw.bkp) simulates the reactive distillation as a 7-tray column with HI ionic dissociation and HI dissociation to form H2 and I2 on all trays. Both reactions are modeled as being at equilibrium. The HI ionic dissociation and associated thermo model parameters give a good description of the available thermodynamic data. The column feed is at its bubble point at 300°C and enters the column on tray 5. A liquid side draw is taken from tray 3. The distillate rate is set to 5 kmol/hr and the boil up rate is set to 2.0. The convergence strategy is as follows. The column was first converged without the H2 production. Now the equilibrium of the HI dissociation to H2 was set to a relatively low value and the reactions were assumed to occur on trays 2-7. Next reaction on tray 1 was added. Finally, the equilibrium constant for HI dissociation to H2 was gradually raised to the correct value. Once convergence was achieved, estimates were generated for the column. The column will now converge reliably for reasonable perturbations of feed and operating conditions.

A sensitivity study has been done to analyze how the H2 production and purity of the bottom varies with liquid side draw. The simulation predicts that as the side draw is increased, the H2 production decreases and the water content of the bottom decreases. Of course, other sensitivity studies can be set up to study the column characteristics.

One possible issue is that the simulation predicts a maximum in the temperature profile, i.e., the bottom tray is at a (slightly) lower temperature than the tray above it. Modification of the boil up rate did not change this trend. This trend is unusual, but is not thought to be absurd.

It is not clear from the Roth-Knoche paper[5] whether the side draw is vapor or liquid. It does seem to be a vapor draw since this stream is used to heat the in-coming column feed. The second bkp file (ReacDistVapDraw.bkp) simulated the same column configuration as the first case, but with a vapor side draw.

Preliminary results suggest that the liquid side draw is better because the hydrogen production is higher and also very little hydrogen escapes in the liquid side draw.

The reactive-distillation simulation models presented in this section are preliminary and more work needs to be done to establish reliable models for this section.

APPENDIX-1 - SECTION 1 MODEL

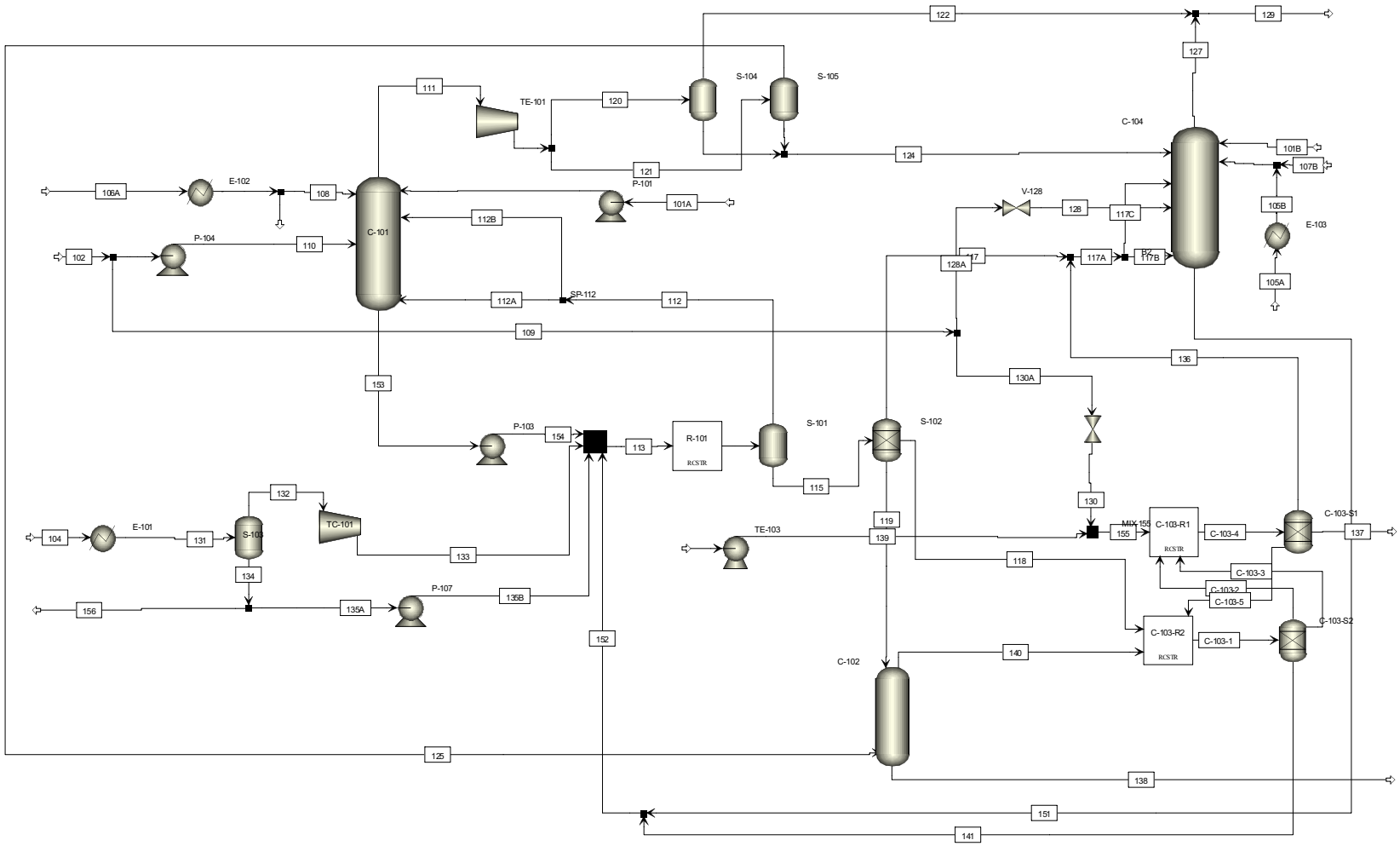

APPENDIX-2 - SECTION 2 MODEL

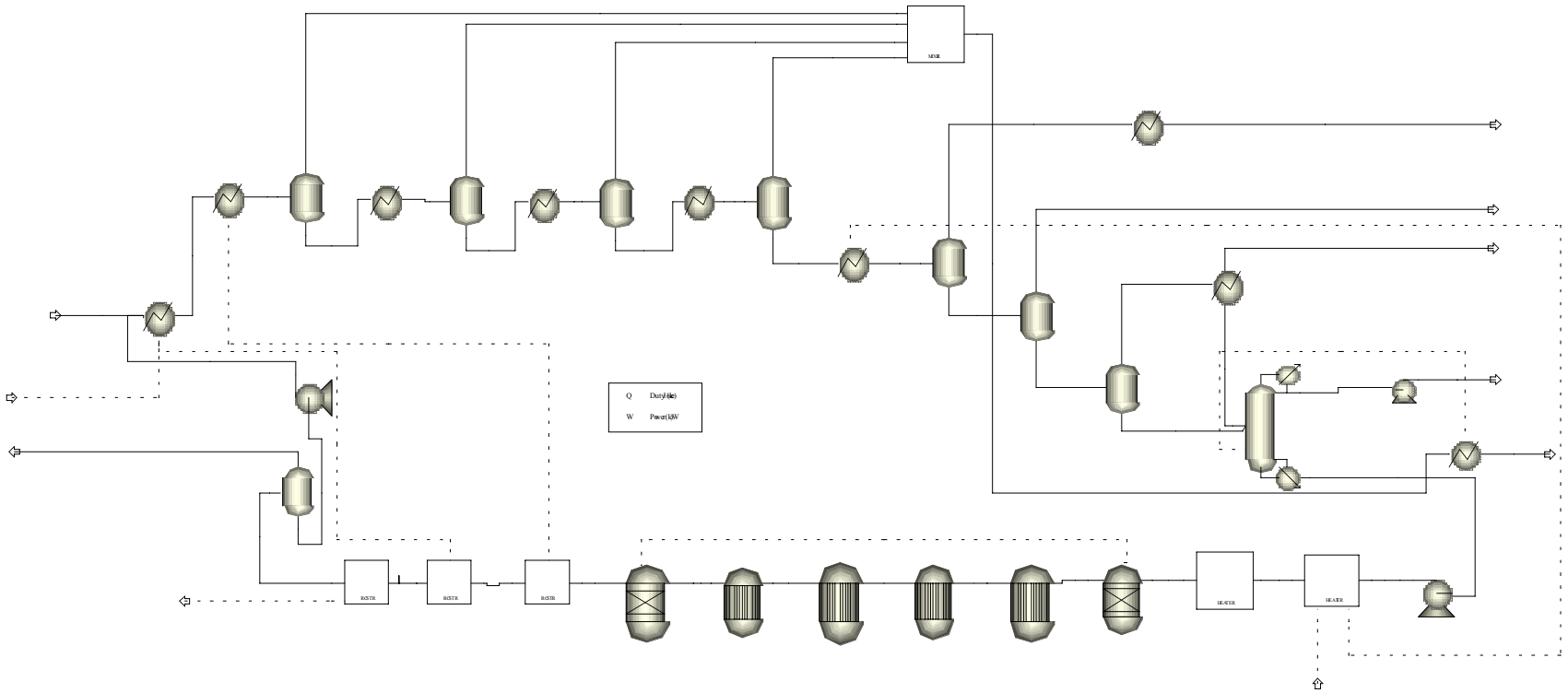

APPENDIX 3 - INPUT SUMMARY OF SECTION 1 MODEL (SECTION1-04,BKP)

```
TITLE 'Section 1 Model for the Sulfur-Iodine Cycle'

IN-UNITS MET PRESSURE=MPa PDROP=MPa INVERSE-PRES='1/bar'

DEF-STREAMS CONVEN ALL

SIM-OPTIONS
   IN-UNITS MET VOLUME-FLOW='cum/hr' ENTHALPY-FLO='MMkcal/hr'  &
      HEAT-TRANS-C='kcal/hr-sqm-K' PRESSURE=bar TEMPERATURE=C  &
      VOLUME=cum DELTA-T=C HEAD=meter MOLE-DENSITY='kmol/cum'  &
      MASS-DENSITY='kg/cum' MOLE-ENTHALP='kcal/mol'  &
      MASS-ENTHALP='kcal/kg' HEAT=MMkcal MOLE-CONC='mol/l'  &
      PDROP=bar
   SIM-OPTIONS FLASH-TOL=1E-007 HF-FL3-DAMP=YES

RUN-CONTROL MAX-TIME=9999.

DESCRIPTION "
   Electrolytes Simulation with Metric Units :
   C, bar, kg/hr, kmol/hr, MMkcal/hr, cum/hr.

   Property Method: ELECNRTL

   Flow basis for input: Mass

   Stream report composition: Mass flow
   "

DATABANKS PURE10  / AQUEOUS  / SOLIDS  / INORGANIC  /  &
      ASPENPCD

PROP-SOURCES PURE10  / AQUEOUS  / SOLIDS  / INORGANIC  /  &
      ASPENPCD

COMPONENTS
   H2O H2O /
   H2SO4 H2SO4 /
   SO2 O2S /
   SO3 O3S /
   HI HI /
   I2 I2 /
```

```
   H2 H2 /
   N2 N2 /
   CO2 CO2 /
   O2 O2 /
   AR AR /
   H3O+ H3O+ /
   HSO4- HSO4- /
   SO4-2 SO4-2 /
   I- I- /
   SAIPAIR H2SO4 /
   I2-S I2 /
   HIX I2 /
   HE HE

HENRY-COMPS HC-1 SO2 CO2 N2 O2 AR H2

HENRY-COMPS HENRY H2

CHEMISTRY CH2SO4
   IN-UNITS SI
   STOIC 1 H2SO4 -1.0 / H2O -1.0 / H3O+ 1.0 / HSO4- 1.0
   STOIC 2 HSO4- -1.0 / H2O -1.0 / H3O+ 1.0 / SO4-2 1.0
   STOIC 3 H2O -1. / SO3 -1. / H2SO4 1.

CHEMISTRY CH2SO4HT
   IN-UNITS MET ENTHALPY-FLO='kcal/hr' PRESSURE=torr  &
      TEMPERATURE=C DELTA-T=C ELEC-POWER=Watt PDROP=torr
   STOIC 1 SO3 -1. / H2O -1. / H2SO4 1.
   STOIC 2 H2O -1. / H2SO4 -1. / SAIPAIR 2.
   K-STOIC 2 A=-10.447219 B=5574.5057

CHEMISTRY H2SO4
   IN-UNITS SI PRESSURE=torr TEMPERATURE=C PDROP='N/sqm'
   STOIC 1 H2SO4 -1.0 / H2O -1.0 / H3O+ 1.0 / HSO4- 1.0
   STOIC 2 HSO4- -1.0 / H2O -1.0 / H3O+ 1.0 / SO4-2 1.0

CHEMISTRY H2SO4-HI
   IN-UNITS MET VOLUME-FLOW='cum/hr' ENTHALPY-FLO='MMkcal/hr'  &
      HEAT-TRANS-C='kcal/hr-sqm-K' PRESSURE=bar TEMPERATURE=C  &
      VOLUME=cum DELTA-T=C HEAD=meter MOLE-DENSITY='kmol/cum'  &
      MASS-DENSITY='kg/cum' MOLE-ENTHALP='kcal/mol'  &
      MASS-ENTHALP='kcal/kg' HEAT=MMkcal MOLE-CONC='mol/l'  &
      PDROP=bar
   STOIC 1 H2SO4 -1. / H2O -1. / H3O+ 1. / HSO4- 1.
   STOIC 2 HI -1. / I2 -0.25 / H2O -1. / HIX 1.
   K-STOIC 2 A=8.96374989
```

```
CHEMISTRY HI-FULL
   IN-UNITS MET VOLUME-FLOW='cum/hr' ENTHALPY-FLO='MMkcal/hr'  &
      HEAT-TRANS-C='kcal/hr-sqm-K' PRESSURE=bar TEMPERATURE=C  &
      VOLUME=cum DELTA-T=C HEAD=meter MOLE-DENSITY='kmol/cum'  &
      MASS-DENSITY='kg/cum' MOLE-ENTHALP='kcal/mol'  &
      MASS-ENTHALP='kcal/kg' HEAT=MMkcal MOLE-CONC='mol/l'  &
      PDROP=bar
   STOIC 1 HI -1. / H2O -1. / H3O+ 1. / I- 1.
   STOIC 3 HI -2. / I2 1. / H2 1.
   K-STOIC 3 A=17.38265099 B=-14058.06029 C=9.099622987  &
      D=-0.110628785
   SALT I2-S I2 1.
   K-SALT I2-S A=-9.228072963 B=-1083.684565 C=2.019221642

CHEMISTRY HI-H2
   IN-UNITS MET VOLUME-FLOW='cum/hr' ENTHALPY-FLO='MMkcal/hr'  &
      HEAT-TRANS-C='kcal/hr-sqm-K' PRESSURE=bar TEMPERATURE=C  &
      VOLUME=cum DELTA-T=C HEAD=meter MOLE-DENSITY='kmol/cum'  &
      MASS-DENSITY='kg/cum' MOLE-ENTHALP='kcal/mol'  &
      MASS-ENTHALP='kcal/kg' HEAT=MMkcal MOLE-CONC='mol/l'  &
      PDROP=bar
   STOIC 1 HI -1. / H2O -1. / H3O+ 1. / I- 1.
   STOIC 2 HI -2. / I2 1. / H2 1.

CHEMISTRY HI-I2
   IN-UNITS MET VOLUME-FLOW='cum/hr' ENTHALPY-FLO='MMkcal/hr'  &
      HEAT-TRANS-C='kcal/hr-sqm-K' PRESSURE=bar TEMPERATURE=C  &
      VOLUME=cum DELTA-T=C HEAD=meter MOLE-DENSITY='kmol/cum'  &
      MASS-DENSITY='kg/cum' MOLE-ENTHALP='kcal/mol'  &
      MASS-ENTHALP='kcal/kg' HEAT=MMkcal MOLE-CONC='mol/l'  &
      PDROP=bar
   STOIC 1 HI -1. / H2O -1. / H3O+ 1. / I- 1.

CHEMISTRY HI-NOCMP
   IN-UNITS MET VOLUME-FLOW='cum/hr' ENTHALPY-FLO='MMkcal/hr'  &
      HEAT-TRANS-C='kcal/hr-sqm-K' PRESSURE=bar TEMPERATURE=C  &
      VOLUME=cum DELTA-T=C HEAD=meter MOLE-DENSITY='kmol/cum'  &
      MASS-DENSITY='kg/cum' MOLE-ENTHALP='kcal/mol'  &
      MASS-ENTHALP='kcal/kg' HEAT=MMkcal MOLE-CONC='mol/l'  &
      PDROP=bar
   STOIC 1 HI -1. / H2O -1. / H3O+ 1. / I- 1.
   K-STOIC 1 A=-228.8380747 B=12587.48013 C=40.68593363  &
      D=-0.098379992

FLOWSHEET
```

```
  BLOCK S-102 IN=115 OUT=117 118 119
  BLOCK E-102 IN=106A OUT=106B
  BLOCK C-101 IN=101AA 108 110 112A 112B OUT=111 153
  BLOCK P-101 IN=101A OUT=101AA
  BLOCK SP-102 IN=102 OUT=110A 109
  BLOCK P-104 IN=110A OUT=110
  BLOCK SP-106 IN=106B OUT=108 107
  BLOCK E-101 IN=104 OUT=131
  BLOCK S-103 IN=131 OUT=132 134
  BLOCK TC-101 IN=132 OUT=133
  BLOCK P-103 IN=153 OUT=154
  BLOCK SP-134 IN=134 OUT=156 135A
  BLOCK MIX-134 IN=152 133 154 135B OUT=113
  BLOCK S-101 IN=114 OUT=112 115
  BLOCK TE-101 IN=111 OUT=1
  BLOCK SP-111 IN=1 OUT=120 121
  BLOCK S-104 IN=120 OUT=122 123
  BLOCK S-105 IN=121 OUT=125 124A
  BLOCK MIX-124 IN=123 124A OUT=124
  BLOCK MIX-127 IN=127 122 OUT=129
  BLOCK SP-109 IN=109 OUT=128A 130A
  BLOCK V-128 IN=128A OUT=128
  BLOCK MX-126 IN=107B 105B OUT=126
  BLOCK E-103 IN=105A OUT=105B
  BLOCK MIX-117 IN=136 117 OUT=117A
  BLOCK C-102 IN=125 119 OUT=140 138
  BLOCK V-130 IN=130A OUT=130
  BLOCK MIX-155 IN=130 139 OUT=155
  BLOCK TE-103 IN=103 OUT=139
  BLOCK P-107 IN=135A OUT=135B
  BLOCK C-104 IN=124 128 117B 126 101B 117C OUT=127 151
  BLOCK R-101 IN=113 OUT=114
  BLOCK C-103-R1 IN=155 C-103-2 C-103-3 OUT=C-103-4
  BLOCK C-103-R2 IN=140 118 C-103-5 OUT=C-103-1
  BLOCK C-103-S1 IN=C-103-4 OUT=136 137 C-103-5
  BLOCK C-103-S2 IN=C-103-1 OUT=C-103-2 C-103-3 141
  BLOCK MIX-152 IN=141 151 OUT=152
  BLOCK SP-112 IN=112 OUT=112A 112B
  BLOCK B2 IN=117A OUT=117B 117C

PROPERTIES ELECNRTL HENRY-COMPS=HC-1 CHEMISTRY=H2SO4-HI  &
      TRUE-COMPS=NO
  PROPERTIES NRTL-RK / STEAMNBS

PROP-REPLACE ELECNRTL ELECNRTL
  MODEL VL0CONS
```

```
PROP-DATA
   PROP-LIST ATOMNO / NOATOM
   PVAL H3O+ 1 8 / 3. 1.

PROP-DATA
   PROP-LIST ATOMNO / NOATOM
   PVAL HIX 1 53 8 / 3. 1.5 1.

PROP-DATA
   PROP-LIST ATOMNO / NOATOM
   PVAL SAIPAIR 1 16 8 / 2. 0.5 2.5

PROP-DATA H2S04-2
   IN-UNITS SI
   PROP-LIST DGAQFM
   PVAL HSO4- -7.55910E+08
   PVAL SO4-2 -7.44530E+08

PROP-DATA H2S04-2
   IN-UNITS SI MOLE-ENTHALP='kcal/mol'
   PROP-LIST DHAQFM
   PVAL HSO4- -207.8
   PVAL SO4-2 -217.17541

PROP-DATA H2SO4-1
   IN-UNITS SI
   PROP-LIST DHFORM / RKTZRA / DGFORM / TB
   PVAL H2SO4 -735130000 / 0.1936342 / -653470000 / 590.51
   PROP-LIST DHFORM / RKTZRA / TC / PC / VC / ZC /  &
      OMEGA / DGFORM / TB / MW
   PVAL SAIPAIR -510035701.8 / 0.25 / 925. / 17600000.0 /  &
      .240 / .20 / .46660 / -1.024420E+09 / 2573.916342 /  &
      58.04738
   PROP-LIST RKTZRA
   PVAL SO3 .24917730

PROP-DATA HI-PROPS
   IN-UNITS MET VOLUME-FLOW='cum/hr' ENTHALPY-FLO='MMkcal/hr'  &
      HEAT-TRANS-C='kcal/hr-sqm-K' PRESSURE=bar TEMPERATURE=K  &
      VOLUME=cum DELTA-T=C HEAD=meter MOLE-DENSITY='kmol/cum'  &
      MASS-DENSITY='kg/cum' MOLE-ENTHALP='kcal/mol'  &
      MASS-ENTHALP='kcal/kg' HEAT=MMkcal MOLE-CONC='mol/l'  &
      PDROP=bar
   PROP-LIST TC / PC / RKTZRA
   PVAL HI 423.85 / 83.1 / 0.31499751
```

```
PROP-DATA HIX
  IN-UNITS MET VOLUME-FLOW='cum/hr' ENTHALPY-FLO='MMkcal/hr'  &
    HEAT-TRANS-C='kcal/hr-sqm-K' PRESSURE=bar TEMPERATURE=C  &
    VOLUME=cum DELTA-T=C HEAD=meter MOLE-DENSITY='kmol/cum'  &
    MASS-DENSITY='kg/cum' MOLE-ENTHALP='kcal/mol'  &
    MASS-ENTHALP='kcal/kg' HEAT=MMkcal MOLE-CONC='mol/l'  &
    PDROP=bar
  PROP-LIST DHFORM
  PVAL HIX -60.585

PROP-DATA I-
  IN-UNITS MET VOLUME-FLOW='cum/hr' ENTHALPY-FLO='MMkcal/hr'  &
    HEAT-TRANS-C='kcal/hr-sqm-K' PRESSURE=bar TEMPERATURE=C  &
    VOLUME=cum DELTA-T=C HEAD=meter MOLE-DENSITY='kmol/cum'  &
    MASS-DENSITY='kg/cum' MOLE-ENTHALP='kcal/mol'  &
    MASS-ENTHALP='kcal/kg' HEAT=MMkcal MOLE-CONC='mol/l'  &
    PDROP=bar
  PROP-LIST DHAQFM
  PVAL I- -13.181905

PROP-DATA SO2-PUR
  IN-UNITS MET PRESSURE=torr TEMPERATURE=C DELTA-T=C  &
    MOLE-ENTHALP='kJ/kmol' PDROP=torr
  PROP-LIST OMEGA / DHFORM / DGFORM
  PVAL SO2 0.24511 / -297050 / -300590.81

PROP-DATA VLCONS
  IN-UNITS MET VOLUME-FLOW='cum/hr' ENTHALPY-FLO='MMkcal/hr'  &
    HEAT-TRANS-C='kcal/hr-sqm-K' PRESSURE=bar TEMPERATURE=C  &
    VOLUME=cum DELTA-T=C HEAD=meter MOLE-DENSITY='kmol/cum'  &
    MASS-DENSITY='kg/cum' MOLE-ENTHALP='kcal/mol'  &
    MASS-ENTHALP='kcal/kg' HEAT=MMkcal MOLE-CONC='mol/l'  &
    PDROP=bar
  PROP-LIST VLCONS
  PVAL H2O 19.63607
  PVAL H2SO4 65.7589
  PVAL SO3 44.2912
  PVAL SO2 43.8228
  PVAL CO2 35.0189
  PVAL N2 34.6723
  PVAL O2 28.0225
  PVAL AR 28.6156
  PVAL SAIPAIR 42.13265
  PVAL I2 68.081606
  PVAL HI 45.675239
```

```
  PVAL H2 28.612729

PROP-DATA VLSTD
  IN-UNITS MET VOLUME-FLOW='cum/hr' ENTHALPY-FLO='MMkcal/hr'  &
    HEAT-TRANS-C='kcal/hr-sqm-K' PRESSURE=bar TEMPERATURE=C  &
    VOLUME=cum DELTA-T=C HEAD=meter MOLE-DENSITY='kmol/cum'  &
    MASS-DENSITY='kg/cum' MOLE-ENTHALP='kcal/mol'  &
    MASS-ENTHALP='kcal/kg' HEAT=MMkcal MOLE-CONC='mol/l'  &
    PDROP=bar
  PROP-LIST VLSTD
  PVAL H3O+ 100
  PVAL HSO4- 100
  PVAL SO4-2 100
  PVAL I- 100

PROP-DATA CPAQ0-1
  IN-UNITS MET VOLUME-FLOW='cum/hr' ENTHALPY-FLO='MMkcal/hr'  &
    MOLE-HEAT-CA='J/kmol-K' HEAT-TRANS-C='kcal/hr-sqm-K'  &
    PRESSURE=bar TEMPERATURE=K VOLUME=cum DELTA-T=C  &
    HEAD=meter MOLE-DENSITY='kmol/cum' MASS-DENSITY='kg/cum'  &
    MOLE-ENTHALP='kcal/mol' MASS-ENTHALP='kcal/kg' HEAT=MMkcal  &
    MOLE-CONC='mol/l' PDROP=bar
  PROP-LIST CPAQ0
  PVAL HSO4- -1588028.5 7970.75904 -10.997292
  PVAL SO4-2 -293000.0
  PVAL I- -401345.64 67.4256945 0 0 0 0 0 2000

PROP-DATA CPDIEC-1
  IN-UNITS MET VOLUME-FLOW='cum/hr' ENTHALPY-FLO='MMkcal/hr'  &
    HEAT-TRANS-C='kcal/hr-sqm-K' PRESSURE=bar TEMPERATURE=C  &
    VOLUME=cum DELTA-T=C HEAD=meter MOLE-DENSITY='kmol/cum'  &
    MASS-DENSITY='kg/cum' MOLE-ENTHALP='kcal/mol'  &
    MASS-ENTHALP='kcal/kg' HEAT=MMkcal MOLE-CONC='mol/l'  &
    PDROP=bar
  PROP-LIST CPDIEC
  PVAL H2SO4 101 0 298.15
  PVAL SO3 2 0 298.15
  PVAL HI 5.01 0 298.15
  PVAL I2 59.0736361 31989.38 298.15
  PVAL HIX 59.0736361 31989.38 298.15

PROP-DATA CPIG-1
  IN-UNITS SI
  PROP-LIST CPIG
  PVAL H2SO4 13511.530 231.2640 .1720030 -.0008403250  &
    .0000006328290 0.0 0.0 2000.0 20800.0 0.0 1.0
```

```
PROP-DATA CPIG-1
   IN-UNITS SI MOLE-HEAT-CA='cal/mol-K'
   PROP-LIST CPIG
   PVAL O2 7.13482399 -2.68379765E-03 1.02868233E-05  &
      -8.78879899E-09 2.40152413E-12 0 100 1500 7.13482399  &
      -2.68379765E-03 1.0
   PVAL N2 7.144511 -1.741872E-03 4.305735E-06 -2.233520E-09  &
      3.210279E-13 0 223.15 1473.15 7.144511 -1.741872E-03  &
      1.0

PROP-DATA CPIGDP-1
   IN-UNITS MET PRESSURE=torr TEMPERATURE=K DELTA-T=C  &
      PDROP=torr
   PROP-LIST CPIGDP
   PVAL SO3 10.19959828 13.26622531 1682.83741 11.72823786  &
      758.8417648 273.15 1273.15
   PVAL CO2 7.221512359 7.666971279 1308.635376 5.247592522  &
      580.9717756 220 1100
   PVAL HIX 35.05246698 1901.199985 1847.059597 476.4006902  &
      2000 50 1200

PROP-DATA CPIGDP-1
   IN-UNITS MET PRESSURE=torr TEMPERATURE=C DELTA-T=C  &
      PDROP=torr
   PROP-LIST CPIGDP
   PVAL SO2 8.446786448 5.44747727 1091.383023 2.980809212  &
      582.8526095 273.15 1773.15

PROP-DATA DHVLDP-1
   IN-UNITS SI
   PROP-LIST DHVLDP
   PVAL SO3 1.1E8 0.51119681 1.65460533 -1.4727676 0 250  &
      1000

PROP-DATA DHVLWT-1
   IN-UNITS SI
   PROP-LIST DHVLWT
   PVAL H2SO4 79050000.0 298.150 .3502 0.1565 2.0
   PVAL SAIPAIR 60836600 298.150 .38 0 2.0
   PVAL HIX 1 298.15 .38 0 2

PROP-DATA IONMUB-1
   IN-UNITS MET ENTHALPY-FLO='kcal/hr' PRESSURE=torr  &
      TEMPERATURE=K DELTA-T=C MOLE-VOLUME='cum/kmol'  &
      ELEC-POWER=Watt PDROP=torr
```

```
   PROP-LIST IONMUB
   PVAL HSO4- 0.01597359 0.00023995

PROP-DATA MULDIP-1
   IN-UNITS MET ENTHALPY-FLO='kcal/hr' PRESSURE=torr  &
      TEMPERATURE=K VISCOSITY='N-sec/sqm' DELTA-T=C  &
      ELEC-POWER=Watt PDROP=torr
   PROP-LIST MULDIP
   PVAL H2SO4 -112.96105 7497.04869 14.7608891 0 0 273.15  &
      500
   PVAL SO3 -150.66701 9073.65901 20 0 0 273 400

PROP-DATA PLXANT-1
   IN-UNITS MET VOLUME-FLOW='cum/hr' ENTHALPY-FLO='MMkcal/hr'  &
      HEAT-TRANS-C='kcal/hr-sqm-K' PRESSURE='N/sqm' TEMPERATURE=K  &
      VOLUME=cum DELTA-T=C HEAD=meter MOLE-DENSITY='kmol/cum'  &
      MASS-DENSITY='kg/cum' MOLE-ENTHALP='kcal/mol'  &
      MASS-ENTHALP='kcal/kg' HEAT=MMkcal MOLE-CONC='mol/l'  &
      PDROP=bar
   PROP-LIST PLXANT
   PVAL H2O 72.550 -7206.70 0.0 0.0 -7.13850 .0000040460  &
      2.0 273.160 647.290
   PVAL H2SO4 37.60588121 -11216.33992 0 -0.011998736 0 0 2  &
      273.15 700
   PVAL SAIPAIR 14.72992607 -8246.41 0 0.0 0 0 2 273.15  &
      3000

PROP-DATA PLXANT-1
   IN-UNITS MET VOLUME-FLOW='cum/hr' ENTHALPY-FLO='MMkcal/hr'  &
      HEAT-TRANS-C='kcal/hr-sqm-K' PRESSURE=bar TEMPERATURE=K  &
      VOLUME=cum DELTA-T=C HEAD=meter MOLE-DENSITY='kmol/cum'  &
      MASS-DENSITY='kg/cum' MOLE-ENTHALP='kcal/mol'  &
      MASS-ENTHALP='kcal/kg' HEAT=MMkcal MOLE-CONC='mol/l'  &
      PDROP=bar
   PROP-LIST PLXANT
   PVAL HI 96.04852687 -4602.079856 0 0.024745309  &
      -15.08465485 0 2 237.6 573

PROP-DATA PLXANT-1
   IN-UNITS MET VOLUME-FLOW='cum/hr' ENTHALPY-FLO='MMkcal/hr'  &
      HEAT-TRANS-C='kcal/hr-sqm-K' PRESSURE=bar TEMPERATURE=C  &
      VOLUME=cum DELTA-T=C HEAD=meter MOLE-DENSITY='kmol/cum'  &
      MASS-DENSITY='kg/cum' MOLE-ENTHALP='kcal/mol'  &
      MASS-ENTHALP='kcal/kg' HEAT=MMkcal MOLE-CONC='mol/l'  &
      PDROP=bar
   PROP-LIST PLXANT
```

```
   PVAL I2 107.768055 -9387.6354 0 0.01240622 -15.167451  &
      1.1981E-19 6 113.65 545.85

;INSERT 1 MH2SO4 H2O H2SO4
;  CVAL DHFORM  1 1 -.735D9
;  CVAL DHFORM 1 1  -1.13085D9

PROP-DATA HENRY-1
   IN-UNITS MET VOLUME-FLOW='cum/hr' ENTHALPY-FLO='MMkcal/hr'  &
      HEAT-TRANS-C='kcal/hr-sqm-K' PRESSURE='N/sqm' TEMPERATURE=K  &
      VOLUME=cum DELTA-T=C HEAD=meter MOLE-DENSITY='kmol/cum'  &
      MASS-DENSITY='kg/cum' MOLE-ENTHALP='kcal/mol'  &
      MASS-ENTHALP='kcal/kg' HEAT=MMkcal MOLE-CONC='mol/l'  &
      PDROP=bar
   PROP-LIST HENRY
   BPVAL SO2 SO3 83.96060 -5578.80 -8.761520 0.0 273.0 373.0
   BPVAL SO2 H2SO4 83.96060 -5578.80 -8.761520 0.0 273.0  &
      373.0
   BPVAL CO2 SO3 170.71260 -8477.7110 -21.957430 .0057807480  &
      273.0 500.0
   BPVAL CO2 H2SO4 170.71260 -8477.7110 -21.957430 .0057807480  &
      273.0 500.0
   BPVAL N2 SO3 176.5070 -8432.770 -21.5580 -.008436240 273.0  &
      346.0
   BPVAL N2 H2SO4 176.5070 -8432.770 -21.5580 -.008436240  &
      273.0 346.0
   BPVAL O2 SO3 155.9210 -7775.060 -18.39740 -.009443540  &
      274.0 348.0
   BPVAL O2 H2SO4 155.9210 -7775.060 -18.39740 -.009443540  &
      274.0 348.0
   BPVAL SO2 H2O 26.56470 -2872.960 -.302880 0.0 283.0 386.0
   BPVAL CO2 H2O 171.3780 -8741.550 -21.6690 .001102590 273.0  &
      353.0
   BPVAL N2 H2O 176.5070 -8432.770 -21.5580 -.008436240 273.0  &
      346.0
   BPVAL O2 H2O 155.9210 -7775.060 -18.39740 -.009443540  &
      274.0 348.0
   BPVAL AR H2O 180.9910000 -8137.130000 -23.25470000  &
      3.06357000E-3 274.0000000 347.0000000
   BPVAL AR H2SO4 180.9910000 -8137.130000 -23.25470000  &
      3.06357000E-3 274.0000000 347.0000000

PROP-DATA HENRY-1
   IN-UNITS MET VOLUME-FLOW='cum/hr' ENTHALPY-FLO='MMkcal/hr'  &
      HEAT-TRANS-C='kcal/hr-sqm-K' PRESSURE=bar TEMPERATURE=C  &
      VOLUME=cum DELTA-T=C HEAD=meter MOLE-DENSITY='kmol/cum'  &
```

```
      MASS-DENSITY='kg/cum' MOLE-ENTHALP='kcal/mol'  &
      MASS-ENTHALP='kcal/kg' HEAT=MMkcal MOLE-CONC='mol/l'  &
      PDROP=bar
   PROP-LIST HENRY
   BPVAL H2 H2O 180.0660745 -6993.510000 -26.31190000  &
      .0150431000 .8500000000 65.85000000
   BPVAL H2 I2 180.0660745 -6993.510000 -26.31190000  &
      .0150431000 .8500000000 65.85000000
   BPVAL H2 HI 177.0660745 -6993.510000 -26.31190000  &
      .0150431000 .8500000000 65.85000000

PROP-DATA NRTL-1
   IN-UNITS MET VOLUME-FLOW='cum/hr' ENTHALPY-FLO='MMkcal/hr'  &
      HEAT-TRANS-C='kcal/hr-sqm-K' PRESSURE=bar TEMPERATURE=K  &
      VOLUME=cum DELTA-T=C HEAD=meter MOLE-DENSITY='kmol/cum'  &
      MASS-DENSITY='kg/cum' MOLE-ENTHALP='kcal/mol'  &
      MASS-ENTHALP='kcal/kg' HEAT=MMkcal MOLE-CONC='mol/l'  &
      PDROP=bar
   PROP-LIST NRTL
   BPVAL H2O CO2 10.0640 -3268.1350 .20 0.0 0.0 0.0 273.150  &
      473.150
   BPVAL CO2 H2O 10.0640 -3268.1350 .20 0.0 0.0 0.0 273.150  &
      473.150
   BPVAL SO3 H2SO4 5.83914569 -614.29263 .2000000 0.0 0.0  &
      0.0 0.0 1000.000
   BPVAL H2SO4 SO3 0.0 0.0 .2000000 0.0 0.0 0.0 0.0  &
      1000.000
   BPVAL H2O H2SO4 0 0.0 .200000 0.0 0.0 0.0 0.0 1000.000
   BPVAL H2SO4 H2O 0 0.0 .200000 0.0 0.0 0.0 0.0 1000.000
   BPVAL SAIPAIR H2SO4 0 -1550.1937 .200000 0.0 0.0 0.0 0.0  &
      1000.000
   BPVAL H2SO4 SAIPAIR 0 969.798206 .200000 0.0 0.0 0.0 0.0  &
      1000.000
   BPVAL SAIPAIR H2O 0 813.139247 .200000 0.0 0.0 0.0 0.0  &
      1000.000
   BPVAL H2O SAIPAIR 0 -2470.0714 .200000 0.0 0.0 0.0 0.0  &
      1000.000
   BPVAL SAIPAIR SO3 0 0.0 .200000 0.0 0.0 0.0 0.0  &
      1000.000
   BPVAL SO3 SAIPAIR 0 0.0 .200000 0.0 0.0 0.0 0.0  &
      1000.000
   BPVAL I2 H2O -8.0628127 3942.57202 0.3 0 0 0.00336012 0  &
      1000
   BPVAL H2O I2 23.6689347 -1492.3546 0.3 0 0 -0.0347553 0  &
      1000
   BPVAL I2 HI 0.0 223 .200000 0.0 0.0 0.0 0.0 1000.000
```

```
   BPVAL HI I2 0.0 223 .200000 0.0 0.0 0.0 0.0 1000.000
   BPVAL HI H2O 0.0 -84 .2 0.0 0.0 0.0 0.0 1000.000
   BPVAL H2O HI 0.0 1380 .2 0.0 0.0 0.0 0.0 1000.000
   BPVAL HIX H2O -4.974829 0 0.30 0 0 0 0 1000
   BPVAL H2O HIX 3.76556829 0 0.30 0 0 0 0 1000
   BPVAL HIX H2SO4 0 0.0 .30 0.0 0.0 0.0 0.0 1000.000
   BPVAL H2SO4 HIX 0 0.0 .30 0.0 0.0 0.0 0.0 1000.000
   BPVAL HIX I2 -2.4516656 0 .30 0.0 0.0 0.0 0.0 1000.000
   BPVAL I2 HIX 24.8287072 0 .30 0.0 0.0 0.0 0.0 1000.000
   BPVAL I2 H2SO4 9.137883 0 .30 0.0 0.0 0.0 0.0 1000.000
   BPVAL H2SO4 I2 3.16529775 0 .30 0.0 0.0 0.0 0.0  &
      1000.000

PROP-DATA VLCLK-1
   IN-UNITS MET VOLUME-FLOW='cum/hr' ENTHALPY-FLO='MMkcal/hr'  &
      HEAT-TRANS-C='kcal/hr-sqm-K' PRESSURE=bar TEMPERATURE=C  &
      VOLUME=cum DELTA-T=C HEAD=meter MOLE-DENSITY='kmol/cum'  &
      MASS-DENSITY='kg/cum' MOLE-ENTHALP='kcal/mol'  &
      MASS-ENTHALP='kcal/kg' MOLE-VOLUME='cum/kmol' HEAT=MMkcal  &
      MOLE-CONC='mol/l' PDROP=bar
   PROP-LIST VLCLK
   BPVAL H3O+ HSO4- 0.05452132 0.01993186

PROP-DATA GMELCC-1
   IN-UNITS MET VOLUME-FLOW='cum/hr' ENTHALPY-FLO='MMkcal/hr'  &
      HEAT-TRANS-C='kcal/hr-sqm-K' PRESSURE=bar TEMPERATURE=C  &
      VOLUME=cum DELTA-T=C HEAD=meter MOLE-DENSITY='kmol/cum'  &
      MASS-DENSITY='kg/cum' MOLE-ENTHALP='kcal/mol'  &
      MASS-ENTHALP='kcal/kg' HEAT=MMkcal MOLE-CONC='mol/l'  &
      PDROP=bar
   PROP-LIST GMELCC
   PPVAL H2O ( H3O+ HSO4- ) 3.4616695
   PPVAL ( H3O+ HSO4- ) H2O -3.9843446
   PPVAL H2SO4 ( H3O+ HSO4- ) -2.0423396
   PPVAL ( H3O+ HSO4- ) H2SO4 -2.3745922
   PPVAL H2O ( H3O+ SO4-2 ) 8
   PPVAL ( H3O+ SO4-2 ) H2O -4
   PPVAL H2SO4 ( H3O+ SO4-2 ) 8
   PPVAL ( H3O+ SO4-2 ) H2SO4 -4
   PPVAL SO3 ( H3O+ HSO4- ) 8
   PPVAL ( H3O+ HSO4- ) SO3 -4
   PPVAL SO3 ( H3O+ SO4-2 ) 8
   PPVAL ( H3O+ SO4-2 ) SO3 -4
   PPVAL SO2 ( H3O+ HSO4- ) 2.22
   PPVAL ( H3O+ HSO4- ) SO2 -0.32
   PPVAL CO2 ( H3O+ HSO4- ) 2.22
```

```
   PPVAL ( H3O+ HSO4- ) CO2 -0.32
   PPVAL N2 ( H3O+ HSO4- ) 2.22
   PPVAL ( H3O+ HSO4- ) N2 -0.32
   PPVAL O2 ( H3O+ HSO4- ) 2.22
   PPVAL ( H3O+ HSO4- ) O2 -0.32
   PPVAL AR ( H3O+ HSO4- ) 2.22
   PPVAL ( H3O+ HSO4- ) AR -0.32
   PPVAL H2O ( H3O+ I- ) 1.83749491
   PPVAL ( H3O+ I- ) H2O -1.9033674
   PPVAL HI ( H3O+ I- ) 3.96750955
   PPVAL ( H3O+ I- ) HI 4.60780554
   PPVAL I2 ( H3O+ I- ) 3.1136453
   PPVAL ( H3O+ I- ) I2 20
   PPVAL I2 ( H3O+ HSO4- ) 8.1580071
   PPVAL ( H3O+ HSO4- ) I2 5.23308504
   PPVAL HI ( H3O+ HSO4- ) 7.53966142
   PPVAL ( H3O+ HSO4- ) HI -11.850752
   PPVAL HIX ( H3O+ HSO4- ) 1.00588251
   PPVAL ( H3O+ HSO4- ) HIX 0.54890791

PROP-DATA GMELCD-1
   IN-UNITS MET VOLUME-FLOW='cum/hr' ENTHALPY-FLO='MMkcal/hr'  &
      HEAT-TRANS-C='kcal/hr-sqm-K' PRESSURE=bar TEMPERATURE=K  &
      VOLUME=cum DELTA-T=C HEAD=meter MOLE-DENSITY='kmol/cum'  &
      MASS-DENSITY='kg/cum' MOLE-ENTHALP='kcal/mol'  &
      MASS-ENTHALP='kcal/kg' HEAT=MMkcal MOLE-CONC='mol/l'  &
      PDROP=bar
   PROP-LIST GMELCD
   PPVAL H2O ( H3O+ HSO4- ) 2412.88399
   PPVAL ( H3O+ HSO4- ) H2O -511.40017
   PPVAL H2SO4 ( H3O+ HSO4- ) 18.4880871
   PPVAL ( H3O+ HSO4- ) H2SO4 2171.05384
   PPVAL H2O ( H3O+ SO4-2 ) 0
   PPVAL ( H3O+ SO4-2 ) H2O 0
   PPVAL H2SO4 ( H3O+ SO4-2 ) 0
   PPVAL ( H3O+ SO4-2 ) H2SO4 0
   PPVAL ( H3O+ HSO4- ) SO3 0
   PPVAL SO3 ( H3O+ HSO4- ) 0
   PPVAL H2O ( H3O+ I- ) 2259.33865
   PPVAL ( H3O+ I- ) H2O -733.80589
   PPVAL I2 ( H3O+ I- ) -2274.142
   PPVAL ( H3O+ I- ) I2 0

PROP-DATA GMELCE-1
   IN-UNITS MET VOLUME-FLOW='cum/hr' ENTHALPY-FLO='MMkcal/hr'  &
      HEAT-TRANS-C='kcal/hr-sqm-K' PRESSURE=bar TEMPERATURE=C  &
```

```
      VOLUME=cum DELTA-T=C HEAD=meter MOLE-DENSITY='kmol/cum'  &
      MASS-DENSITY='kg/cum' MOLE-ENTHALP='kcal/mol'  &
      MASS-ENTHALP='kcal/kg' HEAT=MMkcal MOLE-CONC='mol/l'  &
      PDROP=bar
   PROP-LIST GMELCE
   PPVAL H2O ( H3O+ HSO4- ) 3.09312155
   PPVAL ( H3O+ HSO4- ) H2O 2.21471832
   PPVAL H2SO4 ( H3O+ HSO4- ) 4.84108255
   PPVAL ( H3O+ HSO4- ) H2SO4 -6.2328899
   PPVAL H2O ( H3O+ SO4-2 ) 0
   PPVAL ( H3O+ SO4-2 ) H2O 0
   PPVAL H2SO4 ( H3O+ SO4-2 ) 0
   PPVAL ( H3O+ SO4-2 ) H2SO4 0
   PPVAL H2O ( H3O+ I- ) 10.8191447
   PPVAL ( H3O+ I- ) H2O -0.8738634

PROP-DATA GMELCN-1
   IN-UNITS MET VOLUME-FLOW='cum/hr' ENTHALPY-FLO='MMkcal/hr'  &
      HEAT-TRANS-C='kcal/hr-sqm-K' PRESSURE=bar TEMPERATURE=C  &
      VOLUME=cum DELTA-T=C HEAD=meter MOLE-DENSITY='kmol/cum'  &
      MASS-DENSITY='kg/cum' MOLE-ENTHALP='kcal/mol'  &
      MASS-ENTHALP='kcal/kg' HEAT=MMkcal MOLE-CONC='mol/l'  &
      PDROP=bar
   PROP-LIST GMELCN
   PPVAL H2O ( H3O+ HSO4- ) .20
   PPVAL ( H3O+ HSO4- ) H2O .20
   PPVAL H2SO4 ( H3O+ HSO4- ) .20
   PPVAL ( H3O+ HSO4- ) H2SO4 .20
   PPVAL H2O ( H3O+ SO4-2 ) .20
   PPVAL ( H3O+ SO4-2 ) H2O .20
   PPVAL H2SO4 ( H3O+ SO4-2 ) .20
   PPVAL ( H3O+ SO4-2 ) H2SO4 .20
   PPVAL SO2 ( H3O+ HSO4- ) .2
   PPVAL ( H3O+ HSO4- ) SO2 .2
   PPVAL H2O ( H3O+ I- ) .32
   PPVAL I2 ( H3O+ I- ) .32
   PPVAL HI ( H3O+ I- ) .32
   PPVAL HI ( H3O+ HSO4- ) .32
   PPVAL I2 ( H3O+ HSO4- ) .32
   PPVAL HIX ( H3O+ HSO4- ) .32

STREAM 101A
   SUBSTREAM MIXED TEMP=298. <K> PRES=0.101
   MOLE-FLOW H2O 0.458

STREAM 101B
```

```
   SUBSTREAM MIXED TEMP=298. <K> PRES=0.101
   MOLE-FLOW H2O 0.4144

STREAM 102
   SUBSTREAM MIXED TEMP=393. <K> PRES=0.185
   MOLE-FLOW H2O 0.1327 / I2 12.1686

STREAM 103
   SUBSTREAM MIXED TEMP=360. <K> PRES=5.066
   MOLE-FLOW H2O 0.002 / I2 1.001

STREAM 104
   SUBSTREAM MIXED TEMP=418. <K> PRES=0.2
   MOLE-FLOW H2O 0.4257 / SO2 1.0129 / O2 0.5

STREAM 105A
   SUBSTREAM MIXED TEMP=422. <K> PRES=0.502
   MOLE-FLOW H2O 4.7446

STREAM 106A
   SUBSTREAM MIXED TEMP=368. <K> PRES=0.45
   MOLE-FLOW H2O 10.7178

STREAM 107B
   SUBSTREAM MIXED TEMP=359.6 <K> PRES=0.42
   MOLE-FLOW H2O 2.8448

STREAM 112A
   SUBSTREAM MIXED TEMP=393. <K> PRES=0.44
   MOLE-FLOW H2O 0.1951 / SO2 0.1963 / I2 0.0154 / O2  &
      0.5

STREAM 113
   SUBSTREAM MIXED TEMP=358.346198 <K> PRES=0.101
   MOLE-FLOW H2O 16.3292658 / H2SO4 0.350677152 / SO2  &
      1.02068478 / HI 0.843455781 / I2 12.7363291 / O2  &
      0.501321312

STREAM 136
   SUBSTREAM MIXED TEMP=393. <K> PRES=0.105
   MOLE-FLOW H2O 0.1568 / SO2 0.0391 / I2 0.0133 / O2  &
      0.0501

STREAM 152
   SUBSTREAM MIXED TEMP=373. <K> PRES=0.5
   MOLE-FLOW H2O 8.8578 / H2SO4 0.218 / HI 0.5828 / I2  &
```

```
      9.5748

STREAM C-103-4
   SUBSTREAM MIXED TEMP=385. <K> PRES=0.105
   MOLE-FLOW H2O 4.3423 / H2SO4 1.006 / SO2 0.04301 / HI  &
      0.14 / I2 6.6177 / O2 0.0501

STREAM C-103-5
   SUBSTREAM MIXED TEMP=360 <K> PRES=0.105
   MOLE-FLOW H2O 0.0135607961 / H2SO4 9.535841E-006 / SO2  &
      0.00127354491 / HI 6.756290E-006 / I2 6.56837432 /  &
      O2 7.935692E-005

BLOCK MIX-117 MIXER
   PARAM T-EST=360. <K>
   PROPERTIES NRTL-RK HENRY-COMPS=HC-1

BLOCK MIX-124 MIXER
   PARAM T-EST=300. <K>
   PROPERTIES NRTL-RK

BLOCK MIX-127 MIXER
   PROPERTIES NRTL-RK HENRY-COMPS=HC-1

BLOCK MIX-134 MIXER

BLOCK MIX-152 MIXER

BLOCK MIX-155 MIXER
   PROPERTIES NRTL-RK HENRY-COMPS=HC-1

BLOCK MX-126 MIXER

BLOCK B2 FSPLIT
   FRAC 117C 0.1
   PROPERTIES NRTL-RK HENRY-COMPS=HC-1

BLOCK SP-102 FSPLIT
   FRAC 109 0.725826
   PROPERTIES NRTL-RK HENRY-COMPS=HC-1

BLOCK SP-106 FSPLIT
   FRAC 107 0.232137

BLOCK SP-109 FSPLIT
   FRAC 128A 0.366
```

```
   PROPERTIES NRTL-RK HENRY-COMPS=HC-1

BLOCK SP-111 FSPLIT
   FRAC 121 0.5
   PROPERTIES NRTL-RK HENRY-COMPS=HC-1

BLOCK SP-112 FSPLIT
   FRAC 112B 0.15
   PROPERTIES NRTL-RK

BLOCK SP-134 FSPLIT
   PARAM NPHASE=1 PHASE=L
   FRAC 156 0.0287
   BLOCK-OPTION FREE-WATER=NO

BLOCK E-101 HEATER
   PARAM TEMP=313. <K> PRES=0.195

BLOCK E-102 HEATER
   PARAM TEMP=359.6 <K> PRES=-0.03

BLOCK E-103 HEATER
   PARAM TEMP=359.6 <K> PRES=0.101

BLOCK TE-103 HEATER
   PARAM TEMP=393. <K> PRES=0.105

BLOCK S-101 FLASH2
   PARAM TEMP=393. <K> PRES=0. NPHASE=3 MAXIT=250 TOL=0.0001
   BLOCK-OPTION FREE-WATER=NO

BLOCK S-103 FLASH2
   PARAM PRES=0. DUTY=0.

BLOCK S-104 FLASH2
   PARAM PRES=0. DUTY=0.
   PROPERTIES NRTL-RK HENRY-COMPS=HC-1

BLOCK S-105 FLASH2
   PARAM PRES=0. DUTY=0.
   PROPERTIES NRTL-RK

BLOCK C-103-S1 FLASH3
   PARAM TEMP=350. <K> PRES=0.105 L2-COMP=I2 MAXIT=150  &
      TOL=1E-005
```

```
BLOCK C-103-S2 FLASH3
   PARAM TEMP=350. <K> PRES=0.105 L2-COMP=I2 MAXIT=150  &
      TOL=1E-005

BLOCK S-102 FLASH3
   IN-UNITS MET VOLUME-FLOW='cum/hr' ENTHALPY-FLO='MMkcal/hr'  &
      HEAT-TRANS-C='kcal/hr-sqm-K' PRESSURE=bar TEMPERATURE=C  &
      VOLUME=cum DELTA-T=C HEAD=meter MOLE-DENSITY='kmol/cum'  &
      MASS-DENSITY='kg/cum' MOLE-ENTHALP='kcal/mol'  &
      MASS-ENTHALP='kcal/kg' HEAT=MMkcal MOLE-CONC='mol/l'  &
      PDROP=bar
   PARAM TEMP=360. <K> PRES=0.11 <MPa> L2-COMP=I2 MAXIT=250  &
      TOL=1E-005

BLOCK C-101 RADFRAC
   PARAM NSTAGE=10 ALGORITHM=NONIDEAL INIT-OPTION=STANDARD  &
      MAXOL=50 CMAXNI0=10. LL-METH=EQ-SOLVE L2-GAMMA=MARGULES  &
      NPHASE=3 DAMPING=MILD
   COL-CONFIG CONDENSER=NONE REBOILER=NONE
   FEEDS 101AA 1 ON-STAGE / 108 1 ON-STAGE / 110 5  &
      ON-STAGE / 112A 10 ON-STAGE / 112B 3 ON-STAGE
   PRODUCTS 111 1 V / 153 10 L
   P-SPEC 1 0.42
   COL-SPECS
   L2-COMPS I2
   L2-STAGES 1 10
   REAC-STAGES 1 10 ACIDP-CR
   RES-TIME 1 10 LTIME=10. <sec>
   T-EST 1 335. <K> / 2 370. <K>
   BLOCK-OPTION FREE-WATER=NO

BLOCK C-102 RADFRAC
   PARAM NSTAGE=10 ALGORITHM=NONIDEAL INIT-OPTION=STANDARD  &
      NPHASE=3 DAMPING=SEVERE
   COL-CONFIG CONDENSER=NONE REBOILER=NONE
   FEEDS 125 10 ON-STAGE / 119 1 ON-STAGE
   PRODUCTS 138 10 L / 140 1 V
   P-SPEC 1 0.101
   COL-SPECS
   L2-COMPS I2
   L2-STAGES 1 10
   T-EST 1 340. <K> / 10 340. <K>
   BLOCK-OPTION FREE-WATER=NO

BLOCK C-104 RADFRAC
   PARAM NSTAGE=10 ALGORITHM=NONIDEAL INIT-OPTION=STANDARD  &
```

```
   NPHASE=3
COL-CONFIG CONDENSER=NONE REBOILER=NONE
FEEDS 124 1 ON-STAGE / 128 5 ON-STAGE / 117B 10  &
   ON-STAGE / 126 1 ON-STAGE / 101B 1 ON-STAGE / 117C  &
   3 ON-STAGE
PRODUCTS 151 10 L / 127 1 V
P-SPEC 1 0.101
COL-SPECS
L2-COMPS I2
L2-STAGES 1 10
REAC-STAGES 1 10 ACIDP-CR
RES-TIME 1 10 LTIME=10. <sec>
T-EST 1 368.8 <K> / 2 369.3 <K> / 3 369.3 <K> / 4  &
   369.3 <K> / 5 369.3 <K> / 6 369. <K> / 7 368.9 <K> /  &
   8 368.9 <K> / 9 368.9 <K> / 10 364.7 <K>
L-EST 1 8.21 / 2 8.218 / 3 8.218 / 4 8.218 / 5  &
   11.35 / 6 11.34 / 7 11.34 / 8 11.34 / 9 11.34 /  &
   10 10.87
V-EST 1 0.6459 / 2 0.8299 / 3 0.8377 / 4 0.838 / 5  &
   0.838 / 6 0.6975 / 7 0.6899 / 8 0.6894 / 9  &
   0.6893 / 10 0.6919
X-EST 1 H2O 0.99843 / 1 H2SO4 5.2852E-024 / 1 I2  &
   0.0015695 / 1 O2 1.1602E-006 / 2 H2O 0.99836 / 2  &
   I2 0.0016342 / 2 O2 9.0123E-007 / 3 H2O 0.99836 /  &
   3 H2SO4 1.1852E-025 / 3 I2 0.0016363 / 3 O2  &
   8.9281E-007 / 3 HI 1.2401E-025 / 4 H2O 0.99836 / 4  &
   H2SO4 2.1302E-025 / 4 I2 0.0016363 / 4 O2  &
   8.9254E-007 / 5 H2O 0.71476 / 5 H2SO4 1.6466E-025 /  &
   5 I2 0.28523 / 5 O2 9.2644E-007 / 6 H2O 0.71462 /  &
   6 H2SO4 2.366E-025 / 6 I2 0.28538 / 6 O2  &
   1.1134E-006 / 7 H2O 0.71461 / 7 H2SO4 3.9291E-025 /  &
   7 I2 0.28539 / 7 O2 1.1258E-006 / 8 H2O 0.71461 /  &
   8 H2SO4 1.2757E-024 / 8 I2 0.28539 / 8 O2  &
   1.1267E-006 / 9 H2O 0.71477 / 9 H2SO4 4.8082E-015 /  &
   9 I2 0.28523 / 9 O2 1.1267E-006 / 9 HI 7.1159E-016 / &
   10 H2O 0.69688 / 10 H2SO4 0.0041563 / 10 I2  &
   0.29064 / 10 O2 4.5394E-006 / 10 HI 0.0083126
Y-EST 1 H2O 0.85744 / 1 I2 0.064065 / 1 O2 0.078496 /  &
   1 SO2 8.9869E-025 / 2 H2O 0.8736 / 2 I2 0.065377 /  &
   2 O2 0.061019 / 2 SO2 8.4479E-024 / 3 H2O 0.87413 /  &
   3 I2 0.06542 / 3 O2 0.06045 / 4 H2O 0.87415 / 4  &
   I2 0.065421 / 4 O2 0.060432 / 4 SO2 6.1264E-025 /  &
   5 H2O 0.87415 / 5 I2 0.065421 / 5 O2 0.060431 /  &
   6 H2O 0.86289 / 6 I2 0.064507 / 6 O2 0.072603 /  &
   6 SO2 1.3283E-025 / 7 H2O 0.86214 / 7 I2 0.064447 /  &
   7 O2 0.073409 / 8 H2O 0.86209 / 8 I2 0.064443 /  &
```

```
      8 O2 0.073464 / 9 H2O 0.86209 / 9 I2 0.064443 /  &
      9 O2 0.073467 / 9 SO2 7.5189E-025 / 10 H2O 0.8642 /  &
      10 H2SO4 7.8806E-014 / 10 I2 0.062609 / 10 O2  &
      0.073196 / 10 HI 1.1663E-014 / 10 SO2 1.8195E-025
   BLOCK-OPTION FREE-WATER=NO

BLOCK C-103-R1 RCSTR
   PARAM VOL=1. <cum> TEMP=350. <K> PRES=0.105 NPHASE=1  &
      PHASE=L
   BLOCK-OPTION FREE-WATER=NO
   REACTIONS RXN-IDS=BUNSEN

BLOCK C-103-R2 RCSTR
   PARAM VOL=1. <cum> TEMP=350. <K> PRES=0.105 NPHASE=1  &
      PHASE=L
   BLOCK-OPTION FREE-WATER=NO
   REACTIONS RXN-IDS=BUNSEN

BLOCK R-101 RCSTR
   PARAM VOL=1. <cum> TEMP=393. <K> PRES=0.44 NPHASE=1 PHASE=L
   BLOCK-OPTION FREE-WATER=NO
   REACTIONS RXN-IDS=BUNSEN

BLOCK P-101 PUMP
   PARAM PRES=0.45

BLOCK P-103 PUMP
   PARAM PRES=0.5

BLOCK P-104 PUMP
   PARAM PRES=0.45
   PROPERTIES NRTL-RK HENRY-COMPS=HC-1

BLOCK P-107 PUMP
   PARAM PRES=0.5

BLOCK TC-101 COMPR
   PARAM TYPE=ISENTROPIC PRES=0.5

BLOCK TE-101 COMPR
   PARAM TYPE=ISENTROPIC PRES=0.101 NPHASE=2 MAXIT=100  &
      TOL=1E-005
   PROPERTIES NRTL-RK HENRY-COMPS=HC-1
   BLOCK-OPTION FREE-WATER=NO

BLOCK V-128 VALVE
```

```
   PARAM P-OUT=0.101
   PROPERTIES NRTL-RK HENRY-COMPS=HC-1

BLOCK V-130 VALVE
   PARAM P-OUT=0.105
   PROPERTIES NRTL-RK

EO-CONV-OPTI

CONV-OPTIONS
   PARAM CHECKSEQ=NO

STREAM-REPOR MOLEFLOW MOLEFRAC

PROPERTY-REP NOPCES PROP-DATA DFMS PARAM-PLUS

REACTIONS ACIDP-CE REAC-DIST
   REAC-DATA 1 PHASE=L KBASIS=MOLE-GAMMA
   STOIC 1 H2O -2. / I2 -1. / SO2 -1. / HI 2. / H2SO4  &
      1.

REACTIONS ACIDP-CR REAC-DIST
   REAC-DATA 1 KINETIC
   RATE-CON 1 PRE-EXP=0.01 ACT-ENERGY=0. T-REF=100. <C>
   STOIC 1 H2O -2. / SO2 -1. / I2 -1. / H2SO4 1. / HI  &
      2.
   POWLAW-EXP 1 H2O 1. / SO2 1. / I2 1.

REACTIONS H2-EQUIL REAC-DIST
   IN-UNITS MET VOLUME-FLOW='cum/hr' ENTHALPY-FLO='MMkcal/hr'  &
      HEAT-TRANS-C='kcal/hr-sqm-K' PRESSURE=bar TEMPERATURE=C  &
      VOLUME=cum DELTA-T=C HEAD=meter MOLE-DENSITY='kmol/cum'  &
      MASS-DENSITY='kg/cum' MOLE-ENTHALP='kcal/mol'  &
      MASS-ENTHALP='kcal/kg' HEAT=MMkcal MOLE-CONC='mol/l'  &
      PDROP=bar
   REAC-DATA 1 PHASE=V KBASIS=P
   K-STOIC 1 A=-2.3258476 B=-1233.571
   STOIC 1 HI -2. / I2 1. / H2 1.

REACTIONS H2-HI-EQ REAC-DIST
   IN-UNITS MET VOLUME-FLOW='cum/hr' ENTHALPY-FLO='MMkcal/hr'  &
      HEAT-TRANS-C='kcal/hr-sqm-K' PRESSURE=bar TEMPERATURE=C  &
      VOLUME=cum DELTA-T=C HEAD=meter MOLE-DENSITY='kmol/cum'  &
      MASS-DENSITY='kg/cum' MOLE-ENTHALP='kcal/mol'  &
      MASS-ENTHALP='kcal/kg' HEAT=MMkcal MOLE-CONC='mol/l'  &
      PDROP=bar
```

```
   REAC-DATA 1 PHASE=V KBASIS=FUG
   REAC-DATA 2
   K-STOIC 1 A=-2.325847579 B=-1233.570988
   K-STOIC 2 A=-228.8380747 B=12587.48013 C=40.68593363  &
      D=-0.098379992
   STOIC 1 HI -2. / I2 1. / H2 1.
   STOIC 2 HI -1. / H2O -1. / H3O+ 1. / I- 1.

REACTIONS H2SO4DIS REAC-DIST
   IN-UNITS MET ENTHALPY-FLO='kcal/hr' PRESSURE=torr  &
      TEMPERATURE=C DELTA-T=C ELEC-POWER=Watt PDROP=torr
   REAC-DATA 1
   STOIC 1 SO3 -1. / H2O -1. / H2SO4 1.

REACTIONS ACIDPR-R POWERLAW
   REAC-DATA 1 EQUIL PHASE=V
   STOIC 1 MIXED H2O -2. / I2 -1. / SO2 -1. / HI 2. /  &
      H2SO4 1.

REACTIONS BUNSEN POWERLAW
   REAC-DATA 1
   RATE-CON 1 PRE-EXP=3E-006 ACT-ENERGY=1. <kcal/mol>  &
      T-REF=100. <C>
   STOIC 1 MIXED H2O -2. / SO2 -1. / I2 -1. / HI 2. /  &
      H2SO4 1.
   POWLAW-EXP 1 MIXED H2O 1. / MIXED SO2 1. / MIXED I2  &
      1.

REACTIONS H2SO4R POWERLAW
   IN-UNITS MET ENTHALPY-FLO='kcal/hr' PRESSURE=torr  &
      TEMPERATURE=C DELTA-T=C ELEC-POWER=Watt PDROP=torr
   REAC-DATA 1 EQUIL PHASE=V
   STOIC 1 MIXED SO3 -1. / H2O -1. / H2SO4 1.
```

APPENDIX 4 - INPUT SUMMARY OF SECTION 2 MODEL (SECTION2-01.BKP)

```
TITLE 'GA Sulfur/Iodine Cycle - Section II'

IN-UNITS MET ENERGY=kJ ENTHALPY='J/kmol' ENTROPY='J/kmol-K'  &
      VOLUME-FLOW='cum/hr' ENTHALPY-FLO='kJ/sec' FORCE=Newton  &
      MOLE-HEAT-CA='J/kmol-K' HEAT-TRANS-C='Watt/sqm-K'  &
      TEMPERATURE=C DELTA-T=C MOLE-ENTHALP='kJ/kmol'  &
      MASS-ENTHALP='kJ/kg' MOLE-ENTROPY='J/kmol-K'  &
      MASS-ENTROPY='J/kg-K' ELEC-POWER=Watt MASS-HEAT-CA='J/kg-K'  &
      UA='J/sec-K' HEAT=kJ NUM-CONC='no/cum' MASS-CONC='kg/cum'  &
      FLUX='cum/sqm-sec' MOLE-CONC='kmol/cum'  &
      NUM-CON-RATE='no/cum-sec' VOL-HEAT-CAP='J/cum-K'  &
      HEAT-FLUX='Watt/m' POP-DENSITY='no/m/cum'  &
      INVERSE-HT-C='sqm-K/Watt' VOL-ENTHALPY='kJ/cum'

DEF-STREAMS CONVEN ALL

SIM-OPTIONS
   IN-UNITS SI PRESSURE=torr TEMPERATURE=C PDROP='N/sqm'
   SIM-OPTIONS FLASH-MAXIT=100 FLASH-TOL=1E-007

RUN-CONTROL MAX-TIME=1000.

DESCRIPTION "

   "

DATABANKS PURE10  / AQUEOUS  / SOLIDS  / INORGANIC  /  &
      ASPENPCD

PROP-SOURCES PURE10  / AQUEOUS  / SOLIDS  / INORGANIC  /  &
      ASPENPCD

COMPONENTS
   H2O H2O /
   H2SO4 H2SO4 /
   SO3 O3S /
   H3O+ H3O+ /
   HSO4- HSO4- /
   SO4-2 SO4-2 /
   SO2 O2S /
   CO2 CO2 /
```

```
   N2 N2 /
   O2 O2 /
   AR AR /
   IONPAIR H2SO4 /
   HE HE /
   H2S2O7 H2SO4

HENRY-COMPS HC-1 SO2 CO2 N2 O2 AR

CHEMISTRY CH2SO4
   IN-UNITS SI
   STOIC 1 H2SO4 -1.0 / H2O -1.0 / H3O+ 1.0 / HSO4- 1.0
   STOIC 2 HSO4- -1.0 / H2O -1.0 / H3O+ 1.0 / SO4-2 1.0
   STOIC 3 H2O -1. / SO3 -1. / H2SO4 1.

CHEMISTRY CH2SO4HT
   IN-UNITS MET ENTHALPY-FLO='kcal/hr' PRESSURE=torr  &
      TEMPERATURE=C DELTA-T=C ELEC-POWER=Watt PDROP=torr
   STOIC 1 SO3 -1. / H2O -1. / H2SO4 1.
   STOIC 2 H2O -1. / H2SO4 -1. / IONPAIR 2.
   K-STOIC 2 A=-10.447219 B=5574.5057

CHEMISTRY H2SO4
   IN-UNITS SI PRESSURE=torr TEMPERATURE=C PDROP='N/sqm'
   STOIC 1 H2SO4 -1.0 / H2O -1.0 / H3O+ 1.0 / HSO4- 1.0
   STOIC 2 HSO4- -1.0 / H2O -1.0 / H3O+ 1.0 / SO4-2 1.0

CHEMISTRY H2SO4HT
   IN-UNITS MET ENTHALPY-FLO='kcal/hr' PRESSURE=torr  &
      TEMPERATURE=C DELTA-T=C ELEC-POWER=Watt PDROP=torr
   STOIC 1 H2SO4 -1. / H2O -1. / IONPAIR 2.
   K-STOIC 1 A=-10.447219 B=5574.5057

FLOWSHEET
   BLOCK FLASH1 IN=1 OUT=2A 2
   BLOCK FLASH2 IN=3 OUT=4A 4
   BLOCK FLASH3 IN=5 OUT=6A 6
   BLOCK FLASH4 IN=7 OUT=8A 8
   BLOCK FLASH5 IN=9 OUT=10A 10
   BLOCK COOLER2 IN=10A OUT=10B
   BLOCK PUMP1 IN=13 OUT=14
   BLOCK VAPORIZR IN=15 OUT=16
   BLOCK PREVAPOR IN=14 S2 S3 OUT=15
   BLOCK RECUP1 IN=16 S1 OUT=17
   BLOCK DECOMP1 IN=17 OUT=18
   BLOCK DECOMP2 IN=18 OUT=19
```

```
   BLOCK RECUP2 IN=21 OUT=22 S1
   BLOCK COLUMN IN=12 12C S6 OUT=13A 13
   BLOCK FLASH8 IN=25 OUT=PRODUCT 26
   BLOCK PUMP2 IN=26 OUT=27
   BLOCK DECOMP3 IN=19 OUT=20
   BLOCK DECOMP4 IN=20 OUT=21
   BLOCK PREHEAT IN=27 FEED S5 S4B OUT=0
   BLOCK PUMP3 IN=13A OUT=13B
   BLOCK MIXER IN=4A 6A 8A 2A OUT=1B
   BLOCK COOLER1 IN=1B OUT=1C S6
   BLOCK HDECOMP4 IN=HE1 OUT=HE2
   BLOCK HDECOMP3 IN=HE2 OUT=HE3
   BLOCK HDECOMP2 IN=HE3 OUT=HE4
   BLOCK HDECOMP1 IN=HE4 OUT=HE5
   BLOCK HVAPORZR IN=HE5 OUT=HE6
   BLOCK HPREVAPR IN=HE6 OUT=HE7
   BLOCK HFLASH4 IN=HE7 OUT=HE8
   BLOCK HFLASH3 IN=HE8 OUT=HE9
   BLOCK HFLASH2 IN=HE9 OUT=HE10
   BLOCK HPREHEAT IN=HE10 OUT=HE11
   BLOCK HX1 IN=0 S4A OUT=1
   BLOCK FLASH6 IN=10 OUT=11A 11
   BLOCK FLASH7 IN=11 OUT=12A 12
   BLOCK HX5 IN=8 OUT=9 S2
   BLOCK HX2 IN=2 OUT=3
   BLOCK HX3 IN=4 OUT=5
   BLOCK HX4 IN=6 OUT=7
   BLOCK SEPARTR1 IN=12A OUT=12B 12C
   BLOCK COOLERA IN=22 OUT=23 S4A
   BLOCK COOLERB IN=23 OUT=24 S4B
   BLOCK COOLERC IN=24 OUT=25 S4C

PROPERTIES ELECNRTL HENRY-COMPS=HC-1 CHEMISTRY=CH2SO4  &
      TRUE-COMPS=NO
   PROPERTIES NRTL / NRTL-RK / STEAMNBS

SP-ROUTE PHILPC01 PHILPC 1 PHILPC01
   MODEL VL0CONS

PROP-DATA
   PROP-LIST ATOMNO / NOATOM
   PVAL IONPAIR 1 16 8 / 2. 0.5 2.5

PROP-DATA DATA1
   IN-UNITS SI
   PROP-LIST DHFORM / RKTZRA / DGFORM / TB
```

```
   PVAL H2SO4 -735130000 / 0.1936342 / -653470000 / 590.51
   PROP-LIST DHFORM / RKTZRA / TC / PC / VC / ZC /  &
      OMEGA / DGFORM / TB / MW
   PVAL H2S2O7 -1111000000 / 0.25687684 / 925. / 6400000.0 /  &
      .240 / .20 / .46660 / -1.024420E+09 / 2573.916342 /  &
      178.1437
   PVAL IONPAIR -510035701.8 / 0.25 / 925. / 17600000.0 /  &
      .240 / .20 / .46660 / -1.024420E+09 / 2573.916342 /  &
      58.04738
   PROP-LIST RKTZRA
   PVAL SO3 .24917730

PROP-DATA DATA2
   IN-UNITS SI
   PROP-LIST DGAQFM
   PVAL HSO4- -7.55910E+08
   PVAL SO4-2 -7.44530E+08

PROP-DATA DATA2
   IN-UNITS SI MOLE-ENTHALP='kcal/mol'
   PROP-LIST DHAQFM
   PVAL HSO4- -207.8
   PVAL SO4-2 -217.17541

PROP-DATA PURE-1
   IN-UNITS MET PRESSURE=torr TEMPERATURE=C DELTA-T=C  &
      MOLE-ENTHALP='kJ/kmol' PDROP=torr
   PROP-LIST OMEGA / DHFORM / DGFORM
   PVAL SO2 0.24511 / -297050 / -300590.81

PROP-DATA VLCONS
   IN-UNITS MET ENTHALPY-FLO='kcal/hr' PRESSURE=torr  &
      TEMPERATURE=C DELTA-T=C ELEC-POWER=Watt PDROP=torr
   PROP-LIST VLCONS
   PVAL H2O 18.5064
   PVAL H2SO4 65.7589
   PVAL SO3 44.2912
   PVAL H2S2O7 110.0501
   PVAL SO2 43.8228
   PVAL CO2 35.0189
   PVAL N2 34.6723
   PVAL O2 28.0225
   PVAL AR 28.6156
   PVAL IONPAIR 42.13265

PROP-DATA VLSTD
```

```
   IN-UNITS MET PRESSURE=torr TEMPERATURE=C DELTA-T=C  &
      PDROP=torr
   PROP-LIST VLSTD
   PVAL H3O+ 100
   PVAL HSO4- 100
   PVAL SO4-2 100

PROP-DATA CPAQ0-1
   IN-UNITS SI
   PROP-LIST CPAQ0
   PVAL HSO4- -1588028.5 7970.75904 -10.997292
   PVAL SO4-2 -293000.0

PROP-DATA CPDIEC-1
   IN-UNITS SI
   PROP-LIST CPDIEC
   PVAL H2SO4 101 0 298.15
   PVAL SO3 2 0 298.15

PROP-DATA CPIG-1
   IN-UNITS SI
   PROP-LIST CPIG
   PVAL H2SO4 13511.530 231.2640 .1720030 -.0008403250  &
      .0000006328290 0.0 0.0 2000.0 20800.0 0.0 1.0
   PVAL H2S2O7 29681.3 421.151 -0.271854

PROP-DATA CPIG-1
   IN-UNITS SI MOLE-HEAT-CA='cal/mol-K'
   PROP-LIST CPIG
   PVAL O2 7.13482399 -2.68379765E-03 1.02868233E-05  &
      -8.78879899E-09 2.40152413E-12 0 100 1500 7.13482399  &
      -2.68379765E-03 1.0
   PVAL N2 7.144511 -1.741872E-03 4.305735E-06 -2.233520E-09  &
      3.210279E-13 0 223.15 1473.15 7.144511 -1.741872E-03  &
      1.0

PROP-DATA CPIGDP-1
   IN-UNITS MET PRESSURE=torr TEMPERATURE=K DELTA-T=C  &
      PDROP=torr
   PROP-LIST CPIGDP
   PVAL SO3 10.19959828 13.26622531 1682.83741 11.72823786  &
      758.8417648 273.15 1273.15
   PVAL CO2 7.221512359 7.666971279 1308.635376 5.247592522  &
      580.9717756 220 1100

PROP-DATA CPIGDP-1
```

```
   IN-UNITS MET PRESSURE=torr TEMPERATURE=C DELTA-T=C  &
      PDROP=torr
   PROP-LIST CPIGDP
   PVAL SO2 8.446786448 5.44747727 1091.383023 2.980809212  &
      582.8526095 273.15 1773.15

PROP-DATA DHVLDP-1
   IN-UNITS SI
   PROP-LIST DHVLDP
   PVAL SO3 1.1E8 0.51119681 1.65460533 -1.4727676 0 250  &
      1000

PROP-DATA DHVLWT-1
   IN-UNITS SI
   PROP-LIST DHVLWT
   PVAL H2SO4 79050000.0 298.150 .3502 0.1565 2.0
   PVAL H2S2O7 159050000 298.150 .38 0 2.0
   PVAL IONPAIR 60836600 298.150 .38 0 2.0

PROP-DATA IONMUB-1
   IN-UNITS MET ENTHALPY-FLO='kcal/hr' PRESSURE=torr  &
      TEMPERATURE=K DELTA-T=C MOLE-VOLUME='cum/kmol'  &
      ELEC-POWER=Watt PDROP=torr
   PROP-LIST IONMUB
   PVAL HSO4- 0.01597359 0.00023995

PROP-DATA MULDIP-1
   IN-UNITS MET ENTHALPY-FLO='kcal/hr' PRESSURE=torr  &
      TEMPERATURE=K VISCOSITY='N-sec/sqm' DELTA-T=C  &
      ELEC-POWER=Watt PDROP=torr
   PROP-LIST MULDIP
   PVAL H2SO4 -112.96105 7497.04869 14.7608891 0 0 273.15  &
      500
   PVAL H2S2O7 -12.742544 2926.56599 0 0 0 273.15 500
   PVAL SO3 -150.66701 9073.65901 20 0 0 273 400

PROP-DATA PLXANT-1
   IN-UNITS SI
   PROP-LIST PLXANT
   PVAL H2O 72.550 -7206.70 0.0 0.0 -7.13850 .0000040460  &
      2.0 273.160 647.290
   PVAL H2SO4 37.60588121 -11216.33992 0 -0.011998736 0 0 2  &
      273.15 700
   PVAL H2S2O7 14.72992607 -8246.41 0 0.0 0 0 2 273.15  &
      3000
   PVAL IONPAIR 14.72992607 -8246.41 0 0.0 0 0 2 273.15  &
```

```
      3000

;INSERT 1 MH2SO4 H2O H2SO4
;  CVAL DHFORM  1 1 -.735D9
;  CVAL DHFORM 1 1  -1.13085D9

PROP-DATA HENRY-1
   IN-UNITS SI
   PROP-LIST HENRY
   BPVAL SO2 SO3 83.96060 -5578.80 -8.761520 0.0 273.0 373.0
   BPVAL SO2 H2SO4 83.96060 -5578.80 -8.761520 0.0 273.0  &
      373.0
   BPVAL CO2 SO3 170.71260 -8477.7110 -21.957430 .0057807480  &
      273.0 500.0
   BPVAL CO2 H2SO4 170.71260 -8477.7110 -21.957430 .0057807480  &
      273.0 500.0
   BPVAL N2 SO3 176.5070 -8432.770 -21.5580 -.008436240 273.0  &
      346.0
   BPVAL N2 H2SO4 176.5070 -8432.770 -21.5580 -.008436240  &
      273.0 346.0
   BPVAL O2 SO3 155.9210 -7775.060 -18.39740 -.009443540  &
      274.0 348.0
   BPVAL O2 H2SO4 155.9210 -7775.060 -18.39740 -.009443540  &
      274.0 348.0
   BPVAL SO2 H2O 26.56470 -2872.960 -.302880 0.0 283.0 386.0
   BPVAL CO2 H2O 171.3780 -8741.550 -21.6690 .001102590 273.0  &
      353.0
   BPVAL N2 H2O 176.5070 -8432.770 -21.5580 -.008436240 273.0  &
      346.0
   BPVAL O2 H2O 155.9210 -7775.060 -18.39740 -.009443540  &
      274.0 348.0
   BPVAL AR H2O 180.9910000 -8137.130000 -23.25470000  &
      3.06357000E-3 274.0000000 347.0000000
   BPVAL AR H2SO4 180.9910000 -8137.130000 -23.25470000  &
      3.06357000E-3 274.0000000 347.0000000

PROP-DATA NRTL-1
   IN-UNITS SI
   PROP-LIST NRTL
   BPVAL H2O CO2 10.0640 -3268.1350 .20 0.0 0.0 0.0 273.150  &
      473.150
   BPVAL CO2 H2O 10.0640 -3268.1350 .20 0.0 0.0 0.0 273.150  &
      473.150
   BPVAL SO3 H2S2O7 4.66903268 -218.88919 .2000000 0.0 0.0  &
      0.0 0.0 1000.000
   BPVAL H2S2O7 SO3 -0.6508244 -425.28909 .2000000 0.0 0.0  &
```

```
      0.0 0.0 1000.000
   BPVAL SO3 H2SO4 5.83914569 -614.29263 .2000000 0.0 0.0  &
      0.0 0.0 1000.000
   BPVAL H2SO4 SO3 0.0 0.0 .2000000 0.0 0.0 0.0 0.0  &
      1000.000
   BPVAL H2SO4 H2S2O7 4.95052339 -456.99931 .2000000 0.0 0.0  &
      0.0 0.0 1000.000
   BPVAL H2S2O7 H2SO4 -2.3508099 -88.510187 .2000000 0.0 0.0  &
      0.0 0.0 1000.000
   BPVAL H2O H2SO4 0 0.0 .200000 0.0 0.0 0.0 0.0 1000.000
   BPVAL H2SO4 H2O 0 0.0 .200000 0.0 0.0 0.0 0.0 1000.000
   BPVAL IONPAIR H2SO4 0 -1550.1937 .200000 0.0 0.0 0.0 0.0  &
      1000.000
   BPVAL H2SO4 IONPAIR 0 969.798206 .200000 0.0 0.0 0.0 0.0  &
      1000.000
   BPVAL IONPAIR H2O 0 813.139247 .200000 0.0 0.0 0.0 0.0  &
      1000.000
   BPVAL H2O IONPAIR 0 -2470.0714 .200000 0.0 0.0 0.0 0.0  &
      1000.000
   BPVAL IONPAIR SO3 0 0.0 .200000 0.0 0.0 0.0 0.0  &
      1000.000
   BPVAL SO3 IONPAIR 0 0.0 .200000 0.0 0.0 0.0 0.0  &
      1000.000

PROP-DATA VLCLK-1
   IN-UNITS SI
   PROP-LIST VLCLK
   BPVAL H3O+ HSO4- 0.05452132 0.01993186

PROP-DATA GMELCC-1
   IN-UNITS SI
   PROP-LIST GMELCC
   PPVAL H2O ( H3O+ HSO4- ) 3.4616695
   PPVAL ( H3O+ HSO4- ) H2O -3.9843446
   PPVAL H2SO4 ( H3O+ HSO4- ) -2.0423396
   PPVAL ( H3O+ HSO4- ) H2SO4 -2.3745922
   PPVAL H2O ( H3O+ SO4-2 ) 8
   PPVAL ( H3O+ SO4-2 ) H2O -4
   PPVAL H2SO4 ( H3O+ SO4-2 ) 8
   PPVAL ( H3O+ SO4-2 ) H2SO4 -4
   PPVAL SO3 ( H3O+ HSO4- ) 8
   PPVAL ( H3O+ HSO4- ) SO3 -4
   PPVAL SO3 ( H3O+ SO4-2 ) 8
   PPVAL ( H3O+ SO4-2 ) SO3 -4
   PPVAL SO2 ( H3O+ HSO4- ) 2.22
   PPVAL ( H3O+ HSO4- ) SO2 -0.32
```

```
   PPVAL CO2 ( H3O+ HSO4- ) 2.22
   PPVAL ( H3O+ HSO4- ) CO2 -0.32
   PPVAL N2 ( H3O+ HSO4- ) 2.22
   PPVAL ( H3O+ HSO4- ) N2 -0.32
   PPVAL O2 ( H3O+ HSO4- ) 2.22
   PPVAL ( H3O+ HSO4- ) O2 -0.32
   PPVAL AR ( H3O+ HSO4- ) 2.22
   PPVAL ( H3O+ HSO4- ) AR -0.32

PROP-DATA GMELCD-1
   IN-UNITS SI
   PROP-LIST GMELCD
   PPVAL H2O ( H3O+ HSO4- ) 2412.88399
   PPVAL ( H3O+ HSO4- ) H2O -511.40017
   PPVAL H2SO4 ( H3O+ HSO4- ) 18.4880871
   PPVAL ( H3O+ HSO4- ) H2SO4 2171.05384
   PPVAL H2O ( H3O+ SO4-2 ) 0
   PPVAL ( H3O+ SO4-2 ) H2O 0
   PPVAL H2SO4 ( H3O+ SO4-2 ) 0
   PPVAL ( H3O+ SO4-2 ) H2SO4 0
   PPVAL ( H3O+ HSO4- ) SO3 0
   PPVAL SO3 ( H3O+ HSO4- ) 0

PROP-DATA GMELCE-1
   IN-UNITS SI
   PROP-LIST GMELCE
   PPVAL H2O ( H3O+ HSO4- ) 3.09312155
   PPVAL ( H3O+ HSO4- ) H2O 2.21471832
   PPVAL H2SO4 ( H3O+ HSO4- ) 4.84108255
   PPVAL ( H3O+ HSO4- ) H2SO4 -6.2328899
   PPVAL H2O ( H3O+ SO4-2 ) 0
   PPVAL ( H3O+ SO4-2 ) H2O 0
   PPVAL H2SO4 ( H3O+ SO4-2 ) 0
   PPVAL ( H3O+ SO4-2 ) H2SO4 0

PROP-DATA GMELCN-1
   IN-UNITS SI
   PROP-LIST GMELCN
   PPVAL H2O ( H3O+ HSO4- ) .20
   PPVAL ( H3O+ HSO4- ) H2O .20
   PPVAL H2SO4 ( H3O+ HSO4- ) .20
   PPVAL ( H3O+ HSO4- ) H2SO4 .20
   PPVAL H2O ( H3O+ SO4-2 ) .20
   PPVAL ( H3O+ SO4-2 ) H2O .20
   PPVAL H2SO4 ( H3O+ SO4-2 ) .20
   PPVAL ( H3O+ SO4-2 ) H2SO4 .20
```

```
   PPVAL SO2 ( H3O+ HSO4- ) .2
   PPVAL ( H3O+ HSO4- ) SO2 .2

PROP-SET PHI PHIMX SUBSTREAM=MIXED PHASE=V L

PROP-SET XTRUE
   IN-UNITS SI
   PROPNAME-LIS XTRUE SUBSTREAM=MIXED PHASE=L

STREAM 17
   SUBSTREAM MIXED TEMP=523.719782 PRES=7
   MOLE-FLOW H2O 1.45555744 / H2SO4 0.284363 / SO3  &
      1.28492895

STREAM FEED
   IN-UNITS MET ENTHALPY-FLO='kcal/hr' PRESSURE=torr  &
      TEMPERATURE=C DELTA-T=C ELEC-POWER=Watt PDROP=torr
   SUBSTREAM MIXED TEMP=120. PRES=35. <atm>
   MOLE-FLOW H2O 4. / H2SO4 1.

STREAM HE1
   SUBSTREAM MIXED TEMP=947. PRES=50. MOLE-FLOW=35.
   MOLE-FRAC HE 1.

DEF-STREAMS HEAT S1

DEF-STREAMS HEAT S2

DEF-STREAMS HEAT S3

STREAM S3
   INFO HEAT DUTY=2.8616

DEF-STREAMS HEAT S4A

DEF-STREAMS HEAT S4B

DEF-STREAMS HEAT S4C

DEF-STREAMS HEAT S5

STREAM S5
   INFO HEAT DUTY=5.85521191

DEF-STREAMS HEAT S6
```

```
BLOCK MIXER MIXER
   PARAM PRES=35. MAXIT=99 T-EST=350.
   PROPERTIES ELECNRTL CHEMISTRY=H2SO4HT TRUE-COMPS=NO

BLOCK COOLER1 HEATER
   PARAM TEMP=120. PRES=35.
   PROPERTIES ELECNRTL CHEMISTRY=H2SO4HT

BLOCK COOLER2 HEATER
   IN-UNITS MET ENTHALPY-FLO='kcal/hr' PRESSURE=torr  &
      TEMPERATURE=C DELTA-T=C ELEC-POWER=Watt PDROP=torr
   PARAM TEMP=120. PRES=8. <atm>

BLOCK HDECOMP1 HEATER
   PARAM PRES=50. DUTY=-16.4394816 NPHASE=1 PHASE=V
   PROPERTIES NRTL
   BLOCK-OPTION FREE-WATER=NO

BLOCK HDECOMP2 HEATER
   PARAM PRES=50. DUTY=-11.9676961 NPHASE=1 PHASE=V
   PROPERTIES NRTL
   BLOCK-OPTION FREE-WATER=NO

BLOCK HDECOMP3 HEATER
   PARAM PRES=50. DUTY=-10.7578098 NPHASE=1 PHASE=V
   PROPERTIES NRTL
   BLOCK-OPTION FREE-WATER=NO

BLOCK HDECOMP4 HEATER
   PARAM PRES=50. DUTY=-10.2635833 NPHASE=1 PHASE=V
   PROPERTIES NRTL
   BLOCK-OPTION FREE-WATER=NO

BLOCK HFLASH2 HEATER
   PARAM PRES=50. DUTY=-12.9446947 NPHASE=1 PHASE=V
   PROPERTIES NRTL
   BLOCK-OPTION FREE-WATER=NO

BLOCK HFLASH3 HEATER
   PARAM PRES=50. DUTY=-7.89692688 NPHASE=1 PHASE=V
   PROPERTIES NRTL
   BLOCK-OPTION FREE-WATER=NO

BLOCK HFLASH4 HEATER
   PARAM PRES=50. DUTY=-7.98866144 NPHASE=1 PHASE=V
   PROPERTIES NRTL
```

```
   BLOCK-OPTION FREE-WATER=NO

BLOCK HPREHEAT HEATER
   PARAM PRES=50. DUTY=-4.5545 NPHASE=1 PHASE=V
   PROPERTIES NRTL
   BLOCK-OPTION FREE-WATER=NO

BLOCK HPREVAPR HEATER
   PARAM PRES=50. DUTY=-4.38398 NPHASE=1 PHASE=V
   PROPERTIES NRTL
   BLOCK-OPTION FREE-WATER=NO

BLOCK HVAPORZR HEATER
   PARAM PRES=50. DUTY=-35.5093925 NPHASE=1 PHASE=V
   PROPERTIES NRTL
   BLOCK-OPTION FREE-WATER=NO

BLOCK HX1 HEATER
   PARAM PRES=35.
   PROPERTIES ELECNRTL CHEMISTRY=H2SO4HT TRUE-COMPS=NO

BLOCK HX2 HEATER
   PARAM TEMP=346. PRES=35.
   PROPERTIES ELECNRTL CHEMISTRY=H2SO4HT TRUE-COMPS=NO

BLOCK HX3 HEATER
   PARAM TEMP=358. PRES=35.
   PROPERTIES ELECNRTL CHEMISTRY=H2SO4HT TRUE-COMPS=NO

BLOCK HX4 HEATER
   PARAM TEMP=371. PRES=35.
   PROPERTIES ELECNRTL CHEMISTRY=H2SO4HT TRUE-COMPS=NO

BLOCK HX5 HEATER
   PARAM TEMP=308. PRES=35.
   PROPERTIES ELECNRTL CHEMISTRY=H2SO4HT TRUE-COMPS=NO

BLOCK PREHEAT HEATER
   PARAM PRES=35.
   PROPERTIES ELECNRTL CHEMISTRY=H2SO4HT TRUE-COMPS=NO

BLOCK PREVAPOR HEATER
   IN-UNITS MET ENTHALPY-FLO='kcal/hr' PRESSURE=torr  &
      TEMPERATURE=C DELTA-T=C ELEC-POWER=Watt PDROP=torr
   PARAM PRES=7. <atm> NPHASE=1 PHASE=L MAXIT=99 T-EST=411.
   PROPERTIES ELECNRTL CHEMISTRY=H2SO4HT TRUE-COMPS=NO
```

```
   BLOCK-OPTION FREE-WATER=NO

BLOCK VAPORIZR HEATER
   IN-UNITS MET ENTHALPY-FLO='kcal/hr' PRESSURE=torr  &
      TEMPERATURE=C DELTA-T=C ELEC-POWER=Watt PDROP=torr
   PARAM TEMP=411. VFRAC=0.99 NPHASE=2 MAXIT=99
   PROPERTIES ELECNRTL CHEMISTRY=CH2SO4HT TRUE-COMPS=YES
   BLOCK-OPTION FREE-WATER=NO

BLOCK FLASH1 FLASH2
   IN-UNITS MET ENTHALPY-FLO='kcal/hr' PRESSURE=torr  &
      TEMPERATURE=C DELTA-T=C ELEC-POWER=Watt PDROP=torr
   PARAM PRES=35. <atm> DUTY=0.
   PROPERTIES ELECNRTL CHEMISTRY=H2SO4HT TRUE-COMPS=NO

BLOCK FLASH2 FLASH2
   IN-UNITS MET ENTHALPY-FLO='kcal/hr' PRESSURE=torr  &
      TEMPERATURE=C DELTA-T=C ELEC-POWER=Watt PDROP=torr
   PARAM PRES=35. <atm> DUTY=0.
   PROPERTIES ELECNRTL CHEMISTRY=H2SO4HT TRUE-COMPS=NO

BLOCK FLASH3 FLASH2
   IN-UNITS MET ENTHALPY-FLO='kcal/hr' PRESSURE=torr  &
      TEMPERATURE=C DELTA-T=C ELEC-POWER=Watt PDROP=torr
   PARAM PRES=35. <atm> DUTY=0.
   PROPERTIES ELECNRTL CHEMISTRY=H2SO4HT TRUE-COMPS=NO

BLOCK FLASH4 FLASH2
   IN-UNITS MET ENTHALPY-FLO='kcal/hr' PRESSURE=torr  &
      TEMPERATURE=C DELTA-T=C ELEC-POWER=Watt PDROP=torr
   PARAM PRES=35. <atm> DUTY=0.
   PROPERTIES ELECNRTL CHEMISTRY=H2SO4HT TRUE-COMPS=NO

BLOCK FLASH5 FLASH2
   IN-UNITS MET ENTHALPY-FLO='kcal/hr' PRESSURE=torr  &
      TEMPERATURE=C DELTA-T=C ELEC-POWER=Watt PDROP=torr
   PARAM PRES=8. <atm> DUTY=0. <kJ/sec>
   PROPERTIES ELECNRTL CHEMISTRY=H2SO4HT TRUE-COMPS=NO

BLOCK FLASH6 FLASH2
   PARAM PRES=2. DUTY=0.
   PROPERTIES ELECNRTL CHEMISTRY=CH2SO4 TRUE-COMPS=NO

BLOCK FLASH7 FLASH2
   PARAM PRES=50. <mmHg> DUTY=0.
   PROPERTIES ELECNRTL CHEMISTRY=CH2SO4 TRUE-COMPS=NO
```

```
BLOCK FLASH8 FLASH2
   IN-UNITS MET ENTHALPY-FLO='kcal/hr' PRESSURE=torr  &
      TEMPERATURE=C DELTA-T=C ELEC-POWER=Watt PDROP=torr
   PARAM PRES=7. <atm> DUTY=0.05
   PROPERTIES ELECNRTL HENRY-COMPS=HC-1 CHEMISTRY=CH2SO4  &
      TRUE-COMPS=NO

BLOCK SEPARTR1 FLASH2
   PARAM TEMP=135. PRES=50. <mmHg>

BLOCK COLUMN RADFRAC
   IN-UNITS MET ENTHALPY-FLO='kcal/hr' PRESSURE=torr  &
      TEMPERATURE=C DELTA-T=C ELEC-POWER=Watt PDROP=torr
   PARAM NSTAGE=8 ALGORITHM=NONIDEAL INIT-OPTION=STANDARD  &
      DAMPING=MILD
   COL-CONFIG CONDENSER=TOTAL
   FEEDS 12 4 / 12C 4
   FEEDS S6 8
   PRODUCTS 13 8 L / 13A 1 L
   P-SPEC 1 50. <mmHg>
   COL-SPECS MOLE-B=1.74 MOLE-RR=0.75
   REAC-STAGES 1 8 H2SO4D
   T-EST 1 38. / 2 38. / 3 38.8 / 4 146.5 / 5 166.2 /  &
      6 190.9 / 7 205.2 / 8 210.7
   PROPERTIES ELECNRTL CHEMISTRY=H2SO4 TRUE-COMPS=NO

BLOCK DECOMP1 RGIBBS
   IN-UNITS MET ENTHALPY-FLO='kcal/hr' PRESSURE=torr  &
      TEMPERATURE=C DELTA-T=C ELEC-POWER=Watt PDROP=torr
   PARAM TEMP=875. <K> PRES=7. <atm> NPHASE=1
   PROD H2O / H2SO4 / SO3 / SO2 / O2
   PROPERTIES NRTL-RK HENRY-COMPS=HC-1 TRUE-COMPS=YES

BLOCK DECOMP2 RGIBBS
   IN-UNITS MET ENTHALPY-FLO='kcal/hr' PRESSURE=torr  &
      TEMPERATURE=C DELTA-T=C ELEC-POWER=Watt PDROP=torr
   PARAM TEMP=955. <K> PRES=7. <atm>
   PROD H2O / H2SO4 / SO3 / SO2 / O2
   PROPERTIES NRTL-RK HENRY-COMPS=HC-1 TRUE-COMPS=YES

BLOCK DECOMP3 RGIBBS
   IN-UNITS MET ENTHALPY-FLO='kcal/hr' PRESSURE=torr  &
      TEMPERATURE=C DELTA-T=C ELEC-POWER=Watt PDROP=torr
   PARAM TEMP=1027. <K> PRES=7. <atm>
   PROD H2SO4 / H2O / SO3 / SO2 / O2
```

```
   PROPERTIES NRTL-RK HENRY-COMPS=HC-1

BLOCK DECOMP4 RGIBBS
   IN-UNITS MET ENTHALPY-FLO='kcal/hr' PRESSURE=torr  &
      TEMPERATURE=C DELTA-T=C ELEC-POWER=Watt PDROP=torr
   PARAM TEMP=827. PRES=7. <atm> CHEMEQ=YES
   PROD H2O / H2SO4 / SO3 / SO2 / O2
   PROPERTIES NRTL-RK HENRY-COMPS=HC-1

BLOCK RECUP1 RGIBBS
   IN-UNITS MET ENTHALPY-FLO='kcal/hr' PRESSURE=torr  &
      TEMPERATURE=C DELTA-T=C ELEC-POWER=Watt PDROP=torr
   PARAM PRES=7. <atm>
   PROD H2O / H2SO4 / SO3
   PROPERTIES NRTL-RK HENRY-COMPS=HC-1 TRUE-COMPS=YES

BLOCK RECUP2 RGIBBS
   IN-UNITS MET ENTHALPY-FLO='kcal/hr' PRESSURE=torr  &
      TEMPERATURE=C DELTA-T=C ELEC-POWER=Watt PDROP=torr
   PARAM TEMP=431. PRES=7. <atm>
   PROD H2SO4 / H2O / SO3 / SO2 / O2
   PROD-FRAC SO2 1. / O2 1.
   PROPERTIES NRTL-RK HENRY-COMPS=HC-1 TRUE-COMPS=YES

BLOCK COOLERA RCSTR
   PARAM VOL=10. TEMP=336.6 PRES=7. NPHASE=2
   PROPERTIES ELECNRTL HENRY-COMPS=HC-1 CHEMISTRY=H2SO4HT  &
      TRUE-COMPS=NO
   BLOCK-OPTION FREE-WATER=NO
   REACTIONS RXN-IDS=H2SO4R

BLOCK COOLERB RCSTR
   PARAM VOL=10. TEMP=140. PRES=7. NPHASE=2
   PROPERTIES ELECNRTL HENRY-COMPS=HC-1 CHEMISTRY=H2SO4  &
      TRUE-COMPS=NO
   BLOCK-OPTION FREE-WATER=NO
   REACTIONS RXN-IDS=H2SO4R

BLOCK COOLERC RCSTR
   PARAM VOL=10. TEMP=120. PRES=7. NPHASE=2
   PROPERTIES ELECNRTL HENRY-COMPS=HC-1 CHEMISTRY=H2SO4  &
      TRUE-COMPS=NO
   BLOCK-OPTION FREE-WATER=NO
   REACTIONS RXN-IDS=H2SO4R

BLOCK PUMP1 PUMP
```

```
   IN-UNITS MET ENTHALPY-FLO='kcal/hr' PRESSURE=torr  &
      TEMPERATURE=C DELTA-T=C ELEC-POWER=Watt PDROP=torr
   PARAM PRES=7. <atm>

BLOCK PUMP2 PUMP
   IN-UNITS MET ENTHALPY-FLO='kcal/hr' PRESSURE=torr  &
      TEMPERATURE=C DELTA-T=C ELEC-POWER=Watt PDROP=torr
   PARAM PRES=35. <atm>

BLOCK PUMP3 PUMP
   PARAM PRES=1.

DESIGN-SPEC QHX1
   DEFINE TCOOLB BLOCK-VAR BLOCK=COOLERB VARIABLE=TEMP  &
      SENTENCE=PARAM
   DEFINE T1 STREAM-VAR STREAM=1 SUBSTREAM=MIXED VARIABLE=TEMP
   SPEC "T1" TO "330"
   TOL-SPEC ".1"
   VARY BLOCK-VAR BLOCK=COOLERA VARIABLE=TEMP SENTENCE=PARAM
   LIMITS "320" "360"

DESIGN-SPEC QPREHEAT
   DEFINE T0 STREAM-VAR STREAM=0 SUBSTREAM=MIXED VARIABLE=TEMP
   DEFINE QS5 INFO-VAR INFO=HEAT VARIABLE=DUTY STREAM=S5
   SPEC "T0" TO "307"
   TOL-SPEC ".1"
   VARY INFO-VAR INFO=HEAT VARIABLE=DUTY STREAM=S5
   LIMITS ".01" "50"

EO-CONV-OPTI

CALCULATOR CDECOMP1
   DEFINE QDC1 BLOCK-VAR BLOCK=DECOMP1 VARIABLE=QCALC  &
      SENTENCE=PARAM
   DEFINE DHDC1 BLOCK-VAR BLOCK=HDECOMP1 VARIABLE=DUTY  &
      SENTENCE=PARAM
F     DHDC1=-1*QDC1
   READ-VARS QDC1
   WRITE-VARS DHDC1

CALCULATOR CDECOMP2
   DEFINE QDC2 BLOCK-VAR BLOCK=DECOMP2 VARIABLE=QCALC  &
      SENTENCE=PARAM
   DEFINE DHDC2 BLOCK-VAR BLOCK=HDECOMP2 VARIABLE=DUTY  &
      SENTENCE=PARAM
F     DHDC2=-1*QDC2
```

```
   READ-VARS QDC2
   WRITE-VARS DHDC2

CALCULATOR CDECOMP3
   DEFINE QDC3 BLOCK-VAR BLOCK=DECOMP3 VARIABLE=QCALC  &
      SENTENCE=PARAM
   DEFINE DHDC3 BLOCK-VAR BLOCK=HDECOMP3 VARIABLE=DUTY  &
      SENTENCE=PARAM
F     DHDC3=-1*QDC3
   READ-VARS QDC3
   WRITE-VARS DHDC3

CALCULATOR CDECOMP4
   DEFINE DDC4 BLOCK-VAR BLOCK=DECOMP4 VARIABLE=QCALC  &
      SENTENCE=PARAM
   DEFINE DHDC4 BLOCK-VAR BLOCK=HDECOMP4 VARIABLE=DUTY  &
      SENTENCE=PARAM
F     DHDC4=-1*DDC4
   READ-VARS DDC4
   WRITE-VARS DHDC4

CALCULATOR CFLASH2
   DEFINE QHX2 BLOCK-VAR BLOCK=HX2 VARIABLE=QCALC  &
      SENTENCE=PARAM
   DEFINE DHF2 BLOCK-VAR BLOCK=HFLASH2 VARIABLE=DUTY  &
      SENTENCE=PARAM
F     DHF2=-1*QHX2
   READ-VARS QHX2
   WRITE-VARS DHF2

CALCULATOR CFLASH3
   DEFINE QHX3 BLOCK-VAR BLOCK=HX3 VARIABLE=QCALC  &
      SENTENCE=PARAM
   DEFINE DHF3 BLOCK-VAR BLOCK=HFLASH3 VARIABLE=DUTY  &
      SENTENCE=PARAM
F     DHF3=-1*QHX3
   READ-VARS QHX3
   WRITE-VARS DHF3

CALCULATOR CFLASH4
   DEFINE QHX4 BLOCK-VAR BLOCK=HX4 VARIABLE=QCALC  &
      SENTENCE=PARAM
   DEFINE DHF4 BLOCK-VAR BLOCK=HFLASH4 VARIABLE=DUTY  &
      SENTENCE=PARAM
F     DHF4=-1*QHX4
   READ-VARS QHX4
```

```
   WRITE-VARS DHF4

CALCULATOR CPREHEAT
   DEFINE QS5 INFO-VAR INFO=HEAT VARIABLE=DUTY STREAM=S5
   DEFINE DHPH BLOCK-VAR BLOCK=HPREHEAT VARIABLE=DUTY  &
      SENTENCE=PARAM
F     DHPH=-1*QS5
   READ-VARS QS5
   WRITE-VARS DHPH

CALCULATOR CPREVAPR
   DEFINE QPV INFO-VAR INFO=HEAT VARIABLE=DUTY STREAM=S3
   DEFINE DHPV BLOCK-VAR BLOCK=HPREVAPR VARIABLE=DUTY  &
      SENTENCE=PARAM
F     DHPV=-1*QPV
   READ-VARS QPV
   WRITE-VARS DHPV

CALCULATOR CVAPORZR
   DEFINE QVZR BLOCK-VAR BLOCK=VAPORIZR VARIABLE=QCALC  &
      SENTENCE=PARAM
   DEFINE DHVZR BLOCK-VAR BLOCK=HVAPORZR VARIABLE=DUTY  &
      SENTENCE=PARAM
F     DHVZR=-1*QVZR
   READ-VARS QVZR
   WRITE-VARS DHVZR

CONV-OPTIONS
   PARAM CHECKSEQ=NO

STREAM-REPOR MOLEFLOW MASSFLOW MOLEFRAC MASSFRAC  &
      PROPERTIES=XTRUE PHI

PROPERTY-REP NOPCES PROP-DATA DFMS PARAM-PLUS

REACTIONS H2SO4D REAC-DIST
   IN-UNITS MET ENTHALPY-FLO='kcal/hr' PRESSURE=torr  &
      TEMPERATURE=C DELTA-T=C ELEC-POWER=Watt PDROP=torr
   REAC-DATA 1 PHASE=V KBASIS=FUG
   K-STOIC 1 A=-29.001873 B=11677.3085
   STOIC 1 SO3 -1. / H2O -1. / H2SO4 1.

REACTIONS H2SO4R POWERLAW
   IN-UNITS MET ENTHALPY-FLO='kcal/hr' PRESSURE=torr  &
      TEMPERATURE=C DELTA-T=C ELEC-POWER=Watt PDROP=torr
   REAC-DATA 1 EQUIL PHASE=V KBASIS=FUGACITY
```

K-STOIC 1 A=-29.00187343 B=11677.30851
STOIC 1 MIXED SO3 -1. / H2O -1. / H2SO4 1.

APPENXIS 5 - INPUT SUMMARY OF SECTION 3 MODEL - REACDISTLIQDRAW.BKP)

```
TITLE 'Section 3 Model - Reactive Distillation, Liquid Draw'

IN-UNITS MET VOLUME-FLOW='cum/hr' ENTHALPY-FLO='MMkcal/hr'  &
      HEAT-TRANS-C='kcal/hr-sqm-K' PRESSURE=bar TEMPERATURE=C  &
      VOLUME=cum DELTA-T=C HEAD=meter MOLE-DENSITY='kmol/cum'  &
      MASS-DENSITY='kg/cum' MOLE-ENTHALP='kcal/mol'  &
      MASS-ENTHALP='kcal/kg' HEAT=MMkcal MOLE-CONC='mol/l'  &
      PDROP=bar

DEF-STREAMS CONVEN ALL

SIM-OPTIONS FLASH-TOL=1E-007 HF-FL3-DAMP=YES MAXSOL-CHECK=NO

RUN-CONTROL MAX-TIME=9999.

DESCRIPTION "
   Electrolytes Simulation with Metric Units :
   C, bar, kg/hr, kmol/hr, MMkcal/hr, cum/hr.

   Property Method: ELECNRTL

   Flow basis for input: Mass

   Stream report composition: Mass flow
   "

DATABANKS ASPENPCD  / AQUEOUS  / SOLIDS  / INORGANIC  /  &
      PURE10

PROP-SOURCES ASPENPCD  / AQUEOUS  / SOLIDS  / INORGANIC  /  &
      PURE10

COMPONENTS
   H2O H2O /
   I2 I2 /
   HI HI /
   I- I- /
   H3O+ H3O+ /
   I2-S I2 /
   H2 H2

HENRY-COMPS HENRY H2
```

```
CHEMISTRY HI-FULL
   STOIC 1 HI -1. / H2O -1. / H3O+ 1. / I- 1.
   STOIC 3 HI -2. / I2 1. / H2 1.
   K-STOIC 3 A=17.38265099 B=-14058.06029 C=9.099622987  &
      D=-0.110628785
   SALT I2-S I2 1.
   K-SALT I2-S A=-9.228072963 B=-1083.684565 C=2.019221642

CHEMISTRY HI-H2
   STOIC 1 HI -1. / H2O -1. / H3O+ 1. / I- 1.
   STOIC 2 HI -2. / I2 1. / H2 1.

CHEMISTRY HI-I2
   STOIC 1 HI -1. / H2O -1. / H3O+ 1. / I- 1.
   K-STOIC 1 A=-228.8380747 B=12587.48013 C=40.68593363  &
      D=-0.098379992

FLOWSHEET
   BLOCK COLUMN IN=FEED OUT=TOP BOTTOM SIDELIQ SIDEVAP
   BLOCK B3 IN=TOP OUT=H2PROD COND

PROPERTIES ELECNRTL HENRY-COMPS=HENRY CHEMISTRY=HI-I2  &
      TRUE-COMPS=NO
   PROPERTIES NRTL-RK

PROP-REPLACE ELECNRTL ELECNRTL
   MODEL VL0CONS

PROP-DATA
   PROP-LIST ATOMNO / NOATOM
   PVAL H3O+ 1 8 / 3. 1.

PROP-DATA HI-PROPS
   IN-UNITS MET VOLUME-FLOW='cum/hr' ENTHALPY-FLO='MMkcal/hr'  &
      HEAT-TRANS-C='kcal/hr-sqm-K' PRESSURE=bar TEMPERATURE=K  &
      VOLUME=cum DELTA-T=C HEAD=meter MOLE-DENSITY='kmol/cum'  &
      MASS-DENSITY='kg/cum' MOLE-ENTHALP='kcal/mol'  &
      MASS-ENTHALP='kcal/kg' HEAT=MMkcal MOLE-CONC='mol/l'  &
      PDROP=bar
   PROP-LIST TC / PC / RKTZRA
   PVAL HI 423.85 / 83.1 / 0.31499751

PROP-DATA I-
   IN-UNITS MET VOLUME-FLOW='cum/hr' ENTHALPY-FLO='MMkcal/hr'  &
      HEAT-TRANS-C='kcal/hr-sqm-K' PRESSURE=bar TEMPERATURE=C  &
```

```
      VOLUME=cum DELTA-T=C HEAD=meter MOLE-DENSITY='kmol/cum'  &
      MASS-DENSITY='kg/cum' MOLE-ENTHALP='kcal/mol'  &
      MASS-ENTHALP='kcal/kg' HEAT=MMkcal MOLE-CONC='mol/l'  &
      PDROP=bar
   PROP-LIST DHAQFM
   PVAL I- -13.181905

PROP-DATA VLCONS
   IN-UNITS MET VOLUME-FLOW='cum/hr' ENTHALPY-FLO='MMkcal/hr'  &
      HEAT-TRANS-C='kcal/hr-sqm-K' PRESSURE=bar TEMPERATURE=C  &
      VOLUME=cum DELTA-T=C HEAD=meter MOLE-DENSITY='kmol/cum'  &
      MASS-DENSITY='kg/cum' MOLE-ENTHALP='kcal/mol'  &
      MASS-ENTHALP='kcal/kg' HEAT=MMkcal MOLE-CONC='mol/l'  &
      PDROP=bar
   PROP-LIST VLCONS
   PVAL H2O 19.63607
   PVAL I2 68.081606
   PVAL HI 45.675239
   PVAL H2 28.612729

PROP-DATA VLSTD
   IN-UNITS MET VOLUME-FLOW='cum/hr' ENTHALPY-FLO='MMkcal/hr'  &
      HEAT-TRANS-C='kcal/hr-sqm-K' PRESSURE=bar TEMPERATURE=C  &
      VOLUME=cum DELTA-T=C HEAD=meter MOLE-DENSITY='kmol/cum'  &
      MASS-DENSITY='kg/cum' MOLE-ENTHALP='kcal/mol'  &
      MASS-ENTHALP='kcal/kg' HEAT=MMkcal MOLE-CONC='mol/l'  &
      PDROP=bar
   PROP-LIST VLSTD
   PVAL I- 100
   PVAL H3O+ 100

PROP-DATA CPDIEC-1
   IN-UNITS MET VOLUME-FLOW='cum/hr' ENTHALPY-FLO='MMkcal/hr'  &
      HEAT-TRANS-C='kcal/hr-sqm-K' PRESSURE=bar TEMPERATURE=C  &
      VOLUME=cum DELTA-T=C HEAD=meter MOLE-DENSITY='kmol/cum'  &
      MASS-DENSITY='kg/cum' MOLE-ENTHALP='kcal/mol'  &
      MASS-ENTHALP='kcal/kg' HEAT=MMkcal MOLE-CONC='mol/l'  &
      PDROP=bar
   PROP-LIST CPDIEC
   PVAL HI 5.01 0 298.15
   PVAL I2 59.0736361 31989.38 298.15

PROP-DATA PLXANT-1
   IN-UNITS MET VOLUME-FLOW='cum/hr' ENTHALPY-FLO='MMkcal/hr'  &
      HEAT-TRANS-C='kcal/hr-sqm-K' PRESSURE=bar TEMPERATURE=K  &
      VOLUME=cum DELTA-T=C HEAD=meter MOLE-DENSITY='kmol/cum'  &
```

```
      MASS-DENSITY='kg/cum' MOLE-ENTHALP='kcal/mol'  &
      MASS-ENTHALP='kcal/kg' HEAT=MMkcal MOLE-CONC='mol/l'  &
      PDROP=bar
   PROP-LIST PLXANT
   PVAL HI 96.04852687 -4602.079856 0 0.024745309  &
      -15.08465485 0 2 237.6 573

PROP-DATA HENRY-1
   IN-UNITS MET VOLUME-FLOW='cum/hr' ENTHALPY-FLO='MMkcal/hr'  &
      HEAT-TRANS-C='kcal/hr-sqm-K' PRESSURE=bar TEMPERATURE=C  &
      VOLUME=cum DELTA-T=C HEAD=meter MOLE-DENSITY='kmol/cum'  &
      MASS-DENSITY='kg/cum' MOLE-ENTHALP='kcal/mol'  &
      MASS-ENTHALP='kcal/kg' HEAT=MMkcal MOLE-CONC='mol/l'  &
      PDROP=bar
   PROP-LIST HENRY
   BPVAL H2 H2O 180.0660745 -6993.510000 -26.31190000  &
      .0150431000 .8500000000 65.85000000
   BPVAL H2 I2 180.0660745 -6993.510000 -26.31190000  &
      .0150431000 .8500000000 65.85000000
   BPVAL H2 HI 177.0660745 -6993.510000 -26.31190000  &
      .0150431000 .8500000000 65.85000000

PROP-DATA NRTL-1
   IN-UNITS MET VOLUME-FLOW='cum/hr' ENTHALPY-FLO='MMkcal/hr'  &
      HEAT-TRANS-C='kcal/hr-sqm-K' PRESSURE=bar TEMPERATURE=K  &
      VOLUME=cum DELTA-T=C HEAD=meter MOLE-DENSITY='kmol/cum'  &
      MASS-DENSITY='kg/cum' MOLE-ENTHALP='kcal/mol'  &
      MASS-ENTHALP='kcal/kg' HEAT=MMkcal MOLE-CONC='mol/l'  &
      PDROP=bar
   PROP-LIST NRTL
   BPVAL I2 H2O -8.0628127 3942.57202 0.3 0 0 0.00336012 0  &
      1000
   BPVAL H2O I2 23.6689347 -1492.3546 0.3 0 0 -0.0347553 0  &
      1000
   BPVAL I2 HI 0.0 223 .200000 0.0 0.0 0.0 0.0 1000.000
   BPVAL HI I2 0.0 223 .200000 0.0 0.0 0.0 0.0 1000.000
   BPVAL HI H2O 0.0 -84 .2 0.0 0.0 0.0 0.0 1000.000
   BPVAL H2O HI 0.0 1380 .2 0.0 0.0 0.0 0.0 1000.000

PROP-DATA GMELCC-1
   IN-UNITS MET VOLUME-FLOW='cum/hr' ENTHALPY-FLO='MMkcal/hr'  &
      HEAT-TRANS-C='kcal/hr-sqm-K' PRESSURE=bar TEMPERATURE=C  &
      VOLUME=cum DELTA-T=C HEAD=meter MOLE-DENSITY='kmol/cum'  &
      MASS-DENSITY='kg/cum' MOLE-ENTHALP='kcal/mol'  &
      MASS-ENTHALP='kcal/kg' HEAT=MMkcal MOLE-CONC='mol/l'  &
      PDROP=bar
```

```
   PROP-LIST GMELCC
   PPVAL H2O ( H3O+ I- ) 1.83749491
   PPVAL ( H3O+ I- ) H2O -1.9033674
   PPVAL HI ( H3O+ I- ) 3.96750955
   PPVAL ( H3O+ I- ) HI 4.60780554
   PPVAL I2 ( H3O+ I- ) 3.1136453
   PPVAL ( H3O+ I- ) I2 20

PROP-DATA GMELCD-1
   IN-UNITS MET VOLUME-FLOW='cum/hr' ENTHALPY-FLO='MMkcal/hr'  &
      HEAT-TRANS-C='kcal/hr-sqm-K' PRESSURE=bar TEMPERATURE=K  &
      VOLUME=cum DELTA-T=C HEAD=meter MOLE-DENSITY='kmol/cum'  &
      MASS-DENSITY='kg/cum' MOLE-ENTHALP='kcal/mol'  &
      MASS-ENTHALP='kcal/kg' HEAT=MMkcal MOLE-CONC='mol/l'  &
      PDROP=bar
   PROP-LIST GMELCD
   PPVAL H2O ( H3O+ I- ) 2259.33865
   PPVAL ( H3O+ I- ) H2O -733.80589
   PPVAL I2 ( H3O+ I- ) -2274.142
   PPVAL ( H3O+ I- ) I2 0

PROP-DATA GMELCE-1
   IN-UNITS MET VOLUME-FLOW='cum/hr' ENTHALPY-FLO='MMkcal/hr'  &
      HEAT-TRANS-C='kcal/hr-sqm-K' PRESSURE=bar TEMPERATURE=C  &
      VOLUME=cum DELTA-T=C HEAD=meter MOLE-DENSITY='kmol/cum'  &
      MASS-DENSITY='kg/cum' MOLE-ENTHALP='kcal/mol'  &
      MASS-ENTHALP='kcal/kg' HEAT=MMkcal MOLE-CONC='mol/l'  &
      PDROP=bar
   PROP-LIST GMELCE
   PPVAL H2O ( H3O+ I- ) 10.8191447
   PPVAL ( H3O+ I- ) H2O -0.8738634

PROP-DATA GMELCN-1
   IN-UNITS MET VOLUME-FLOW='cum/hr' ENTHALPY-FLO='MMkcal/hr'  &
      HEAT-TRANS-C='kcal/hr-sqm-K' PRESSURE=bar TEMPERATURE=C  &
      VOLUME=cum DELTA-T=C HEAD=meter MOLE-DENSITY='kmol/cum'  &
      MASS-DENSITY='kg/cum' MOLE-ENTHALP='kcal/mol'  &
      MASS-ENTHALP='kcal/kg' HEAT=MMkcal MOLE-CONC='mol/l'  &
      PDROP=bar
   PROP-LIST GMELCN
   PPVAL H2O ( H3O+ I- ) .32
   PPVAL I2 ( H3O+ I- ) .32
   PPVAL HI ( H3O+ I- ) .32

PROP-SET CPMX CPMX UNITS='cal/gm-K' SUBSTREAM=MIXED
```

```
PROP-SET XTRUE XTRUE SUBSTREAM=MIXED PHASE=L
;  "True component mole fractions in liquid phase"


STREAM FEED
   SUBSTREAM MIXED TEMP=300. VFRAC=0. MOLE-FLOW=125.8  &
      FREE-WATER=NO NPHASE=2 PHASE=V
   MOLE-FRAC H2O 51. / I2 39. / HI 10.

BLOCK B3 FLASH2
   PARAM TEMP=25. PRES=0.

BLOCK COLUMN RADFRAC
   PARAM NSTAGE=7 NPA=0 ALGORITHM=NONIDEAL MAXOL=100  &
      TOLOL=0.001 LL-METH=EQ-SOLVE NPHASE=2 DAMPING=SEVERE
   COL-CONFIG CONDENSER=PARTIAL-V REBOILER=KETTLE
   FEEDS FEED 5 ON-STAGE
   PRODUCTS BOTTOM 7 L / SIDELIQ 3 L MOLE-FLOW=50. / TOP  &
      1 V / SIDEVAP 3 V MOLE-FLOW=0.01
   P-SPEC 1 45.
   COL-SPECS DP-STAGE=0. MOLE-D=5. MOLE-BR=2.
   REAC-STAGES 1 7 H2-EQUIL
   T-EST 1 254.1 / 2 283.3 / 3 292.4 / 4 297.3 / 5  &
      298.8 / 6 299.3 / 7 297.5
   L-EST 1 81.73 / 2 97.94 / 3 69.99 / 4 83.02 / 5  &
      211.3 / 6 212.4 / 7 70.79
   V-EST 1 5. / 2 86.73 / 3 102.9 / 4 125. / 5 138. /  &
      6 140.5 / 7 141.6
   X-EST 1 H2O 0.87044 / 1 I2 0.014897 / 1 HI 0.1146 /  &
      1 H2 6.5908E-005 / 2 H2O 0.8181 / 2 I2 0.071324 /  &
      2 HI 0.11057 / 2 H2 4.7046E-006 / 3 H2O 0.74169 /  &
      3 I2 0.1472 / 3 HI 0.1111 / 3 H2 1.5166E-006 / 4  &
      H2O 0.65379 / 4 I2 0.24216 / 4 HI 0.10405 / 4 H2  &
      8.8491E-007 / 5 H2O 0.57041 / 5 I2 0.33743 / 5 HI  &
      0.092165 / 5 H2 7.1702E-007 / 6 H2O 0.55243 / 6  &
      I2 0.36037 / 6 HI 0.0872 / 6 H2 5.602E-007 / 7  &
      H2O 0.33942 / 7 I2 0.61157 / 7 HI 0.049013 / 7  &
      H2 6.0167E-007
   Y-EST 1 H2O 0.60752 / 1 I2 0.00016147 / 1 HI 0.073899 / &
      1 H2 0.31842 / 2 H2O 0.85528 / 2 I2 0.01035 / 2  &
      HI 0.11965 / 2 H2 0.014721 / 3 H2O 0.80787 / 3  &
      I2 0.055877 / 3 HI 0.13277 / 3 H2 0.0034801 / 4  &
      H2O 0.73633 / 4 I2 0.13008 / 4 HI 0.13208 / 4 H2  &
      0.0015071 / 5 H2O 0.68397 / 5 I2 0.18841 / 5 HI  &
      0.12666 / 5 H2 0.00096263 / 6 H2O 0.68681 / 6 I2  &
      0.19999 / 6 HI 0.11248 / 6 H2 0.00071653 / 7 H2O  &
```

```
    0.65893 / 7 I2 0.2353 / 7 HI 0.10524 / 7 H2  &
    0.00052939
  PROPERTIES ELECNRTL HENRY-COMPS=HENRY CHEMISTRY=HI-I2  &
    TRUE-COMPS=NO
  BLOCK-OPTION TERM-LEVEL=4 FREE-WATER=NO

EO-CONV-OPTI

SENSITIVITY SIDEFLOW
  DEFINE H2PROD MOLE-FLOW STREAM=TOP SUBSTREAM=MIXED  &
    COMPONENT=H2
  DEFINE BOTXW MOLE-FRAC STREAM=BOTTOM SUBSTREAM=MIXED  &
    COMPONENT=H2O
  DEFINE BOTFW MOLE-FLOW STREAM=BOTTOM SUBSTREAM=MIXED  &
    COMPONENT=H2O
  TABULATE 1 "H2PROD"
  TABULATE 2 "BOTXW"
  TABULATE 3 "BOTFW"
  VARY BLOCK-VAR BLOCK=COLUMN VARIABLE=MOLE-FLOW  &
    SENTENCE=PRODUCTS ID1=SIDELIQ
  RANGE LOWER="50" UPPER="75" INCR="5"

CONV-OPTIONS
  PARAM CHECKSEQ=NO

STREAM-REPOR MOLEFLOW MASSFLOW MOLEFRAC MASSFRAC  &
    PROPERTIES=XTRUE CPMX

PROPERTY-REP NOPCES PROP-DATA DFMS PARAM-PLUS

REACTIONS H2-EQUIL REAC-DIST
  REAC-DATA 1 PHASE=V KBASIS=P
  K-STOIC 1 A=-2.3258476 B=-1233.571
  STOIC 1 HI -2. / I2 1. / H2 1.

REACTIONS H2-HI-EQ REAC-DIST
  REAC-DATA 1 PHASE=V KBASIS=FUG
  REAC-DATA 2
  K-STOIC 1 A=-2.325847579 B=-1233.570988
  K-STOIC 2 A=-228.8380747 B=12587.48013 C=40.68593363  &
    D=-0.098379992
  STOIC 1 HI -2. / I2 1. / H2 1.
  STOIC 2 HI -1. / H2O -1. / H3O+ 1. / I- 1.
```

APPENDIX 6 - INPUT SUMMARY OF SECTION 3 MODEL – REACTDISTVAPDRAW.BKP)

```
TITLE 'Section 3 Model - Reactive Distillation, Vapor Draw'

IN-UNITS MET VOLUME-FLOW='cum/hr' ENTHALPY-FLO='MMkcal/hr'  &
      HEAT-TRANS-C='kcal/hr-sqm-K' PRESSURE=bar TEMPERATURE=C  &
      VOLUME=cum DELTA-T=C HEAD=meter MOLE-DENSITY='kmol/cum'  &
      MASS-DENSITY='kg/cum' MOLE-ENTHALP='kcal/mol'  &
      MASS-ENTHALP='kcal/kg' HEAT=MMkcal MOLE-CONC='mol/l'  &
      PDROP=bar

DEF-STREAMS CONVEN ALL

SIM-OPTIONS FLASH-TOL=1E-007 HF-FL3-DAMP=YES MAXSOL-CHECK=NO

RUN-CONTROL MAX-TIME=9999.

DESCRIPTION "
   Electrolytes Simulation with Metric Units :
   C, bar, kg/hr, kmol/hr, MMkcal/hr, cum/hr.

   Property Method: ELECNRTL

   Flow basis for input: Mass

   Stream report composition: Mass flow
   "

DATABANKS ASPENPCD  / AQUEOUS  / SOLIDS  / INORGANIC  /  &
      PURE10

PROP-SOURCES ASPENPCD  / AQUEOUS  / SOLIDS  / INORGANIC  /  &
      PURE10

COMPONENTS
   H2O H2O /
   I2 I2 /
   HI HI /
   I- I- /
   H3O+ H3O+ /
   I2-S I2 /
   H2 H2
```

```
HENRY-COMPS HENRY H2

CHEMISTRY FULL
   STOIC 1 HI -1. / H2O -1. / H3O+ 1. / I- 1.
   STOIC 3 HI -2. / I2 1. / H2 1.
   K-STOIC 3 A=17.38265099 B=-14058.06029 C=9.099622987  &
      D=-0.110628785
   SALT I2-S I2 1.
   K-SALT I2-S A=-9.228072963 B=-1083.684565 C=2.019221642

CHEMISTRY HI-H2
   STOIC 1 HI -1. / H2O -1. / H3O+ 1. / I- 1.
   STOIC 2 HI -2. / I2 1. / H2 1.

CHEMISTRY HI-I2
   STOIC 1 HI -1. / H2O -1. / H3O+ 1. / I- 1.
   K-STOIC 1 A=-228.8380747 B=12587.48013 C=40.68593363  &
      D=-0.098379992

FLOWSHEET
   BLOCK COLUMN IN=FEED OUT=TOP BOTTOM SIDELIQ SIDEVAP
   BLOCK H2COND IN=TOP OUT=H2PROD COND

PROPERTIES ELECNRTL HENRY-COMPS=HENRY CHEMISTRY=HI-I2  &
      TRUE-COMPS=NO
   PROPERTIES NRTL-RK

PROP-REPLACE ELECNRTL ELECNRTL
   MODEL VL0CONS

PROP-DATA
   PROP-LIST ATOMNO / NOATOM
   PVAL H3O+ 1 8 / 3. 1.

PROP-DATA HI-PROPS
   IN-UNITS MET VOLUME-FLOW='cum/hr' ENTHALPY-FLO='MMkcal/hr'  &
      HEAT-TRANS-C='kcal/hr-sqm-K' PRESSURE=bar TEMPERATURE=K  &
      VOLUME=cum DELTA-T=C HEAD=meter MOLE-DENSITY='kmol/cum'  &
      MASS-DENSITY='kg/cum' MOLE-ENTHALP='kcal/mol'  &
      MASS-ENTHALP='kcal/kg' HEAT=MMkcal MOLE-CONC='mol/l'  &
      PDROP=bar
   PROP-LIST TC / PC / RKTZRA
   PVAL HI 423.85 / 83.1 / 0.31499751

PROP-DATA I-
   IN-UNITS MET VOLUME-FLOW='cum/hr' ENTHALPY-FLO='MMkcal/hr'  &
```

```
      HEAT-TRANS-C='kcal/hr-sqm-K' PRESSURE=bar TEMPERATURE=C  &
      VOLUME=cum DELTA-T=C HEAD=meter MOLE-DENSITY='kmol/cum'  &
      MASS-DENSITY='kg/cum' MOLE-ENTHALP='kcal/mol'  &
      MASS-ENTHALP='kcal/kg' HEAT=MMkcal MOLE-CONC='mol/l'  &
      PDROP=bar
   PROP-LIST DHAQFM
   PVAL I- -13.181905

PROP-DATA VLCONS
   IN-UNITS MET VOLUME-FLOW='cum/hr' ENTHALPY-FLO='MMkcal/hr'  &
      HEAT-TRANS-C='kcal/hr-sqm-K' PRESSURE=bar TEMPERATURE=C  &
      VOLUME=cum DELTA-T=C HEAD=meter MOLE-DENSITY='kmol/cum'  &
      MASS-DENSITY='kg/cum' MOLE-ENTHALP='kcal/mol'  &
      MASS-ENTHALP='kcal/kg' HEAT=MMkcal MOLE-CONC='mol/l'  &
      PDROP=bar
   PROP-LIST VLCONS
   PVAL H2O 19.63607
   PVAL I2 68.081606
   PVAL HI 45.675239
   PVAL H2 28.612729

PROP-DATA VLSTD
   IN-UNITS MET VOLUME-FLOW='cum/hr' ENTHALPY-FLO='MMkcal/hr'  &
      HEAT-TRANS-C='kcal/hr-sqm-K' PRESSURE=bar TEMPERATURE=C  &
      VOLUME=cum DELTA-T=C HEAD=meter MOLE-DENSITY='kmol/cum'  &
      MASS-DENSITY='kg/cum' MOLE-ENTHALP='kcal/mol'  &
      MASS-ENTHALP='kcal/kg' HEAT=MMkcal MOLE-CONC='mol/l'  &
      PDROP=bar
   PROP-LIST VLSTD
   PVAL I- 100
   PVAL H3O+ 100

PROP-DATA CPDIEC-1
   IN-UNITS MET VOLUME-FLOW='cum/hr' ENTHALPY-FLO='MMkcal/hr'  &
      HEAT-TRANS-C='kcal/hr-sqm-K' PRESSURE=bar TEMPERATURE=C  &
      VOLUME=cum DELTA-T=C HEAD=meter MOLE-DENSITY='kmol/cum'  &
      MASS-DENSITY='kg/cum' MOLE-ENTHALP='kcal/mol'  &
      MASS-ENTHALP='kcal/kg' HEAT=MMkcal MOLE-CONC='mol/l'  &
      PDROP=bar
   PROP-LIST CPDIEC
   PVAL HI 5.01 0 298.15
   PVAL I2 59.0736361 31989.38 298.15

PROP-DATA PLXANT-1
   IN-UNITS MET VOLUME-FLOW='cum/hr' ENTHALPY-FLO='MMkcal/hr'  &
      HEAT-TRANS-C='kcal/hr-sqm-K' PRESSURE=bar TEMPERATURE=K  &
```

```
      VOLUME=cum DELTA-T=C HEAD=meter MOLE-DENSITY='kmol/cum'  &
      MASS-DENSITY='kg/cum' MOLE-ENTHALP='kcal/mol'  &
      MASS-ENTHALP='kcal/kg' HEAT=MMkcal MOLE-CONC='mol/l'  &
      PDROP=bar
   PROP-LIST PLXANT
   PVAL HI 96.04852687 -4602.079856 0 0.024745309  &
      -15.08465485 0 2 237.6 573

PROP-DATA HENRY-1
   IN-UNITS MET VOLUME-FLOW='cum/hr' ENTHALPY-FLO='MMkcal/hr'  &
      HEAT-TRANS-C='kcal/hr-sqm-K' PRESSURE=bar TEMPERATURE=C  &
      VOLUME=cum DELTA-T=C HEAD=meter MOLE-DENSITY='kmol/cum'  &
      MASS-DENSITY='kg/cum' MOLE-ENTHALP='kcal/mol'  &
      MASS-ENTHALP='kcal/kg' HEAT=MMkcal MOLE-CONC='mol/l'  &
      PDROP=bar
   PROP-LIST HENRY
   BPVAL H2 H2O 180.0660745 -6993.510000 -26.31190000  &
      .0150431000 .8500000000 65.85000000
   BPVAL H2 I2 180.0660745 -6993.510000 -26.31190000  &
      .0150431000 .8500000000 65.85000000
   BPVAL H2 HI 177.0660745 -6993.510000 -26.31190000  &
      .0150431000 .8500000000 65.85000000

PROP-DATA NRTL-1
   IN-UNITS MET VOLUME-FLOW='cum/hr' ENTHALPY-FLO='MMkcal/hr'  &
      HEAT-TRANS-C='kcal/hr-sqm-K' PRESSURE=bar TEMPERATURE=K  &
      VOLUME=cum DELTA-T=C HEAD=meter MOLE-DENSITY='kmol/cum'  &
      MASS-DENSITY='kg/cum' MOLE-ENTHALP='kcal/mol'  &
      MASS-ENTHALP='kcal/kg' HEAT=MMkcal MOLE-CONC='mol/l'  &
      PDROP=bar
   PROP-LIST NRTL
   BPVAL I2 H2O -8.0628127 3942.57202 0.3 0 0 0.00336012 0  &
      1000
   BPVAL H2O I2 23.6689347 -1492.3546 0.3 0 0 -0.0347553 0  &
      1000
   BPVAL I2 HI 0.0 223 .200000 0.0 0.0 0.0 0.0 1000.000
   BPVAL HI I2 0.0 223 .200000 0.0 0.0 0.0 0.0 1000.000
   BPVAL HI H2O 0.0 -84 .2 0.0 0.0 0.0 0.0 1000.000
   BPVAL H2O HI 0.0 1380 .2 0.0 0.0 0.0 0.0 1000.000

PROP-DATA GMELCC-1
   IN-UNITS MET VOLUME-FLOW='cum/hr' ENTHALPY-FLO='MMkcal/hr'  &
      HEAT-TRANS-C='kcal/hr-sqm-K' PRESSURE=bar TEMPERATURE=C  &
      VOLUME=cum DELTA-T=C HEAD=meter MOLE-DENSITY='kmol/cum'  &
      MASS-DENSITY='kg/cum' MOLE-ENTHALP='kcal/mol'  &
      MASS-ENTHALP='kcal/kg' HEAT=MMkcal MOLE-CONC='mol/l'  &
```

```
      PDROP=bar
   PROP-LIST GMELCC
   PPVAL H2O ( H3O+ I- ) 1.83749491
   PPVAL ( H3O+ I- ) H2O -1.9033674
   PPVAL HI ( H3O+ I- ) 3.96750955
   PPVAL ( H3O+ I- ) HI 4.60780554
   PPVAL I2 ( H3O+ I- ) 3.1136453
   PPVAL ( H3O+ I- ) I2 20

PROP-DATA GMELCD-1
   IN-UNITS MET VOLUME-FLOW='cum/hr' ENTHALPY-FLO='MMkcal/hr'  &
      HEAT-TRANS-C='kcal/hr-sqm-K' PRESSURE=bar TEMPERATURE=K  &
      VOLUME=cum DELTA-T=C HEAD=meter MOLE-DENSITY='kmol/cum'  &
      MASS-DENSITY='kg/cum' MOLE-ENTHALP='kcal/mol'  &
      MASS-ENTHALP='kcal/kg' HEAT=MMkcal MOLE-CONC='mol/l'  &
      PDROP=bar
   PROP-LIST GMELCD
   PPVAL H2O ( H3O+ I- ) 2259.33865
   PPVAL ( H3O+ I- ) H2O -733.80589
   PPVAL I2 ( H3O+ I- ) -2274.142
   PPVAL ( H3O+ I- ) I2 0

PROP-DATA GMELCE-1
   IN-UNITS MET VOLUME-FLOW='cum/hr' ENTHALPY-FLO='MMkcal/hr'  &
      HEAT-TRANS-C='kcal/hr-sqm-K' PRESSURE=bar TEMPERATURE=C  &
      VOLUME=cum DELTA-T=C HEAD=meter MOLE-DENSITY='kmol/cum'  &
      MASS-DENSITY='kg/cum' MOLE-ENTHALP='kcal/mol'  &
      MASS-ENTHALP='kcal/kg' HEAT=MMkcal MOLE-CONC='mol/l'  &
      PDROP=bar
   PROP-LIST GMELCE
   PPVAL H2O ( H3O+ I- ) 10.8191447
   PPVAL ( H3O+ I- ) H2O -0.8738634

PROP-DATA GMELCN-1
   IN-UNITS MET VOLUME-FLOW='cum/hr' ENTHALPY-FLO='MMkcal/hr'  &
      HEAT-TRANS-C='kcal/hr-sqm-K' PRESSURE=bar TEMPERATURE=C  &
      VOLUME=cum DELTA-T=C HEAD=meter MOLE-DENSITY='kmol/cum'  &
      MASS-DENSITY='kg/cum' MOLE-ENTHALP='kcal/mol'  &
      MASS-ENTHALP='kcal/kg' HEAT=MMkcal MOLE-CONC='mol/l'  &
      PDROP=bar
   PROP-LIST GMELCN
   PPVAL H2O ( H3O+ I- ) .32
   PPVAL I2 ( H3O+ I- ) .32
   PPVAL HI ( H3O+ I- ) .32

PROP-SET CPMX CPMX UNITS='cal/gm-K' SUBSTREAM=MIXED
```

```
PROP-SET XTRUE XTRUE SUBSTREAM=MIXED PHASE=L
;  "True component mole fractions in liquid phase"


STREAM FEED
   SUBSTREAM MIXED TEMP=300. VFRAC=0. MOLE-FLOW=125.8  &
      FREE-WATER=NO NPHASE=2 PHASE=V
   MOLE-FRAC H2O 51. / I2 39. / HI 10.

BLOCK H2COND FLASH2
   PARAM TEMP=25. PRES=0.

BLOCK COLUMN RADFRAC
   PARAM NSTAGE=7 NPA=0 ALGORITHM=NONIDEAL MAXOL=100  &
      TOLOL=0.001 LL-METH=EQ-SOLVE NPHASE=2 DAMPING=SEVERE
   COL-CONFIG CONDENSER=PARTIAL-V REBOILER=KETTLE
   FEEDS FEED 5 ON-STAGE
   PRODUCTS BOTTOM 7 L / SIDELIQ 3 L MOLE-FLOW=0.01 / TOP  &
      1 V / SIDEVAP 3 V MOLE-FLOW=65.
   P-SPEC 1 45.
   COL-SPECS DP-STAGE=0. MOLE-D=5. MOLE-BR=2.
   REAC-STAGES 1 7 H2-EQUIL
   T-EST 1 279.6 / 2 293.6 / 3 297.7 / 4 298.6 / 5  &
      299. / 6 299.5 / 7 293.7
   L-EST 1 27.97 / 2 36.08 / 3 41.47 / 4 42.05 / 5  &
      164.9 / 6 167.4 / 7 55.79
   V-EST 1 5. / 2 32.97 / 3 41.08 / 4 111.5 / 5 112.1 / &
      6 109.1 / 7 111.6
   X-EST 1 H2O 0.78822 / 1 I2 0.085191 / 1 HI 0.12658 /  &
      1 H2 1.4145E-005 / 2 H2O 0.71926 / 2 I2 0.1683 /  &
      2 HI 0.11244 / 2 H2 1.6259E-006 / 3 H2O 0.63274 /  &
      3 I2 0.26479 / 3 HI 0.10247 / 3 H2 8.858E-007 /  &
      4 H2O 0.57934 / 4 I2 0.32644 / 4 HI 0.094222 / 4  &
      H2 7.7414E-007 / 5 H2O 0.53347 / 5 I2 0.37983 / 5  &
      HI 0.086697 / 5 H2 7.3458E-007 / 6 H2O 0.53032 /  &
      6 I2 0.386 / 6 HI 0.083683 / 6 H2 5.5273E-007 /  &
      7 H2O 0.25121 / 7 I2 0.71353 / 7 HI 0.035264 / 7  &
      H2 6.9707E-007
   Y-EST 1 H2O 0.70292 / 1 I2 0.014439 / 1 HI 0.24059 /  &
      1 H2 0.04205 / 2 H2O 0.77528 / 2 I2 0.071543 / 2  &
      HI 0.1497 / 2 H2 0.0034711 / 3 H2O 0.71727 / 3  &
      I2 0.14587 / 3 HI 0.13545 / 3 H2 0.0014157 / 4  &
      H2O 0.68517 / 4 I2 0.18258 / 4 HI 0.13119 / 4 H2  &
      0.0010648 / 5 H2O 0.66486 / 5 I2 0.20598 / 5 HI  &
      0.12826 / 5 H2 0.00090347 / 6 H2O 0.6778 / 6 I2  &
```

```
      0.20988 / 6 HI 0.11165 / 6 H2 0.00067324 / 7 H2O  &
      0.66987 / 7 I2 0.2228 / 7 HI 0.10676 / 7 H2  &
      0.00056708
   PROPERTIES ELECNRTL HENRY-COMPS=HENRY CHEMISTRY=HI-I2  &
      TRUE-COMPS=NO
   BLOCK-OPTION TERM-LEVEL=4 FREE-WATER=NO

EO-CONV-OPTI

CONV-OPTIONS
   PARAM CHECKSEQ=NO

STREAM-REPOR MOLEFLOW MASSFLOW MOLEFRAC MASSFRAC  &
      PROPERTIES=XTRUE CPMX

PROPERTY-REP NOPCES PROP-DATA DFMS PARAM-PLUS

REACTIONS H2-EQUIL REAC-DIST
   REAC-DATA 1 PHASE=V KBASIS=P
   K-STOIC 1 A=-2.3258476 B=-1233.571
   STOIC 1 HI -2. / I2 1. / H2 1.

REACTIONS H2-HI-EQ REAC-DIST
   REAC-DATA 1 PHASE=V KBASIS=FUG
   REAC-DATA 2
   K-STOIC 1 A=-2.325847579 B=-1233.570988
   K-STOIC 2 A=-228.8380747 B=12587.48013 C=40.68593363  &
      D=-0.098379992
   STOIC 1 HI -2. / I2 1. / H2 1.
   STOIC 2 HI -1. / H2O -1. / H3O+ 1. / I- 1.
```

REFERENCES

[1] International Energy Outlook 2000: DOE/EIA-0484(2000), The Energy Information Administration of the Department of Energy (www.eia.doe.gov).

[2] Annual Energy Outlook 2000 with projections to 2020: DOE/EIA-0383 (2000), The Energy Information Administration of the Department of Energy (www.eia.doe.gov).

[3] Norman, J.H, Besenbruch, G.E., Brown, L.C., O'Keefe, D.R., and Allen, C.L., "Thermochemical Water-Splitting Cycle, Bench-Scale Investigations, and Process Engineering," final report for the period February 1977 through December 31, 1981, DOE/ET/26225-1, GA-A16713, May 1982.

[4] Brown, L.C., Bresenbruch, G. E., Funk, J. E., Marshall, A. C., Pickard, P. S., and Showalter, "High Efficiency Generation of Hydrogen Fuel Using Nuclear Power," presented at the AIChE Spring National Meeting, New Orleans, March 11-15, 2002.

[5] Roth, M., and Knoche, K.F., "Thermochemical Water Splitting Through Direct HI-Decomposition from $H_2O/HI/I_2$ Solutions," J. Hydrogen Energy, 14, 545-549 (1989).

[6] Chen, C-C., Britt, H.I., Boston, J.F., and Evans, L.B., "Extension and Application of the Pitzer Equation for Vapor-Liquid Equilibrium of Aqueous Electrolyte Systems with Molecular Species," AIChE J., 25, 820 (1979).

[7] Chen, C-C., Britt, H.I., Boston, J.F., and Evans, L.B., "Local Composition Model for Excess Gibbs Energy of Electrolyte Systems," AIChE J., 28, 588 (1982).

[8] Chen, C-C. and Evans, L.B., "A Local Composition Model for the Excess Gibbs Energy of Aqueous Electrolyte Systems," AIChE J., 32, 444 (1986).

[9] Aspen Plus Electrolytes Manual, Aspen Technology, Inc. August, 1988.

[10] Wüster, Günter, "p, v, T – und Dampfdruckmessungen zur Bestimmung Thermodynamischer Eigenschaften Starker Elektrolyte bei Erhöhtem Druck," doctoral thesis, University of Aachen (1979).

[11] Mathias, P. M., Chen, C-C, Zou, B. Randolph III, D. L., and Doering, F. J., "A Representation of the Thermodynamic Properties of Sulfuric Acid and Oleum," presented at the AIChE Annual Meeting, Reno, NE, 4-9 November, 2001.

[12] Randolph III, D. L., Doering, F. J., and Mathias, P. M., "Process Simulation of Sulfuric Acid Plants with the Correct Physical Properties," presented at Clearwater 2002, Annual Convention on Phosphate Fertilizer & Sulfuric Acid Technology, Sheraton Sand Key Resort, Clearwater Beach, Florida, June 14- 15, 2002.

[13] Gmitro, J. I., and Vermeulen, t., Vapor-Liquid Equilibrium for Aqueous Sulfuric Acid," AIChE Journal, 10, 740 (1964).

[14] Kim, S. H., and Roth, M., "Enthalpies of Dilution and Excess Molar Enthalpies of an Aqueous Solution of Sulfuric Acid," J. Chem. Eng. Data, 46, 138-14 (2001).

[15] Fasullo, o. T., "Sulfuric Acid: Use and Handling,' mc-Graw-Hill, New York, 1965.

[16] Kracek, F. C., "Solubilities in the System Water-Iodine to 200°C, J. Phys. Chem. 35, 417 (1931).

[17] O'Keefe, D. R., and Norman, J. H., "Vapor Pressure, Iodine Solubility and Hydrogen

[18] Neumann, Dirk, "Phasengleichgewichte von HJ/H2O/J2 – Lösungen," thesis, Lehrstuhl für Thermodynamik, RWTH Aachen, 5100 Aachen, Germany (1987).

[19] CRC Handbook of Chemistry and Physics, 56th Edition (1975).

[20] Haase, R., Naas, H., and Thumm, H., : Z. Phys. Chem. NF, 37, 210 (1963).

[21] Norman, J. H., liquid-liquid equilibrium data for the HI-I2-H2O ternary system (1984)

[22] Engels, H., and Knoche, K. F., "Vapor Pressures of the System HI/H2O/I2 and H2," Int. J. Hydrogen Energy, 11, 703 (1986)

[23] Roth, M., and Knoche, K.F., "Thermochemical Water Splitting Through Direct HI-Decomposition from $H_2O/HI/I_2$ Solutions," J. Hydrogen Energy, 14, 545-549 (1989).

[24] Sakurai, M., Nakajima, H., Onuki, K., and Shimizu, S., "Preliminary Process Analysis for the Closed Cycle Operation of the Iodine-Sulfur Thermochemical Hydrogen Production Process," Int. J. Hydrogen Energy, **24**, 603-612 (1999).

[25] Sakurai, M., Nakajima, H., Onuki, K., and Shimizu, S., "Investigation of the 2-Liquid Phase Separation Characteristics on the Iodine-Sulfur Thermochemical Hydrogen Production Process" Int. J. Hydrogen Energy, **25**, 605-611 (2000).

[26] Sakurai, M, personal communication, July 2002.

APPENDIX D
SYSTEM MODEL FOR HYBRID H_2-PRODUCTION/ELECTRICAL POWER SYSTEM REACTOR

System Model for Hybrid H_2-Production/Electrical Power Reactor System

by

Al Marshal, Sandia National Laboratories

1. Background

Hydrogen may someday provide a clean and bountiful alternative to fossil fuels. One possible approach for generating hydrogen uses a high temperature nuclear reactor as a heat source along with a sulfur-iodine thermochemical cycle. The basic process for hydrogen production for a sulfur-iodine cycle is carried out using the following cycle reactions [1].

(1) $H_2SO_4 \rightarrow SO_2 + H_2O + \_ O_2$ 850 C

(2) $2HI \rightarrow I_2 + H_2$ 300 C

(3) $H_2O + SO_2 + I_2 \rightarrow 2HI + H_2SO_4$ 100 C

The lower temperature requirements for the HI decomposition loop suggest that an electrical power production topping cycle can be used to provide electricity needed to operate the system and to provide surplus electrical power. By using a topping cycle the net efficiency for a hydrogen production system may be improved.

This memorandum describes a simple MATHCAD model for the analysis of a hybrid hydrogen production/electrical power generation reactor system. Although the model assumes a gas-cooled reactor with a He coolant, all H_2 production and electricity production processes take place on the secondary side of a heat exchanger. Thus, other types of high-temperature reactor systems can be studied by modifying only the reactor model.

The MATHCAD model actually consists of three separate models:

1. A hydrogen production reactor system (no electricity generation).
2. An electrical production reactor system (no hydrogen production).
3. A hybrid hydrogen production / electricity generation system.

Systems 1 and 2 are included to assess the effectiveness of the hybrid system relative to hydrogen-only and electrical power-only systems.

2. Model Components:

The three types of systems and the model components for those systems are discussed in the following:

2.1 Hydrogen Production System

The basic components of the hydrogen production system model are illustrated schematically in Fig. 1. The model components include the reactor, the sulfuric acid decomposition subsystem, and the hydrogen iodide decomposition subsystem. The nuclear reactor provides the heat required for the sulfuric acid decomposition and the HI decomposition loops. Heat is passed to these loops through heat exchange surfaces. The sulfuric acid production process ($SO_2+I_2+2H_2O \rightarrow H_2SO_4 + 2HI$) is exothermic and does not require heat addition to achieve reaction temperatures; consequently, for simplicity, this process is not explicitly modeled.

A simplified schematic of the helium side of the sulfuric acid decomposition subsystem, is shown in Fig. 2 for a system using an intermediate heat exchanger between the reactor helium and the helium flowing through the sulfuric acid decomposition subsystem. For this example the maximum and minimum helium temperatures are 947 C and 340 C [2]. The sulfuric acid decomposition subsystem requirements are included in this preliminary model by assuming a single heat exchanger path (HX1), without an intermediate heat exchanger. The thermal power requirements and inlet and outlet temperatures across the entire loop are specified. In addition, an approximation is used to account for entrance and exit pressure drop losses for the multiple heat exchange interfaces (as well as other pressure losses). The same approach is used for the HI decomposition loop (approximated by a single heat exchanger, HX3).

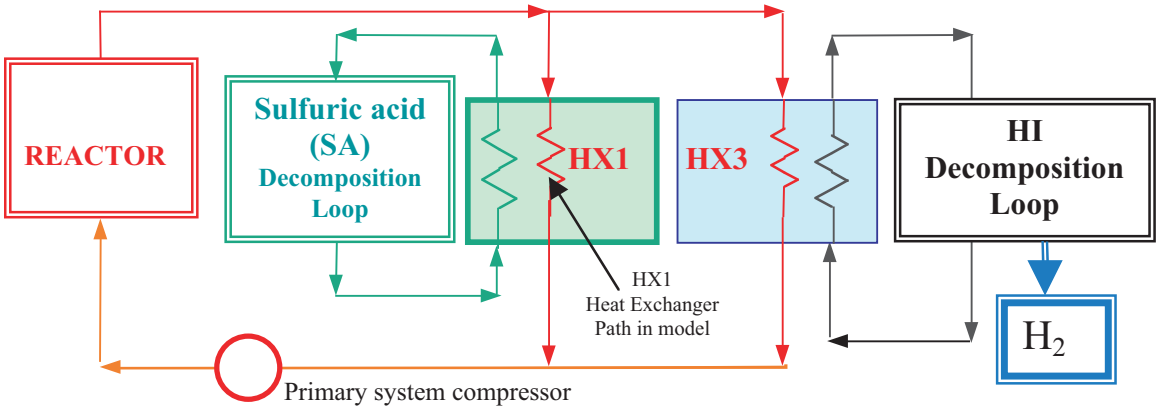

Fig. 1 Reactor hydrogen production system model components

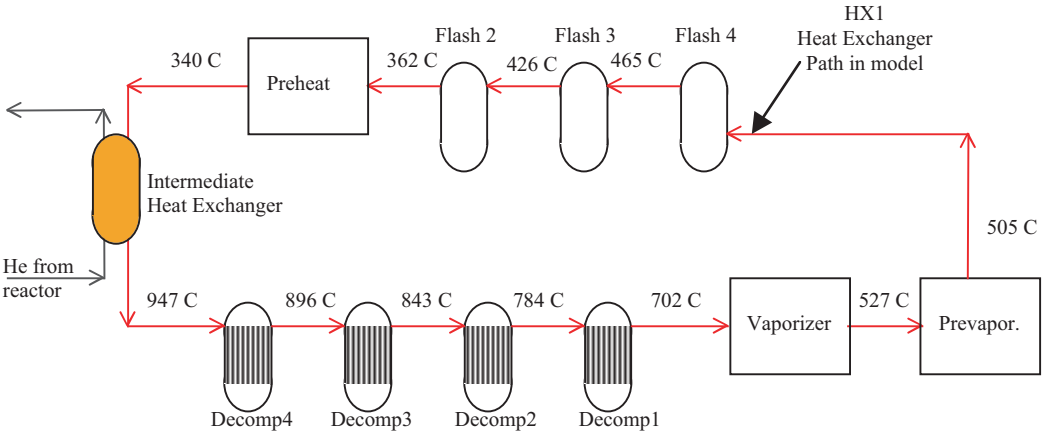

Fig. 2 Simplified schematic of helium side of sulfuric acid decomposition loop.

2.2 Electricity Generation System

The basic components of the model for the reactor-electrical power system are illustrated in Fig. 3. The model assumes a direct Brayton electrical power cycle using two compression stages with inter-cooling and a recuperator.

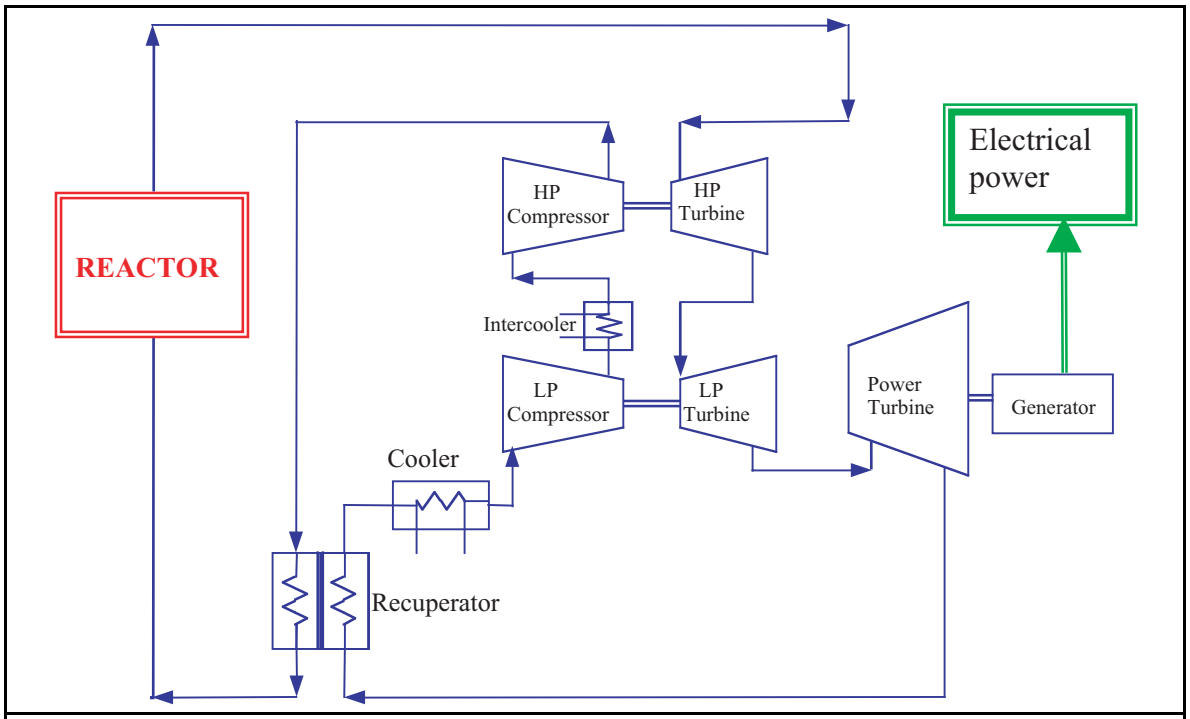

Fig. 3 Gas cooled reactor electrical generation system.

2.3 Hydrogen/Electricity Generation System

The basic model components of the hybrid system are illustrated in Fig. 4. The components include the reactor and primary loop, the sulfuric acid decomposition

subsystem, the electrical power generation subsystem, and the hydrogen iodide decomposition subsystem. It is assumed that essentially all of the heat transferred to the sulfuric acid decomposition loop at Heat Exchanger 1 (HX1) is used within the cycle [2]. A heat exchanger (HX2) is used with a secondary side Brayton cycle in order to allow the flow to be divided between the sulfuric acid decomposition loop (approximately constant pressure) and the electrical power loop (isentropic expansion). As discussed previously, an electrical power production topping cycle is used to provide electricity needed to operate the system and to produce surplus electrical power. The helium exiting from the power turbine passes through a HX3 to provide heat for the HI decomposition process before entering the recuperator.

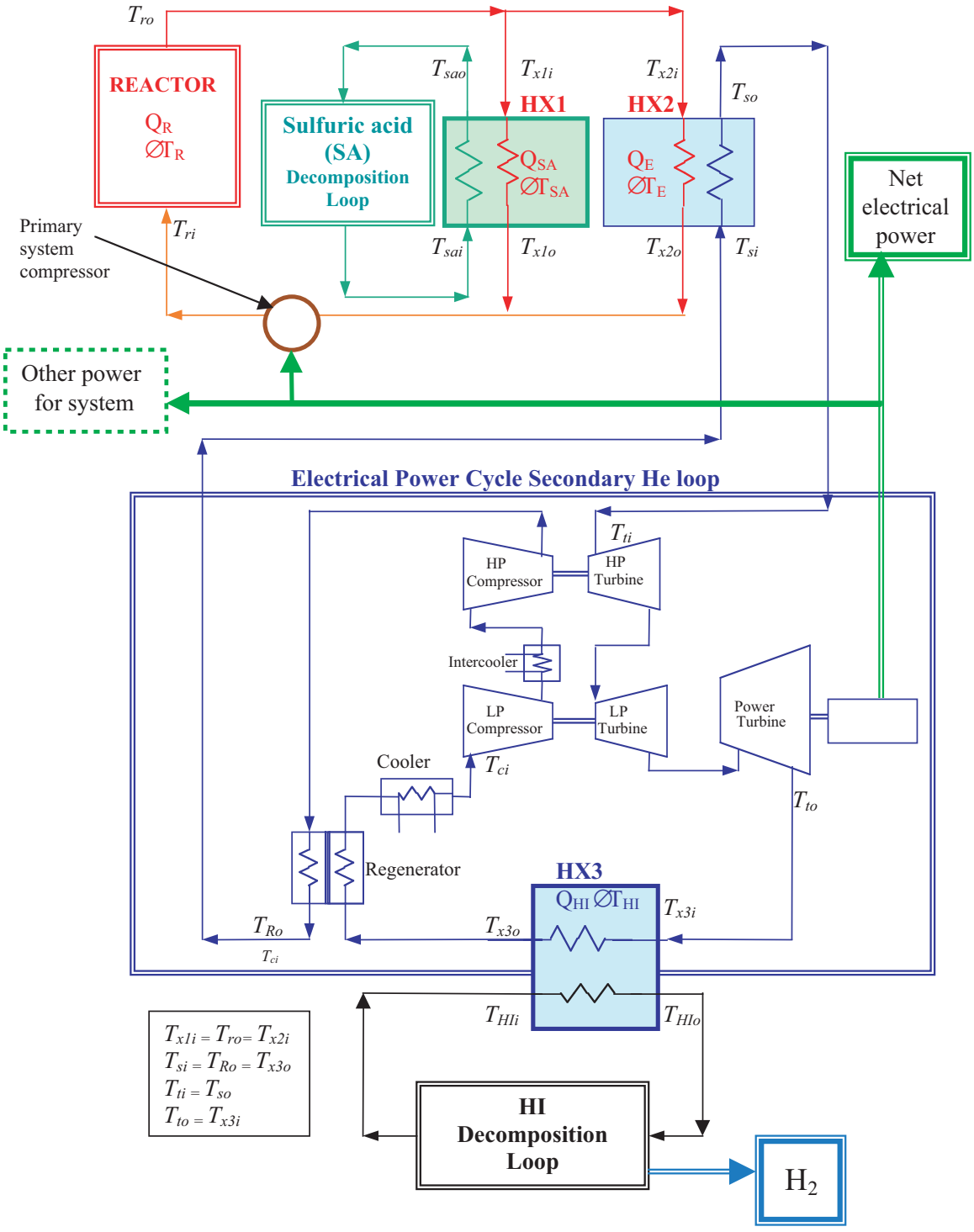

Fig. 4. Schematic Flow Diagram of a Hybrid H2/Electricity Production System

3. Model Input Requirements

The MATHCAD models are incorporated in the reverse of the order discussed in Sections 1 and 2; i.e., the hybrid system is discussed first, the electrical power-only system

next, and the hydrogen production-only system last. The input data required for these models is presented in the following:

3.1 Hybrid System

HQ Energy released (Ws/per gram of H_2)

Hpr Hydrogen production rate desired (kg/hr)

Esa Total energy required for sulfuric acid decompos. cycle per kg H_2 (Whr/kg H_2)

Ehi Total energy required for HI decompos. cycle per kg H_2 produced (Whr/kg H_2)

Pden Core power density

LD Core length to diameter ratio

Tw Cooling water average temperature (K)

Tsao Heat exchanger 1 sulfuric acid loop outlet temperature (K)

Thio Heat exchanger 3 hydrogen iodide loop outlet temperature (K)

Tsai Heat exchanger 1 sulfuric acid loop inlet temperature (K)

Thii Heat exchanger 3 hydrogen iodide loop inlet temperature (K)

ΔTr Reactor temperature difference (outlet-inlet) (K)

ε1 Heat exchanger 1 effectiveness

ε2 Heat exchanger 2 effectiveness

ε3 Heat exchanger 3 effectiveness

εR Recuperator effectiveness

De Core flow channel hydraulic diameter (cm)

D1 HX1 flow channel hydraulic diameter (cm)

D2 HX2 flow channel hydraulic diameter (cm)

D3 HX3 flow channel hydraulic diameter (cm)

DR Recuperator flow channel hydraulic diameter (cm)

fc (Core flow cross section area)/(core cross section area)

FHX1 (Heat exchanger 1 flow cross section area)/(core flow cross section area)

FHX2 (Heat exchanger 2 flow cross section area)/(core flow cross section area)

FHX3 (Heat exchanger 3 flow cross section area)/(core flow cross section area)

FR (1-side of the recuperator flow cross section area)/(core flow area)

p Core outlet pressure (Mpa)

LDsa Length/D1 pressure loss adjustment for entrance, exits, etc for HX1 loop

LDhi Length/D3 pressure loss adjustment for entrance, exits, etc for HX3 loop

LDe Length/DR pressure loss adjustment for entrance, exits, etc for Brayton loop

γ Specific heat ratio for helium

cp Specific heat at constant pressure for helium (Ws/gK)

ηc Compressor efficiency

ηt Turbine efficiency

Ne Primary compressor power multiplier to obtain electrical power to operate system

Qeth Range of additional thermal power studied for electricity production (W)

3.2 Electricity-only System (additional input data)

Teti Range of turbine inlet temperatures (K)

rp Pressure ratio

3.3 Hydrogen-only System (modified input data)

Ne Primary compressor power multiplier to obtain electrical power to operate system

4. Calculational Model

In the following, the basic computational model and some preliminary predictions are presented for the three system types:

4.1 Hybrid System

Helium temperatures

Tx1i = Tsai +(1/ε1)(Tsao –Tsai)	**HX1 T_{inlet} (helium)** Required temperature for given heat exchanger effectiveness [3] for ΔT on He side is less than ΔT on H_2SO_4 side. Assumes no intermediate loop between reactor and H_2SO_4 decomposition loop,
Tro = Tx1i	**Reactor T_{outlet} (helium)** = HX1 inlet temperature
Tri = Tro – ΔTr	**Reactor T_{inlet} (helium)**
Tx1o = Tri	**HX 1 T_{outlet} (helium)** = reactor inlet temp
Tx2i = Tx1i	**HX2 T_{inlet} (helium)** Same as HX1
Tx2o = Tx1o	**HX2 T_{outlet} (helium)** Same as HX1

Power requirements

Qsa = Hpr x Esa	**Thermal power for sulfuric acid decomp. loop** (W)
Qhi = Hpr x Ehi (W)	**Thermal power for hydrogen iodide decomp. loop**
QH=Qsa + Qh	**Total thermal power for hydrogen production** (W)
P = QH + Qeth	**Total reactor power required** (W)

Secondary Side Temperatures

$Tx3i = Thii + (1/\varepsilon 3)(Thio - Thii)$

HX 3 T_{inlet} (helium)

Required temperature for ΔT on He side is < ΔT on hydrogen-iodide side

$Tx2i = Tsi + (1/\varepsilon 2)(Tso - Tsi)$ (1)

$mrs\ (cp)\ (Tso - Tsi) = Qeth + Qhi$ (2)

$mrs\ (cp)\ (Tx3i - Tsi) = Qhi$ (3)

(mrs = mass flow rate on secondary side)

Three simultaneous equations were solved to obtain the expressions for computing the three unknowns Tso, Tsi, and mrs -used in the following:

$\alpha = 1 + Qeth/Qhi$

HX2 secondary side helium T_{inlet}

Define α & β, use to compute Tsi

$\beta = (1 + \alpha)/\varepsilon 2$

$Tsi = (Tx2i - \beta\ Tx3i)/(1 - \beta)$

$Tso = (1 + \alpha)(Tx3i - Tsi) + Tsi$

HX2 secondary side helium T_{outlet}

Use α & β to compute Tso.

$Tto = Tx3i$

Turbine T_{outlet}

Must equal required HX3 inlet temp.

$Tti = Tso$

Turbine T_{outlet}

Equals secondary outlet temp.

$Tci = Tw$

Compressor T_{inlet}

Equals cooling water temp.

$Tx3o = Tsi$

HX3 T_{outlet}

Equals secondary inlet temp.

Plots of helium temperatures for the reactor outlet, turbine inlet, turbine outlet, and the secondary side inlet are presented as a function of the excess thermal power used for

electricity generation (Qeth) in Fig. 5. A hydrogen production rate of 10^3 kg/hr was used to generate Fig. 5.

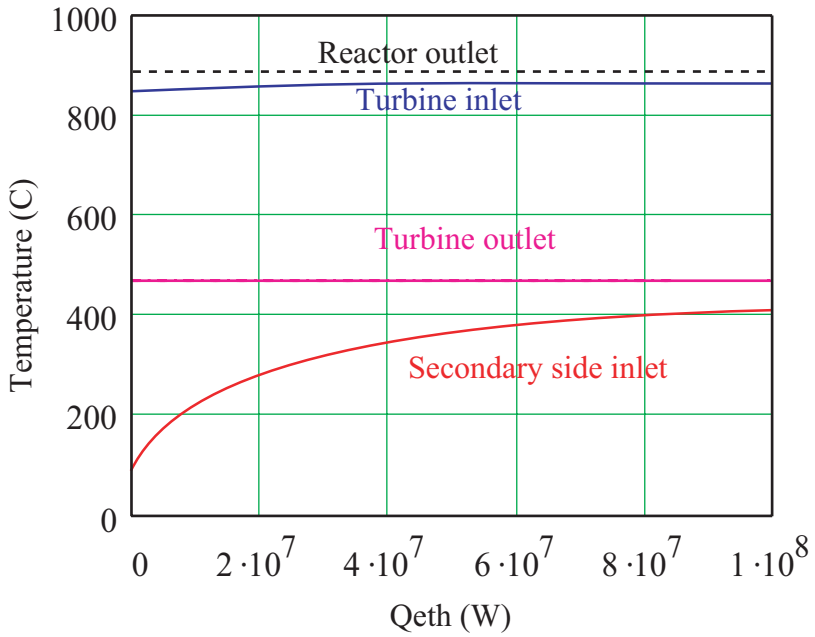

Fig. 5 Hybrid system temperatures vs. Qeth.

Mass Flow Rates and Pressure Ratio

$mr1 = Qsa\ [(cp)(\Delta Tr)]^{-1}$ **Helium mass flow rate in HX1** (g/s)

$mr2 = (Qhi + Qeth)\ [(cp)(\Delta Tr)]^{-1}$ **Helium mass flow rate in HX2** (g/s)

$mrc = mr1 + mr2$ **Core mass flow rate** (g/s)

$mrs = (Qhi)\ [(cp)(Tx3i - Tx3o)]^{-1}$ **He mass flow rate in HX2 secondary side** (g/s)

$rp = (Tto/Tti)^{(\gamma-1)/\gamma}$ **Pressure ratio**

Set by Tti & Tto [4]

Core geometry

No thermal modeling of heat transfer within the core is used. Reactor parameters are assumed to be known and available as input parameters.

$V = P/Pden$	**Volume** = power/(core power density)
$D = (4V/\pi\ LD)^{1/3}$	**Diameter** in terms of volume and core L/D
$L = D \times LD$	**Length**
$A = \pi\ (D/2)^{12}$	**Cross section area**
$Ac = fc \times A$	**Flow cross section area**

Average helium parameters

$Tah = Tro - \Delta Tr/2$	Define two **average temperatures** h=high & l=low two obtain high and low temperature parameter sets.
$Tal = 700$	All components will be grouped as either h or l sets.
$pl = p\ (1 + 1/2.9)/2$	Define low pressure assuming rp = 2.9
Use linear fittings for computing parameters	Obtain high and low temperature sets for **density, viscosity, & thermal conductivity**

Helium velocities

He velocities in core, recuperator, heat exchangers

Compute flow cross section areas and use mass flow rates and densities to compute velocities

$v = mr/A\rho$	General expression for velocity

Pressure drops

Core

$frf = 0.184$	Core friction factor [5]

$(De\ vc\ \rho h/\mu h)^{0.2}$

$\Delta pc = [(frf\ )(L)(\rho h)(vc)^2]/2De$ Pressure drop in core [5]

Includes 10^{-7} multiplier to convert to MPa

Recuperator

$fR = \dfrac{0.184}{(DR\ vR\ \rho l/\mu l)^{0.2}}$ Recuperator friction factor

$h = 0.023 DR^{-0.2}\ v^{0.8}\ k\ (\rho/\mu)^{0.8}$ Use convective heat transfer coefficient from [6].

$= U$ Ignore conduction losses in recuperator

$(U)(Aht) = (mr\ x\ cp)/(1/\varepsilon R - 1)$ From [7]

$ARx = [\pi(DR)^2\ n]/4$ ARx = flow x-sec area, n = number of channels

$Aht = \pi(DR)\ LR\ n$ Aht = heat transfer area

$vR = mr/[(ARx)\ \rho]$ velocity

By substitution, using these equations, we obtain the following expression for recuperator length

$LR = \dfrac{\mu l^{0.8}\ cp\ (mrs/ARx)^{0.2}\ DR^{1.2}}{(\varepsilon R^{-1}-1)\ 4(0.023)\ kl}$ Recuperator length

Pressure drop in recuperator

$R = (LR+DR\ Lde)\ fR\ \rho l$ Define R for ΔpR eq.

includes LDe correction to length

$\Delta pR = [R\,(vR)^2]/2DR$

HX1

$Csa = \frac{(mr1)\,cp\,(Tx1i - Tx1o)}{\varepsilon 1(Tx1i - Tsai)}$ Sulfuric acid side (mass flow rate)(cp) [3]

(based on heat exchanger effectiveness equation)

$C1 = \frac{(Tx1i - Tx1o)}{\varepsilon 1(Tx1i - Tsai)}$ $\frac{\text{He side (mass flow rate)(cp)}}{\text{Sulfuric acid side (mass flow rate)(cp)}}$

$U1 = \frac{0.023\,(vH1)^{0.8}\,(\rho h)^{0.8}\,kh}{D1^{0.2}\,(\mu h)^{0.8}}$ HX1 heat transfer coef.

Ignores conduction through HX walls

HX1 length

$K1 = -4\,\frac{AHx1\,U1(1 - C1)}{D1\,Csa1}$ Define parameter K1 for use in length eq.

$L1 = (1/K1)\,\ln[(\varepsilon 1 - 1)/(\varepsilon 1 C1 - 1)]$ Based on expression for computing HX effect.

$fHx1 = \frac{0.184}{(D1\,vH1\,\rho h/\mu h)^{0.2}}$ HX1 friction factor

Pressure drop in HX1

$HH1 = fHx1(L1 + D1\,LDsa)\rho h$ Define HH1

Includes LDsa correction to length

$\Delta pHx1 = HH1(vH1)^2]/2D1$

HX2

$\Delta pHx2 = \Delta pHx1$ Pressure drop in HX2

Pressure drop across HX2 must equal ΔpHx1

Secondary Side

$CSs = mrs(cp)$ Secondary side (mass flow rate)(cp)

$Cs = mr2/mrs$ HX2 Primary side (mass flow rate)(cp) / Secondary side (mass flow rate)(cp)

(cp same for both sides)

$$Us = \frac{0.023\ (vHs)^{0.8}\ (\rho h)^{0.8}\ kh}{Ds^{0.2}\ (\mu h)^{0.8}}$$ HX2 heat transfer coef. for secondary side

$$Ks = -4\ \frac{AHs\ Us(1-Cs)}{Ds\ CSs}$$ HX2 heat transfer coef.

Define Ks.

$Ls = (1/Ks)\ \ln[(\varepsilon 2-1)/(\varepsilon 2\ Cs - 1)]$ HX2 length

$$fHs = \frac{0.184}{(Ds\ vHs\ \rho h/\mu h)^{0.2}}$$ HX2 friction factor

$HHs = (fHs)(Ls)(\rho h\}$ Pressure drop in secondary of HX2

Define HHs

$\Delta ps = [HHs\ (vHs)^2]/2\ Ds$

HX3

$$Chi = \frac{(mrs)\ cp\ (Tx3i - Tx3o)}{\varepsilon 3(Tx3i - Thii)}$$ HI side of HX3 (mass flow rate)(cp)

$$C3 = \frac{(Tx3i - Tx3o)}{\varepsilon 3(Tx3i - Thii)}$$ He side (mass flow rate)(cp) / HI side (mass flow rate)(cp)

$$U3 = \frac{0.023\ (vH3)^{0.8}\ (\rho l)^{0.8}\ kl}{D3^{0.2}\ (\mu l)^{0.8}}$$ HX3 heat transfer coef.

$$K3 = -\ 4\ \frac{AHx3\ U3(1-\ C3)}{D3\ Chi3}$$ HX3 length

Define K3

$$L3 = (1/K3)\ \ln[(\varepsilon 3-1)/\ (\varepsilon 3\ C3-1)]$$

$$fHx3 = \frac{0.184}{(D3\ vH3\ \rho l/\mu l)^{0.2}}$$ HX3 friction factor

$HH3 = fHx3(L3+ D3\ LDhi)(\rho l)$ Pressure drop in HX1

Define HH3

$\Delta pH3 = [\ HH3\ (vH3)^2]/2D3$ Includes LDhi correction for length

---

Actual Pressure ratios

$rpT = p/[(p/rp - \Delta pR) - \Delta pH3]$ Compute max /min pressures on primary side

$rpC = rp\ (p + \Delta pH2 + \Delta pR)\ /\ p$ Compute max /min pressures on compressor side

Primary side compressor power and electrical power for system

$Ppmax = p + \Delta pc$ Compute max and min pressure on primary side

$ppmin = p - \Delta pH1$

$Wp = mrc\ cp\ Tri[1-(ppmax/ppmin)^{-(\gamma-1)/\gamma}]$ **Compressor work** as enthalpy rise in compressor [4]

$Qemin = Ne\ Wp$ **Electrical power required by system**

Using work required for primary side compressor, estimate total electrical power required by the system as a multiple of Wp.

Efficiencies

$Xa = Tti\{1-\varepsilon R[1-\eta t(1-(rpT)^{-(\gamma-1)/\gamma})]\}$ **Heat input** (W)

From [4], includes recuperator effect and Xb power used for HI decomp.

$= Tci\{(1-\varepsilon R)\{1+\eta c^{-1}\,[(rpT)^{(\gamma-1)/\gamma}-1]\}$

$X = Xa + Xb$

$QRs = mrs\ cp\ X + Qhi$

$Ya = Tti\ (\eta t)[\ 1-(rpC)^{-(\gamma-1)/\gamma}]$ **Electrical Power output** (W)

Note that the expression. for an intercooler in Ref [4] eq. 7-30 appears to be in error. Using Ref. [8], I find that the pressure ratio expression in the compressor work eq. should be $rp^{(\gamma-1)/2\gamma}$

$Yb = Ttc(2/\eta c)\,[(rpC)^{(\gamma-1)/2\gamma}-1]\}$

$Y = Ya + Yb$

$W = mrs\ cp\ Y$

$WH = Hpr\ (HQ/3.6)$ **Power equivalent of H_2 Produced** (W)

Energy equivalent for H_2 combustion.

3.6 is for units conversion

Qtot = QRs + Qsa **Total thermal power produced** (W)

$\eta T = \frac{W + WH - Qemin}{Qtot}$ **Net efficiency (elec. + H_2 energy)** (W)

For the parameters assumed in the trial run, the efficiency is obtained as a function of the ratio of the thermal power used for hydrogen production to the total thermal power used for both electricity production and hydrogen production; i.e.,

$$fh = QH/ Qtot$$

A plot of the total efficiency as a function of fh is given in Fig. 6 for hydrogen production rates of 10^3 kg/hr. Note that for 10^3 kg/hr, the efficiency decreases (slightly) from about 52.5% as the fraction of power used for hydrogen production increases to 0.8. For low hydrogen production rates the efficiency increases up to about 53%.

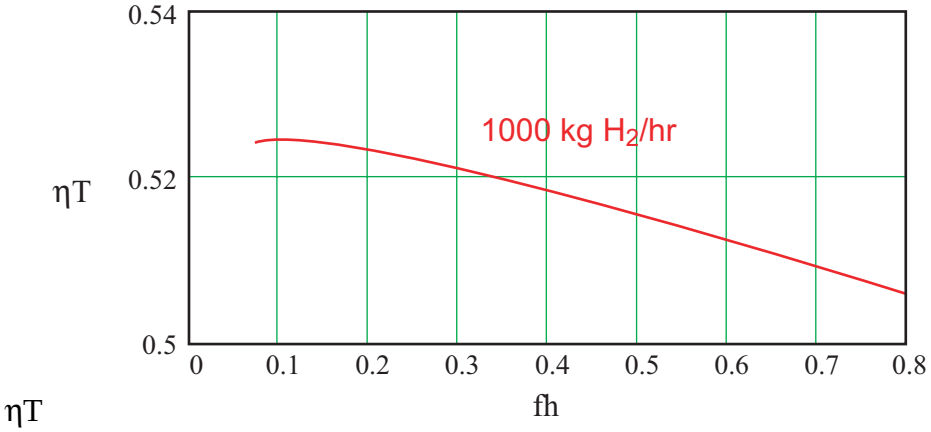

Fig. 6 Total (hydrogen + electricity) efficiency vs. fraction of thermal power used for hydrogen production.

Figure 7 presents the total efficiency as a function of the thermal power for electricity (Qeth) for several hydrogen production rates. Note that efficiencies for low hydrogen production rates peak at low Qeth, and efficiencies for high hydrogen production rates peak at high Qeth. Also note that for high hydrogen production rates, no solution exists at low Qeth.

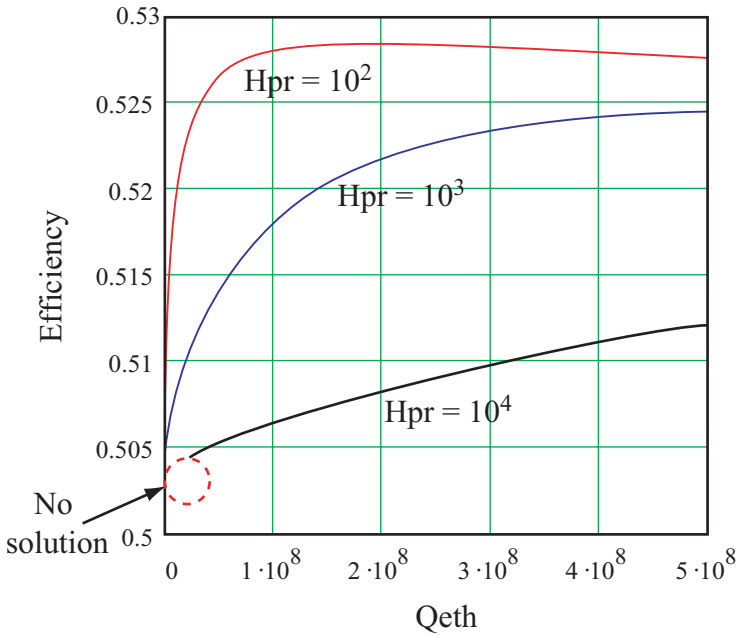

Fig. 7 Total (hydrogen + electricity) efficiency vs. additional thermal power for electricity.

The electrical power and equivalent hydrogen power produced for hydrogen production rates of 10^3 and 5 x 10^3 are plotted as a function of Qeth in Fig. 8. The total reactor power is plotted as a function of Qeth for several hydrogen production rates in Fig. 9.

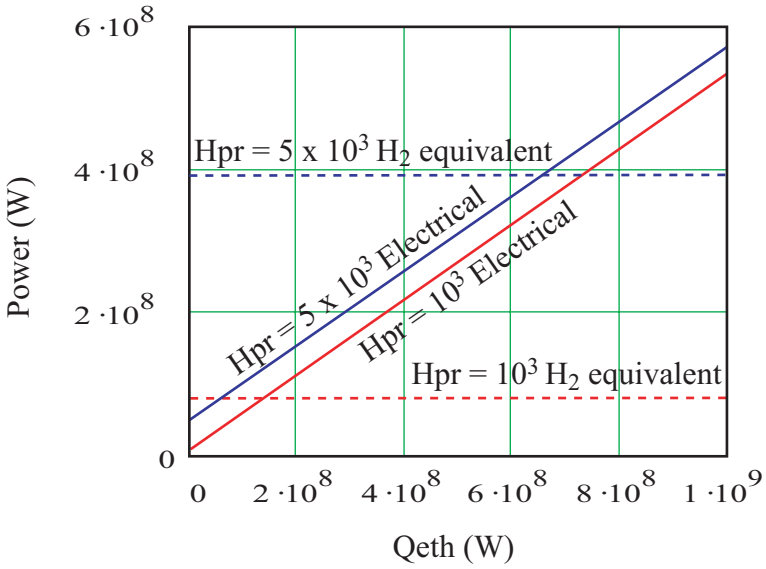

Fig. 8 Electrical and hydrogen (equivalent) power vs. additional thermal power for electricity.

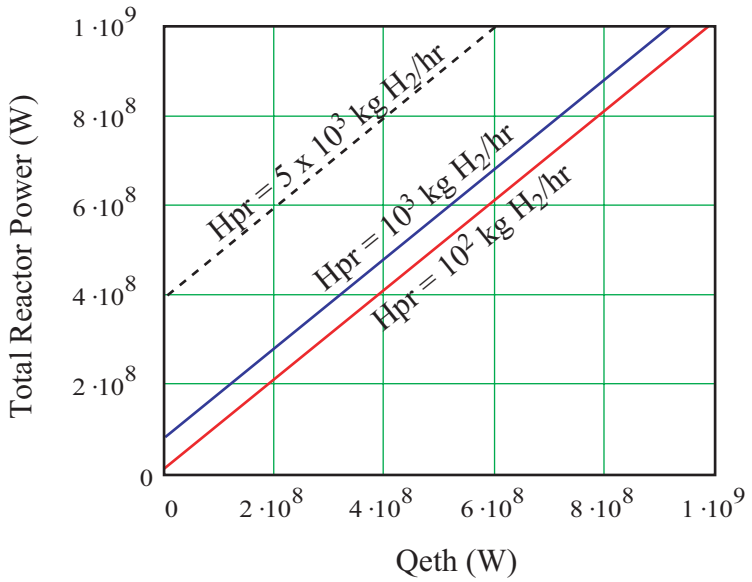

Fig. 9 Total reactor power vs. additional thermal power or electricity for several hydrogen production rates.

4.2 Electrical–only System

Helium temperatures

Troo=Teti — **Reactor outlet temperature** = turbine inlet temperature (direct Brayton)

Tri = Troo–ΔTr — **Reactor inlet temperature**

Tto = Teti $rp^{(1-\gamma)/\gamma}$ — **Turbine outlet temperature**

Set by selected pressure ratio and turbine inlet temperature

The remainder of the electrical-only model is similar to the hybrid model.

The electrical efficiency as a function of turbine inlet temperature is compared to the Carnot efficiency in Fig. 10. The predicted efficiencies are in good agreement with predictions made by General Atomics [9].

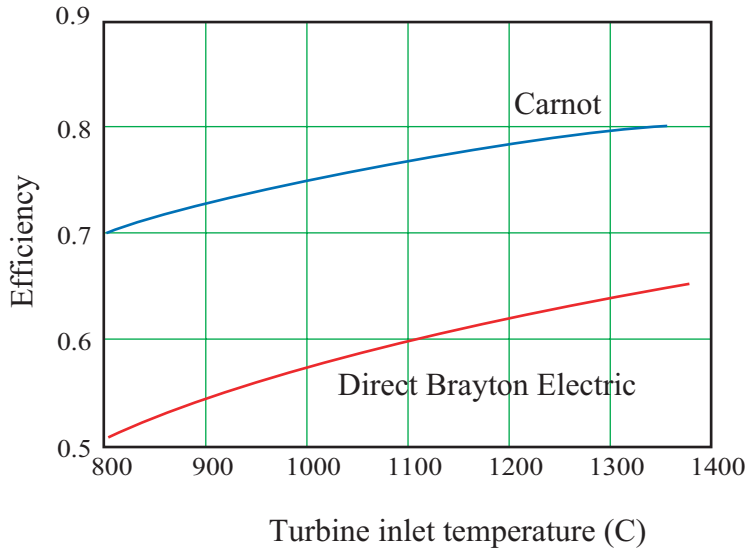

Fig. 10 Electrical efficiency and Carnot efficiency vs, turbine inlet temperature for an electrical-only direct Brayton system.

The electrical efficiency vs. Qeth for an electricity-only plant is compared to the total efficiency of a hybrid system in Fig11. The top curve is for an electrical-only system operating at the reactor outlet temperature (888 C) of the hybrid system. The 1% increase in efficiency, relative to a hybrid system efficiency, is due primarily to the operation of the electrical-only system as a direct Brayton system (without an intermediate heat exchanger). When the same turbine inlet temperature as the hybrid system is used (equivalent to an indirect electrical only system), the efficiency is only very slightly better than the efficiency of the hybrid system with no hydrogen production. This small difference is probably due the temperature constraints and pressure losses imposed by the heat exchangers. Note that for the hybrid system producing 10^3 kg/hr, the efficiency is a few percent lower than the electrical-only system efficiency at zero electrical power production, and the efficiency approaches the electrical-only efficiency at high Qeth.

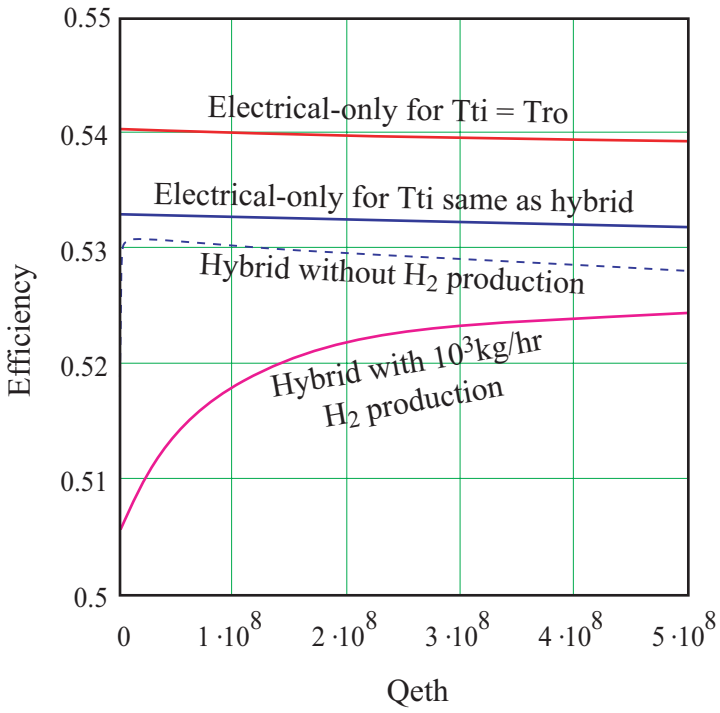

Fig. 11 Electrical efficiency for electrical-only and hybrid systems vs. Qeth.

4.3 Hydrogen–only System

The hydrogen-only model is similar to the hybrid model. Figure 12 compares the efficiency vs. hydrogen production rate of an electrical-only system and the hybrid system. Note that the efficiencies for the hybrid system are bracketed by the efficiencies for the electrical-only and the hydrogen-only efficiencies.

5. Conclusions

The results presented in this memorandum were based on a preliminary model using trial input data. Better input data and a more sophisticated model may alter the predictions somewhat. Nonetheless, the model predicts total efficiencies of 50% or more for a range of hydrogen production rates. Although the efficiencies for a hybrid system are better than for a hydrogen-only system, the improvement is not substantial. Furthermore, the efficiency of an electrical-only system is predicted to be greater than the efficiency of a hybrid system. If these predictions are correct, the efficiency benefits gained must be compared to the capital cost of a hybrid system to assess the best system design for a hydrogen production plant.

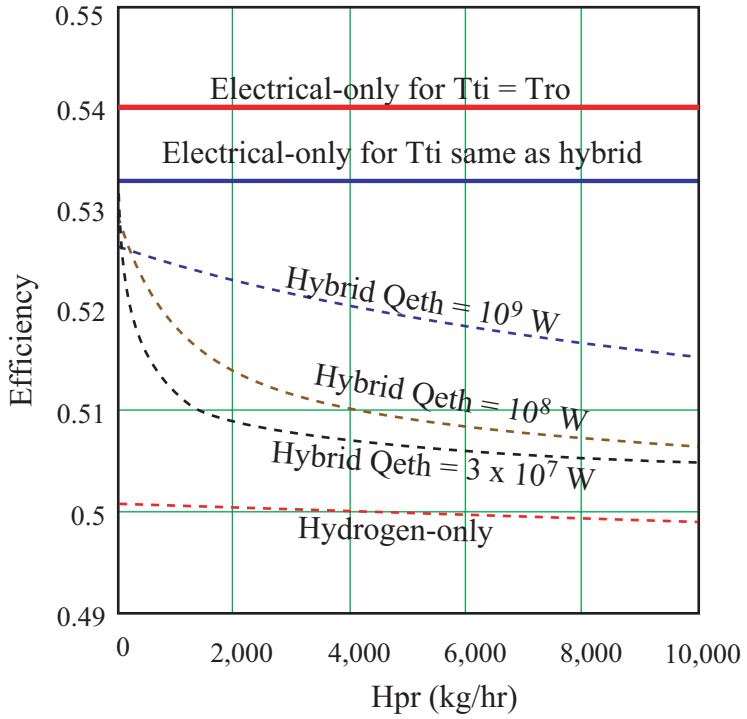

Fig. 12 Electrical efficiency for electrical-only, hydrogen-only, and hybrid systems vs. hydrogen production rate.

References:

1. L. C. Brown, *High efficiency Generation of Fuels Using Nuclear Power*, NERI Proposal, January 29, 1999.

2. J. E. Funk, personal communication, March 2002.

3. J. R. Welty, C. E. Wicks, and R.E. Wilson, *Fundamentals of Momentum, Heat, and Mass Transfer*, John Wiley & Sons, 1969.

4. M. M. El-Wakil, *Nuclear Energy Conversion*, International Textbook Co., 1982.

5. M. M. El-Wakil, *Nuclear Heat Transport*, International Textbook Co., 1978.

6. Kreith, *Principles of Heat Transport*

7. A. F. Mills, *Heat Transfer*, Second Edition, Prentice Hall, 1999.

8. Memphis.edu/courses/01f/MECH3312/Ch8.pdf

9. *Very High Efficiency Reactor for Electricity and Transportation-Fuel Production*, GACP 211-001, Jan. 19, 2001.